E-ISSN: 2148-6247

Turkish Journal of PHARMACEUTICAL SCIENCES

An Official Journal of the Turkish Pharmacists' Association, Academy of Pharmacy

Volume: 19 Issue: 5 October 2022

www.turkjps.org

PubMed Central PubMed Scopus TR DİZİN

galenos Publishing House

Turkish Journal of
PHARMACEUTICAL SCIENCES

Turkish Journal of
PHARMACEUTICAL SCIENCES

Turkish Journal of
PHARMACEUTICAL SCIENCES

AIMS AND SCOPE

The Turkish Journal of Pharmaceutical Sciences is the only scientific periodical publication of the Turkish Pharmacists' Association and has been published since April 2004.
Turkish Journal of Pharmaceutical Sciences journal is regularly published 6 times in a year (February, April, June, August, October, December). The issuing body of the journal is Galenos Yayinevi/Publishing House level. The aim of Turkish Journal of Pharmaceutical Sciences is to publish original research papers of the highest scientific and clinical value at an international level.
The target audience includes specialists and professionals in all fields of pharmaceutical sciences.
The editorial policies are based on the "Recommendations for the Conduct, Reporting, Editing, and Publication of Scholarly Work in Medical Journals (ICMJE Recommendations)" by the International Committee of Medical Journal Editors (20, archived at http://www.icmje.org/) rules.

Editorial Independence

Turkish Journal of Pharmaceutical Sciences is an independent journal with independent editors and principles and has no commerical relationship with the commercial product, drug or pharmaceutical company regarding decisions and review processes upon articles.

ABSTRACTED/INDEXED IN

PubMed
PubMed Central
Web of Science-Emerging Sources Citation Index (ESCI)
SCOPUS SJR
TÜBİTAK/ULAKBİM TR Dizin
ProQuest
Chemical Abstracts Service (CAS)
EBSCO
EMBASE
GALE
Index Copernicus
Analytical Abstracts
International Pharmaceutical Abstracts (IPA)
Medicinal & Aromatic Plants Abstracts (MAPA)
British Library
CSIR INDIA
GOALI
Hinari
OARE
ARDI
AGORA
Türkiye Atıf Dizini
Türk Medline
UDL-EDGE
J- Gate
Idealonline
CABI

OPEN ACCESS POLICY

This journal provides immediate open access to its content on the principle that making research freely available to the public supports a greater global exchange of knowledge.
Open Access Policy is based on the rules of the Budapest Open Access Initiative (BOAI) http://www.budapestopenaccessinitiative.org/. By "open access" to peer-reviewed research literature, we mean its free availability on the public internet, permitting any users to read, download, copy, distribute, print, search, or link to the full texts of these articles, crawl them for indexing, pass them as data to software, or use them for any other lawful purpose, without financial, legal, or technical barriers other than those inseparable from gaining access to the internet itself. The only constraint on reproduction and distribution, and the only role for copyright in this domain, should be to give authors control over the integrity of their work and the right to be properly acknowledged and cited.

CORRESPONDENCE ADDRESS

All correspondence should be directed to the Turkish Journal of Pharmaceutical Sciences Editorial Board

Post Address: Turkish Pharmacists' Association, Mustafa Kemal Mah 2147.Sok No:3 06510 Çankaya/Ankara, TÜRKİYE
Phone: +90 (312) 409 81 00
Fax: +90 (312) 409 81 09
Web Page: http://turkjps.org
E-mail: turkjps@gmail.com

PERMISSIONS

Requests for permission to reproduce published material should be sent to the publisher.
Publisher: Erkan Mor
Adress: Molla Gürani Mah. Kaçamak Sok. 21/1 Fındıkzade, Fatih, Istanbul, Türkiye
Telephone: +90 212 621 99 25
Fax: +90 212 621 99 27
Web page: http://www.galenos.com.tr/en
E-mail: info@galenos.com.tr

ISSUING BODY CORRESPONDING ADDRESS

Issuing Body : Galenos Yayınevi
Address: Molla Gürani Mah. Kaçamak Sk. No: 21/, 34093 İstanbul, Türkiye
Phone: +90 212 621 99 25 Fax: +90 212 621 99 27
E-mail: info@galenos.com.tr

MATERIAL DISCLAIMER

The author(s) is (are) responsible for the articles published in the JOURNAL.
The editors, editorial board and publisher do not accept any responsibility for the articles.

Publisher Contact
Address: Molla Gürani Mah. Kaçamak Sk. No: 21/1
34093 İstanbul, Türkiye
Phone: +90 (212) 621 99 25 **Fax:** +90 (212) 621 99 27
E-mail: info@galenos.com.tr/yayin@galenos.com.tr
Web: www.galenos.com.tr | **Publisher Certificate Number:** 14521

Publication Date: October 2022
E-ISSN: 2148-6247
International scientific journal published bimonthly.

Turkish Journal of
PHARMACEUTICAL SCIENCES

INSTRUCTIONS TO AUTHORS

Turkish Journal of Pharmaceutical Sciences journal is published 6 times (February, April, June, August, October, December) per year and publishes the following articles:

- Research articles
- Reviews (only upon the request or consent of the Editorial Board)
- Preliminary results/Short communications/Technical notes/Letters to the Editor in every field of pharmaceutical sciences.

The publication language of the journal is English.

The Turkish Journal of Pharmaceutical Sciences does not charge any article submission or processing charges.

A manuscript will be considered only with the understanding that it is an original contribution that has not been published elsewhere.

The Journal should be abbreviated as "Turk J Pharm Sci" when referenced.

The scientific and ethical liability of the manuscripts belongs to the authors and the copyright of the manuscripts belongs to the Journal. Authors are responsible for the contents of the manuscript and accuracy of the references. All manuscripts submitted for publication must be accompanied by the Copyright Transfer Form [copyright transfer]. Once this form, signed by all the authors, has been submitted, it is understood that neither the manuscript nor the data it contains have been submitted elsewhere or previously published and authors declare the statement of scientific contributions and responsibilities of all authors.

Experimental, clinical and drug studies requiring approval by an ethics committee must be submitted to the JOURNAL with an ethics committee approval report including approval number confirming that the study was conducted in accordance with international agreements and the Declaration of Helsinki (revised 2013) (http://www.wma.net/en/30publications/10policies/b3/). The approval of the ethics committee and the fact that informed consent was given by the patients should be indicated in the Materials and Methods section. In experimental animal studies, the authors should indicate that the procedures followed were in accordance with animal rights as per the Guide for the Care and Use of Laboratory Animals (http://oacu.od.nih.gov/regs/guide/guide.pdf) and they should obtain animal ethics committee approval.

Authors must provide disclosure/acknowledgment of financial or material support, if any was received, for the current study.

If the article includes any direct or indirect commercial links or if any institution provided material support to the study, authors must state in the cover letter that they have no relationship with the commercial product, drug, pharmaceutical company, etc. concerned; or specify the type of relationship (consultant, other agreements), if any.

Authors must provide a statement on the absence of conflicts of interest among the authors and provide authorship contributions.

All manuscripts submitted to the journal are screened for plagiarism using the 'iThenticate' software. Results indicating plagiarism may result in manuscripts being returned or rejected.

The Review Process

This is an independent international journal based on double-blind peer-review principles. The manuscript is assigned to the Editor-in-Chief, who reviews the manuscript and makes an initial decision based on manuscript quality and editorial priorities. Manuscripts that pass initial evaluation are sent for external peer review, and the Editor-in-Chief assigns an Associate Editor. The Associate Editor sends the manuscript to at least two reviewers (internal and/or external reviewers). The Associate Editor recommends a decision based on the reviewers' recommendations and returns the manuscript to the Editor-in-Chief. The Editor-in-Chief makes a final decision based on editorial priorities, manuscript quality, and reviewer recommendations. If there are any conflicting recommendations from reviewers, the Editor-in-Chief can assign a new reviewer.

The scientific board guiding the selection of the papers to be published in the Journal consists of elected experts of the Journal and if necessary, selected from national and international authorities. The Editor-in-Chief, Associate Editors may make minor corrections to accepted manuscripts that do not change the main text of the paper.

In case of any suspicion or claim regarding scientific shortcomings or ethical infringement, the Journal reserves the right to submit the manuscript to the supporting institutions or other authorities for investigation. The Journal accepts the responsibility of initiating action but does not undertake any responsibility for an actual investigation or any power of decision.

The Editorial Policies and General Guidelines for manuscript preparation specified below are based on "Recommendations for the Conduct, Reporting, Editing, and Publication of Scholarly Work in Medical Journals (ICMJE Recommendations)" by the International Committee of Medical Journal Editors (20, archived at http://www.icmje.org/).

Preparation of research articles, systematic reviews and meta-analyses must comply with study design guidelines:

CONSORT statement for randomized controlled trials (Moher D, Schultz KF, Altman D, for the CONSORT Group. The CONSORT statement revised recommendations for improving the quality of reports of parallel group randomized trials. JAMA 2001; 285: 1987-91) (http://www.consort-statement.org/);

PRISMA statement of preferred reporting items for systematic reviews and meta-analyses (Moher D, Liberati A, Tetzlaff J, Altman DG, The PRISMA Group. Preferred Reporting Items for Systematic Reviews and Meta-Analyses: The PRISMA Statement. PLoS Med 2009; 6(7): e1000097.) (http://www.prisma-statement.org/);

STARD checklist for the reporting of studies of diagnostic accuracy (Bossuyt PM, Reitsma JB, Bruns DE, Gatsonis CA, Glasziou PP, Irwig LM, et al., for the STARD Group. Towards complete and accurate reporting of studies of diagnostic accuracy: the STARD initiative. Ann Intern Med 2003;138:40-4.) (http://www.stard-statement.org/);

STROBE statement, a checklist of items that should be included in reports of observational studies (http://www.strobe-statement.org/);

MOOSE guidelines for meta-analysis and systemic reviews of observational studies (Stroup DF, Berlin JA, Morton SC, et al. Meta-analysis of observational studies in epidemiology: a proposal for reporting Meta-analysis of observational Studies in Epidemiology (MOOSE) group. JAMA 2000; 283: 2008-12).

Turkish Journal of
PHARMACEUTICAL SCIENCES

INSTRUCTIONS TO AUTHORS

GENERAL GUIDELINES

Manuscripts can only be submitted electronically through the Journal Agent website (http://journalagent.com/tjps/) after creating an account. This system allows online submission and review.

Format: Manuscripts should be prepared using Microsoft Word, size A4 with 2.5 cm margins on all sides, 12 pt Arial font and 1.5 line spacing.

Abbreviations: Abbreviations should be defined at first mention and used consistently thereafter. Internationally accepted abbreviations should be used; refer to scientific writing guides as necessary.

Cover letter: The cover letter should include statements about manuscript type, single-Journal submission affirmation, conflict of interest statement, sources of outside funding, equipment (if applicable), for original research articles.

ETHICS COMMITTEE APPROVAL

The editorial board and our reviewers systematically ask for ethics committee approval from every research manuscript submitted to the Turkish Journal of Pharmaceutical Sciences. If a submitted manuscript does not have ethical approval, which is necessary for every human or animal experiment as stated in international ethical guidelines, it must be rejected on the first evaluation.

Research involving animals should be conducted with the same rigor as research in humans; the Turkish Journal of Pharmaceutical Sciences asks original approval document to show implements the 3Rs principles. If a study does not have ethics committee approval or authors claim that their study does not need approval, the study is consulted to and evaluated by the editorial board for approval.

SIMILARITY

The Turkish Journal of Pharmaceutical Sciences is routinely looking for similarity index score from every manuscript submitted before evaluation by the editorial board and reviewers. The journal uses iThenticate plagiarism checker software to verify the originality of written work. There is no acceptable similarity index; but, exceptions are made for similarities less than 15 %.

REFERENCES

Authors are solely responsible for the accuracy of all references.

In-text citations: References should be indicated as a superscript immediately after the period/full stop of the relevant sentence. If the author(s) of a reference is/are indicated at the beginning of the sentence, this reference should be written as a superscript immediately after the author's name. If relevant research has been conducted in Türkiye or by Turkish investigators, these studies should be given priority while citing the literature.

Presentations presented in congresses, unpublished manuscripts, theses, Internet addresses, and personal interviews or experiences should not be indicated as references. If such references are used, they should be indicated in parentheses at the end of the relevant sentence in the text, without reference number and written in full, in order to clarify their nature.

References section: References should be numbered consecutively in the order in which they are first mentioned in the text. All authors should be listed regardless of number. The titles of Journals should be abbreviated according to the style used in the Index Medicus.

Reference Format

Journal: Last name(s) of the author(s) and initials, article title, publication title and its original abbreviation, publication date, volume, the inclusive page numbers. Example: Collin JR, Rathbun JE. Involutional entropion: a review with evaluation of a procedure. Arch Ophthalmol. 1978;96:1058-1064.

Book: Last name(s) of the author(s) and initials, book title, edition, place of publication, date of publication and inclusive page numbers of the extract cited.

Example: Herbert L. The Infectious Diseases (1st ed). Philadelphia; Mosby Harcourt; 1999:11;1-8.

Book Chapter: Last name(s) of the author(s) and initials, chapter title, book editors, book title, edition, place of publication, date of publication and inclusive page numbers of the cited piece.

Example: O'Brien TP, Green WR. Periocular Infections. In: Feigin RD, Cherry JD, eds. Textbook of Pediatric Infectious Diseases (4th ed). Philadelphia; W.B. Saunders Company;1998:1273-1278.

Books in which the editor and author are the same person: Last name(s) of the author(s) and initials, chapter title, book editors, book title, edition, place of publication, date of publication and inclusive page numbers of the cited piece. Example: Solcia E, Capella C, Kloppel G. Tumors of the exocrine pancreas. In: Solcia E, Capella C, Kloppel G, eds. Tumors of the Pancreas. 2nd ed. Washington: Armed Forces Institute of Pathology; 1997:145-210.

TABLES, GRAPHICS, FIGURES, AND IMAGES

All visual materials together with their legends should be located on separate pages that follow the main text.

Images: Images (pictures) should be numbered and include a brief title. Permission to reproduce pictures that were published elsewhere must be included. All pictures should be of the highest quality possible, in

JPEG format, and at a minimum resolution of 300 dpi.

Tables, Graphics, Figures: All tables, graphics or figures should be enumerated according to their sequence within the text and a brief descriptive caption should be written. Any abbreviations used should be defined in the accompanying legend. Tables in particular should be explanatory and facilitate readers' understanding of the manuscript, and should not repeat data presented in the main text.

MANUSCRIPT TYPES

Original Articles

Clinical research should comprise clinical observation, new techniques or laboratories studies. Original research articles should include title, structured abstract, key words relevant to the content of the article, introduction, materials and methods, results, discussion, study limitations, conclusion references, tables/figures/images and

Turkish Journal of
PHARMACEUTICAL SCIENCES

INSTRUCTIONS TO AUTHORS

acknowledgement sections. Title, abstract and key words should be written in both Turkish and English. The manuscript should be formatted in accordance with the above-mentioned guidelines and should not exceed 16 A4 pages.

Title Page: This page should include the title of the manuscript, short title, name(s) of the authors and author information. The following descriptions should be stated in the given order:

1. Title of the manuscript (Turkish and English), as concise and explanatory as possible, including no abbreviations, up to 135 characters

2. Short title (Turkish and English), up to 60 characters

3. Name(s) and surname(s) of the author(s) (without abbreviations and academic titles) and affiliations

4. Name, address, e-mail, phone and fax number of the corresponding author

5. The place and date of scientific meeting in which the manuscript was presented and its abstract published in the abstract book, if applicable

Abstract: A summary of the manuscript should be written in both Turkish and English. References should not be cited in the abstract. Use of abbreviations should be avoided as much as possible; if any abbreviations are used, they must be taken into consideration independently of the abbreviations used in the text. For original articles, the structured abstract should include the following sub-headings:

Objectives: The aim of the study should be clearly stated.

Materials and Methods: The study and standard criteria used should be defined; it should also be indicated whether the study is randomized or not, whether it is retrospective or prospective, and the statistical methods applied should be indicated, if applicable.

Results: The detailed results of the study should be given and the statistical significance level should be indicated.

Conclusion: Should summarize the results of the study, the clinical applicability of the results should be defined, and the favorable and unfavorable aspects should be declared.

Keywords: A list of minimum , but no more than 5 key words must follow the abstract. Key words in English should be consistent with "Medical Subject Headings (MESH)" (www.nlm.nih.gov/mesh/MBrowser.html). Turkish key words should be direct translations of the terms in MESH.

Original research articles should have the following sections:

Introduction: Should consist of a brief explanation of the topic and indicate the objective of the study, supported by information from the literature.

Materials and Methods: The study plan should be clearly described, indicating whether the study is randomized or not, whether it is retrospective or prospective, the number of trials, the characteristics, and the statistical methods used.

Results: The results of the study should be stated, with tables/figures given in numerical order; the results should be evaluated according to the statistical analysis methods applied. See General Guidelines for details about the preparation of visual material.

Discussion: The study results should be discussed in terms of their favorable and unfavorable aspects and they should be compared with the literature. The conclusion of the study should be highlighted.

Study Limitations: Limitations of the study should be discussed. In addition, an evaluation of the implications of the obtained findings/results for future research should be outlined.

Conclusion: The conclusion of the study should be highlighted.

Acknowledgements: Any technical or financial support or editorial contributions (statistical analysis, English/Turkish evaluation) towards the study should appear at the end of the article.

References: Authors are responsible for the accuracy of the references. See General Guidelines for details about the usage and formatting required.

Review Articles

Review articles can address any aspect of clinical or laboratory pharmaceuticals. Review articles must provide critical analyses of contemporary evidence and provide directions of or future research. Most review articles are commissioned, but other review submissions are also welcome. Before sending a review, discussion with the editor is recommended.

Reviews articles analyze topics in depth, independently and objectively. The first chapter should include the title in Turkish and English, an unstructured summary and key words. Source of all citations should be indicated. The entire text should not exceed 25 pages (A, formatted as specified above).

Turkish Journal of
PHARMACEUTICAL SCIENCES

CONTENTS

Turk J Pharm Sci 2022;19(5):488-497
DOI: 10.4274/tjps.galenos.2021.48861

ORIGINAL ARTICLE

Stability Indicating Assay Method for the Quantitative Determination of Olaparib in Bulk and Pharmaceutical Dosage Form

Antima CHAUDHARY[1], Rajiv TONK[1], Pankaj DAGUR[2], Suddhasattya DEY[3], Manik GHOSH[2]*

[1]Delhi Pharmaceutical Sciences and Research University, Department of Pharmaceutical Chemistry, New Delhi, India
[2]Birla Institute of Technology, Department of Pharmaceutical Sciences and Technology, Ranchi, India
[3]Sanaka Educational Trust's Group of Institutions, Department of Pharmacy, Durgapur West Bengal, India

ABSTRACT

Objectives: Olaparib is an orally active poly (ADP-ribose) PARP (polymerases) inhibitor known to destroy cancer cells with BRCA1 or BRCA2 deficiency. An authentic, fast, distinct, and reliable reverse phase-high performance liquid chromatography (RP-HPLC) method was developed and promptly validated in tablet formulations for olaparib estimation.

Materials and Methods: The proposed method focuses on the separation of olaparib in reverse phase mode using a Waters symmetry C18 (150 x 4.6 mm, 5 µm) analytical column with a flow rate of 1.0 mL/min and the injection volume was kept at 20 µL. The optimized mobile phase consists of ammonium acetate buffer (pH adjusted to 3.5 by glacial acetic acid): methanol in the ratio of 50:50 v/v.

Results: The eluents were measured at 254 nm and the retention time for the drug encircled was about 4.32 min. The stress degradation studies of olaparib were conducted under acidic, alkaline, oxidative, photolytic and thermal conditions to demonstrate the stability of the drug. The regression value of 0.998 showed that the developed method was linear over the range of 80 µg/mL to 120 µg/mL. The developed RP-HPLC method is accurate and precise. The method was statistically validated as *per* International Conference on Harmonization guidelines.

Conclusion: The proposed method is suitable and can be applied for the quantitative estimation of olaparib without any interference of the excipients used in the drug formulations.

Key words: Olaparib, poly ADP-ribose polymerase (PARP) inhibitor, RP-HPLC, waters, ICH and validation

INTRODUCTION

During the last decade, inactivation of poly (ADP-ribose) polymerase (PARP), a nuclear enzyme associated with many operations including DNA repair and cell death, has emerged as a possible individualized cancer therapeutic approach.[1-4] In cancer cells with a defective DNA damage repair system, such as those produced by *BRCA* gene mutations, PARP inhibitors, a new class of anticancer drugs, can cause tumor-specific synthetic lethality.[5-8] Olaparib (Figure 1), veliparib, niraparib, and rucaparib are potent PARP inhibitors that have recently moved through advanced clinical studies as combination and/or solo-targeted therapies, especially in breast and ovarian malignancies. Olaparib (Lynparza®) was the first medication to be approved for use in individuals with BRCA-mutated ovarian

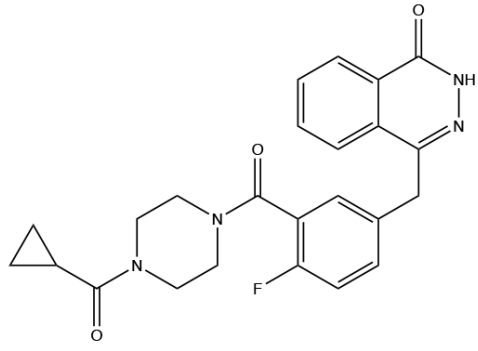

Figure 1. Chemical structure of olaparib

*Correspondence: manik@bitmesra.ac.in, Phone: +9430360991, ORCID-ID: orcid.org/0000-0003-2846-2971
Received: 31.08.2021, Accepted: 18.10.2021

cancer by the European Commission (2014) and the United States Food and Drug Administration (2015).[5,9,10]

PARP inhibitors hold a lot of therapeutic potential and will likely be employed in many cancer therapies in the future.[10] However, preclinical and clinical studies have revealed that tumor cell sensitivity to PARP inhibitors varies significantly, indicating that treatment efficacy must be enhanced.[11] Because PARP is an intracellular target, a crucial element influencing tumour cell sensitivity and the efficacy of a PARP-targeted treatment is the quantity of PARP inhibitors reaching the intracellular compartment.[12] PARP inhibitors, like any other intracellular target medicine, are affected by processes such as excretion, metabolism,[13] drug absorption, and expression/upregulation of transmembrane drug efflux transporters.[14,15] The latter, which is particularly significant for PARP inhibitors, was discovered as a key resistance mechanism during early preclinical trials.[16-18]

Analytical method validation assures that diverse high performance liquid chromatography (HPLC) analytical procedures provide consistent and reproducible results; it is an important stage in the development of novel dosage forms since it provides information on accuracy, linearity, precision, detection, and quantification limits. "The goal of validation of an analytical procedure is to demonstrate that it is suitable for its intended purpose", according with the International Conference on Harmonization (ICH) guideline. Validation data must now be sent to the appropriate authorities during the medication development process. The validation of analytical methods is governed by a set of guidelines from the ICH and the United States Pharmacopeia.

Olaparib has not yet been formally included in any of the official pharmacopeias, and there is no documented reverse phase (RP)-HPLC technique for quantifying olaparib in pharmaceutical formulations, according to a comprehensive literature assessment.[19,20] However, only a few techniques for estimating olaparib concentrations in human plasma using UHPLC10 and liquid chromatography-tandem mass spectrometry (LC-MS/MS) have been reported.[21,22] This work aimed to create a genuine, quick, distinct, and reliable analytical technique for quantifying olaparib in pharmaceutical formulations using RP-HPLC, which was validated according to ICH guidelines. A proven method for quantifying olaparib in bulk and pharmaceutical formulations was successfully implemented.

MATERIALS AND METHODS

Chemical and reagents

The various laboratory batch samples and reference standard (99.92%) of olaparib were provided by AstraZeneca Pharma. HPLC grade methanol was procured from Merck Sigma-Aldrich. Milli-Q purified water a Milli-Q plus purification system from Millipore was utilized during experimental studies. HPLC grade ammonium acetate was obtained from Rankem.

Instrument

In the study, a Waters HPLC 2695 sequence with a pump, auto sampler, auto injector, variable wavelength detector, and 2690 PDA detector with thermostatic column compartment was used. Operation control of the instrument and data collection was done by empower 3 software.

Optimization of chromatographic conditions

The HPLC method was optimized with objective to estimation olaparib in tablet formulation. Several mobile phases in isocratic mode, along with various columns, were considered to achieve a sharp peak with the base line. The tailing factor, the sharpness of the peak, and symmetry were considered for selectivity, sensitivity, and appropriate chromatographic conditions suitable for the column and the mobile phase. Different flow rates were also attempted and fixed at 1 mL/min for the optimized method. The eluents were also checked for their maximum absorbance in the PDA detector and fixed at 254 nm as a detection wavelength. The temperature of the column was maintained at 25°C.

Preparation of mobile phase

The mobile phase was prepared at a ratio of 50:50 v/v of buffer and methanol. Ammonium acetate buffer was created by dissolving 1.0 g of ammonium acetate in a sufficient volume of Milli-Q water (1000 mL). The pH of the solution was adjusted to 3.5 using glacial acetic acid. The mobile phase was degassed by sonication and it filtered using a 0.45 µ membrane filter. Methanol was used as the diluent. The ultraviolet detector was set at a wavelength of 254 nm.

Preparation of standard solutions

The standard stock solution of olaparib was prepared by weighing 25 mg olaparib into a 25 mL volumetric flask, sonicating until dissolved, and finally, the volume was made up to 25 mL with methanol. Appropriate dilutions were made from the above 1.0 mg/mL solution and transferred to a 100 mL volumetric flask, where the final volume was made by the mobile phase. Before the filling the vials for chromatographic analysis, the solution was passed through a membrane filter of diameter 0.45 µ.

Sample solution preparation for estimating marketed tablet formulation

Twenty tablets were accurately weighed, powdered and was added to 25 mL of diluent in a volumetric flask followed by sonication till it was completely dissolved. Finally, the volume was made up to 50 mL. Appropriate dilution was made to obtain a concentration of 100 µg/mL as a stock solution. Different dilutions were prepared from the stock solution and chromatographic analysis was carried out. Before filling the vial for chromatographic analysis, the solution was filtered *via* a 0.45 µ membrane filter.

Method validation

The optimized method developed for olaparib was validated in accordance with the ICH guideline Q2 (R1) for evaluating linearity, precision, accuracy, specificity, robustness, ruggedness, system suitability, analytical solution stability, and force degradation.

Linearity

The linearity range of an analytical method was assessed by injecting the standard dilution in duplicates over five different concentrations made in the range of 80 µg/mL to 120 µg/mL. The calibration curve was plotted with the analyte peak area against the analyte concentration to ensure the linearity of the analytical method being developed.

Precision and intermediate precision

The intra-and inter-day precision was determined in terms of the peak area difference of drug solutions for three consecutive days. A relative standard deviation (RSD) was calculated from the alteration of peak area to represent the intra- and inter-day precision.

Intra- and inter-day precision were performed at three different concentration levels of 80, 100, and 120 µg/mL. The repeatability study was performed by injecting six replicates of standard preparations of concentration 100 µg/mL.

Accuracy

The accuracy of the developed method was verified by spiking olaparib, which was performed by spiking olaparib with a standard at three different concentrations: 90%, 100%, and 110%. Triplicate analysis of these samples was performed and the results were in the form of RSD% and recovery percentage.

Specificity

The specificity of the method was established by analyzing standard substances against potent interferences. Specificity was assessed by injecting standard, sample, placebo, and blank preparations into HPLC. The recovery was measured.

Robustness

Alterations were made deliberately in chromatographic parameters such as the composition of the mobile phase, mobile phase pH, and flow rate. These variations were evaluated for column efficiency, asymmetry factor along with their RSD%.

Ruggedness

Different analysts were considered for the ruggedness study. Solutions of 100 µg/mL were prepared and injected by two different analysts and the result was given in the form of RSD%.

Assay of standard formulation of lynparza (olaparib)

Twenty tablets were weighed and crushed to powder. A quantity of this powder equivalent to 50 mg was taken in a 50 mL volumetric flask to which 25 mL diluent was added. The solution was sonicated for 30 min, and the volume was adjusted up to the mark with diluent. The solution was further diluted to obtain a concentration of 100 µg/mL of olaparib. Before the filling the vials for chromatographic analysis, the solution was passed through a 0.45 µ membrane filter.

System suitability

System suitability parameters such as tailing factor, resolution, theoretical plates, and percent RSD were assessed by injecting a blank observed by six replicates of the olaparib standard as well as sample solutions at a concentration of 100 µg/mL.

Limit of detection (LOD) and limit of quantification (LOQ)

LOD and LOQ were calculated from the calibration according to the formulas mentioned;

LOD = 3.3 SD/Slope

LOQ = 10 SD/Slope

or detection limit= 3.3 σ/s, quantification limit= 10 σ/s, where σ is the standard deviation of *y*- intercept of the regression line, and s is the slope of the calibration curve.

Solution stability

The stability of the analytical solution was established by injecting the standard solution at a periodic interval of 48 h by maintaining the temperature of the auto sampler at room temperature. The solution response was measured and the percentage differences in the peak area have been calculated.

Force degradation study

According to the ICH guideline Q1A (R2), a force degradation study of olaparib was conducted under stress conditions. The olaparib active pharmaceutical ingredient (100 µg/mL) was subjected to hydrolysis (acid and alkali), peroxide, thermal, and photolytic degradation for the stability study.

Acid degradation

A standard solution of 5 mL olaparib was taken in a 50 mL clean and dry volumetric flask. To the volumetric flask, 2.5 mL of 5 M HCl was added and kept for 30 min. After the completion of 30 min, neutralize the solution was with 2.5 mL of 5 M NaOH and the 50 mL volume was made by the mobile phase. Finally, filtering the solution was done with a 0.45 µm filter. The filtered solution was introduced into HPLC and the peak area was compared with the standard chromatogram.

Alkali degradation

A standard solution of 5 mL olaparib was taken in a 50 mL clean and dry volumetric flask. To the volumetric flask, 2.5 mL of 5 M NaOH was added and kept for 30 min. After 30 min, the solution was neutralized with 2.5 mL of 5 M HCl, and the mobile phase was responsible for 50 mL volume. Finally, the prepared solution was filtered with a 0.45 µm filter. The filtered solution was introduced into HPLC and the peak area was compared with the standard chromatogram.

Peroxide degradation

A standard solution of 1.0 mL olaparib was taken in a 10 mL clean and dry volumetric flask. To the volumetric flask, 1 mL of 30% H_2O_2 was added and kept in the flask for 30 min. After the completion of the 30 min, a volume of 10 mL was made by the mobile phase. Finally, the prepared solution was filtered with a 0.45 µm filter. The filtered solution was then introduced into HPLC and the peak area was compared with the standard chromatogram.

Thermal degradation

The powdered sample of olaparib was spread on a petri dish with 1.0 mm thickness and kept at 70°C in a hot air oven for 3 h. 25 mg of the sample was taken in a 25 mL clean and dry

volumetric flask. 10 mL solution was pipette out and the volume of 100 mL was made by the mobile phase. Finally, the prepared solution was filtered with a 0.45 µm filter. The filtered solution was introduced into HPLC and the peak area was compared with the standard chromatogram.

Photolytic degradation

The powdered sample of olaparib was spread on a petri dish 1.0 mm thickness and kept in direct sunlight for 3 h. 25 mg of the sample was taken in a 25 mL clean and dry volumetric flask. 10 mL solution was pipette out and the volume of 100 mL was made by the mobile phase. Finally, the prepared solution was filtered with a 0.45 µm filter. The filtered solution was introduced into HPLC and the peak area was compared with the standard chromatogram.

Statistical analysis

Statistical data were not used during the experiments.

RESULTS

Method development

Chromatographic separation

Various chromatographic systems (RP-HPLC) were considered to optimize the separation of olaparib. Olaparib separation was performed on the column C18 (150 mm x 4.6 mm, 5 µm). The mobile phase was a combination that included 500 mL methanol, 500 mL buffer, and 1.0 mL of glacial acetic acid, pH adjusted to 3.5 ± 0.05 with ammonium acetate. The flow rate was set to 1.0 mL/min and the detector was set to 254 nm. The injection volume was kept at 20 µL. The retention time for olaparib was found to be 4.32 min as shown in Figure 2.

Calibration curve

The calibration curve was prepared and evaluated using the least square method within the Microsoft Excel® program. The coefficient of determination (R^2), slope and intercept for olaparib were 0.998, 23599, and 66731, respectively. The linear equation was found to be $y = 23599x + 66731$ and the calibration curve is shown in Figure 2.

Validation of the method

Linearity

The analytical calibration curve was plotted for olaparib and was found to be linear in the specified ranges (80-120 µg/mL) indicating a correlation coefficient R^2 of 0.99 (acceptance limit >0.98). The slope of the straight line was found to be 23599 and the intercept was found to be 66731. The results are reported in Table 1 and the calibration curve is shown in Figure 2.

Precision and intermediate precision

The precision value was reported in terms of RSD%. The RSD% for olaparib was found to be <2.0% for both inter- and intra-day precision, indicating satisfactory precision (Table 2). The inter-day precision was found to be within 0.05-0.98, whereas intra-day precision was found to be within 0.06-0.43.

Accuracy

The accuracy of this method is determined by a recovery study conducted using standard addition methods at six concentration levels, first 90%, 100%, and 110%. The spiked sample solutions were assayed in triplicate and the obtained results were compared with the expected results and expressed as the

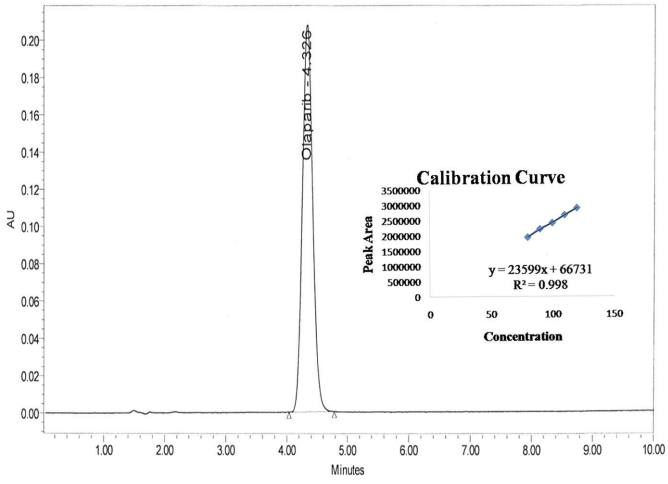

Figure 2. HPLC chromatogram of olaparib at 254 nm. Inset: Calibration curve of olaparib

HPLC: High performance liquid chromatography

Table 1. Linear regression equation generated from validation of olaparib: Slope, intercept, and coefficient of determination

Concentration (mg/mL)	Concentration (µg/mL)	Peak Area 1	Peak area 2	Peak area 3	Average Area
0.080	80	1938729	1945764	1942428	1942307
0.090	90	2215489	2215608	2210027	2213708
0.100	100	2413316	2411985	2415423	2413575
0.110	110	2671899	2672202	2663858	2669319.600
0.120	120	2894206	2891855	2897362	2894474.300
Slope	-	-	-	-	23599
Intercept	-	-	-	-	66731
R^2 (correlation)	(Coefficient)	-	-	-	0.998

percentage of recovery reported in Table 3. The recovery was found to be within the limit.

Specificity

The developed analytical method should reflect that there was no interference due to the presence of excipients in the formulation. The recovery and RSD% of olaparib were measured and were within the limits summarized in Table 4. The recovery was found to be 100.81-101.71 and RSD% was within 0.10-0.80.

Robustness

The method was found to be robust, ensuring that upon applying small variations to the chromatographic conditions in terms of flow rate, mobile phase composition, and pH variation in the mobile phase, no significant changes are detected. The robustness data were expressed in terms of RSD% was found to be 0.68 and is given in Table 5.

Ruggedness

Analyst 1 and analyst 2 performed the ruggedness test and the results are summarized in Table 6 as RSD% was found to be 1.48.

Table 2a. Intra-day precision

Concentration (µg/mL)	Peak area	Concentration found (µg/mL)	Average	SD	RSD%
80	1942307	79.477	79.475	0.149	0.187
80	1945764	79.623	-	-	-
80	1938729	79.325	-	-	-
100	2475997	102.092	101.585	0.440	0.433
100	2458935	101.369	-	-	-
100	2457207	101.296	-	-	-
120	2894210	119.813	119.862	0.073	0.061
120	2894544	119.828	-	-	-
120	2897362	119.947	-	-	-

SD: Standard deviation (n: 3), RSD: Relative standard deviation

Table 2b. Inter-day precision

Concentration (µg/mL)	Peak area	Concentration found (µg/mL)	Average	SD	RSD%
80	1939789	79.370	79.417	0.043	0.054
80	1941781	79.455	-	-	-
80	1941161	79.428	-	-	-
100	2442327	100.665	101.802	1.005	0.986
100	2487270	102.569	-	-	-
100	2477898	102.172	-	-	-
120	2894277	119.816	119.868	0.157	0.131
120	2892563	119.743	-	-	-
120	2899665	120.044	-	-	-

SD: Standard deviation (n: 3), RSD: Relative standard deviation

Table 2c. Repeatability

Concentration (µg/mL)	Peak area	Concentration found (µg/mL)	Average	SD	RSD%
100	2443258	100.704	100.959	0.250	0.248
100	2448178	100.913	-	-	-
100	2446070	100.824	-	-	-
100	2444889	100.774	-	-	-
100	2457432	101.305	-	-	-
100	2455724	101.232	-	-	-

SD: Standard deviation, RSD: Relative standard deviation

System suitability

The system suitability test is an important element of chromatographic analysis since it ensures that the chromatographic system's accuracy and repeatability are sufficient for analysis. It was performed with six replicate injections of the standard solution of olaparib. The retaining of olaparib was found to be 4.32 min, having a tailing factor of not more than 1.17 in all peaks, indicating good peak symmetry. Theoretical plates were found to be 3160. The results are reported in Table 7.

Detection limit and quantification limit

The LOD and LOQ of olaparib were found to be 0.49 µg/mL and 1.49 µg/mL, respectively.

Assay of standard formulation of lynparza (olaparib)

Assay validation provides reliability assurance during normal use, and is sometimes referred to as "the process of providing documented evidence that the method is doing what it intends to do". The purity by HPLC is determined by the percentage recovery of olaparib. The developed method was very accurate, precise and robust as recovery percentage was within 100±2 given in Figure 3a and Table 8.

Analytical solution stability

The olaparib sample solution was stable for 24 h at room temperature. The stability results were analyzed for the percentage difference from zero time injection, where there was no decrease in the peak areas of the drug nor a shifting of retention time was detected. The observations obtained from the stability phenomenon are reported in Table 9.

Force degradation study

The drug degradation study was conducted in acid, alkaline, and oxidation solutions to determine the stability of the drug under different conditions.

Acid degradation

The acid degradation of olaparib was carried out at different concentrations of (1-5 M) HCl until it was degraded for a period of 30 min. The degraded chromatogram and the non-degraded chromatogram were compared and the percentage of degradation was calculated. The chromatogram is given in (Figure 3b) and the results are summarized in Table 10. Acid degradation was found to be 12.69% for 5 M HCl.

Table 3. Accuracy observation table

Recovery level	API added (mg)	API recovered (mg)	Recovery%	Average recovery%	RSD%
90%	-	22.110	98.680	-	-
90%	24.900	22.100	98.610	98.650	0.230
90%	-	22.500	100.390	-	-
100%	-	24.720	99.290	-	-
100%	24.900	24.920	100.070	99.680	0.140
100%	-	25.060	100.000	-	-
110%	-	26.920	98.300	-	-
110%	24.900	26.900	98.220	98.260	0.050
110%	-	26.870	98.110	-	-

RSD: Relative standard deviation, API: Active pharmaceutical ingredient

Table 4. Specificity table of olaparib

Analyte	Added%	Excipient amount added (mg)	Concentration found (µg/mL)	Recovery%	Average recovery%	SD	RSD%
Olaparib	50	5	100.705	100.705	100.814	0.105	0.104
(10 mg)	50	5	100.913	100.913	-	-	-
	50	5	100.824	100.824	-	-	-
	100	10	100.774	100.774	100.915	0.342	0.340
	100	10	101.305	101.305	-	-	-
	100	10	100.665	100.665	-	-	-
	150	15	102.569	102.57	101.710	0.892	0.877
	150	15	100.789	100.789	-	-	-
	150	15	101.773	101.774	-	-	-

SD: Standard deviation, RSD: Relative standard deviation

Alkali degradation

The alkali degradation of olaparib was carried out at different concentrations of (1-5 M) NaOH until it was degraded. The degraded chromatogram and the non-degraded chromatogram were compared and the percentage of degradation was calculated. The chromatogram is given in Figure 4a and the results are summarized in Table 9. Alkali degradation was found to be 2.60% at 5 M NaOH.

Peroxide degradation

Peroxide degradation of olaparib was carried out at a concentration of 30%. A comparative study of the peroxide degraded olaparib chromatogram and the non-degraded chromatogram was conducted to calculate the 2.55% degradation. The chromatogram is given in Figure 4b and the results are summarized in Table 10.

Thermal degradation

Thermal degradation of the drug was found to be negligible. The olaparib drug was found to be thermal stable as there was no degradation when exposed to thermal conditions. The chromatogram is given in Figure 5a, and the results are summarized in Table 10.

Photolytic degradation

Degradation by photolysis of olaparib was found to be negligible. The olaparib drug was found to be light stable as there was no degradation when exposed to light. The chromatogram is given in (Figure 5b) and the results are summarized in Table 10.

DISCUSSION

Olaparib is a new drug, so almost no method is available to estimate olaparib in bulk and pharmaceutical dosage form. Therefore, our present aim was to develop a new, compatible, stable, robust method for the determination of olaparib in bulk and formulations by RP-HPLC.

According to the ICH guidelines, the developed method was validated for the following parameters: system suitability, linearity, accuracy, precision, robustness, and analytical

Table 5. Robustness study with flow rate, pH, and mobile phase composition

Sample ID	Analytical condition	Olaparib input (mg)	Olaparib recovery (mg)	Olaparib recovery (%)	Mean recovery olaparib (%)	SD	RSD%
1	Flow rate: 1.1 mL/min Mobile phase pH: 3.5 Mobile phase ratio: 50:50 Column: C18 (150 mm x 4.6 mm, 5 µm)	25	24.860	99.500	100.060	0.680	0.680
2	Flow rate: 0.9 mL/min Mobile phase pH: 3.5 Mobile phase ratio: 50:50 Column: C18 (150 mm x 4.6 mm, 5 µm)	25	25.090	100.300			
3	Flow rate: 1 mL/min Mobile phase pH: 3.6 Mobile phase ratio: 50:50 Column: C18 (150 mm x 4.6 mm, 5 µm)	25	24.820	99.200			
4	Flow rate: 1 mL/min Mobile phase pH: 3.4 Mobile phase ratio: 50:50 Column: C18 (150 mm x 4.6 mm, 5 µm)	25	25.110	100.400			
5	Flow rate: 1 mL/min Mobile phase pH: 3.5 Mobile phase ratio: 55:45 Column: C18 (150 mm x 4.6 mm, 5 µm)	25	24.980	99.900			
6	Flow rate: 1 mL/min Mobile phase pH: 3.5 Mobile phase ratio: 45:55 Column: C18 (150 mm x 4.6 mm, 5 µm)	25	25.290	101.100			

solution stability. The RSD% value was well below 2 and the percentage recovery was within the limit of 100±2. The stability of the drugs is a immense issue during formulation and still no stability data have been reported. To determine the stability of olaparib, we conducted a force degradation study.

The drug was found to be very stable, when exposed to heat and light. It was also found to be quite stable under both acidic and basic conditions. Higher concentrations of acids and bases (5 M) could degrade the drug, too, by 12.69% under acidic conditions, whereas in the case of basic and oxidation

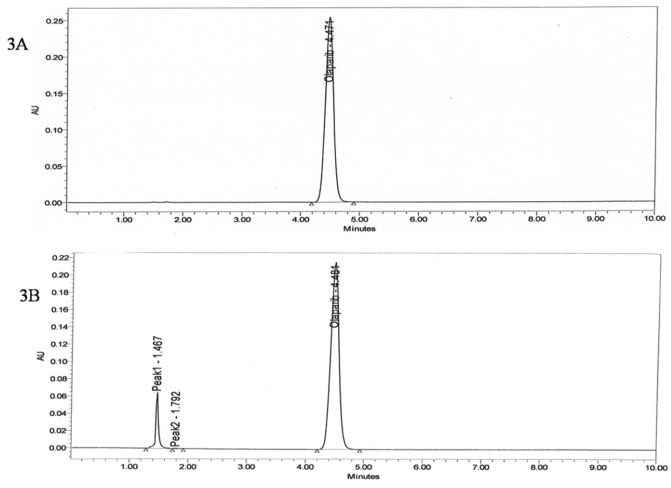

Figure 3. A) Chromatogram showing assay of standard formulation, B) Chromatogram of acid-degraded olaparib

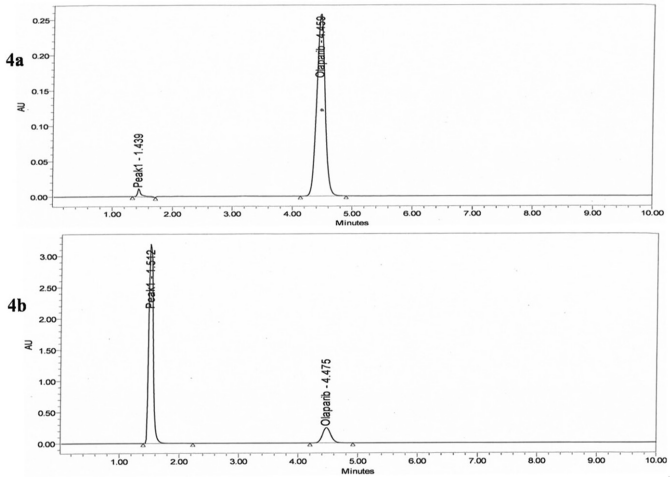

Figure 4. a) Chromatogram of base degraded olaparib, b) Chromatogram of hydrogen peroxide degraded olaparib

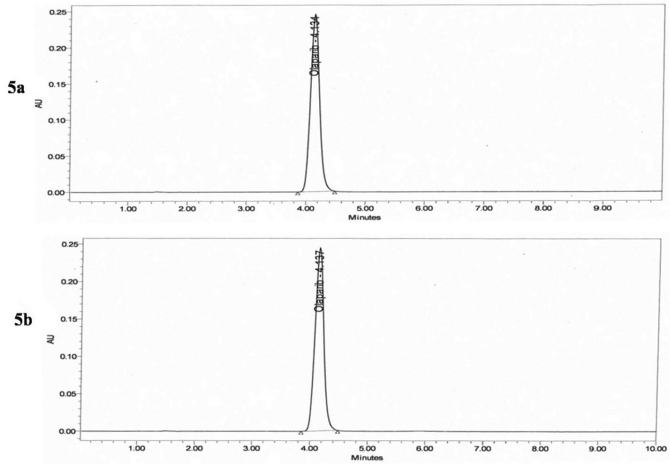

Figure 5. a) Chromatogram of thermal degraded olaparib, b) Chromatogram of photolytic degraded olaparib

Table 6. Ruggedness of olaparib

S. no.	Analyst 1 (assay%)	Assay percent olaparib	Analyst 2 (assay%)
1	99.390		100.560
2	100.210		99.640
3	98.040		99.800
4	102.690		100.410
5	99.980		100.200
6	101.560		97.100
Mean	100.480		99.620
RSD% Overall percentage RSD	1.660	1.480	1.290

RSD: Relative standard deviation

Table 7. System suitability parameters and achieved values parameters

Values achieved in the validation phenomenon	
Theoretical plates	3160
Retention time	4.32 minutes
Asymmetry	1.170
RSD	0.240%

RSD: Relative standard deviation

Table 8. Summery of validation

Parameter	Acceptable limit	Remark
Accuracy	98.260-99.680	Passed
Specificity	0.100-0.800	Passed
Precision	0.056-0.980	Passed
Linearity	0.998	Passed
Ruggedness and Robustness	1.480 and 0.680	Passed
Assay	98.680%	Passed

Table 9. Solution stability data

Time	Inject	Time	Difference (sec)	Area	Calculation
Initial	9	2	0	2442536	0.00
After 1 h	10	9	67	2450664	0.00
After 24 h	10	5	1436	2473824	-0.01

Table 10. Force degradation data

Type of degradation	Area	Degradation%	Peak purity
No degradation (standard chromatogram 100 µg/mL)	2443258	-	Passed
2.5 mL of 5 M HCl (acidic)	2133134.666	12.690	Passed
2.5 mL 5 M NaOH (alkaline)	2507018.666	2.600	Passed
1 mL of 30% H_2O_2 (peroxide)	2380875	2.550	Passed
Thermal degradation	2443258	0	Passed
Photolytic degradation	2443258	0	Passed

conditions, degradation was found to be 2.60% and 2.55%. Under thermal and photolytic conditions, they were found to be stable.

CONCLUSION

The developed method in RP-HPLC was established to be simple, cost-effective, accurate, and robust; so that, it can be extensively applied for estimating any formulations of olaparib. This degradation study was conducted on HPLC for the first time. As the HPLC method is less cost-effective compared with the LC-MS method, this will prove an effective method for estimating olaparib.

Degradation studies were conducted and from the study we can conclude that the degradation of olaparib was very low in the case of basic and oxidation conditions, whereas in the case of acidic degradation by HCl, the highest degradation was observed. The degradation was found to be 12.69%. No degradations were found in the case of thermal and photolytic conditions. The drug olaparib can be considered a very stable drug in all conditions except the acidic condition.

ACKNOWLEDGMENTS

The authors are grateful to the Department of Delhi Pharmaceutical Sciences and Research University, New Delhi (India) for providing the facilities for working and to the laboratory assistance.

Ethics

Ethics Committee Approval: Not applicable.

Informed Consent: Not applicable.

Peer-review: Externally peer-reviewed.

Authorship Contributions

Concept: A.C., R.T., Design: A.C., R.T., S.D., Data Collection or Processing: A.C., P.D., Analysis or Interpretation: M.G., S.D., A.C., P.D., Literature Search: A.C., P.D., Writing: M.G., S.D., A.C., P.D.

Conflict of Interest: No conflict of interest was declared by the authors.

Financial Disclosure: The authors declared that this study received no financial support.

REFERENCES

1. Dizdar O, Arslan C, Altundag K. Advances in PARP inhibitors for the treatment of breast cancer. Expert Opin Pharmacother. 2015;16:2751-2758.
2. Ferraris DV. Evolution of poly(ADP-ribose) polymerase-1 (PARP-1) inhibitors. From concept to clinic. J Med Chem. 2010;53:4561-4584.
3. Lupo B, Trusolino L. Inhibition of poly(ADP-ribosyl)ation in cancer: old and new paradigms revisited. Biochim Biophys Acta. 2014;1846:201-215.
4. Schreiber V, Dantzer F, Ame JC, de Murcia G. Poly(ADP-ribose): novel functions for an old molecule. Nat Rev Mol Cell Biol. 2006;7:517-528.
5. Brown JS, Kaye SB, Yap TA. PARP inhibitors: the race is on. Br J Cancer. 2016;114:713-715.
6. Murai J, Huang SY, Das BB, Renaud A, Zhang Y, Doroshow JH, Ji J, Takeda S, Pommier Y. Trapping of PARP1 and PARP2 by clinical PARP inhibitors. Cancer Res. 2012;72:5588-5599.
7. Tangutoori S, Baldwin P, Sridhar S. PARP inhibitors: a new era of targeted therapy. Maturitas. 2015;81:5-9.
8. Murata S, Zhang C, Finch N, Zhang K, Campo L, Breuer EK. Predictors and modulators of synthetic lethality: an update on PARP inhibitors and personalized medicine. Biomed Res Int. 2016;2016:2346585.
9. Deeks ED. Olaparib: first global approval. Drugs. 2015;75:231-240.
10. O'Connor MJ. Targeting the DNA damage response in cancer. Mol Cell. 2015;60:547-560.
11. Dollery CT. Intracellular drug concentrations. Clin Pharmacol Ther. 2013;93:263-266.
12. Fojo T, Bates S. Mechanisms of resistance to PARP inhibitors-three and counting. Cancer Discov. 2013;3:20-23.
13. Lord CJ, Ashworth A. Mechanisms of resistance to therapies targeting BRCA-mutant cancers. Nat Med. 2013;19:1381-1388.
14. Dufour R, Daumar P, Mounetou E, Aubel C, Kwiatkowski F, Abrial C, Vatoux C, Penault-Llorca F, Bamdad M. BCRP and *P*-gp relay overexpression in triple negative basal-like breast cancer cell line: a prospective role in resistance to olaparib. Sci Rep. 2015;5:12670.
15. Aoki D, Chiyoda T. PARP inhibitors and quality of life in ovarian cancer. Lancet Oncol. 2018;19:1012-1014.
16. Weil MK, Chen AP. PARP inhibitor treatment in ovarian and breast cancer. Curr Probl Cancer. 2011;35:7-50.
17. Faraoni I, Aloisio F, De Gabrieli A, Consalvo MI, Lavorgna S, Voso MT, Lo-Coco F, Graziani G. The poly(ADP-ribose) polymerase inhibitor olaparib induces up-regulation of death receptors in primary acute myeloid leukemia blasts by NF-κB activation. Cancer Lett. 2018;423:127-138.

18. Liu CH, Chang Y, Wang PH. Poly(ADP-ribose) polymerase (PARP) inhibitors and ovarian cancer. Taiwan J Obstet Gynecol. 2017;56:713-714.

19. Nijenhuis CM, Lucas L, Rosing H, Schellens JH, Beijnen JH. Development and validation of a high-performance liquid chromatography-tandem mass spectrometry assay quantifying olaparib in human plasma. J Chromatogr B Analyt Technol Biomed Life Sci. 2013;940:121-125.

20. Daumar P, Dufour R, Dubois C, Penault-Llorca F, Bamdad M, Mounetou E. Development and validation of a high-performance liquid chromatography method for the quantitation of intracellular PARP inhibitor olaparib in cancer cells. J Pharm Biomed Anal. 2018;152:74-80.

21. Roth J, Peer CJ, Mannargudi B, Swaisland H, Lee JM, Kohn EC, Figg WD. A sensitive and robust ultra HPLC assay with tandem mass spectrometric detection for the quantitation of the PARP inhibitor olaparib (AZD2281) in human plasma for pharmacokinetic application. Chromatography. 2014;1:82-95.

22. Nijenhuis CM, Rosing H, Schellens JH, Beijnen JH. Development and validation of a high-performance liquid chromatography-tandem mass spectrometry assay quantifying vemurafenib in human plasma. J Pharm Biomed Anal. 2014;88:630-635.

Turk J Pharm Sci 2022;19(5):498-504
DOI: 10.4274/tjps.galenos.2021.97572

ORIGINAL ARTICLE

Investigation of Selected Medicinal Plants for Their Anti-Obesity Properties

Sıla Özlem ŞENER[1]*, Eylül CILIZ[2], Berre Nur ÖZTEKİN[2], Merve BADEM[3], Ufuk ÖZGEN[2]

[1]University of Health Sciences Türkiye, Gülhane Faculty of Pharmacy, Department of Pharmacognosy, Ankara, Türkiye
[2]Karadeniz Technical University, Faculty of Pharmacy, Department of Pharmacognosy, Trabzon, Türkiye
[3]Karadeniz Technical University, Faculty of Pharmacy, Department of Biochemistry, Trabzon, Türkiye

ABSTRACT

Objectives: Obesity, which is a risk factor for diabetes, hypertension, cardiovascular diseases, and cancer, is caused serious health problems and economic costs on a global scale. Nowadays, pancreatic lipase inhibitors that cause inhibition of lipid digestion and lipid absorption are one of the limited treatment approaches for obesity. Plant-derived secondary metabolites can be used for treating obesity. The aim of this study was to research the antiobesity potential of *Amaranthus albus* L. (Amaranthaceae), *Helichrysum compactum* Boiss. (Asteraceae), *Chenopodium album* L. (Chenopodiaceae), and *Agrimonia eupatoria* L. (Rosaceae).

Materials and Methods: To detect the antiobesity potentials of the plants, *in vitro* lipase inhibitory activity studies by spectroscopic method and quantitative analysis studies of some anti-obesity effective secondary metabolites by reversed-phase high performance liquid chromatography (RP-HPLC) technique were carried out.

Results: *In vitro* lipase inhibitory studies showed that all plant extracts possess lipase inhibitory effect, and the highest lipase inhibitory potential was observed for *H. compactum* (IC_{50}: 45.70 µg/mL ± 2.3618). According to HPLC analyses, *p*-coumaric acid (0.27 mg/g) in *A. albus*; benzoic acid (0.33 mg/g) in *C. album*; vanillic acid (7.32 mg/g), syringaldehyde (14.97 mg/g), quercetin (4.66 mg/g), *p*-coumaric acid (0.71 mg/g), and benzoic acid (3.43 mg/g) in *H. compactum*; *p*-coumaric acid (0.71 mg/g) and benzoic acid (3.43 mg/g) in *A. eupatoria* were detected.

Conclusion: In conclusion, *H. compactum* is the most remarkable natural source for the study. The fact remains that all plants may be promising candidates for treating obesity.

Key words: *Agrimonia eupatoria*, *Amaranthus albus*, *Chenopodium album*, *Helichrysum compactum*, obesity

INTRODUCTION

Obesity is expressed as abnormal or excessive fat accumulation resulting from the imbalance between energy intake and consumption.[1-3] Obesity is directly related to coronary artery diseases, cerebrovascular diseases, hypertension, hyperlipidemia, diabetes, pulmonary embolism, sleep apnea, gynecological abnormalities, osteoarthritis, psychiatric diseases, and many cancers.[4-9] It also causes high economic expenses globally.[10] Some medicinal treatment approaches have been developed to treat and prevent obesity except for classical approaches like decreasing diet calories and increasing physical activity.[11,12] Inhibition of adipocyte differentiation, stimulation of energy consumption, suppression of the *FAS* gene, lipase enzyme inhibition, appetite suppression, and anti-inflammatory approach can be given as examples of these medicinal approaches.[13]

Pancreatic lipase (PL) is a 449 amino acid single chain glycoprotein. 90% of dietary fat consist of triglycerides (TG) and must be hydrolyzed in order to be absorbed. PL converts 50-70% TGs into fatty acids (FA) and monoglycerides (MG). MGs released by lipid hydrolysis and free FA are absorbed by adipose tissue to form mixed micelles with bile salts, cholesterol, and lysophosphatidic acid.[14] PL inhibition, one of the therapeutic approaches for prevention and treatment of obesity, creates an antiobesity effect through decreasing intestinal lipid absorption.[15]

Natural products have become popular for development of safe and effective antiobesity drugs.[9] Herbal sources included

*Correspondence: silaozlem.sener@sbu.edu.tr, Phone: +90 506 394 58 87, ORCID-ID: orcid.org/0000-0001-7679-7165
Received: 27.07.2021, Accepted: 19.10.2021

effective secondary metabolites like benzoic acid, vanillic acid, syringaldehyde, *p*-coumaric acid, sinapic acid, and quercetin, have therapeutic potential for treating obesity.[16] It has been proven that the consumption of some plant-based foods with phenolic content is associated with the prevention of obesity.

The traditional use of all species for many years, their phenolic content potential, and their obesity-related effects like antioxidant and anti-inflammatory have guided the study. The purpose of this article is to investigate the antiobesity effect of *Amaranthus albus* L. (Amaranthaceae), *Helichrysum compactum* Boiss. (Asteraceae), *Chenopodium album* L. (Chenopodiaceae), and *Agrimonia eupatoria* L. (Rosaceae) through *in vitro* lipase inhibitory effect and quantitative high performance liquid chromatography (HPLC) analysis studies.

MATERIALS AND METHODS

Plant materials and preparation of extracts

Identification of *A. albus*, *H. compactum*, *C. album*, and *A. eupatoria* were carried out by Prof. Dr. Ufuk Özgen and Asst. Prof. Dr. Merve Badem. Herbarium samples of *A. albus* (1145 m, Kürekçili village, Akkuş, Ordu, AEF 26904), *H. compactum* (1190 m, Ormancık village, Akkuş, Ordu, AEF 26823), *C. album* (1145 m, Kürekçili village, Akkuş, Ordu, AEF 26902), and *A. eupatoria* (1290 m, Karaçal village, Akkuş, Ordu, AEF 26905) were deposited in the Herbarium of the Faculty of Pharmacy of Ankara University.

The aerial parts of the species *A. albus, H. compactum, C. album,* and *A. eupatoria* were powdered to prepare the methanol extracts. The powdered plant materials (~ 200 g) were extracted with ~ 500 mL methanol in a 30°C shaker incubator for 24 h and then filtered. After this process was repeated thrice, the filtrates were combined and evaporated to dryness.

Lipase enzyme inhibition

Dried methanolic extracts of the aerial parts of *A. albus, H. compactum, C. album,* and *A. eupatoria* were diluted with buffer solution (0.1 M Tris-HCl buffer, pH: 8.0) with final concentrations to be 12.5, 25, 50, 100, and 200 µg/mL in microplates. The levels of lipase inhibition were determined using a substrate *p*-nitrophenylbutyrate (*p*-NPB) (CAS: 2635-84-9). Basic principle of the method is based on determining the absorbance of *p*-nitrophenol using the spectroscopic method. *p*-Nitrophenol has a yellow color, which is formed because of the interaction of *p*-NPB with the lipase enzyme.[17] Orlistat was used as a positive control. Orlistat was diluted with buffer solution (0.1 M tris-HCl buffer, pH: 8.0) to be 6.25, 12.5, 25, 50, and 100 µg/mL final concentrations in the microplate. Absorbance measurements of the samples were carried out by a spectrophotometer (SPECTROstar Nano-BMG LABTECH).

The experimental procedure is designed by coding microplates A, B, C, and D. Microplates are designed with these ingredients: A, 90 µL enzyme solution [crudeporcine PL type II (Sigma, EC 3.1.1.3) - (200 units/mL)], 5 µL substrate solution (10 mM *p*-NPB acetonitrile solution); 5 µL buffer solution (0.1 M tris-HCl buffer, pH: 8.0); B, 90 µL enzyme solution [(crudeporcine PL type II (Sigma, EC 3.1.1.3) - (200 units/mL)], 10 µL buffer solution (0.1 M tris-HCl buffer, pH: 8.0); C, 90 µL enzyme solution [crudeporcine PL type II (Sigma, EC 3.1.1.3) - (200 units/mL)], 5 µL sample solution, 5 µL substrate solution (10 mM *p*-NPB acetonitrile solution); D, 90 µL enzyme solution [crudeporcine PL type II (Sigma, EC 3.1.1.3) - (200 units/mL)], 5 µL sample solution, 5 µL buffer solution (0.1 M tris-HCl buffer pH: 8.0). Before the substrate solutions were added to the wells containing substrate solutions, each microplate was incubated at 37°C for 15 min in the incubator (Memmert), after which the substrate solutions were added to the relevant wells, and each microplate was subjected to incubation again at 37°C for 15 min. Absorbance of samples was measured at 405 nm wavelength. Each sample was performed triple.

Lipase enzyme inhibition values were calculated with the absorbance values of A, B, C, and D using the formula. The formula is given below.

% Pancreatic lipase inhibition= [[(A-B)-(C-D)]/(A-B)]*100

The chart was constituted with percentage enzyme inhibition values determined at the end of the experiment and the logarithm of the concentration (ordinate and absis). Then, the inhibitor concentration 50 (IC_{50}) values of the samples that cause 50% inhibition of the lipase enzyme were determined from the chart equation.

Statistical analysis

Three repetitions of each experiment were carried out. The results were reported as mean ± standard deviation. The Kolmogorov-Smirnov test was used to determine compatibility with the normal distribution. The analysis of Kruskal-Wallis and Mann-Whitney *U* tests were employed to compare variations between the groups. Statistical significance level was considered $p<0.05$.

HPLC analysis

HPLC (Shimadzu Corporation, LC 20AT, Kyoto, Japan) device was used in the analysis, containing a Zorbax C18 (150 x 4.6 mm, 5 µm) column.

The prepared sample solutions were dragged 3 times under the analysis conditions stated below. HPLC chromatograms prepared from sample solutions were compared with the retention times of 7 different phenolic compounds. Initially, qualitative definitions were realized with the detector signals. For the quantitative analysis of 7 different compounds in the sample solutions, during the validation studies of HPLC method, 5, 10, 25, 50, and 100 µg/mL standard mixture solutions were dragged five times under the specified HPLC analysis conditions, and then the calibration curve obtained from the peak areas and relevant concentrations were used. *p*-Hydroxybenzoic acid, vanillic acid, syringaldehyde, *p*-coumaric acid, sinapic acid, benzoic acid, and quercetin were analyzed by the HPLC method with validated analysis conditions. To separate these 7 compounds in the column, various preliminary trials were made, the appropriate gradient program was determined,

and the method was validated. It has been observed that the compounds are separated by high resolution.[6,18]

Preparation of sample

HPLC-grade methanol was added to the dry methanol extracts of the species at a final concentration of 10 mg/mL, and the solutions were transferred to HPLC vials, after being filtered through 0.45 µm membrane filters.

HPLC analysis conditions

HPLC analysis was performed using the validated method.[6,18] The flow rate is 1.5 mL/min, and the injection volume is 20 µL. For analysis, solvent systems of A solution: 100% methanol and B solution: 2% acetic acid: water (pH 2.65) were used. The gradient elution program was applied 0-3 minutes 20:80 (solution A: solution B); 4-6 minutes 30:70 (solution A: solution B); 7-9 minutes 40:60 (solution A: solution B); 10-11 minutes 45:55 (solution A: solution B); 12-13 minutes 50:50 (solution A: solution B); 14-15 minutes 60:40 (A solution: B solution) and 16 min 80:20 (A solution: B solution). Measurements were carried out at wavelengths of 200, 210, 220, 230, 240, 250, 260, 270, 280, and 320 nm.

RESULTS

Results of lipase inhibition

After *in vitro* lipase enzyme inhibition studies, IC_{50} level of orlistat was used as positive control, and dry methanolic extracts prepared from *A. albus*, *C. album*, *H. compactum*, and *A. eupatoria* species were determined on lipase. It was determined that the graph created as the logarithm of percent enzyme inhibition values of orlistat and species the concentration it belongs to was linear (Figure 1). IC_{50} value of orlistat was determined as 8.05 ± 0.8615 µg/mL.

The percentage lipase inhibition levels at different concentrations of the methanol extract prepared from *A. albus*, *C. album*, *H. compactum*, and *A. eupatoria* species are expressed in Figure 2.

IC_{50} values of methanol extracts prepared from *A. albus*, *C. album*, *H. compactum*, and *A. eupatoria* species were determined as 106.02 ± 4.5125, 177.82 ± 8.6325, 45.70 ± 2.3618, and 94.18 ± 5.2569 µg/mL, respectively.

Results of HPLC analysis

The phenolic compounds and benzoic contents in the extracts of screened species were expressed as mg/g extract (Table 1). Chromatographic results of the extracts were presented in addition (Figure 3).

DISCUSSION

Obesity is expressed as abnormal or excess fat accumulation resulting from the imbalance between energy intake and consumption.[1-3] Obesity is directly related to coronary artery disease, cerebrovascular disease, hypertension,

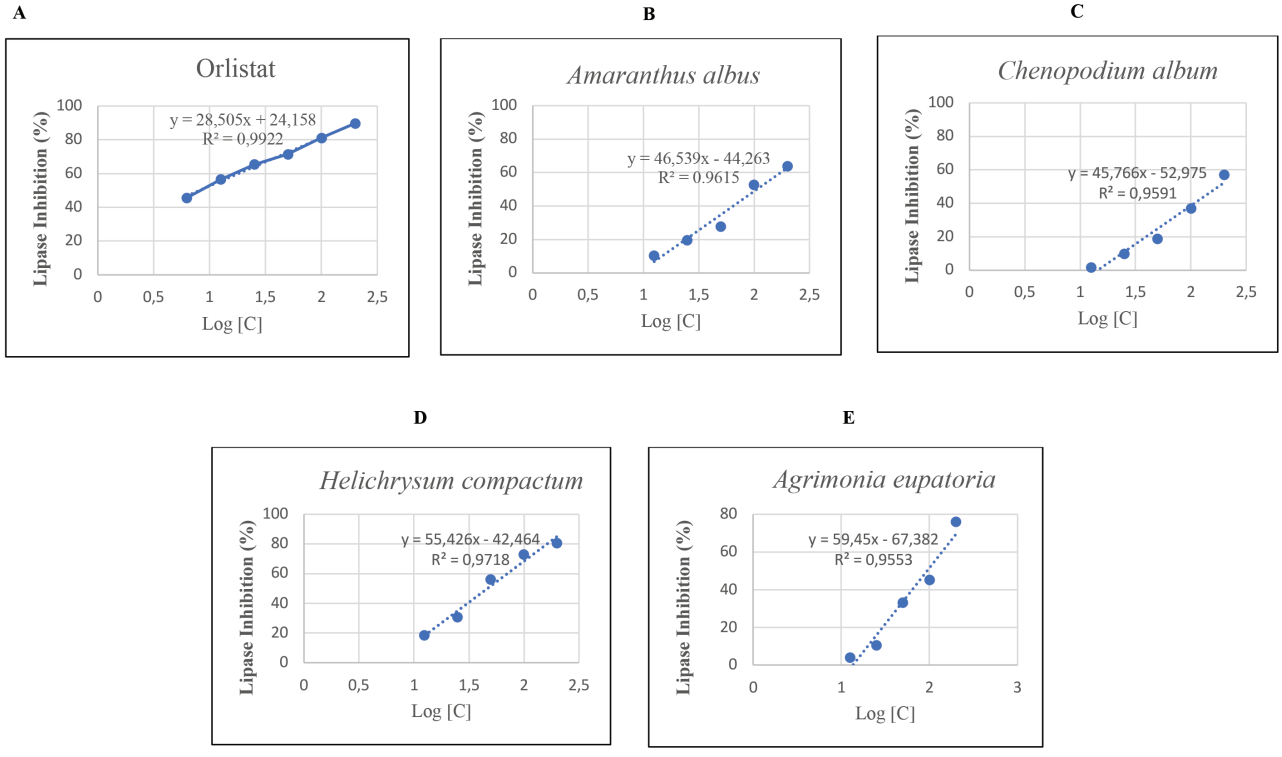

Figure 1. The graph created in the form of lipase inhibition (%) values of orlistat and the logarithm of the concentration it belongs to (A), the graph created in the form of lipase inhibition (%) values of *Amaranthus albus* and the logarithm of the concentration it belongs to (B), the graph created in the form of lipase inhibition (%) values of *Chenopodium album* and the logarithm of the concentration it belongs to (C), the graph created in the form of lipase inhibition (%) values of *Helichrysum compactum* and the logarithm of the concentration it belongs to (D), the graph created in the form of lipase inhibition (%) values of *Agrimonia eupatoria* and the logarithm of the concentration it belongs to (E)

hyperlipidemia, diabetes, pulmonary embolism, sleep apnea, gynecological abnormalities, osteoarthritis, psychiatric diseases, and many cancer diseases.[4-9] Obesity also causes high economic expenses in Türkiye as worldwide. So, the reduction of obesity is important for the economic burden related to obesity.[10]

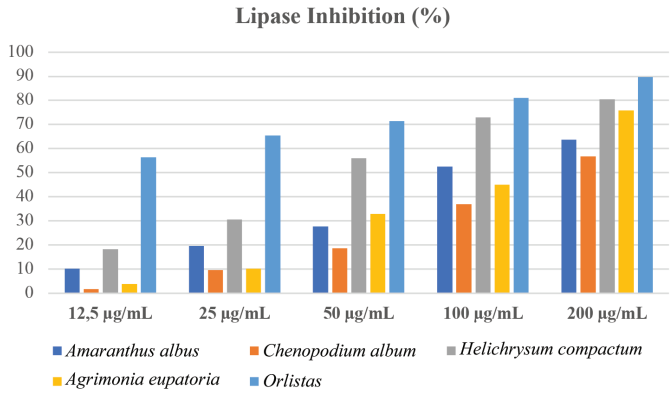

Figure 2. Lipase inhibition (%) values of the species and orlistat at different concentrations

Some treatment approaches have been developed to treat and prevent obesity except for diet or increasing physical activity.[11,12] Inhibition of adipocyte differentiation, stimulation of energy expenditure, suppression of *FAS* gene, inhibition of PL, suppression of appetite, and anti-inflammatory approach can be given as examples of these strategies.[13]

PL is responsible for the conversion of 50-70% TG to FA and MG. Inhibition of PL allows reduces fat absorption and therefore to reduces energy intake.[19]

Phenolic compounds play an important role for treating obesity. It has been proven that consuming some plant-derived food with phenolic content is associated with the prevention of obesity.[20] Vanillic acid has been proved to have an anti-inflammatory effect in rats fed a high-fat diet and provides a regulatory effect on insulin resistance-induced hyperinsulinemia, hyperglycemia, and hyperlipidemia.[16] Previous studies showed that *p*-coumaric

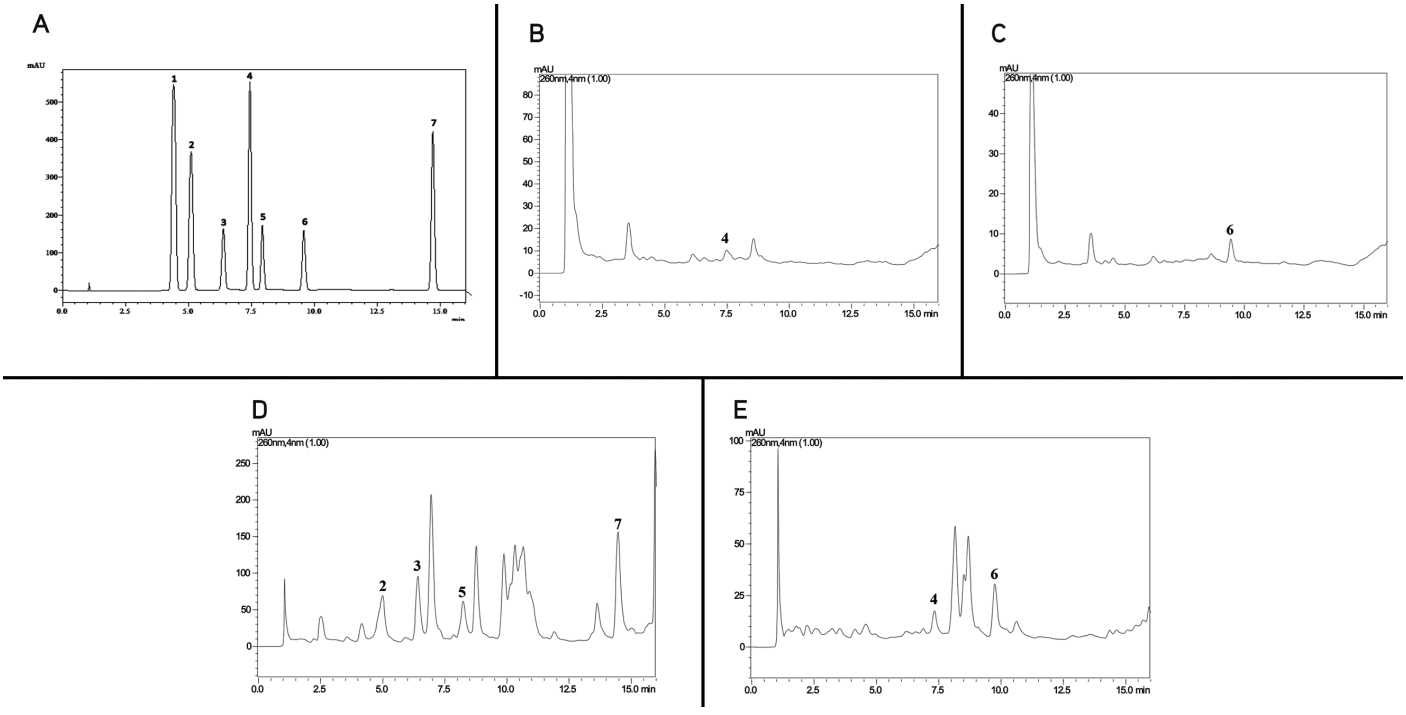

Figure 3. HPLC chromatogram of phenolic standards, Peak identification:[18] 1: *p*-hydroxy benzoic acid, 2: vanillic acid, 3: syring aldehyde, 4: *p*-coumaric acid, 5: sinapic acid, 6: benzoic acid, 7: quercetin (A), HPLC chromatogram of the methanol extract of *Amaranthus albus* (B), HPLC chromatogram of the methanol extract of *Chenopodium album* (C), HPLC Chromatogram of the methanol extract of Helichrysum compactum (D), HPLC Chromatogram of the methanol extract of *Agrimonia eupatoria* (E)

Table 1. Phenolic compounds and benzoic acid contents of their species

Species	*p*-Hydroxybenzoic acid	Vanilic acid	Syringaldehyde	*p*-Coumaric acid	Sinapic acid	Benzoic acid	Quercetin
	mg/g extract						
Amaranthus albus	-	-	-	0.27	-	-	-
Chenopodium album	-	-	-	-	-	0.33	-
Helichrysum compactum	-	7.32	14.97	-	0.30	-	4.66
Agrimonia eupatoria	-	-	-	0.71	-	3.43	-

acid and sinapic acid decrease pro-inflammatory adipokines such as tumor necrosis factor-α in obese mice and increase the level of anti-inflammatory cytokines such as adiponectin, thereby both phenolic compounds causing reduced obesity and obesity-related complications.[21]

Syringaldehyde has been presented to positively affect hyperglycemia by increasing the GLUT-4 transporter and mRNA levels in muscles of diabetic rats.[22] Benzoic acid-derived compounds improved lipid metabolism and diabetes by regulating plasma insulin, glucose, low-density lipoprotein, and TG in streptozotocin-induced diabetic rats.[23] A study on the antiobesity effect of quercetin showed that quercetin reduced body weight, liver fat accumulation, blood glucose, plasma, and liver triacylglycerol levels in a high-fat diet-fed mice.[24]

HPLC analysis was performed and lipase inhibitory effects were evaluated to reveal the potential of *A. albus*, *C. album*, *H. compactum,* and *A. eupatoria* in treating obesity with this study.

Amaranthus genus has been used for osteoarthritis, rheumatoid arthritis, gonorrhea, inflammation, hemorrhoids, and antibacterial effect, traditionally.[25,26] Terpenoids, flavonoids, tannins, alkaloids, sterols, cardiac glycosides, and saponins were determined for *Amaranthus* genus in previous phytochemical studies. Phenolic compounds of ellagic, ferulic, and gallic acids, quercetin, rutin, *p*-coumaric, sinapic, syringic acid, and vanillic acid, have been detected on the *Amaranthus* genus previously.[27] Previous biological activity studies revealed analgesic, anti-inflammatory, antifungal, antioxidant, enzyme inhibition, and hepatoprotective effects of *Amaranthus* genus.[28-31] Because of *in vitro* lipase inhibitor activity tests, IC_{50} value of *A. albus* was determined as 106.02 ± 4.5125 µg/mL. *p*-Coumaric acid among analyzed phenolic contents was detected *via* HPLC for the species. The anti-obesity effect of *A. albus* may be due to *p*-coumaric acid. Also, HPLC signals except for *p*-coumaric acid may be related to phenolic content determined by previous studies on *Amaranthus* genus. Furthermore, this state may contribute to the obesity effect. Simultaneously, the anti-inflammatory, antioxidant, and hepatoprotective effects of the species revealed by previous studies may contribute to the potential therapeutic effect of the plant for obesity.

C. album is traditionally used to treat peptic ulcers, dyspepsia, swelling, pharyngoplasty, splenopathy, ophthalmopathy, fatigue, liver disorders, spleen enlargement, intestinal ulcers, and burns.[32,33] Apart from these uses, it has also been observed to have antiparasitic, diuretic, hepatoprotective, laxative, and sedative effects.[33] Terpenoids, flavonoids, tannins, alkaloids, sterols, cardiac glycosides, and saponins were found in the content of *C. album*.[32] Lots of phenolic components such as quercetin, quercetin 3-*O*-glycosides, quercetin 3-*O*-xylosylglucoside, quercetin-3-*O*-rhamnoglucoside, isorhamnetin, kaempferol, kaempferol 3-*O*-glycosides, kaempferol 3-*O*-β-diglucoside, kaempferol-3-*O*-arabinoglucoside *etc*., have been defined in previous studies.[32] Biological activity studies revealed anthelmintic, antidiarrheal, anticancer, antimicrobial, antinociceptive, antioxidant, antipruritic, hepatoprotective, and sperm immobilization effects of *C. album*.[32-40] IC_{50} value of lipase inhibition was evaluated as 177.82 ± 8.6325 µg/mL for *C. album*. According to HPLC analysis, benzoic acid was determined. *C. album* may inhibit lipase inhibition potential because of benzoic acid content. Also, other HPLC signals, except for benzoic acid, may be based on phenolic components mentioned in previous literature.

H. compactum is used for kidney diseases and kidney stones, stomach pain, heart rhythm regulation, liver disease, burn and wound treatment, hand and foot cracks, diarrhea, and asthma treatment, traditionally.[41] *H. compactum* has been revealed to have terpenoids, flavonoids, tannins, alkaloids, sterols, cardiac glycosides, and saponins.[42] It was determined that phenolic compounds, *e.g.* apigenin, apigenin-7-*O*-glucoside, kaempferol, kaempferol-3-*O*-glucoside, 3,5-dihydroxy-6,7,8- kaempferol-3-*O*-glucoside, luteolin, luteolin-7-*O*-glucoside, luteolin-4′,7-di-*O*-glucoside, and naringenin were isolated from *H. compactum.*[42] Other signals observed on the HPLC chromatogram may be related to these phenolic compounds, and therefore lipase activity. Biological activity studies showed that it had antioxidant and antibacterial effects.[42-44] *In vitro* lipase inhibitory activity analysis on *H. compactum*, the IC_{50} value was evaluated as 45.70 ± 2.3618 µg/mL. Vanillic acid, syringaldehyde, sinapic acid, and quercetin were determined as phenolic compounds by HPLC analysis. Other HPLC signals can be related to the potential phenolic content mentioned in previous studies. Therefore, the lipase inhibitory effect may be due to its potential phenolic content and compounds detected in this study.

A. eupatoria is traditionally used to treat cold, bleeding, tuberculosis, skin diseases, urinary disorders, intestinal infections, ulcers, and antidiabetic, anti-inflammatory, cholagogue, hemostatic, antibacterial, fungicidal, aggregate, and diuretic effects.[45,46] In phytochemical analysis studies, terpenoids, flavonoids, tannins, alkaloids, sterols, cardiac glycosides, and saponins were found in *A. eupatoria*. Phenolic components of astragalin, apigenin 7-*O*-D-glucuronide, apigenin-7-*O*-glucopyranoside, catechin, ellagic acid 4-*O*-glucopyranoside, quercetin, kaempferol-3-*O*-rhamnoside, kaempferol-3-*O*-glucopyranoside, tiliroside, and rutin isolated from *A. eupatoria* previously may be related to other HPLC signals.[45] Biological activity studies revealed analgesic, antibacterial, antidiabetic, anti-inflammatory, anticoagulant, antinociceptive, antioxidant, antitumor, antiviral, and hepatoprotective effects of *A. eupatoria*.[46-55] In the study, the IC_{50} value for lipase inhibition was stated as 94.18 ± 5.2569 µg/mL, and *p*-coumaric and benzoic acids were identified *via* HPLC analysis. Anti-obesity activity of *A. eupatoria* may be based on phenolic compounds of *p*-coumaric acid and benzoic acid. Also, other phenolic components observed in HPLC analysis can be related to phenolic content aforementioned in previous studies. Simultaneously, antidiabetic, anti-inflammatory, antioxidant, and hepatoprotective effects reported in literature studies may contribute to the potential therapeutic effect of the species for treating obesity.

According to HPLC analysis, the highest phenolic content was found in *H. compactum,* followed by *A. eupatoria, C. album, A. albus.* When the lipase inhibitory effects of four species were evaluated, it was observed that the order of activity, respectively,

was *H. compactum, A. eupatoria, A. albus,* and *C. album*. In this study, the relationship between phenolic compounds and lipase inhibitory effects has been proven again, and the therapeutic potential of these species has been demonstrated for obesity.

Study limitations

The value of these species in treating obesity, which is a global health problem, can be demonstrated more comprehensively with toxicological analysis studies, formulation studies, standardization studies, and clinical studies on the antiobesity effect.

CONCLUSION

Because of this study, the relationship between phenolic compounds and lipase inhibitory effects has been proven and concluded that *A. albus, H. compactum, C. album, A. eupatoria* species could be used as potential therapeutic agents for treating obesity.

Ethics

Ethics Committee Approval: Ethical approval does not require for the study.

Informed Consent: Not necessary.

Authorship Contributions

Concept: S.Ö.Ş., Design: S.Ö.Ş., E.C., U.Ö., Data Collection or Processing: S.Ö.Ş., E.C., B.N.Ö., M.B., Analysis or Interpretation: S.Ö.Ş., E.C., B.N.Ö., M.B., Literature Search: S.Ö.Ş., E.C., B.N.Ö., Writing: S.Ö.Ş., E.C., U.Ö.

Conflict of Interest: No conflict of interest was declared by the authors.

Financial Disclosure: The study was supported by Turkish Scientific and Technical Research Council (TUBITAK) (project number: 1919B012001065).

REFERENCES

1. T.R. Ministry of Health, General Directorate of Health Promotion. Turkey body weight perception survey. Ankara. 2012;894:1-64.
2. Hruby A, Hu FB. The epidemiology of obesity: a big picture. Pharmacoeconomics. 2015;33:673-689.
3. Aktar N, Qureshi NK, Ferdous HS. Obesity: a review of pathogenesis and management strategies in adult. Delta Med J. 2017;5:35-48.
4. Rippe JM, Crossley S, Ringer R. Obesity as a chronic disease: modern medical and lifestyle management. J Am Diet Assoc. 1998;98(10 Suppl 2):S9-15.
5. Feng S, Reuss L, Wang Y. Potential of natural products in the inhibition of adipogenesis through regulation of PPARγ expression and/or its transcriptional activity. Molecules. 2016;21:1278.
6. Şener SÖ. Pharmacognosic studies on some *Cirsium* Mill. (Asteraceae) species. (PhD thesis). Ankara: Ankara University Institute of Health Sciences; 2019.
7. Kim GS, Park HJ, Woo JH, Kim MK, Koh PO, Min W, Ko YG, Kim CH, Won CK, Cho JH. *Citrus aurantium* flavonoids inhibit adipogenesis through the Akt signaling pathway in 3T3-L1 cells. BMC Complement Altern Med. 2012;12:31.
8. Kusunoki J, Kanatani A, Moller DE. Modulation of fatty acid metabolism as a potential approach to the treatment of obesity and the metabolic syndrome. Endocrine. 2006;29:91-100.
9. Yun JW. Possible anti-obesity therapeutics from nature-a review. Phytochemistry. 2010;71:1625-1641.
10. Yiğit A, Yiğit V. Economic burden of obesity-related comorbidities in Turkey. GUJHS. 2019;8:223-230.
11. Bonamichi B, Bezerra Parente E, dos Santos RB, Beltzhoover R, Lee J, Nunes Salles JE. The challenge of obesity treatment: a review of approved drugs and new therapeutic targets. J Eat Disord. 2018;4:1-10.
12. Kaila B, Raman M. Obesity: a review of pathogenesis and management strategies. Can J Gastroenterol. 2008;22:61-68.
13. Jhade D, Paarakh PM, Gavani U. Isolation of phytoconstituents from the leaves of *Chenopodium album* Linn. J Pharm Res. 2009;2:1192-1193.
14. Birari RB, Bhutani KK. Pancreatic lipase inhibitors from natural sources: unexplored potential. Drug Discov Today. 2007;12:879-889.
15. Hirose M, Ando T, Shofiqur R, Umeda K, Kodama Y, Nguyen SV, Goto T, Shimada M, Nagaoka S. Anti-obesity activity of hen egg anti-lipase immunoglobulin yolk, a novel pancreatic lipase inhibitor. Nutr Metab (Lond). 2013;10:70.
16. Kwon DH, Kwon HY, Kim HJ, Chang EJ, Kim MB, Yoon SK, Song EY, Yoon DY, Lee YH, Choi IS, Choi YK. Inhibition of hepatitis B virus by an aqueous extract of *Agrimonia eupatoria* L. Phytother Res. 2005;19:355-358.
17. Pang Z, Wu N, Zhang X, Avallone R, Croci T, Dressler H, Palejwala V, Ferrara P, Tocci MJ, Polites HG. GPR40 is partially required for insulin secretion following activation of beta3-adrenergic receptors. Mol Cell Endocrinol. 2010;325:18-25.
18. Korkmaz N, Sener SO, Akkaya S, Badem M, Aliyazicioglu R, Abudayyak M, Oztas E, Ozgen U. Investigation of antioxidant, cytotoxic, tyrosinase inhibitory activities, and phenolic profiles of green, white, and black teas. Turk J Biochem. 2019;44:278-288.
19. Al Shukor N, Ravallec R, Van Camp J, Raes K, Smagghe G. Flavonoids stimulate cholecystokinin peptide secretion from the enteroendocrine STC-1 cells. Fitoterapia. 2016;113:128-131.
20. Hsu CL, Yen GC. Phenolic compounds: evidence for inhibitory effects against obesity and their underlying molecular signaling mechanisms. Mol Nutr Food Res. 2008;52:53-61. Erratum in: Mol Nutr Food Res. 2008;52:624-625.
21. Alam A, Subhan N, Hossain H, Hossain M, Reza HM, Rahman M, Ullah MO. Hydroxycinnamic acid derivatives: a potential class of natural compounds for the management of lipid metabolism and obesity. Nutr Metab. 2016;13:1-13.
22. Ling BL, Chiu CT, Lu HC, Lin JJ, Kuo CY, Chou FP. Short and long-term impact of lipectomy on expression profile of hepatic anabolic genes in rats: a high fat and high cholesterol diet-induced obese model. PLoS One. 2014;9:e108717.
23. Gayathri M, Kannabiran K. Antidiabetic activity of 2-hydroxy 4-methoxy benzoic acid isolated from the roots of Hemidesmus indicus on streptozotocin-induced diabetic rats. Int J Diabetes & Metabolism. 2009;17:53-57.
24. Ozturk K, Dogan T, Celikkanat S, Ozen A, Demirci H, Kurt O, Turker T, Yilmaz Y, Uygun A. The association of fatty pancreas with subclinical atherosclerosis in nonalcoholic fatty liver disease. Eur J Gastroenterol Hepatol. 2018;30:411-417.

25. Ishtiaq S, Hanif U, Ajaib M, Shaheen S, Afridi MSK, Siddiqui MF. Pharmacognostical and physicochemical characterization of *Amaranthus graecizans* subsp. *silvestris*: an anatomical perspective. Pak J Bot. 2018;50:307-312.
26. Wambugu SN, Mathiu PM, Gakuya DW, Kanui TI, Kabasa JD, Kiama SG. Medicinal plants used in the management of chronic joint pains in Machakos and Makueni counties, Kenya. J Ethnopharmacol. 2011;137:945-955.
27. Peter K, Gandhi P. Rediscovering the therapeutic potential of *Amaranthus* species: a review. Egypt J Basic Appl Sci. 2017;4:196-205.
28. Ishtiaq S, Afridi MSK, Masood N. Amelioration of isoniazid and rifampicin-induced liver toxicity by *Amaranthus graecizans* subsp. *silvestris* in rat. Bangladesh J Pharmacol. 2017;12:354-358.
29. Cevheri C, Küçük Ç. Effects of antifungal of *Amaranthus* extracts on *T. harzianum* and *F. moniliforme* antagonizm. Kafkas Univ Vet Fak Derg. 2012;18:161-165.
30. Adegbola PI, Adetutu A, Olaniyi TD. Antioxidant activity of *Amaranthus* species from the Amaranthaceae family - a review. S Afr J Bot. 2020;133:111-117.
31. Ishtiaq S, Ahmad M, Hanif U, Akbar S, Mehjabeen, Kamran SH. Phytochemical and *in vitro* antioxidant evaluation of different fractions of *Amaranthus graecizans* subsp. *silvestris* (Vill.) Brenan. Asian Pac J Trop Med. 2014;7S1:S342-S347.
32. Poonia A, Upadhayay A. *Chenopodium album* Linn: review of nutritive value and biological properties. J Food Sci Technol. 2015;52:3977-3985.
33. Saini R, Kumar D, Mittal A. Antimicrobial and phytochemical potential of *Chenopodium album* Linn. Int J Sci Technol Res. 2019;8:877-880.
34. Lone BA, Chishti MZ, Bhat FA, Tak H, Bandh SA, Khan A. Evaluation of anthelmintic antimicrobial and antioxidant activity of *Chenopodium album*. Trop Anim Health Prod. 2017;49:1597-1605.
35. Parida S, Patro VJ, Mishra US, Mohapatra L, Sannigrahi S. Anthelmintic potential of crude extracts and its various fractions of different parts of *Pterospermum acerifolium* Linn. Int J Pharm Sci Rev Res. 2010;1:107-111.
36. Nigam V, Paarakh PM. Evaluation of anti-diarrhoeal activity of hydro alcoholic extract of *Chenopodium album* L. Indian J Nat Prod Resour. 2013;4:61-66.
37. Martini L, Brzezinski P. The demonstration that amongs myriads of palliative anticancer plants, there is one that is endowed by a synergical action: the *Chenopodium album*, that avoids the biotranformation of a benign skin tumor to malignant. Our Dermatol Online. 2018;9:316-319.
38. Laghari AH, Memon S, Nelofar A, Khan KM, Yasmin A. Determination of free phenolic acids and antioxidant activity of methanolic extracts obtained from fruits and leaves of *Chenopodium album*. Food Chem. 2011;126:1850-1855.
39. Vijay N, Padmaa M. Hepatoprotective activity of *Chenopodium album* Linn. against paracetamol induced liver damage. Pharmacologyonline. 2011;3:312-328.
40. Kumar S, Biswas S, Mandal D, Roy HN, Chakraborty S, Kabir SN, Banerjee S, Mondal NB. *Chenopodium album* seed extract: a potent sperm-immobilizing agent both *in vitro* and *in vivo*. Contraception. 2007;75:71-78.
41. Eroğlu HE, Aksoy A, Hamzaoğlu E, Budak U, Albayrak S. Cytogenetic effects of nine *Helichrysum taxa* in human lymphocytes culture. Cytotechnology. 2009;59:65-72.
42. Süzgeç S, Meriçli AH, Houghton PJ, Cubukçu B. Flavonoids of *Helichrysum compactum* and their antioxidant and antibacterial activity. Fitoterapia. 2005;76:269-272.
43. Albayrak S, Aksoy A, Sagdic O, Hamzaoglu E. Compositions, antioxidant and antimicrobial activities of *Helichrysum* (Asteraceae) species collected from Turkey. Food Chem. 2010;119:114-122.
44. Süzgeç S. Pharmacognosic Studies on *Helichrysum compactum* Boiss. (PhD thesis). İstanbul: Istanbul University Institute of Health Sciences, Department of Pharmacognosy. 2002;222.
45. Al-Snafi AE. The pharmacological and therapeutic importance of *Agrimonia eupatoria*-a review. Asian J Pharm Sci Technol. 2015;5:112-117.
46. Pour MG, Mirazi N, Moradkhani S, Rafieian-Kopaei M, Rahimi-Madiseh M. A comprehensive review on phytochemical, pharmacological and therapeutic properties of *Agrimonia eupatoria* L. J Herbmed Pharmacol. 2020;10:14-30.
47. Santos TN, Costa G, Ferreira JP, Liberal J, Francisco V, Paranhos A, Cruz MT, Castelo-Branco M, Figueiredo IV, Batista MT. Antioxidant, anti-inflammatory, and analgesic activities of *Agrimonia eupatoria* L. infusion. Evid-Based Complement Altern Med. 2017:1-13.
48. Copland A, Nahar L, Tomlinson CT, Hamilton V, Middleton M, Kumarasamy Y, Sarker SD. Antibacterial and free radical scavenging activity of the seeds of *Agrimonia eupatoria*. Fitoterapia. 2003;74:133-135.
49. Ghaima KK. Antibacterial and wound healing activity of some *Agrimonia eupatoria* extracts. Baghdad Sci J. 2013;10:152-160.
50. Kuczmannová A, Balažová A, Račanská E, Kameníková M, Fialová S, Majerník J, Nagy M, Gál P, Mučaji P. *Agrimonia eupatoria* L. and *Cynara cardunculus* L. water infusions: comparison of anti-diabetic activities. Molecules. 2016;21:564.
51. Lee KH, Rhee KH. Anti-nociceptive effect of *Agrimonia eupatoria* extract on a cisplatin induced neuropathic model. Afr J Tradit Complement Altern Med. 2016;13:139-144.
52. Tsirigotis-Maniecka M, Pawlaczyk-Graja I, Ziewiecki R, Balicki S, Matulová M, Capek P, Czechowski F, Gancarz R. The polyphenolic-polysaccharide complex of *Agrimonia eupatoria* L. as an indirect thrombin inhibitor - isolation and chemical characterization. Int J Biol Macromol. 2019;125:124-132.
53. Correia H, González-Paramás A, Amaral MT, Santos-Buelga C, Batista MT. Polyphenolic profile characterization of *Agrimonia eupatoria* L. by HPLC with different detection devices. Biomed Chromatogr. 2006;20:88-94.
54. Ad'hiah AH, Al-Bederi ON, Al-Sammarrae KW. Cytotoxic effects of *Agrimonia eupatoria* L. against cancer cell lines *in vitro*. J Assoc Arab Univ Basic Appl Sci. 2013;14:87-92.
55. Yoon SJ, Koh EJ, Kim CS, Zee OP, Kwak JH, Jeong WJ, Kim JH, Lee SM. *Agrimonia eupatoria* protects against chronic ethanol-induced liver injury in rats. Food Chem Toxicol. 2012;50:2335-2341.

Turk J Pharm Sci 2022;19(5):505-512
DOI: 10.4274/tjps.galenos.2021.51882

ORIGINAL ARTICLE

Dexamethasone and Citicoline Mitigate Cisplatin-Induced Peripheral Neuropathy: A Novel Experimental Study in Mice

Farid MASOUD[1,2*], Bohloul HABIBI-ASL[1*], Mohammad CHARKHPOUR[1], Yashar ASADPOUR[3], Javad MAHMOUDI[4]

[1]Tabriz University of Medical Sciences, Faculty of Pharmacy, Department of Pharmacology, Tabriz, Iran
[2]Radboud University Medical Center, Radboud Institute for Molecular Life Sciences, Nijmegen, Netherlands
[3]Tabriz University of Medical Sciences, Student Research Committee and Faculty of Pharmacy, Tabriz, Iran
[4]Tabriz University of Medical Sciences, Neurosciences Research Center, Tabriz, Iran

ABSTRACT

Objectives: Given the rising prevalence of cisplatin-induced peripheral neuropathy (CisIPN), investigations to alleviate its adverse effects are required. Oxidative stress and free radical development are essential pathways of CisIPN. Specifically, dexamethasone and citicoline are characterized by anti-inflammatory and antioxidant activities that might reduce CisIPN incidence and severity. The current study assessed the possible impacts of novel interventions, dexamethasone, and, citicoline on CisIPN.

Materials and Methods: Seventy-two male mice were randomly allocated into nine groups (n: 8/each group). Different doses of dexamethasone (7.5, 15, 30 mg/kg, *i.p.*), citicoline (10, 20, 40 mg/kg, *i.p.*), and the combination (dexamethasone 7.5 mg/kg + citicoline 10 mg/kg, *i.p.*) were injected in the first three days and one day before receiving cisplatin (2 mg/kg, *i.p.*). The tail-flick method was used for assessing nociception. Besides, malondialdehyde (MDA), interleukin-1 beta (IL-1β), tumor necrosis factor-α (TNF-α), total antioxidant capacity (TAC), and mice weight differences (ΔW) were measured.

Results: Different doses of dexamethasone and citicoline enhanced latency time ($p<0.05$). Moreover, dexamethasone 15 mg/kg diminished the level of MDA and increased TAC ($p<0.05$) and in 30 mg/kg, MDA was reduced ($p<0.05$). Besides, 20 and 40 mg/kg of citicoline reduced MDA and elevated TAC ($p<0.05$), and 10 mg/kg merely reduced MDA ($p<0.05$). Dexamethasone in all doses declined IL-1β and TNF-α levels, and citicoline only at 40 mg/kg lessened their levels ($p<0.05$). Interestingly, ΔW declined more in the dexamethasone and citicoline groups than the cisplatin group ($p<0.05$).

Conclusion: Dexamethasone and citicoline attenuate CisIPN through anti-inflammatory activity, improving the antioxidant capacity, and inhibiting lipid peroxidation.

Key words: Cisplatin, citicoline, dexamethasone, oncology, peripheral neuropathy

INTRODUCTION

Peripheral neuropathy is driven by an injury to the peripheral nervous system and can originate from various factors, such as *diabetes mellitus*, vitamin insufficiency, autoimmune diseases, and particular medications.[1,2]

Unquestionably, chemotherapy-induced peripheral neuropathy (CIPN) is the most frequent medication-IPN that has occurred predominantly with platinum-based drugs, and it affects approximately half of the patients, who received these medications.[3,4] Although the incidence of its symptoms is determined by numerous factors such as the drug's physicochemical properties, dose, duration, liver function, and age, the intolerable symptoms usually persist for several weeks after the drug discontinuation.[5]

Cisplatin (*cis*-diamminedichloroplatinum II) has been administered to treat several solid malignancies, such as ovarian, lung, and testicular carcinomas.[6] However, serious side effects, including neurotoxicity, ototoxicity, and nephrotoxicity, affect patients' quality of life, may lead to treatment discontinuation, and consequently, its clinical usage has been limited.[7,8] Specifically, CisIPN symptoms are associated with sensory disturbances that occur more frequently than autonomic and

*Correspondence: habibiaslbohlool@gmail.com, habibib@tbzmed.ac.ir, - faridmasoud@gmail.com, farid.masoud@ru.nl, Phone: +98 (411) 3341315, +31 644915009,
ORCID-ID: orcid.org/0000-0001-8427-9149, orcid.org/0000-0003-1823-3702
Received: 15.07.2021, Accepted: 19.10.2021

movement signs; its hallmarks are incorporated weakness in the hands, gait disturbance, weakness in movements, orthostatic hypotension, and altered sexual activity.[9,10] Interestingly, the exact mechanism of CisIPN has not been determined; however, some studies have indicated that pro-inflammatory cytokines, especially tumor necrosis factor-α (TNF-α) and interleukin-1 beta (IL-1β), lipid peroxidation, and oxidative stress may demonstrate the accelerated factors in the incidence of CisIPN.[11-13]

Given the potential anti-inflammatory, antioxidant, and neuroprotective activities of dexamethasone and citicoline[14-19] and the lack of a study in this area, we hypothesized that they might act as potential agents to diminish CisIPN occurrence and/or severity. Insights into these aspects are expected to understand dexamethasone and citicoline impacts on CisIPN better. This research has shown the possible prophylactic effects of dexamethasone and citicoline on CisIPN.

MATERIALS AND METHODS

Drugs and chemicals

Cisplatin was provided by Pfizer Inc. (NY, USA). Dexamethasone and citicoline were supplied by Iran Darou Pharmaceutical Co. (Tehran, Iran). Thiobarbituric acid, hydrogen peroxide, *n*-butanol, and phosphoric acid, were obtained from Sigma-Aldrich Inc. (Missouri, USA). Ketamine and xylazine were also purchased from Alfasan Diergeneesmiddelen B.V. (Utrecht, Netherlands).

Animals

Healthy male mice (25-35 g) were purchased from Tabriz University of Medical Sciences Animal Center, housed in a standard polypropylene cage at 25 ± 2°C temperature, and provided 12 hour light/12 hour dark intervals with *ad libitum* feeding. Tabriz University of Medical Sciences Ethics Committee authorized the study protocols and methods (ethical code: IR.TBZMED.VCR.REC.1398.087, May 13, 2019), conformed to the NIH Guide for the Care and Use of Laboratory Animals (8th edition, NRC 2011).

Experimental design

Seventy-two mice were randomly divided into the following nine groups (n: 8/each group) (Figure 1).

(1) Control: The animals received sterile saline (10 mL/kg, *i.p.*) for three consecutive days and the fourth, seventh, eleventh, fourteenth, eighteenth, twenty-first, and twenty-fifth days.

(2) Cisplatin: The animals in the first three days and the sixth,

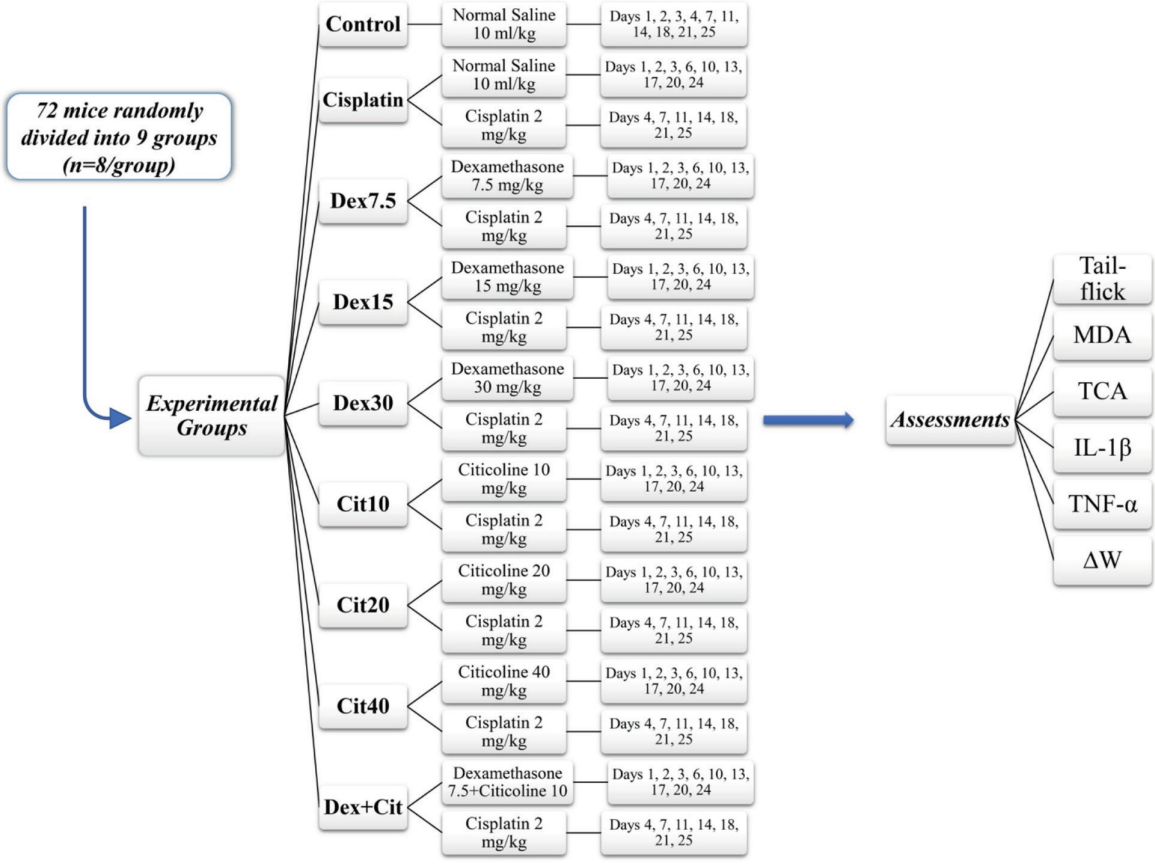

Figure 1. Functional diagram of the experimental groups and the assessments. In all figures, Dex7.5, dexamethasone 7.5 mg/kg; Dex15, dexamethasone 15 mg/kg; Dex30, dexamethasone 30 mg/kg; Cit10, citicoline 10 mg/kg; Cit20, citicoline 20 mg/kg; Cit40, citicoline 40 mg/kg; and Dex + Cit, dexamethasone 7.5 mg/kg and citicoline 10 mg/kg

Dex: Dexamethasone, Cit: Citicoline, Dex + Cit: Dexamethasone 7.5 mg/kg and citicoline 10 mg/kg, MDA: Malondialdehyde, IL-1β: Interleukin-1 beta, TNF-α: Tumor necrosis factor-α, TAC: Total antioxidant capacity, ΔW: Mice weight differences

tenth, thirteenth, seventeenth, twentieth, and twenty-fourth days received sterile saline 10 mL/kg, *i.p.*). Additionally, cisplatin was injected (2 mg/kg, *i.p.*) on the fourth, seventh, eleventh, fourteenth, eighteenth, twenty-first, and twenty-fifth days.

(3) Dex7.5: The animals in the first three days and the sixth, tenth, thirteenth, seventeenth, twentieth, and twenty-fourth days received dexamethasone (7.5 mg/kg, *i.p.*). Besides, on the fourth, seventh, eleventh, fourteenth, eighteenth, twenty-first, and twenty-fifth days, cisplatin 2 mg/kg, *i.p.* was administered.

(4) Dex15: The interventions were identical to those of the Dex7.5 group; however, the dexamethasone dosages were 15 mg/kg.

(5) Dex30: Similar to the conditions in the Dex7.5 group except that the dexamethasone dosages were 30 mg/kg.

(6) Cit10: Same procedure as the Dex7.5 group, but instead of dexamethasone, citicoline 10 mg/kg was administered.

(7) Cit20: Identical procedure as the Dex7.5 group, but instead of dexamethasone, 20 mg/kg of citicoline was injected.

(8) Cit40: The conditions were similar to those in the Dex7.5 group, but 40 mg/kg of citicoline was injected instead of dexamethasone.

(9) Dex + Cit: The conditions were the same as those in the Dex7.5 group; however, instead of dexamethasone, combinations of dexamethasone 7.5 mg/kg and citicoline 10 mg/kg were administered.

In all study groups, the latency time to pain was measured using the tail-flick test on day 0 (before interventions) and repeated on the days fourth, eleventh, eighteenth, twenty-fifth, and twenty-eighths.

Nociception assessment

In the tail-flick method, the thermal light (235 mW/cm^2 and 50°C temperature) created by a lamp beam (20% intensity) from a constant distance to the 3-4 cm of animal's tail end in a special chamber (Ugo Basile 37360 Stoelting Co., IL, USA). The latency time (in seconds) was identified as the elapsed time between the beginning of the tail exposure to the thermal source and its withdrawal.[20] In this study, the maximum time, when the heat stimulus was applied to the animal's tail (cut-off time), was determined for 30 seconds to avoid tail tissue injury. Besides, stimulation was applied to successive sites from the end to the tail's beginning to increase accuracy.

Assessment total antioxidant capacity (TAC)

TAC evaluation was based on ABTS radical reduction and was performed according to the technique by Miller et al.[21] using a commercial kit (Rel Assay Diagnostics, Türkiye). The results were expressed in millimoles *per* liter (mmol/L).

Measurement of malondialdehyde (MDA)

MDA calculation was started by dissolving 500 µL of serum into 3 mL of 1% phosphoric acid. It was applied to the test tube after vortexing 1 mL of 0.67% thiobarbituric acid solution, and after full vortexing, it was put for 45 min in a laboratory water bath. The test tubes were cooled under cold water after the necessary time; 3 mL of normal butanol was applied and vortexed for 2 min, centrifuged for 10 minutes at 3000 rpm; eventually, the supernatant was collected for calculating light absorbance at 532 nm.[22] The results were reported in nanomoles *per* liter (nmol/L).

Weight changes

The animal weights were measured at baseline (day 0) and repeated on days 7, 14, and 28 by an analytical balance (Libror AEU-210, Shimadzu, Japan); their weight changes for each study group were recorded and compared.

Assay of proinflammatory cytokines

Mice were anesthetized intraperitoneally (*i.p.*) by administering a combination of ketamine (50 mg/kg) and xylazine (5 mg/kg); blood samples were obtained from their abdominal aorta and centrifuged at 10000 rpm for 10 minutes at 4°C and collected supernatants were frozen at -80°C to measure the levels of proinflammatory cytokines. Subsequently, TNF-α and IL-1β levels were assessed using ELISA kits (Bender Medsystems, Vienna, Austria). Briefly, in a 96 well plate, 50 mL of standard were inserted, polyclonal antibodies were separately added to all wells, and their surfaces were coated and incubated at room temperature (25°C) for 2 h. Followed by washing, the wells were filled with streptavidin-HRP and incubated at room temperature. Afterward, a colored product parallel to the amount of IL-1β and TNF-α in the sample was formed by adding tetramethylbenzidine substrate solution to all wells. Finally, to prevent the enzyme-reaction, the stop solution was applied to each well, and the relative absorbance of TNF-α and IL-1β were measured spectrophotometrically at 450 nm (Synergy HT, BioTek, USA). The results were standardized to the amount of protein in each sample and expressed as a picograms *per* milligram (pg/mg) of protein.[23]

Statistical analysis

Statistical analyses were conducted using SPSS software 25 (SPSS Inc., Chicago, Illinois). Data from experiments are presented as mean ± standard errors of means. An ANOVA test with Tukey *post-hoc* analysis was used to assess the various treatment regimens' efficacy between the study groups. A $p<0.05$ value was assumed to demonstrate a statistically significant difference.

RESULTS

Different interventions and CisIPN

The comparative effects of different interventions on CisIPN pain hypersensitivity are presented in Figure 2. Cisplatin injection in the cisplatin group on days 25 and 28 significantly diminished the latency time compared with the control group ($p<0.01$) (Figure 2A). Administration of dexamethasone with 7.5 and 15 and mg/kg (Dex7.5 and Dex15 groups) on days 11, 18, 25, and 28 ($p<0.001$) and 30 mg/kg (Dex30 group) on the fourth day ($p<0.05$) and days 25 and 28 ($p<0.001$) could significantly increased the latency time to pain compared with cisplatin group (Figure 2B). Besides, citicoline 10 mg/kg on the fourth day ($p<0.01$) and on days 11, 18, 25, and 28 ($p<0.001$), also at doses

20 and 40 mg/kg on days 28, 25, 18, 11 (p<0.001) substantially increased pain latency time compared to the cisplatin group (Figure 2C). Moreover, co-administration of dexamethasone and citicoline (Dex + Cit group) on days 11 (p<0.01), 18 (p<0.05), 25, and 28 (p<0.001) dramatically improved latency time compared with cisplatin group; however, on day 28 (p<0.01) compared with dexamethasone group (Dex7.5) and on days 11 and 25 (p<0.01), 18 and 28 (p<0.001) in comparison with citicoline group (Cit10) the latency time was declined (Figure 2D).

Changes in mice weights

Administration of cisplatin in the cisplatin group reduced body weight differences (ΔW) compared to the control group (-1.07 ± 0.09 *vs.* 0.14 ± 0.11; p>0.05). Also, dexamethasone at doses of 7.5 and 30 (Dex7.5 and Dex30 groups) decreased ΔW significantly compared to the cisplatin group (-3.03 ± 0.2 *vs.* -1.07 ± 0.09; p<0.001, and -6.29 ± 0.45 *vs.* -1.07 ± 0.09; p<0.001, respectively). However, citicoline at all doses declined ΔW meaningfully compared to the cisplatin group (Cit10, -5.57 ± 0.01 *vs.* -1.07 ± 0.09; p<0.001, Cit20, -4.34 ± 0.07 *vs.* -1.07 ± 0.09; p<0.001, and Cit40, -3.11 ± 0.55 *vs.* -1.07 ± 0.09; p<0.01). Moreover, the combination of dexamethasone and citicoline (Dex + Cit group) reduced ΔW notably compared with the cisplatin group (-4.5 ± 0.25 *vs.* -1.07 ± 0.09; p<0.001), Cit10 group (-4.5 ± 0.25 *vs.* -5.57 ± 0.01; p<0.001), and Dex7.5 group (-4.5 ± 0.25 *vs.* -3.03 ± 0.2; p<0.01) (Table 1).

TAC and MDA levels

Cisplatin administration in the cisplatin group increased MDA significantly compared to the control group (2.52 ± 0.28 *vs.* 1.64 ± 0.09; p<001). The injection of dexamethasone (7.5, 15, and 30 mg/kg) elevated TAC and declined MDA levels compared to the cisplatin group; however, only at the 15 mg/kg (Dex15 group) showed significant differences (p<0.05). Also, the reduced MDA level in the Dex30 group was meaningfully compared the cisplatin group (p<0.05). Similarly, citicoline at all doses elevated TAC and diminished MDA levels compared to the cisplatin group; notably, this outlined changes occurred at doses 10 mg/kg (TAC, 0.57 ± 0.05 *vs.* 0.54 ± 0.04; p>0.05, MDA, 1.46 ± 0.08 *vs.* 2.52 ± 0.28; p<0.01), 20 mg/kg (TAC, 0.75 ± 0.04 *vs.* 0.54 ± 0.04; p<0.05, MDA, 1.73 ± 0.17 *vs.* 2.52 ± 0.28; p<0.05), and 40 mg/kg (TAC, 0.82 ± 0.04 *vs.* 0.54 ± 0.04; p<0.001, MDA, 1.8 ± 0.15 *vs.* 2.52 ± 0.28; p<0.05). Moreover, co-administration of dexamethasone and citicoline (Dex + Cit group) enhanced TAC and reduced MDA

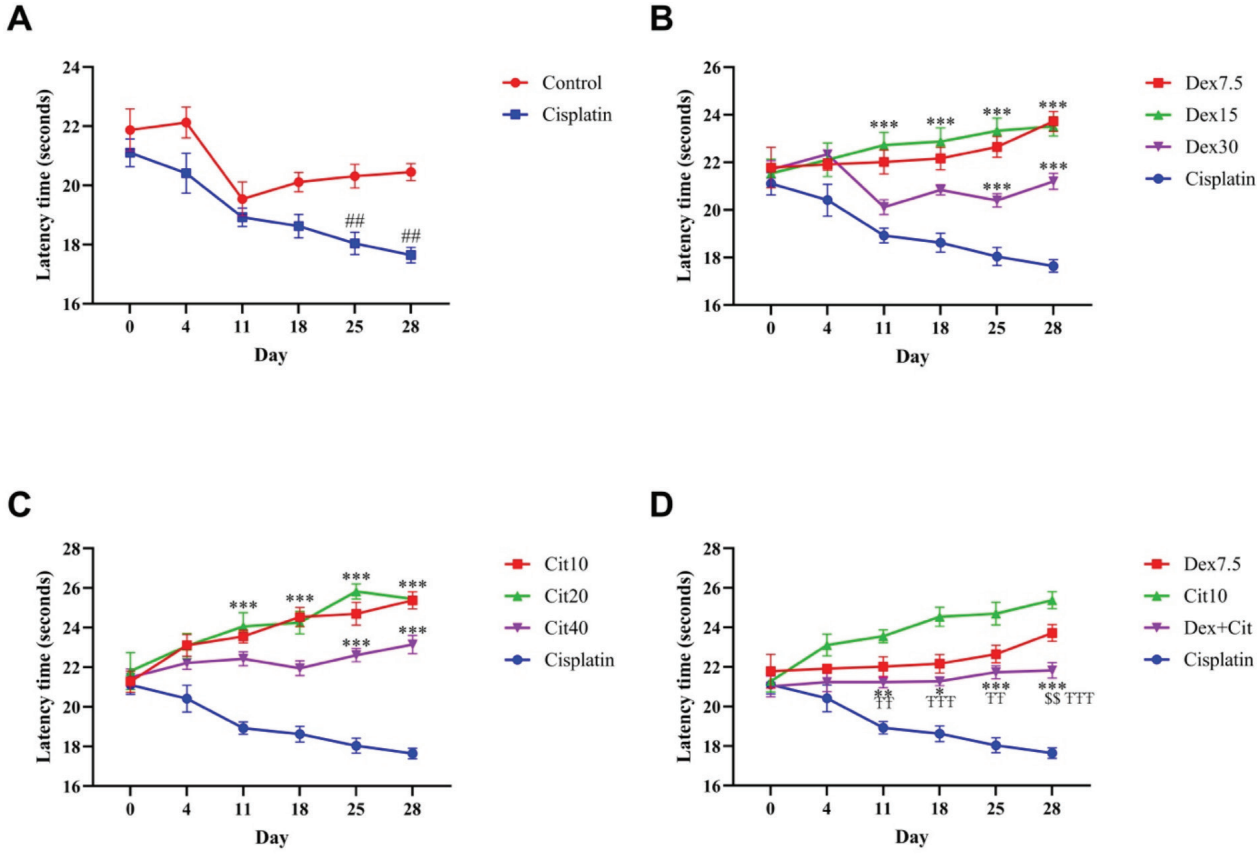

Figure 2. The effect of different interventions on latency times in study groups. (A) Comparison between the control and cisplatin group. (B) Comparing dexamethasone injected groups (Dex7.5, Dex15, Dex30, and Dex + Cit) with the cisplatin group. (C) Comparing with citicoline injected groups (Cit10, Cit20, Cit40, and Dex + Cit) and the cisplatin group. (D) Comparison of the combination group (Dex + Cit) with Dex7.5 and Cit10 groups. Data are provided as mean ± SEM (n: 8/each group). Statistical analyses were conducted using one-way ANOVA with Tukey *post-hoc* analysis

*p<0.05, **p<0.01, ***p<0.001 compared with the cisplatin group. $^{\#\#}p$<0.01 as compared with the control group. $^{\$\$}p$<0.01 as compared with the Dex7.5 group. $^{\tau\tau}p$<0.01 and $^{\tau\tau\tau}p$<0.001 as compared with the Cit10 group. Dex: Dexamethasone, Cit: Citicoline, Dex + Cit: Dexamethasone 7.5 mg/kg and citicoline 10 mg/kg, SEM: Standard error of means

levels compared with the cisplatin group (0.69 ± 0.05 *vs.* 0.54 ± 0.04; $p<0.05$ and 1.55 ± 0.21 *vs.* 2.52 ± 0.28; $p<0.05$, respectively) (Table 2).

TNF-α and IL-1β levels

Figure 3 shows that TNF-α levels in the cisplatin group were significantly enhanced compared with the control group ($p<0.01$). The administration of dexamethasone at doses 7.5 mg/kg (Dex7.5), 15 mg/kg (Dex15), and 30 mg/kg (Dex30) significantly declined the TNF-α levels compared with the cisplatin group ($p<0.05$, $p<0.05$, and $p<0.01$, respectively). Besides, citicoline showed a considerable reduction at dose 40 mg/kg (Cit40) compared with the cisplatin group ($p<0.05$). The combination of dexamethasone and citicoline (Dex + Cit) did not demonstrate significant TNF-α levels change compared to the cisplatin group; nonetheless, its levels diminished considerably compared with the Cit10 group ($p<0.05$).

As shown in Figure 4, the IL-1β level was significantly enhanced in the cisplatin group compared to the control group ($p<0.001$). Additionally of dexamethasone at all doses 7.5 mg/kg (Dex7.5), 15 mg/kg (Dex15), and 30 mg/kg (Dex30), significantly diminished the IL-1β levels compared with the cisplatin group ($p<0.01$, $p<0.01$, and $p<0.001$, respectively). Moreover, citicoline only at dose 40 mg/kg indicated a significant reduction in IL-1β level compared with the cisplatin group ($p<0.05$). Combination of dexamethasone and citicoline (Dex + Cit) did not reveal IL-1β changes considerably than the cisplatin group; however, its levels decremented significantly compared with the Cit10 group ($p<0.01$).

Table 1. Changes in mice weights between study groups

Groups	Day 0	Day 7	Day 14	Day 28	ΔW
Control	28 ± 1.44	29.57 ± 1.41	28.71 ± 1.47	28.14 ± 1.33	0.14 ± 0.11
Cisplatin	27.28 ± 0.68	27.28 ± 0.56	26.85 ± 0.63	26.21 ± 0.77	-1.07 ± 0.09
Dex7.5	30.12 ± 1.5	28.37 ± 1.33	28.12 ± 1.29	27.09 ± 1.3	-3.03 ± 0.2***
Dex15	26.85 ± 0.34	26 ± 0.81	25.57 ± 1.13	23.81 ± 1.35	-3.04 ± 1.01**
Dex30	33.14 ± 0.4	31.85 ± 0.4	28.07 ± 0.78	26.85 ± 0.85	-6.29 ± 0.45***
Cit10	28.14 ± 1.31	26.71 ± 1.2	25.14 ± 1.12	22.57 ± 1.32	-5.57 ± 0.01***
Cit20	27.5 ± 0.61	25.83 ± 0.6	24.08 ± 0.63	23.16 ± 0.54	-4.34 ± 0.07***
Cit40	29.14 ± 1.03	27.57 ± 1.2	27.12 ± 1.3	26.03 ± 1.58	-3.11 ± 0.55**
Dex + Cit	25.83 ± 1.24	25.66 ± 1.4	23.33 ± 1.54$^{\$}$	21.33 ± 1.49$^{\$\$}$	-4.5 ± 0.25***, $^{\$\$}$, $^{\text{ŦŦŦ}}$

Data are provided as mean ± SEM, g. n: 8/each group. [ΔW: Weight changes ($W_{\text{in day 28}}$-$W_{\text{in day 0}}$)]. Dex: Dexamethasone, Cit: Citicoline, Dex + Cit: Dexamethasone 7.5 mg/kg and citicoline 10 mg/kg. **$p<0.01$ and ***$p<0.001$ as compared with the cisplatin group. $^{\$}p<0.05$ and $^{\$\$}p<0.01$ as compared with the Dex7.5 group. $^{\text{ŦŦŦ}}p<0.001$ as compared with the Cit10 group, SEM: Standard error of means

Table 2. TAC and MDA levels in the study groups

Groups	TAC (mmol/L)	MDA (nmol/L)
Control	0.6 ± 0.02	1.64 ± 0.09
Cisplatin	0.54 ± 0.04	2.52 ± 0.28$^{\#\#}$
Dex7.5	0.58 ± 0.03	2.02 ± 0.3
Dex15	0.65 ± 0.03*	1.85 ± 0.16*
Dex30	0.66 ± 0.37	1.65 ± 0.06*
Cit10	0.57 ± 0.05	1.46 ± 0.08**
Cit20	0.75 ± 0.04*	1.73 ± 0.17*
Cit40	0.82 ± 0.04***	1.8 ± 0.15*
Dex + Cit	0.69 ± 0.05*	1.55 ± 0.21*

Data are presented as mean ± SEM. n: 8/each group. Dex: Dexamethasone, Cit10: Citicoline, Dex + Cit: Dexamethasone 7.5 mg/kg and citicoline 10 mg/kg. *$p<0.05$, ** $p<0.01$, and ***$p<0.001$ as compared with the cisplatin group. $^{\#\#}p<0.01$ as compared with the control group, SEM: Standard error of means, TAC: Total antioxidant capacity, MDA: Malondialdehyde

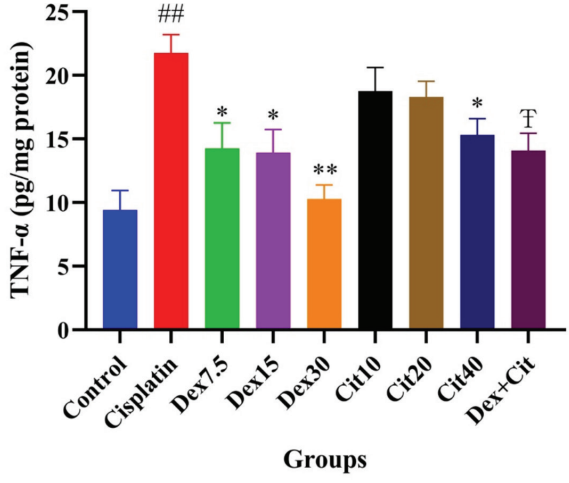

Figure 3. The levels of TNF-α in different groups. Data are presented as mean ± SEM (n: 8/each group)

*$p<0.05$ and **$p<0.01$ compared with the cisplatin group. $^{\#\#}p<0.01$ as compared with the control group. $^{\text{Ŧ}}p<0.05$ as compared with the Cit10 group, Dex: Dexamethasone, Cit: Citicoline, Dex + Cit: Dexamethasone 7.5 mg/kg and citicoline 10 mg/kg, SEM: Standard error of means, TNF-α: Tumor necrosis factor-α

DISCUSSION

The effectiveness of different doses of dexamethasone and citicoline on CisIPN in healthy male mice was evaluated. Administration of dexamethasone in different doses indicated a significant preventive effect on raising latency times at doses 7.5 and 15 mg/kg from the eleventh day, and in 30 mg/kg dose from the 25th day, compared with the cisplatin group. Citicoline in all doses significantly increased the latency time from the 11th day than the cisplatin group. Moreover, co-administration of dexamethasone and citicoline (Dex + Cit group) indicated their significant protective effects from the 11th day compared to the cisplatin and Cit10 groups; however, compared with the Dex7.5 group, a considerable difference was obtained only on the 28th day. Specifically, neither of the interventions (dexamethasone and citicoline) demonstrated a dose-dependent efficacy on latency time; nonetheless, their beneficial impacts on MDA and TAC levels were dose-dependent.

Conventional pharmacological treatments for CisIPN, including tricyclic antidepressants, some anticonvulsants (pregabalin and gabapentin), opioids, and non-steroidal anti-inflammatory drugs, present various side effects, and their efficacy remain unclear. Significantly, inflammation, oxidative stress, altered calcium channel activity, mitochondrial damage, and serotonergic system is associated mechanisms identified in developing CisIPN.[24]

In a study by Takasaki et al.[25] which examined the antagonist effects of glucocorticoid receptors on allodynia and hyperalgesia in mice-induced neuropathic pain, their results showed that dexamethasone exerted its anti-inflammatory and immunosuppressive effects *via* spinal glucocorticoid receptors that play a beneficial target in treating peripheral neuropathy. A meta-analysis study, which included 32 studies (2.697 patients), presented that dexamethasone partnered dosing could decline bortezomib-IPN severity.[26] Moattari et al.[27] found that dexamethasone enhanced sciatic nerve function, regeneration, and histomorphological characteristics followed by sciatic nerve dissection surgery. Additionally, retrospective analyses that included 190 patients demonstrated that dexamethasone could diminish CIPN severity.[28] Findings from a systematic review of dexamethasone combination therapy with thalidomide (12 studies, including 451 patients with multiple myeloma) indicated that dexamethasone could significantly reduce peripheral neuropathy.[29]

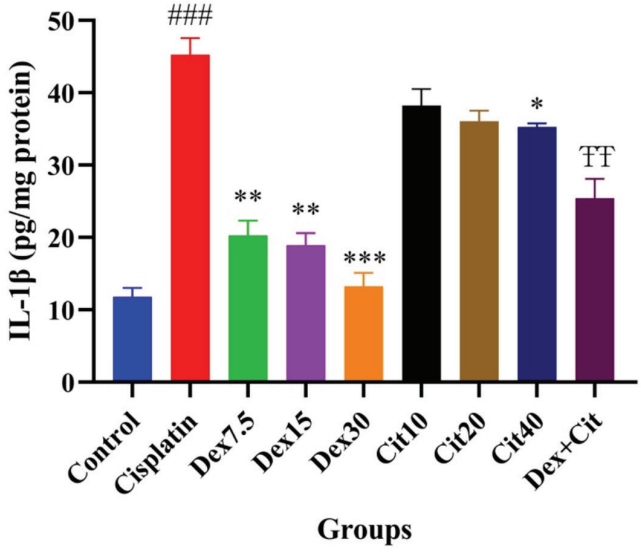

Figure 4. The IL-1β levels in different groups. Data are provided as mean ± SEM (n: 8/each group).

*p<0.05, **p<0.01, and ***p<0.001 compared with the cisplatin group. ###p<0.001 as compared with the control group. ŦŦp<0.01 as compared with the Cit10 group, Dex: Dexamethasone, Cit: Citicoline, Dex + Cit: Dexamethasone 7.5 mg/kg and citicoline 10 mg/kg, SEM: Standard error of means, IL-1β: Interleukin-1 beta

Numerous studies have implied that citicoline demonstrates its neuroprotective properties by increasing sirtuin-1,[30,31] acetylcholine,[32,33] and serotonin,[34] decreasing glutamate levels,[17] anti-inflammation activity *via* blocking phospholipase A2, and diminishing reactive oxygen species generation.[14] Besides, in an experiment using Bagdas et al.[35], they used the Randall-Sellito test to evaluate the pain threshold, which citicoline significantly elevated the pain threshold through central opioid receptors in a neuropathic pain rat model.

TAC has been used to determine antioxidant activity and response to generated free radicals in particular diseases. Low TAC levels could also be inferred from oxidative stress or enhanced exposure to oxidative stress-induced tissue injuries.[36] Additionally, MDA levels have been measured as the primary lipid peroxidation indicator, and its elevated levels are associated with cell damages.[37] Therefore, measuring TAC and MDA are essential factors for assessing the proposed interventions on CisIPN. Kamisli et al.[38] demonstrated that cisplatin triggered lipid peroxidation and diminished antioxidant defense mechanisms in the brain and sciatic nerve. In this study, cisplatin-enhanced MDA and reduced TAC levels may have induced decrement in antioxidant nerve cells' capacity. Alternatively, dexamethasone and citicoline in the relevant groups elevated TAC and diminished MDA levels compared with control and cisplatin groups, which exert profitable outcomes on CisIPN through antioxidant activities.

Considering the glucocorticoids' catabolic impact of on skeletal muscle,[39] it is not surprising that the Dex30 group (dexamethasone 30 mg/kg) demonstrated the lowest ΔW compared with other study groups. Moreover, the ΔW lessened in all cisplatin-treated groups (groups 2-9) compared with the control group, implying the induced weight loss by cisplatin in the above groups. Precisely, cisplatin activates the central nucleus of the amygdala, lateral parabrachial nucleus, and nucleus tractus solitarius neurons'; these regions may trigger weight loss through CGRP/glutamatergic signaling.[40] However, it remains unclear in the current study whether citicoline administration (Cit10, Cit20, Cit40, and Dex + Cit groups) presented a more diminished ΔW than the cisplatin group. Besides, we have not found any study that showed citicoline could attenuate body weights; interestingly, some studies have revealed that citicoline mitigated body weight loss.[41,42]

It has been indicated that proinflammatory cytokines such as IL-1β and TNF-α play a significant role in cisplatin-induced vestibular damage.[43] Also, their expression increased in cisplatin-induced peripheral nerve injuries, contributing to peripheral neuron excitability and sensitization by mediating tetrodotoxin-resistant sodium channels in nociceptors.[44,45] Following immune cell activation, IL-1β and TNF-α generate inflammation, they contribute to the development of peripheral sensitization by producing nerve growth factor and prostaglandin E_2, which triggers pain hypersensitivity in nociceptor dorsal root ganglion neurons. Therefore, inhibiting the synthesis or development of IL-1β and TNF-α exerts anti-inflammatory impacts and acts as an analgesic against inflammatory pain.[46] Our results demonstrated that cisplatin elevated IL-1β and TNF-α levels, and administration of dexamethasone and citicoline attenuated them in the treatment groups (Dex7.5, Dex15, Dex30, Cit10, Cit20, Cit40, and Dex + Cit), suggesting that they have potential activity against CisIPN.

This study revealed that cisplatin-enhanced MDA, TNF-α, and IL-1β levels; and it declined TAC and pain hypersensitivity; nevertheless, in the treatment groups, MDA and proinflammatory cytokines (IL-1β and TNF-α) diminished, and TAC and hypersensitivity to pain were elevated. The neuroprotective effect of dexamethasone and citicoline appears to be conferred *via* anti-inflammatory (declining IL-1β and TNF-α levels) and antioxidant (enhancing the antioxidative capacity and diminishing lipid peroxidation) activities. To our knowledge, this was the first attempt to apply dexamethasone and citicoline in CisIPN, and the evaluation of these two medications is assumed to be novel because they have not been administered for treating CisIPN.

CONCLUSION

The most critical finding of this research is that dexamethasone and citicoline administration, along with cisplatin, increased the latency time and TAC, declined TNF-α and IL-1β, and attenuated lipid peroxidation by reduced MDA levels. We observed that the relevant groups' proposed interventions were better than the control and cisplatin groups in all experiments. The experimental results conclude that since dexamethasone and citicoline have beneficial neuroprotective effects on CisIPN fundamental mechanisms, of clinical studies should be conducted to validate these effects in patients with CisIPN symptoms.

ACKNOWLEDGMENTS

The authors sincerely acknowledge the staff of Pharmacology Laboratory at Faculty of Pharmacy, Tabriz University of Medical Sciences, for supporting this study.

Ethics

Ethics Committee Approval: The study protocols and methods were authorized by Tabriz University of Medical Sciences Ethics Committee (ethical code: IR.TBZMED.VCR.REC.1398.087, May 13, 2019), conformed to the NIH Guide for the Care and Use of Laboratory Animals (8th edition, NRC 2011).

Informed Consent: Not applicable.

Peer-review: Externally peer-reviewed.

Authorship Contributions

Surgical and Medical Practices: F.M., Y.A., Concept: F.M., Y.A., J.M., Design: F.M., B.H.A., Data Collection or Processing: F.M., M.C., Analysis or Interpretation: F.M., B.H.A., Literature Search: F.M., Writing: F.M.

Conflict of Interest: No conflict of interest was declared by the authors.

Financial Disclosure: The authors declared that this study received no financial support.

REFERENCES

1. Authier N, Fialip J, Eschalier A, Coudoré F. Assessment of allodynia and hyperalgesia after cisplatin administration to rats. Neurosci Lett. 2000;291:73-76.
2. Seretny M, Currie GL, Sena ES, Ramnarine S, Grant R, MacLeod MR, Colvin LA, Fallon M. Incidence, prevalence, and predictors of chemotherapy-induced peripheral neuropathy: a systematic review and meta-analysis. Pain. 2014;155:2461-2470.
3. Glare PA, Davies PS, Finlay E, Gulati A, Lemanne D, Moryl N, Oeffinger KC, Paice JA, Stubblefield MD, Syrjala KL. Pain in cancer survivors. J Clin Oncol. 2014;32:1739-1747.
4. Streckmann F, Hess V, Bloch W, Décard BF, Ritzmann R, Lehmann HC, Balke M, Koliamitra C, Oschwald V, Elter T, Zahner L, Donath L, Roth R, Faude O. Individually tailored whole-body vibration training to reduce symptoms of chemotherapy-induced peripheral neuropathy: study protocol of a randomised controlled trial-VANISH. BMJ Open. 2019;9:e024467.
5. Li JQ, Chen SR, Chen H, Cai YQ, Pan HL. Regulation of increased glutamatergic input to spinal dorsal horn neurons by mGluR5 in diabetic neuropathic pain. J Neurochem. 2010;112:162-172.
6. Carozzi VA, Marmiroli P, Cavaletti G. The role of oxidative stress and anti-oxidant treatment in platinum-induced peripheral neurotoxicity. Curr Cancer Drug Targets. 2010;10:670-682.
7. Cavaletti G, Pezzoni G, Pisano C, Oggioni N, Sala F, Zoia C, Ferrarese C, Marmiroli P, Tredici G. Cisplatin-induced peripheral neurotoxicity in rats reduces the circulating levels of nerve growth factor. Neurosci Lett. 2002;322:103-106.
8. So H, Kim H, Lee JH, Park C, Kim Y, Kim E, Kim JK, Yun KJ, Lee KM, Lee HY, Moon SK, Lim DJ, Park R. Cisplatin cytotoxicity of auditory cells requires secretions of proinflammatory cytokines *via* activation of ERK and NF-kappaB. J Assoc Res Otolaryngol. 2007;8:338-355.
9. Bernhardson BM, Tishelman C, Rutqvist LE. Chemosensory changes experienced by patients undergoing cancer chemotherapy: a qualitative interview study. J Pain Symptom Manage. 2007;34:403-412.
10. Kolb NA, Smith AG, Singleton JR, Beck SL, Stoddard GJ, Brown S, Mooney K. The association of chemotherapy-induced peripheral neuropathy symptoms and the risk of falling. JAMA Neurol. 2016;73:860-866.
11. Al Moundhri MS, Al-Salam S, Al Mahrouqee A, Beegam S, Ali BH. The effect of curcumin on oxaliplatin and cisplatin neurotoxicity in rats: some behavioral, biochemical, and histopathological studies. J Med Toxicol. 2013;9:25-33.
12. Chtourou Y, Gargouri B, Kebieche M, Fetoui H. Naringin abrogates cisplatin-induced cognitive deficits and cholinergic dysfunction through

the down-regulation of AChE expression and iNOS signaling pathways in hippocampus of aged rats. J Mol Neurosci. 2015;56:349-362.

13. Guindon J, Deng L, Fan B, Wager-Miller J, Hohmann AG. Optimization of a cisplatin model of chemotherapy-induced peripheral neuropathy in mice: use of vitamin C and sodium bicarbonate pretreatments to reduce nephrotoxicity and improve animal health status. Mol Pain. 2014;10:56.
14. Adibhatla RM, Hatcher JF. Citicoline decreases phospholipase A2 stimulation and hydroxyl radical generation in transient cerebral ischemia. J Neurosci Res. 2003;73:308-315.
15. Gonzalez-Rodriguez PJ, Li Y, Martinez F, Zhang L. Dexamethasone protects neonatal hypoxic-ischemic brain injury *via* L-PGDS-dependent PGD2-DP1-pERK signaling pathway. PLoS One. 2014;9:e114470.
16. Han SR, Yeo SP, Lee MK, Bae YC, Ahn DK. Early dexamethasone relieves trigeminal neuropathic pain. J Dent Res. 2010;89:915-920.
17. Hurtado O, Moro MA, Cárdenas A, Sánchez V, Fernández-Tomé P, Leza JC, Lorenzo P, Secades JJ, Lozano R, Dávalos A, Castillo J, Lizasoain I. Neuroprotection afforded by prior citicoline administration in experimental brain ischemia: effects on glutamate transport. Neurobiol Dis. 2005;18:336-345.
18. Jasielski P, Piędel F, Piwek M, Rocka A, Petit V, Rejdak K. Application of citicoline in neurological disorders: a systematic review. Nutrients. 2020;12:3113.
19. Sun WH, He F, Zhang NN, Zhao ZA, Chen HS. Time dependent neuroprotection of dexamethasone in experimental focal cerebral ischemia: the involvement of NF-κB pathways. Brain Res. 2018;1701:237-245.
20. Bannon AW, Malmberg AB. Models of nociception: hot-plate, tail-flick, and formalin tests in rodents. Curr Protoc Neurosci. 2007;chapter 8: unit 8.9.
21. Miller NJ, Rice-Evans C, Davies MJ, Gopinathan V, Milner A. A novel method for measuring antioxidant capacity and its application to monitoring the antioxidant status in premature neonates. Clin Sci (Lond). 1993;84:407-412.
22. Ohkawa H, Ohishi N, Yagi K. Assay for lipid peroxides in animal tissues by thiobarbituric acid reaction. Anal Biochem. 1979;95:351-358.
23. Najafi M, Noroozi E, Javadi A, Badalzadeh R. Anti-arrhythmogenic and anti-inflammatory effects of troxerutin in ischemia/reperfusion injury of diabetic myocardium. Biomed Pharmacother. 2018;102:385-391.
24. Sisignano M, Baron R, Scholich K, Geisslinger G. Mechanism-based treatment for chemotherapy-induced peripheral neuropathic pain. Nat Rev Neurol. 2014;10:694-707.
25. Takasaki I, Kurihara T, Saegusa H, Zong S, Tanabe T. Effects of glucocorticoid receptor antagonists on allodynia and hyperalgesia in mouse model of neuropathic pain. Eur J Pharmacol. 2005;524:80-83.
26. Kumar SK, Laubach JP, Giove TJ, Quick M, Neuwirth R, Yung G, Rajkumar SV, Richardson PG. Impact of concomitant dexamethasone dosing schedule on bortezomib-induced peripheral neuropathy in multiple myeloma. Br J Haematol. 2017;178:756-763.
27. Moattari M, Moattari F, Kaka G, Mohseni Kouchesfehani H, Sadraie SH, Naghdi M, Mansouri K. Evaluation of dexamethasone treated mesenchymal stem cells for recovery in neurotmesis model of peripheral nerve injury. Neurol Res. 2018;40:1060-1070.
28. Kanbayashi Y, Hosokawa T, Okamoto K, Konishi H, Otsuji E, Yoshikawa T, Takagi T, Taniwaki M. Statistical identification of predictors for peripheral neuropathy associated with administration of bortezomib, taxanes, oxaliplatin or vincristine using ordered logistic regression analysis. Anticancer Drugs. 2010;21:877-881.
29. von Lilienfeld-Toal M, Hahn-Ast C, Furkert K, Hoffmann F, Naumann R, Bargou R, Cook G, Glasmacher A. A systematic review of phase II trials of thalidomide/dexamethasone combination therapy in patients with relapsed or refractory multiple myeloma. Eur J Haematol. 2008;81:247-252.
30. Herskovits AZ, Guarente L. SIRT1 in neurodevelopment and brain senescence. Neuron. 2014;81:471-483.
31. Hurtado O, Hernández-Jiménez M, Zarruk JG, Cuartero MI, Ballesteros I, Camarero G, Moraga A, Pradillo JM, Moro MA, Lizasoain I. Citicoline (CDP-choline) increases sirtuin1 expression concomitant to neuroprotection in experimental stroke. J Neurochem. 2013;126:819-826.
32. Blusztajn JK, Slack BE, Mellott TJ. Neuroprotective actions of dietary choline. Nutrients. 2017;9:815.
33. Synoradzki K, Grieb P. Citicoline: a superior form of choline? Nutrients. 2019;11:1569.
34. Roohi-Azizi M, Torkaman-Boutorabi A, Akhondzadeh S, Nejatisafa AA, Sadat-Shirazi MS, Zarrindast MR. Influence of citicoline on citalopram-induced antidepressant activity in depressive-like symptoms in male mice. Physiol Behav. 2018;195:151-157.
35. Bagdas D, Sonat FA, Hamurtekin E, Sonal S, Gurun MS. The antihyperalgesic effect of cytidine-5'-diphosphate-choline in neuropathic and inflammatory pain models. Behav Pharmacol. 2011;22:589-598.
36. Young IS. Measurement of total antioxidant capacity. J Clin Pathol. 2001;54:339.
37. Parlakpinar H, Tasdemir S, Polat A, Bay-Karabulut A, Vardi N, Ucar M, Acet A. Protective role of caffeic acid phenethyl ester (cape) on gentamicin-induced acute renal toxicity in rats. Toxicology. 2005;207:169-177.
38. Kamisli S, Ciftci O, Kaya K, Cetin A, Kamisli O, Ozcan C. Hesperidin protects brain and sciatic nerve tissues against cisplatin-induced oxidative, histological and electromyographical side effects in rats. Toxicol Ind Health. 2015;31:841-851.
39. Bodine SC, Furlow JD. Glucocorticoids and skeletal muscle. Adv Exp Med Biol. 2015;872:145-176.
40. Alhadeff AL, Holland RA, Nelson A, Grill HJ, De Jonghe BC. Glutamate receptors in the central nucleus of the amygdala mediate cisplatin-induced malaise and energy balance dysregulation through direct hindbrain projections. J Neurosci. 2015;35:11094-11104.
41. Knippenberg S, Skripuletz T, Rath KJ, Thau N, Gudi V, Pul R, Körner S, Dengler R, Stangel M, Petri S. CDP-choline is not protective in the SOD1-G93A mouse model of ALS. Amyotroph Lateral Scler Frontotemporal Degener. 2013;14:284-290.
42. Qian K, Gu Y, Zhao Y, Li Z, Sun M. Citicoline protects brain against closed head injury in rats through suppressing oxidative stress and calpain over-activation. Neurochem Res. 2014;39:1206-1218.
43. Kim HJ, So HS, Lee JH, Park C, Lee JB, Youn MJ, Kim SJ, Yang SH, Lee KM, Kwon KB, Park BH, Park R. Role of proinflammatory cytokines in cisplatin-induced vestibular hair cell damage. Head Neck. 2008;30:1445-1456.
44. Elmarakby AA, Sullivan JC. Relationship between oxidative stress and inflammatory cytokines in diabetic nephropathy. Cardiovasc Ther. 2012;30:49-59.
45. Jin X, Gereau RW. Acute p38-mediated modulation of tetrodotoxin-resistant sodium channels in mouse sensory neurons by tumor necrosis factor-alpha. J Neurosci. 2006;26:246-255.
46. Binshtok AM, Wang H, Zimmermann K, Amaya F, Vardeh D, Shi L, Brenner GJ, Ji RR, Bean BP, Woolf CJ, Samad TA. Nociceptors are interleukin-1beta sensors. J Neurosci. 2008;28:14062-14073.

Turk J Pharm Sci 2022;19(5):513-520
DOI: 10.4274/tjps.galenos.2021.47855

ORIGINAL ARTICLE

Tableting Performance of Maize and Potato Starches Used in Combination as Binder/ Disintegrant in Metronidazole Tablet Formulation

Yonni Eshovo APEJI*, Rejoice Thomas KAIGAMA, Sani Hadi IBRAHIM, Sophie Nock ANYEBE, Aisha Ohunene ABDUSSALAM, Avosuahi Rukayat OYI

Ahmadu Bello University, Department of Pharmaceutics and Industrial Pharmacy, Zaria, Nigeria

ABSTRACT

Objectives: This study aimed to characterize the tableting performance of maize and potato starches, when used in combination either as a disintegrant or binder in solid dosage form development.

Materials and Methods: Wet granulation was used to process metronidazole granules incorporating either maize starch, potato starch, or a combination of the two starches as binders or disintegrant at 10% $^{w}/_{w}$. Granule analysis was carried out on the various formulations and subsequently compressed into tablets weighing approximately 500 mg following the addition of extragranular excipients. Tablet properties were assessed after 24 h of storage.

Results: Analysis of granule properties did not reveal a wide variation across the formulations irrespective of the type and combination of starches used in the formulation either as binder or disintegrant. It was observed, however, that there were slight differences in particle size, bulk and tapped densities of granule formulations containing the combined starch as excipients compared to granule formulations containing individual starch as the excipient. Tablets prepared using the combined starches as binder had lower tensile strength and disintegration time compared to other formulations incorporating the individual starches as binders. However, when evaluated as disintegrant, the tablet formulation containing the combined starches produced tablets with relatively lower disintegration time compared to formulations containing the individual starches as disintegrant.

Conclusion: The study concludes that the combination of maize and potato starches as excipients in tablet formulation influenced the outcome of granule and tablet properties.

Key words: Maize starch, potato starch, binder, disintegrant, tablet, excipient

INTRODUCTION

With regard to oral drug delivery, tablets remain the most commonly prescribed dosage form among health practitioners and this is simply because tablets are easy to administer, relatively stable and less cumbersome to handle compared to other dosage forms like liquid formulations and parenteral.[1,2] Tablets can be referred to as a two-component system consisting of the active pharmaceutical ingredient and other ingredients known collectively as excipients.[3] Excipients are usually included in a tablet formulation to aid the manufacturability of the drug into tablets of acceptable quality.[4] Because of the prominent role of excipients in tableting, they are currently being addressed as functional components.[5]

Though inert, most excipients possess some degree of functionality that makes it possible for drugs not only to be processed into solid compacts but also to ensure that the tablet releases the drug timely to exert its action in the body.[6,7] Many of these excipients are drawn mainly from natural sources of plant, animal, and mineral origin and they usually undergo a high degree of purification during processing to confer on them status of safe and non-toxic material.[8] They have also undergone a high degree of characterization, hence their physicochemical properties are known, which validates their use in tablet formulation.[9,10]

Currently, starch is listed as one of the most commonly used excipients in tablet formulation. Starch is obtained from a wide

*Correspondence: yehonathanapeji@gmail.com, Phone: +2348052622947, ORCID-ID: orcid.org/0000-0002-3116-7570
Received: 31.05.2021, Accepted: 22.10.2021

variety of sources, which including cereals and tuber crops.[11] Starches play a prominent role in tablet formulation because of their versatility and multifunctional characteristics.[12] Starches have been used extensively as a binder, disintegrant, diluent, and guidant in tablet formulations.[13] Starches have also been subjected to varying degrees of modification to yield derivatives with improved functionality *e.g.* pregelatinized starch.[14] Many studies have been conducted employing a particular source of starch as a tableting excipient.[14-17]

Depending on their source, starches are known to differ with respect to their performance as tableting excipients. Many studies have compared the tableting properties of starches from different sources and discovered differences that were statistically significant ($p<0.05$). A study conducted by Olayemi et al.[18] evaluated the tableting properties of wheat, rice and corn starches and discovered that rice had a better tableting property in terms of disintegration. Hence, most studies in the past have employed the use of starch from a single source in tablet formulation. Very few studies have been conducted to explore the combination of starches from various sources in tablet formulation. Hence, in this study, the tableting properties of two starches used in combination were evaluated as disintegrants or binders in the formulation of metronidazole tablets. Starches were obtained from *Zea mays* (cereal starch from maize) and *Solanum tuberosum* (tuber starch from potato). These starches were combined in equal proportion and used as either a binder or disintegrant in metronidazole tablets prepared by wet granulation.

MATERIALS AND METHODS

Materials

Metronidazole (Hopkin and Williams, New Delhi, India), maize starch (Burgoyne Burbidge & Co. India, Mumbai), potato starch (Roquette Pharma, France), acacia (Kerry EMEA region, Draycott mills, Glos. GL115NA, UK), lactose, croscarmellose sodium (DFE pharma, Klever strasse 187, D-47574 Koch, Germany), colloidal silicon dioxide (Evonik Industries, Germany), sodium stearyl fumarate (JRS Pharma GmbH CO.KG, 73494, Rosenberg, Germany) were purchased from their respective companies. All other chemicals used were of pharmaceutical grade.

Methods

Preparation of metronidazole tablets

Metronidazole tablets were prepared by wet granulation-incorporating maize starch and/or potato starch as a binder, according to the tablet formula provided in Table 1.

Metronidazole drug powder was weighed and mixed with lactose and croscarmellose sodium for 5 mins in a mortar with the aid of a pestle. Maize starch paste was prepared as a binder and incorporated into the powder mix to facilitate binding and formation of granules. The wet mass of the powder mix was force-screened through a sieve of 1.6 mm to generate granules and then placed in the oven to dry at 40˚C for 20 min to allow for partial drying. The partially dried granules were passed through another sieve of 1 mm and then returned to the oven for complete drying at 40˚C for 1 h. The dried granules were then kept away in a safe place for further studies. Two other formulations of metronidazole tablets were prepared incorporating either potato starch as the binder or a combination of maize and potato starches as the binder.

The entire process was repeated to prepare three formulations of metronidazole tablets incorporating maize starch and/or potato starch as disintegrants according to the tablet formula given in Table 1.

The granules obtained above were characterized for their physicochemical properties, lubricated with extragranular excipients, and compressed into tablets weighing ~500 mg on an Erweka tablet press using 12 mm punch and die set. The tablets were allowed to relax upon storage and their properties were evaluated after 24 h.

Particle size analysis

The mean granule size (MGS) for each granule formulation was obtained by sieve analysis. A representative quantity of

Table 1. Tablet formula for formulations I-VI

	Formulations containing starches as binders			Formulations containing starches as disintegrants		
Ingredients	**I**	**II**	**III**	**IV**	**V**	**VI**
Metronidazole (40%)	30	30	30	30	30	30
Lactose (40%)	30	30	30	30	30	30
Maize starch (5, 10%)	7.5	-	3.75	7.5	-	3.75
Potato starch (5, 10%)	-	7.5	3.75	-	7.5	3.75
Cros sod (5%)	3.75	3.75	3.75	-	-	-
Acacia (5%)	-	-	-	3.75	3.75	3.75
CSD (4%)	3	3	3	3	3	3
SSF (1%)	0.75	0.75	0.75	0.75	0.75	0.75

I-III: Formulations containing starches as binders
IV-VI: Formulations containing starches as disintegrants
Cros sod: Croscarmellose sodium, CSD: Colloidal silicon dioxide, SSF: Sodium stearyl fumarate

the granules was poured into a nest of sieves arranged in descending order (1000 µm, 710 µm, 300 µm, 180 µm, 125 µm, and pan) and agitated for 10 mins in the Endecott test sieve shaker. The fraction of granules recovered from each sieve was weighed out and the MGS was computed using equation 1 below:

$$MGS = \frac{[\Sigma(\%\, retained) \times (sieve\ size)]}{100} \quad \text{equation (1)}$$

Microscopy

Each sample of granule formulation was viewed under a light microscope and the images of the granules were captured using a digital camera. Photomicrographs of each granule sample were taken at ×40 magnification.

Angle of repose (AoR)

The fixed funnel method was used to measure the AoR of granules.[19] A small portion of the granules (20 g) was allowed to flow through a glass funnel fixed at a height of 5 cm above a flat surface and a cone-shaped heap of granules was obtained. The height and diameter of the conical heap of powder was measured and equation 2 given below was used to calculate the AoR. The AoR was reported as the mean of three replicates for each formulation.

$$Tan\,\theta = \frac{h}{r} \quad \text{equation (2)}$$

Where *h* is the height of the powder, *r* is the radius of the circular base and θ is the AoR.

Bulk and tapped densities

Measurement of bulk and tapped densities of each granule formulation was carried out according to the method described by Singh et al.[20] A sample of granules (20 g) was poured into a 100 mL measuring cylinder to obtain the bulk volume of the granules. The cylinder was then tapped to a constant volume and the volume was recorded as the tapped volume. This was repeated two more times for each granule formulation. Equations 3 and 4 given below were used to calculate bulk and tapped densities, respectively.

$$Bulk\ density\ (BD) = \frac{Mass\ of\ granules}{Bulk\ volume (BV)} \quad \text{equation (3)}$$

$$Tapped\ density\ (TD) = \frac{Mass\ of\ granules}{Tapped\ volume\ (TV)} \quad \text{equation (4)}$$

Carr's index (CI) and Hausner's ratio (HR) were obtained using the equations 5 and 6 below:

$$CI = \frac{TD - BD}{TD} \times 100 \quad \text{equation (5)}$$

$$HR = \frac{TD}{BD} \quad \text{equation (6)}$$

Moisture content (MC) determination

The residual MC of granules was determined using gravimetric analysis. A portion of the granules (1 g) was sampled for each formulation and dried to a constant weight in the hot-air oven at 105°C. MC was then calculated using equation 7 below:

$$\%\, MC = \frac{Initial\ weight - Final\ weight}{Initial\ weight} \times 100\,\% \quad \text{equation (7)}$$

Weight variation tests

The weights of 20 tablets selected at random for each formulation were obtained using an electronic scale. The mean tablet weight was calculated and recorded with the standard deviation.

Content uniformity test

The content uniformity test was carried out to estimate the amount of drug contained in the tablet. The weight of 5 tablets was obtained and powdered using a mortar and pestle. An equivalent weight of one tablet was weighed out from the powdered mass and dissolved in 100 mL of 0.1 N HCl. The mixture was filtered and a dilution of the solution (1 in 100) was prepared with 0.1 N HCl before the absorbance reading was taken at 277 nm using the ultraviolet (UV) spectrophotometer. The percentage drug content was calculated using the straight-line equation, $y = 0.0395x + 0.1314$, generated for the calibration curve of metronidazole, where *y* is the absorbance and *x* is drug concentration (µg/mL).

Tensile strength

The force required to fracture a tablet along its diameter was measured using a Monsanto hardness tester. A mean of 5 determinations was obtained and recorded with its standard deviation. The tensile strength of each tablet formulation was resolved using equation 8 below.

$$TS = \frac{2F}{\pi dt} \quad \text{equation (8)}$$

Where *F* is the breaking force, *d* is the diameter and *t* is the thickness.

Tablet friability

Tablet friability was obtained for each tablet formulation using the Friabilator machine. Ten tablets were sampled at random, and their collective weight was obtained by weighing on an electronic scale. The tablets were transferred into the friabilator, which was allowed to revolve for 4 min at 25 rpm. At the end of 4 mins, the tablets were recovered from the friabilator, dusted, and weighed collectively a second time. Friability was computed as the percent loss in weight using equation 9 below.

$$Friability = \frac{Initial\ weight - Final\ weight}{Initial\ weight} \times 100\,\% \quad \text{equation (9)}$$

Disintegration test

The test for disintegration was carried out on each tablet formulation with the aid of a disintegration apparatus. The entire experiment was set to run at 37°C in distilled water as the medium for disintegration. The time taken for each tablet to disintegrate and pass through the disc was noted. The mean of six replicates was recorded for each formulation.

In vitro dissolution studies

Drug release profile of each tablet formulation was assessed using 0.1 N HCl as sample medium for dissolution. A single tablet was placed in a basket and immersed in a beaker containing 900 mL of 0.1 N HCl regulated at 37°C and allowed to rotate at 100 rpm. Portions (5 mL) were withdrawn intermittently at 5, 10, 20, 30, 45, and 60 mins, respectively, and replaced with an equal volume of 0.1 N HCl after each withdrawal. The collected samples were filtered and sufficiently diluted with 0.1 N HCl before taking the absorbance readings at 277 nm using the UV spectrophotometer (UV-1800 Spectrophotometer, Shimadzu Corporation, USA). The amount of drug released (%) was calculated based on the equation, $y = 0.0395x + 0.1314$, derived from the calibration curve of metronidazole and a plot against time was generated for the six formulations.

Statistical analysis

No statistical analysis was carried out of the results obtained.

RESULTS AND DISCUSSION

Granule properties

Granule properties of formulations containing starches as binders (I-III) are presented in Table 2. Particle size of granules represented as MGS ranged from 309.74 349.69 µm with formulations II and III having the least and largest MGS, respectively. Although, the MGS did not appear to differ significantly across the granule formulations, it was observed that formulation III granules that combined the two starches in equal proportion as a binder had the highest MGS. This can be attributed to the combined cohesive effect of both starches as binders put together. Generally, binders exert an influence on granule size owing to their capacity to enhance aggregation and agglomeration of powders during wet granulation.[21] This is consistent with the findings of Abdallah et al.[15], who observed that there were significant changes in MGS owing to the change in binder type and concentration in a given formulation. The flowability of granules as assessed by measuring the AoR shows that the results of this parameter ranged from 30.32-34.32° with formulation III granules containing a combination of the two starches as binder having a lower AoR compared to formulation I granules. This is a requirement for the successful formulation of robust tablets. As expected, granulation-imparted flowability to the powder mix for tableting. Generally, lower AoR corresponds to an improvement in the flow of granules and powders and this can be attributed to the increase in particle size which was observed in formulation III granules. With respect to flowability of granules and powders, there is interplay of forces including particle size and shape of granules that combine to define the flowability of the granules.[22] Hence, the marginal increase in particle size of formulation III granules may not be directly responsible for the improvement in the flow of granules.

There was a marginal increase in the bulk and tapped densities of formulation III granules containing both starches as binders, suggesting an improvement in the compressibility of granules. This can be attributed to the combined effect of both starches as binders in the formulation resulting in a greater degree of cohesion and subsequently densification during compression.[23] High bulk density corresponds to a greater degree of volume reduction because of decrease in porosity and closer packing of granules.[24] Other parameters like CI and HR did not follow the same relationship as seen with the AoR. However, the values obtained for both parameters confirmed that granules have acceptable flowability. This is based on the requirement that CI and HR should not exceed 20% and 1.2 respectively for good powder and granule flowability.[25] This agrees with the findings of Oyi et al.[26], where the flowability of granules was confirmed to be excellent owing to the low values of CI and HR, respectively.

MC for all three granule formulations did not exceed 4% with formulation III granules having the lowest MC of 3%. Studies have shown that MC is implicated in the flowability of powders and granules and so it is imperative to optimize MC to ensure acceptable flow of granules. This agrees with the findings of Emery[27], whose studies confirmed the role of

Table 2. Granule properties of formulations I-VI

	Formulations containing starch as binder			Formulations containing starch as a disintegrant		
Granule parameters	**I**	**II**	**III**	**IV**	**V**	**VI**
Mean granule size (µm)	337.18	309.74	349.69	386.41	369.73	371.02
Angle of repose (º)	32.32 ± 0.15	30.32 ± 0.58	30.50 ± 0.82	28.66 ± 0.38	29.31 ± 0.37	29.40 ± 0.42
Bulk density (g/cm^3)	0.41 ± 0.01	0.43 ± 0.01	0.44 ± 0.01	0.49 ± 0.01	0.60 ± 0.01	0.64 ± 0.01
Tapped density (g/cm^3)	0.46 ± 0.01	0.51 ± 0.02	0.52 ± 0.01	0.58 ± 0.01	0.70 ± 0.02	0.70 ± 0.02
Carr's index (%)	10.29 ± 2.77	15.22 ± 0.47	15.39 ± 0.24	14.82 ± 0.26	14.93 ± 0.32	9.53 ± 0.21
Hausner's ratio	1.12 ± 0.03	1.18 ± 0.01	1.18 ± 0.00	1.17 ± 0.00	1.18 ± 0.00	1.11 ± 0.00
Moisture content (%)	4	4	3	3	3	2

MC in defining the flowability of a formulation designed for tableting. MC did not differ significantly across the granule formulations, implying that granulation and drying conditions were kept constant.

Photomicrographs of granule formulations (I-III) are displayed in Figure 1. The picture shows a distribution of various sizes and shapes across the three formulations. The photomicrograph did not show a clear distinction as to distinguish each granule formulation, implying that the type of binder used may not have a significant effect on the morphology of granules considering that the binders used had some degree of similarity except for the source of starch. Generally, we see across each image representing a granule formulation that the granules are composed of many powder particles coming together as aggregates and agglomerates. This is essentially the reason for granulation to improve the flowability and compressibility of powders induced by the cohesive effect of binders.[24,28,29] This is consistent with the normal distribution of particle sizes in granules produced by wet granulation.[30] The differences observed in the granule properties were minimal across the three formulations. These slight differences could be attributed to the composition of each formulation as they differed in their binder content. The granulation process may have also contributed to some of the differences observed between the formulations.

Granule properties of formulations containing starch as disintegrant (IV-V) are also presented in Table 2. MGS for the formulations ranges from 371.02-386.41 µm with formulations IV and V having the highest and least MGS. The particle size of the formulations did not appear to differ significantly, however, it was observed that formulation VI containing the combined starches as disintegrant had a relatively similar MGS with formulation V granules, but was lower than that of formulation IV. This implies therefore that the combined effect of both starches as disintegrants did not promote an increase in MGS of granules, as was seen in formulation III, when both starches were incorporated as binders. This may be because incorporating starches as disintegrants promotes disaggregation and fragmentation rather than aggregation and agglomeration, which increases MGS.[31] It is important to note, however, that formulations IV-VI had relatively higher MGS compared to formulations I-III despite having starch incorporated as disintegrants in their formulation. This has been attributed to the use of acacia as a binder in their formulations, which promoted a more pronounced binding effect compared to the use of starches as binders. Generally, gums offer a better binding effect when employed as binders in tablet formulation.[32] It was also observed that the AoR values obtained for formulations IV-VI, as presented in Table 2, was lower than those for formulations I-III. This can be attributed to the larger MGS of formulation IV-VI granules, which directly influences the flow of granules.

The bulk and tapped density values of formulation VI containing both starches as disintegrants were relatively higher compared to formulations IV and V, implying a greater degree of densification occurring in the granules during tapping, which simulates the application of force during compression. This has also been attributed to the MGS of formulation VI granules, which was lower compared to formulation IV. As revealed by other studies, small-sized granules generally facilitate a greater degree of densification because of the ability of the small particles to fill in pore spaces, thereby reducing the porosity and volume occupied by the densely packed granules.[33]

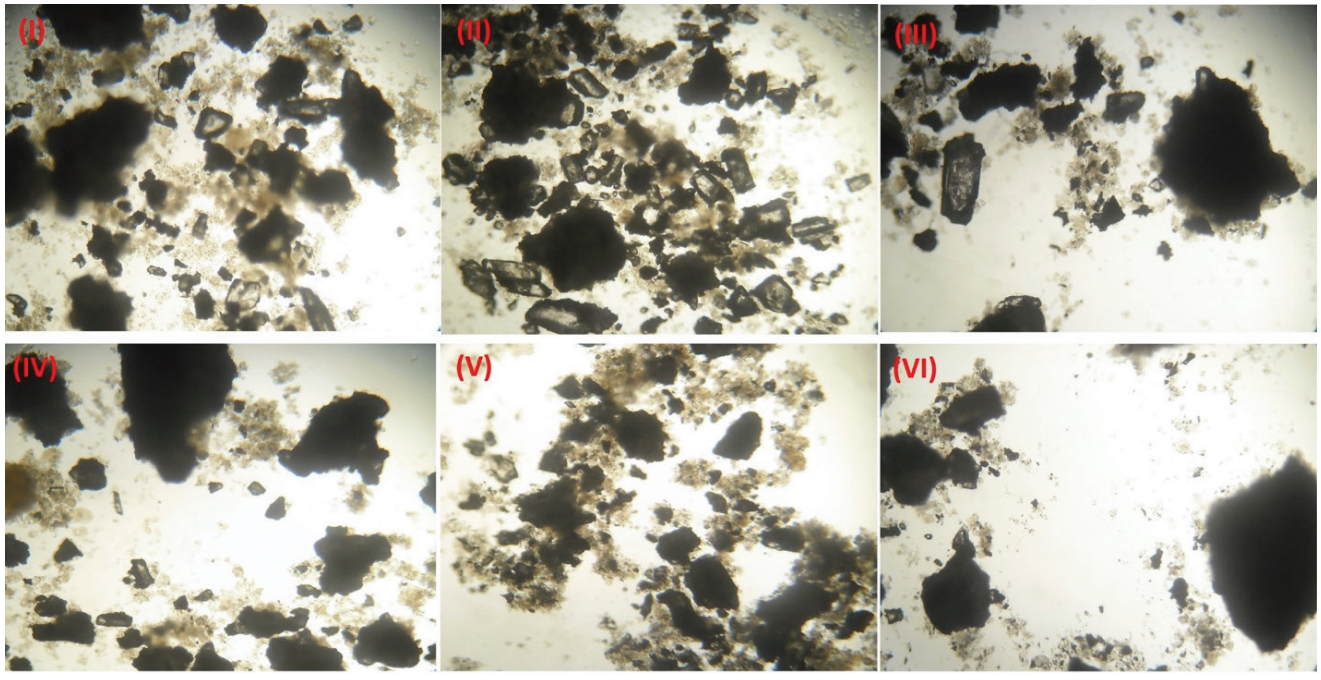

Figure 1. Photomicrographs of granule formulation (I-VI)

The values of CI and HR (Table 2) for formulations IV-VI were consistent with free flowing granules as they ranged from 9.53-14.82% and 1.11-1.18, respectively. MC did not reveal any much difference across formulations IV-VI as it ranged from 2-3%. However, formulation VI containing both starches as disintegrants had a lower MC of 2%. Photomicrographs of formulation IV-VI granules displayed in Figure 1 show similar morphology across the formulations. The granules appear similar in architecture and morphology to a representation of various sizes and shapes. The appearance of the granules does not appear to have been affected significantly by the difference in formulation of granules with respect to the starch type and composition. This implies therefore that the inclusion of excipients in a formulation will exert its effect primarily within the internal structure of the granulation and not necessarily on the external aspects of the granulation. Modification of the external appearance of granules may occur when extragranular excipients are incorporated before tableting.

Physical properties of metronidazole tablets

Tablet properties of formulations I-VI are presented in Table 3. The mean tablet weight of formulations I-III ranged from 490-521 mg, with formulation III having the highest mean tablet weight. This may be related to the larger MGS of formulation III granules, which may have caused preferential filling of the die cavity with large sized granules producing oversized tablets. This is consistent with the findings of Tan et al.[34], who evaluated the effect of granule size on tablet weight variation. Content uniformity of the three tablet formulations reflected the mean tablet weight as formulation III tablets had the highest percentage drug content compared to the other two formulations. This also agrees with the findings of Zaid et al.[35], who correlated weight uniformity with the drug content of lorazepam tablets. The tensile strength of tablets ranged from 0.49-1.14 MPa with formulation II tablets containing potato starch as the binder having the highest mean tensile strength of 1.14 MPa. This is consistent with the report of Szepes[13] in a review published in 2009, where potato starch is described as having multifunctional properties including diluent, binder and disintegrant properties. Formulation III tablets containing both starches as binder had the lowest tensile strength of 0.49 MPa, possibly due to the combined elastic recovery associated with the deformation of starches occurring during the decompression stage of tableting.[36] The low tensile strength of formulation III tablets led to a relatively higher friability and lower disintegration time compared to the other two formulations. This was expected as the low tensile strength of tablets implies that the tablets are brittle and porous in microstructure, thereby facilitating rapid ingress of water leading to fast disintegration.[37] Drug-release profiles shown in Figure 2a. The time taken to release 80% of the drug was under 10 mins for all three formulations. All the formulations therefore passed the test for dissolution as more than 70% of the drug was released in 45 mins.

Tablet properties of formulations IV-VI as presented in Table 3 shows a greater degree of uniformity in tablet weight, possibly due to the excellent flowability of granules, confirmed by the flow indices of AoR, CI and HR. The percentage drug content of all three formulations, however, appeared high, exceeding the recommended range of 95-105% as *per* BP requirements.[38] The tensile strength of tablets ranged from 1.02-1.84 MPa, with formulation VI having the least tensile strength. This could be attributed to the combined effect of both starches exerting their effect as a disintegrant, thereby hindering the formation of interparticulate bonds during compression.[39] Friability and disintegration results were consistent with the tensile strength values recorded across the three formulations (IV-VI) as higher tensile strength of tablets (formulation IV) produced less friable tablets, which took a longer time to disintegrate. Comparing the disintegrant properties of both starches, formulation V tablets containing potato starch as the disintegrant disintegrated faster compared to formulation IV tablets containing maize starch as disintegrant. However, when both starches were combined as disintegrant in formulation VI tablets, the disintegration time was lowered compared to either of the formulations containing the different starches as disintegrant. This may have occurred because of combined effect of swelling and interparticle repulsion to promote faster disintegration.[31]

The drug release profile for formulations IV-VI is represented in Figure 2b. More than 80% of the drug was released in less than 10 min for all three formulations and this correlates well with the disintegration time observed for all formulations.

Table 3. Tablet properties of formulations I-VI

	Formulations containing starch as binder			Formulations containing starch as a disintegrant		
Tablet parameters	**I**	**II**	**III**	**IV**	**V**	**VI**
Mean weight (mg)	490.7 ± 5.46	495.05 ± 3.17	521.9 ± 4.85	499.75 ± 6.82	498.35 ± 7.97	498.60 ± 4.25
Content uniformity (%)	103.5	101.2	114.6	114	112	110
Tensile strength (MN/m^2)	0.99 ± 0.17	1.14 ± 0.05	0.49 ± 0.06	1.84 ± 0.01	1.25 ± 0.05	1.02 ± 0.06
Friability (%)	0.8	0.8	0.9	0.81	0.81	0.60
Disintegration time (min)	0.7 ± 0.19	0.83 ± 0.12	0.30 ± 0.03	14.92 ± 0.20	11.33 ± 1.51	10.83 ± 1.72

MN: Meganewton

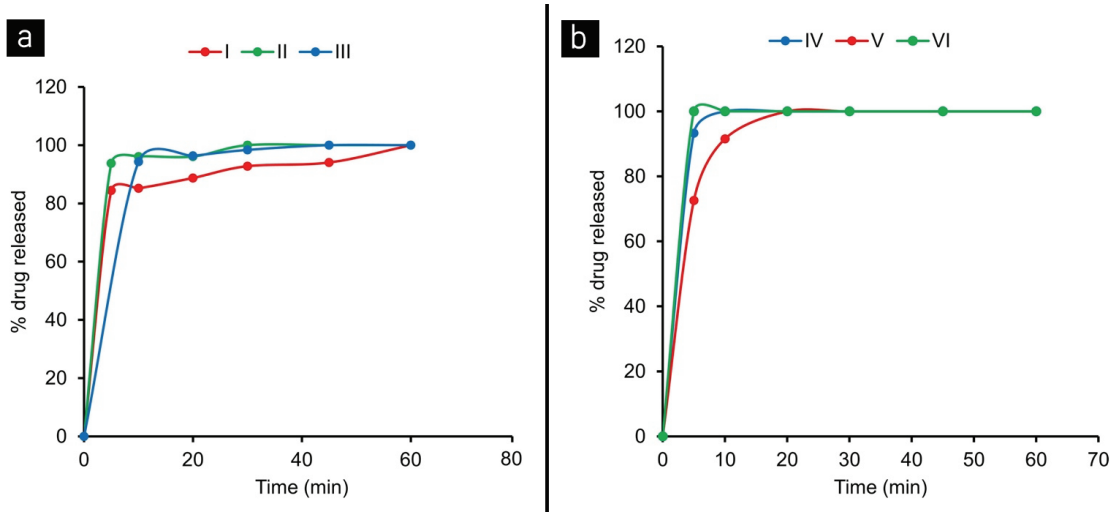

Figure 2. Dissolution profiles for (a) formulations I-III (b) formulations IV-VI

CONCLUSION

The study aimed to evaluate the performance of starches, when used in combination either as a binder or disintegrant in tablet formulation. The outcome of the study shows that combining maize starch and potato starch in equal proportion as a binder did not yield a superior performance compared to the performance of the individual starches in formulation as a binder. However, when both starches where combined in the same proportion as a disintegrant in tablet formulation, they gave a better performance in terms of faster disintegration compared to the performance of the individual starches as disintegrant in a tablet formulation. This implies, therefore, that combining starches of different sources as a tableting excipient may most likely influence its functionality in tablet formulation.

Ethics

Ethics Committee Approval: Not applicable.

Informed Consent: Not applicable.

Peer-review: Externally peer-reviewed.

Authorship Contributions

Concept: Y.E.A., R.T.K., S.H.I., Design: Y.E.A., R.T.K., S.H.I., Data Collection or Processing: R.T.K., S.H.I., Analysis or Interpretation: Y.E.A., R.T.K., S.H.I., S.N.A., A.O.A., A.R.O., Literature Search: R.T.K., S.H.I., Writing: Y.E.A., R.T.K., S.H.I., S.N.A., A.O.A., A.R.O.

Conflict of Interest: No conflict of interest was declared by the authors.

Financial Disclosure: The authors declared that this study received no financial support.

REFERENCES

1. Mohan S. compression physics of pharmaceutical powders: a review. Int J Pharm Sci Res. 2012;3:1580-1592.
2. Patel S, Kaushal AM, Bansal AK. Compression physics in the formulation development of tablets. Crit Rev Ther Drug Carrier Syst. 2006;23:1-65.
3. Meeus L. Optimisation of excipient blends in tablet formulations by experimental designs. Pharma Chem. 2002:37-41.
4. Mangal S, Meiser F, Morton D, Larson I. Particle engineering of excipients for direct compression: understanding the role of material properties. Curr Pharm Des. 2015;21:5877-5889.
5. Moreton RC. Excipient functionality. Pharm Technol. 2004:98-100.
6. Domb AJ, Khan W. Biodegradable polymers as drug carrier systems. In: Dumitriu S, Popa V, eds. Polymeric biomaterials: structure and function, volume 1. Illustrated ed. Florida: CRC Press; 2013:135-174.
7. Rutesh DH. Overview of pharmaceutical excipients used in tablets and capsules. Drug Topics. 2008;152.
8. Pawar HA, Kamat SR, Choudhary PD. An overview of natural polysaccharides as biological macromolecules: their chemical modifications and pharmaceutical applications. Biol Med. 2015;7:1-9.
9. Mangal S, Meiser F, Lakio S, Morton D, Larson I. The role of physico-chemical and bulk characteristics of co-spray dried L-leucine and polyvinylpyrrolidone on glidant and binder properties in interactive mixtures. Int J Pharm. 2015;479:338-348.
10. Okoye EI, Onyekweli AO, Kunle OO. Lacagpregs- a group of novel multifunctional excipients: development and solid state characterization. West African J Pharm. 2014;25:54-75.
11. Li S, Zhang Y, Wei Y, Zhang W, Zhang B. Thermal, pasting and gel textural properties of commercial starches from different botanical sources. J Bioprocess Biotechiq. 2014;4:1-6.
12. Apeji YE, Abdulhakim A, Anyebe SN, Orugun OA, Olowosulu AK, Oyi AR. Performance evaluation of maize starch as a multifunctional excipient in metronidazole tablet formulation. Ars Pharm. 2019;60:161-167.
13. Szepes PSA. Potato starch in pharmaceutical technology – a review. Food. 2009;3:109–117.
14. Adedokun MO, Itiola OA. Material properties and compaction characteristics of natural and pregelatinized forms of four starches. Carbohydr Polym. 2010;79:818-824.
15. Abdallah DB, Charoo NA, Elgorashi AS. Comparative binding and disintegrating property of *Echinochloa colona* starch (difra starch) against maize, sorghum, and cassava starch. Pharm Biol. 2014;52:935-943.

16. Alebiowu G. Studies on the tableting properties of *Sorghum bicolor* Linn (Poaceae) starch I: evaluation of binder types and concentrations on the properties of sorghum starch granulations. Discov Innov. 2001;13:73-77.
17. Alebiowu G, Adeyemi AO. Influence of starch steeping period on dimensionless disintegration values of a paracetamol tablet formulation. Acta Pol Pharm. 2009;66:311-320.
18. Olayemi OJ, Oyi AR, Allagh TS. Comparative evaluation of maize, rice and wheat starch powders as pharmaceutical excipients. Nig J Pharm Sci. 2008;7:131-138.
19. Ogunjimi AT, Alebiowu G. Flow and consolidation properties of neem gum coprocessed with two pharmaceutical excipients. Powder Technol. 2013;246:187-192.
20. Singh I, Kaur B, Juneja P. Preparation and characterization of starch-metal silicate co-precipitates--evaluation as tablet superdisintegrant. Polim Med. 2014;44:157-166.
21. Batra A, Thongsukmak A, Desai D, Serajuddin ATM. The effect of process variables and binder concentration on tabletability of metformin hydrochloride and acetaminophen granules produced by twin screw melt granulation with different polymeric binders. AAPS PharmSciTech. 2021;22:154.
22. Sun CC. Setting the bar for powder flow properties in successful high speed tableting. Powder Technol. 2010;201:106-108.
23. Arida AI, Al-Tabakha MM. Compaction mechanism and tablet strength of cellactose®. Jordan J Pharm Sci. 2008;1:71-82.
24. Szumilo M, Belniak P, Swiader K, Holody E, Poleszak E. Assessment of physical properties of granules with paracetamol and caffeine. Saudi Pharm J. 2017;25:900-905.
25. Ogunjimi AT, Alebiowu G. Neem gum as a binder in a formulated paracetamol tablet with reference to acacia gum BP. AAPS PharmSciTech. 2014;15:500-510.
26. Oyi AR, Allagh TS, Olayemi OJ. Comparative binding effects of wheat, rice and maize starches in chloroquine phosphate tablet formulations. Res J Appl Sci Eng Technol. 2009;1:77-80.
27. Emery E. Flow Properties of selected pharmaceutical powders. 2008. Available from: https://citeseerx.ist.psu.edu/viewdoc/download?doi=10.1.1.557.2667&rep=rep1&type=pdf
28. Andrews GP. Advances in solid dosage form manufacturing technology. Philos Trans Royal Soc A. 2007;365:2935-2949.
29. Tousey MD. The granulation process 101 basic technologies for tablet making. Pharm Technol. 2002:8-12.
30. Manek RV, Builders PF, Kolling WM, Emeje M, Kunle OO. Physicochemical and binder properties of starch obtained from *Cyperus esculentus*. AAPS PharmSciTech. 2012;13:379-388.
31. Desai PM, Liew CV, Heng PWS. Review of disintegrants and the disintegration phenomena. J Pharm Sci. 2016;105:2545-2555.
32. Ogunjimi AT, Alebiowu G. Material and tableting properties of *Azadirachta indica* gum with reference to official acacia gum. Acta Pol Pharm. 2014;71:107-118.
33. Osei-Yeboah F, Feng Y, Sun CC. Evolution of structure and properties of granules containing microcrystalline cellulose and polyvinylpyrrolidone during high-shear wet granulation. J Pharm Sci. 2014;103:207-215.
34. Tan SB, Moreton RC, Smith D. Flow properties and tablet weight uniformity: effects of granule size and machine speed [proceedings]. J Pharm Pharmacol. 1979;31(Suppl):74P.
35. Zaid AN, Al-Ramahi RJ, Ghoush AA, Qaddumi A, Zaaror YA. Weight and content uniformity of lorazepam half-tablets: a study of correlation of a low drug content product. Saudi Pharm J. 2013;21:71-75.
36. Odeku OA, Schmid W, Picker-Freyer KM. Material and tablet properties of pregelatinized (thermally modified) *Dioscorea* starches. Eur J Pharm Biopharm. 2008;70:357-371.
37. Yassin S, Goodwin DJ, Anderson A, Sibik J, Wilson DI, Gladden LF, Zeitler JA. The disintegration process in microcrystalline cellulose based tablets, part 1: influence of temperature, porosity and superdisintegrants. J Pharm Sci. 2015;104:3440-3450.
38. British Pharmacopoeia. British Pharmacopoeia. Volume II. London, UK: Her Majesty's Stationery Office; 2013.
39. Bansal AK, Patel S, Kaushal AM. The effect of starch paste and sodium starch glycolate on the compaction behavior of wet granulated acetaminophen formulations. J Excipients Food Chem. 2011;2:64-72.

Turk J Pharm Sci 2022;19(5):521-529
DOI: 10.4274/tjps.galenos.2021.05252

ORIGINAL ARTICLE

Studies on Almond Gum and Gelucire-Based Pellets Prepared by Extrusion and Spheronization for Sustained Release

Ramesh Venkata KANTETI[1]*, Omar SARHEED[1], Hemant YADAV[1], Quamrul ISLAM[1], Joshua BOATENG[2]

[1]RAK Medical University, College of Pharmaceutical Sciences, Department of Pharmaceutics, Ras al Khaimah, United Arab Emirates
[2]University of Greenwich, Department of Engineering and Science, London, United Kingdom

ABSTRACT

Objectives: The aim of the investigation was to prepare sustained release (SR) pellets of diltiazem hydrochloride employing almond gum and gelucire. The study was performed to explore the suitability of almond gum in the preparation of pellets of diltiazem hydrochloride without the use of microcrystalline cellulose and role and effectiveness of hydrophobic gelucire (43/01) in controlling the drug release.

Materials and Methods: Pellets were prepared by extrusion-spheronization of the blend previously obtained by incorporation of the drug in a mixture of melted gelucire 43/01 and almond gum. A 3^2 factorial design was employed to study the effect of two independent variables, almond gum and gelucire, on the size, friability and drug release from pellets. Scanning electron microscopy, differential scanning calorimetry and infrared spectroscopy were performed to characterize pellets.

Results: Free flowing spherical pellets could be prepared. The 3^2 factorial study revealed that as the proportion of almond gum increased, the size of pellets increased, while increasing gelucire had opposite effect. The yield of pellets prepared in different formulations is in the range of 86 to 92%. The size of the pellets varied from 1128 to 1458 µ. Higher amounts of gelucire resulted in pellets with greater friability, whereas increasing the amount of almond gum yielded pellets with low friability. The pellets exhibited SR of diltiazem and the presence of gelucire in the matrix of the pellets had an enhanced sustaining effect on release.

Conclusion: Dispersion of the drug in gelucire before it was converted to pellets resulted in extended release of drug. The drug release rate changed with changes in the proportion of pellet composition. The results of the study suggest that employing gelucire (43/01) in the preparation of pellets is a useful approach in the design of SR products of highly water-soluble drug such as diltiazem hydrochloride.

Key words: Spheronization, sustained release, pellets, gelucire (43/01), almond gum

INTRODUCTION

Various novel technologies and approaches are being explored for medicinal compounds to be developed as modified release dosage forms. These forms provide significant benefits compared with the immediate release (IR) dosage forms.[1,2] These include less frequency of administration, safer, and effective plasma concentrations and better patient compliance. Many investigations on the design of modified release dosage forms aim to develop single unit forms such as matrix tablets. Fewer studies are conducted on the development of multi-unit forms such as microcapsules or pellets.[3,4] The multi-unit forms have beneficial characteristics such as well-controlled drug release, no burst release of drug and are evenly dispersed in the gastrointestinal tract after oral administration.[5,6] There are some reports on the design of pellets for sustained release (SR).[7,8] While developing a SR dosage form, the approach employed should take into consideration the physicochemical properties of the drug, especially the solubility. This is because controlling the release of highly soluble drugs is difficult because drug release occurs by diffusion form the unit and higher the solubility, more will be the diffusion of the drug. It is essential that the formulation and echnology are appropriately developed.

Extrusion and spheronization is a widely used technique for preparing pellets with different characteristics, including

*Correspondence: venkatramesh@rakmhsu.ac.ae, Phone: +00971503716203, ORCID-ID: orcid.org/0000-0002-7629-2500
Received: 08.09.2021, Accepted: 22.10.2021

obtaining the SR of drugs. Mahrous et al.[7] have developed SR pellets of indomethacin by different concentrations of hydrophilic polymers, polyethylene glycol 4000, hydroxypropyl methylcellulose E5 LV premium (HPMC) and polyvinylpyrrolidone K30. SR matrix pellets of flurbiprofen were developed and drug release optimized by studying the matrix forming units employing HPMC and carbopol.[8] Sriamornsak et al.[9] have prepared alginate pellets of theophylline employing microcrystalline cellulose (MCC). They studied the drug-release properties of the pellets by varying the number of other substances in the formulation, such as sodium alginate and calcium salts. Chatchawalsaisin et al.[10] developed MCC pellets of acetaminophen and diclofenac sodium. They explored a range of levels of glyceryl monostearate to evaluate its effect on spheronization and drug release.

In all these various earlier investigations, MCC is employed as the spheronizing agent to form the pellets. However, of late there has been an increasing interest shown by researchers to develop alternative substances to MCC as spheronizing agents. This is because of adsorption of some drugs to MCC and undesirable chemical interactions between drugs and MCC.[11,12] Several investigators have worked on polymers such as carrageenan, chitosan and starch - dextrin *etc*. to prepare pellets by extrusion and spheronization.[13-15]

For obtaining the SR from the pellets of a highly water-soluble drug, it is essential that the matrix of the pellet does not allow for rapid diffusion of the soluble drug. In this regard, investigators in the past have explored different hydrophilic polymers along with MCC. However, there are only a few studies have been undertaken in which waxy/fatty or lipoidal materials are explored for preparing the pellets.[16,17]

In our present investigation, we studied the role of gelucire (43/01), a fatty polymer, in developing SR matrix pellets by extrusion and spheronization using almond gum as the alternative spheronizing agent to MCC. The gelucires with a low hydrophilic-lipophilic balance value are hydrophobic and are suitable for designing SR products.[18] Almond gum is an exudate obtained from the plant *Amygdalus communis* L.[19] There are some reports of almond gum as a binder in tablet formulations and for obtaining SR.[20] Almond gum nanofibers were investigated and reported to help obtain SR.[21]

In our laboratories, we developed SR matrix tablets of employing almond gum and pellets employing almond gum as a substitute for MCC in the extrusion and spheronization process.[22,23] Therefore, this investigation explores the usefulness of the combination of hydrophobic gelucire and almond gum in preparing SR pellets. Diltiazem hydrochloride was selected as a model, highly water-soluble drug. It is used for treating angina and in the management of hypertension.[24]

MATERIALS AND METHODS

Materials

Diltiazem hydrochloride (gift sample from Julphar Gulf Pharmaceutical Industries (UAE), gelucire (43/01) was a gift sample from Gattefosse (Paris, France). Almond gum was procured from Harekrishna Herbals (India). All other chemicals and solvents were of analytical grade.

Preparation of pellets by extrusion and spheronization

The required quantities of diltiazem hydrochloride were incorporated into gelucire (43/01) which was melted at 50°C. After cooling and solidification, the mixture was ground and sifted through a 250 µm sieve. This powder mixture was employed during the pelletization process rather than the separate quantities of drug and gelucire. The powder mixture was mixed with appropriate quantities of almond gum and wetted with water until a homogenous and cohesive mass was obtained. The mass was then fed manually into an extruder (Shakti model EX-50/SSP120) fitted with a die/screen of 1 mm diameter operated at a speed of 30 rpm. The extruded mass was spheronized in a unit fitted with a crosshatched plate. A spheronization speed of 1000 rpm was employed and the spheronizer was operated for 15 min. The resulting pellets were air dried at room temperature for further use.

To study the effect of variables, pellets were prepared using 3^2 factorial design (Table 1). Amounts of gelucire and almond gum were selected as the two independent variables. The influence of the independent variables on the size, friability of pellets and drug release was studied.

Characterization of the pellets

Yield and drug content

Pellets were weighed after drying and percent yield was calculated employing the formula given below.

$$\text{Percent yield} = \frac{\text{Weight of dried pellets obtained}}{\text{Weight of drug and excipients}} \times 100$$

For determination of drug content, 10 mg pellets were triturated and the drug diltiazem hydrochloride was extracted into distilled water by sonication for 30 min. The solution was filtered and analyzed spectrophotometrically at 240 nm (Shimadzu model UV 1600) after sufficient dilution with water.

Friability, Carr's index, and angle of repose

Friability

For each study, 25 g pellets were mixed with 20 glass beads (3 mm in diameter) and were placed in Roche friabilator and operated for 8 min at 25 rpm. After the study, the pellets were sieved through a sieve of 250 µm opening and the weight of pellets left on the sieve was determined and the friability was calculated using the formula given below.

$$\text{Percent friability} = \frac{W_I - W_F}{W_I} \times 100$$

W_I and W_F are the initial and final weights of the pellets.

Carr's index

Pellets (100 g) were added to a graduated cylinder and density apparatus (VTAP MATIC II). The bulk and tapped densities were

determined. From the obtained values, the Carr's index and Hausner ratio were calculated employing the formulae below.

$$\text{Carr's index} = \frac{\rho_t - \rho_b}{\rho_t} \times 100$$

$$\text{Hausner ratio} = \frac{\rho_t}{\rho_b}$$

ρ_t is the tapped density and ρ_b is the bulk density.

Angle of repose

The angle of repose was measured according to the fixed funnel method. The funnel is positioned in a way that the lower tip of the funnel is at a fixed height of 3 cm from a horizontal surface. The pellets were then passed slowly through the funnel in such a way that the upper tip of the surface of the heap being formed just touched the lower tip of the funnel. The angle of repose is determined from the height and radius of the heap formed.

Average pellet size

The average size of pellets of different formulations was estimated by sieve analysis (electrolab model EMS 8). 100 g pellets were sieved employing a set of sieves. The pore size of different sieves was between 150 and 2000 microns. After shaking the sieve set for 10 min, the weight of pellets on each sieve was determined to determine the size of pellets.

Surface and shape characterization of pellets

The surface and shape of pellets were studied by optical microscopic image observation and scanning electron microscopy (SEM).

Optical microscopy

The pellets were observed employing an Olympus microscope (model BX 53) attached with DP 74 digital camera. The images were taken employing an image analyzer connected to a black and white camera and processed using cellSens software.

SEM

Pellets were placed on carbon tabs (agar scientific) and imaged under low vacuum on a JEOL JSM5310LV SEM at an accelerating voltage of 20 kV. The aspect ratio of the particles was measured by appropriately thresholding the images using AZtec version 3.3 software (Oxford instruments).

Differential scanning calorimetry (DSC)

DSC studies were performed to know about any interaction between diltiazem hydrochloride and the two excipients used in the preparation of pellets. The calorimeter (Shimadzu DSC 60+) was run at a scanning speed of 10°C/minute. The temperature range of heating was 25-250°C. After sealing the samples in aluminum pans, heating was carried out in an inert atmosphere which is maintained by circulating nitrogen gas.

Fourier-transform infrared (FTIR) spectroscopy

The infrared spectroscopic analysis of diltiazem hydrochloride and the mixtures of diltiazem with almond gum and gelucire was performed by attenuated total reflectance sampling interface technique using Agilent model Cary 630.

Drug release study

Release of diltiazem hydrochloride from different pellets was studied by employing USP dissolution rate test apparatus type I. 0.1 N hydrochloric acid for first 2 h and phosphate buffer of pH 7.4 for the remaining 10 h were used as medium for the release study. Pellets containing 90 mg of diltiazem hydrochloride were added to the drug release medium. The various removed sample media at different time points were assayed for diltiazem hydrochloride released by determining the absorbance at 240 nm.

Statistical analysis

Responses obtained from factorial design experiments were subjected to multiple regression analysis using SPSS statistics 24 software. Data obtained on the 3 dependent variables, size of pellets, friability and drug release for all formulations (F1-F9) showed a wide variation, which indicated that the response values of dependent variables highly rely on the independent variables.

Table 1. Details of different formulations with 3^2 factorial design

Formula	Diltiazem hydrochloride (%)	Gelucire (X1) (%)	Almond gum (X2) (%)	Lactose (as filler) (%)
F1	20	10	20	50
F2	20	10	30	40
F3	20	10	40	30
F4	20	20	20	40
F5	20	20	30	30
F6	20	20	40	20
F7	20	30	20	30
F8	20	30	30	20
F9	20	30	40	10

RESULTS AND DISCUSSION

In this investigation, pellets were prepared by extrusion and spheronization without the conventional and widely used spheronizing agent, MCC. Almond gum is investigated as a spheronizing agent and its usefulness in acting as a release retardant matrix material is studied. We previously reported on the SR pellets of furosemide prepared by extrusion and spheronization employing almond gum.[23] Our preliminary investigations on the suitability of almond gum alone for preparing SR pellets of a highly water soluble drug such as diltiazem hydrochloride revealed that although SR could be obtained, the release could not be significantly retarded. So we employed a combination of lipophilic (gelucire 43/01) and hydrophilic (almond gum) materials as release retardants. A 3^2 factorial design (Table 1) was used to determine the effect of the two variables (percentage of almond gum and gelucire) on the three dependent variables, size, and friability of pellets and drug release.

Characterization of pellets

Preliminary characterization

The yield of the pellets prepared in different formulations was between 86 and 92%. The changes in almond gum or the gelucire proportions did not majorly influence the percentage yield. The drug content of various pellets was found to be between 90 and 94%. The results of the study of flow properties are shown in Table 2. From the angle of repose values, it can be concluded that the flow properties were good for the pellets, especially the formulations F1 to F3. An angle of repose value below 25˚ suggests a good flow. An angle of repose lower than 40˚ indicates good flowability, conversely an angle of repose superior to 40˚ is an indication of cohesiveness.[25,26] However, it is observed that as the proportion of gelucire increased, the flow became poorer, as reflected in the various values shown in Table 2. The fatty nature of gelucire probably impedes the flow of the pellets. Also, it is observed that for a given proportion of gelucire, with a higher amount of almond gum, the flow appears to be improving. It was probably because the pellets were becoming more regular and rounded off with higher amounts of almond gum (discussed more in detail below).

The friability of different formulations of pellets was found to be between 0.52 and 3.68%. Pellet formulations, in which the fatty substance gelucire proportion, was higher exhibited higher friability. Pellet friability is an index of pellet strength, with a lower friability reflecting greater pellet strength. Increased amounts of gelucire probably resulted in a decrease in the amount of water available during extrusion stage, resulting in poor quality extrudates which could not be spheronized into pellets of good strength. Reynolds[27] reported their work that by increasing the amount of water content in the extruded mass, the friability problem can be overcome. As the water content increases, the association of water molecules with the binder almond gum will be greater, which will result in higher plasticity and greater binding capacity. As the gelucire proportion increases, it probably has a more impeding effect on the availability of water in the extruded mass, resulting in less compact extrudates and more friable pellets.

Size of the pellets

The sizes of pellets of different formulations are shown in Table 2. The size of the pellets varied as the amounts of gelucire and almond gum in different formulations changed. With increase in the amount of gelucire, the size of the pellets decreased. However, for a given amount of gelucire present, an increase in almond gum-yielded pellets of higher size. So, gelucire and almond gum had negative and positive influences on the size of the pellets, respectively. Uniform wetting of the dough mass is essential for good-quality extrudates to be formed. The presence of gelucire probably hindered the movement of water during extrusion process and the extruded mass had lower plasticity, which is essential during spheronization. Pellets formed from extrudates of higher amounts of gelucire did not have sufficient strength and were broken into smaller pellets during spheronization. As the almond gum concentration increases, the binding strength and the plasticity of the extrudates increases. A similar observation of increase in pellet size with higher binder amount was reported by other investigators.[28,29]

The proportion of the two ingredients, *e.g.* gelucire and almond gum (the two independent variables), also affected the size distribution of the pellets, as shown in Figure 1. With

Table 2. Characteristics of different pellets

Formula	Average size (μ)	Hausner ratio	Carr index	Angle of repose	Friability (%)	Aspect ratio
F1	1260 ± 3.19	1.31 ± 0.12	16.38 ± 2.23	19.21 ± 1.29	0.96 ± 0.05	1.06 ± 0.02
F2	1358 ± 2.66	1.14 ± 0.21	11.27 ± 1.05	16.41 ± 1.65	0.67 ± 0.23	1.03 ± 0.01
F3	1458 ± 3.11	1.09 ± 0.07	9.34 ± 2.45	14.29 ± 1.30	0.52 ± 0.38	1.01 ± 0.04
F4	1128 ± 4.05	1.43 ± 0.17	19.66 ± 2.27	26.38 ±1.61	2.11 ± 0.37	1.08 ± 0.02
F5	1291 ± 3.25	1.28 ± 0.10	17.89 ± 1.92	23.67 ± 0.72	1.96 ± 0.19	1.05 ± 0.05
F6	1360 ± 2.97	1.21 ± 0.07	13.51 ± 2.57	20.85 ± 1.64	1.23 ± 0.14	1.06 ± 0.03
F7	1146 ±1.85	1.53 ± 0.19	24.21 ± 3.18	32.67 ± 2.11	3.68 ± 0.39	1.17 ± 0.01
F8	1201 ± 2.77	1.37 ± 0.14	21.32 ± 2.19	30.37 ± 1.88	3.05 ± 0.45	1.14 ± 0.03
F9	1301 ± 3.26	1.31 ± 0.09	18.45 ± 1.85	29.66 ± 0.91	2.28 ± 0.31	1.13 ± 0.02

increase in the amount of gelucire, not only the average pellet size decreased but also affected the size distribution of the pellets in different formulations. As the amount of gelucire increased, it resulted in a size distribution, which was more. For example; between F1 and F4 formulations, with higher gelucire in F4 and with almond gum being the same in both, pellets of F4 formulation exhibited a non-uniform distribution compared to F1. A similar observation can be made in F2 and F7 formulations, with pellets of F7 formulation showing non-uniformity in distribution.

Surface and shape characterization of pellets

The surface features of pellets were investigated by optical microscopy and SEM. The pellets were found to be spherical in shape and exhibited a smooth surface (Figure 2). However, higher amount of gelucire in the pellet composition (F9 pellets) resulted in pellets, whose surfaces were not smooth and showed irregularity as shown in Figure 2A, whereas with lesser amounts of gelucire and proportionately higher amounts of almond gum (F3 pellets), yielded pellets that are more spherical and have smoother surface as shown in Figure 2B. The SEM photographs are shown in Figure 3 that confirm the spherical and more regular features of the pellets with higher almond gum (Figure 3B) and a surface irregularity with pellets of higher gelucire (Figure 3B).

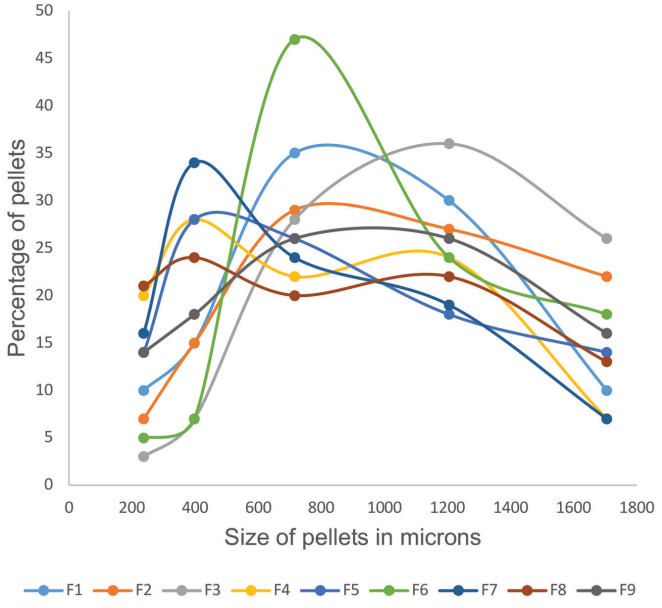

Figure 1. Pellet size distribution curves for different formulations of pellets

An important feature of a pellet is its roundness. Aspect ratios of the pellets were used to express their roundness. Podczeck and Newton[30] have carried out image analysis to evaluate the shape of pellets and suggested an upper value for the aspect ratio of 1.1 for a pellet to be described as spherical. The pellet shape and spherical nature are critical in ensuring the uniform filling of pellets into a hard gelatin capsule. Rowe et al.[31] have reported that an aspect ratio of less than 1.2 will ensure reproducibility of the filling process. Since the pellets made in this investigation needed to be developed into hard gelatin capsules, we determined the aspect ratio of various pellets. The aspect ratio (shown in Table 2) was found to be between 1.01 and 1.17. These values suggest that the pellets prepared are spherical and can be handled easily in the subsequent stages of processing.

DSC

The DSC thermograms of diltiazem hydrochloride and the mixtures of diltiazem with gelucire and almond gum are shown in Figure 4. Diltiazem showed a peak at 212°C, which is due to the melting of the drug.[32] The melting peak of diltiazem was retained at the same temperature even in the mixtures with gelucire and almond gum indicating absence of any interaction between diltiazem and the two excipients used in the pellet preparation.

FTIR spectroscopy

The FTIR spectra of diltiazem hydrochloride and its mixtures with gelucire and almond gum are shown in Figure 5. Diltiazem hydrochloride exhibits strong to medium characteristic absorption peaks at 1743 cm^{-1} (acetate C=O stretch), 1679 cm^{-1} (lactam C=O stretch), 838 cm^{-1} (*O*-substituted aromatic C-H out-of-plane deformation) and 781 cm^{-1} (*p*-substituted aromatic C-H

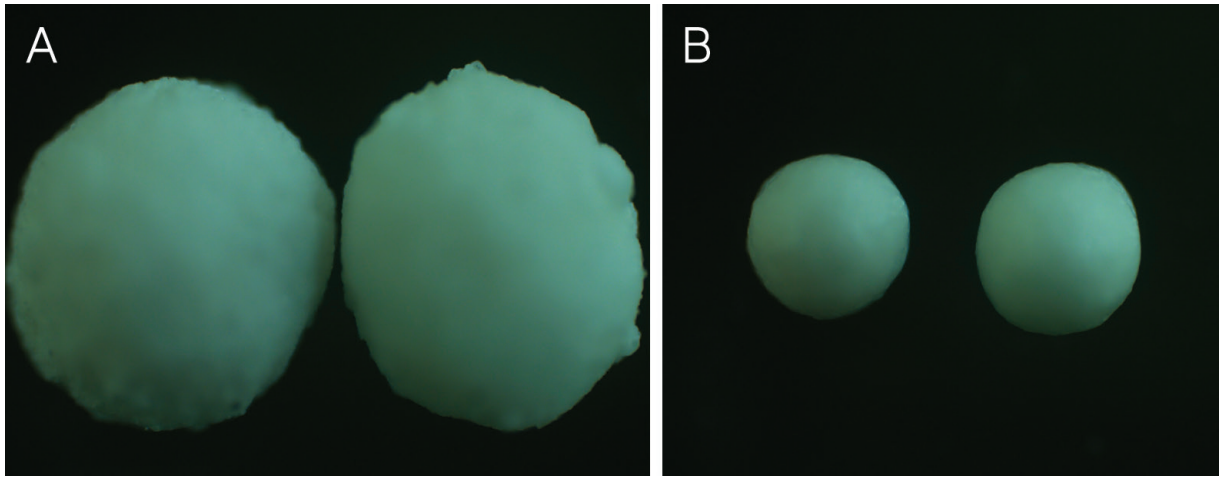

Figure 2. Photomicrograph of pellets F9 (A) and F3 (B)

out-of-plane deformation).[32] These principal peaks of diltiazem were retained in the mixtures of the drug with gelucire and almond gum, suggesting that there is no chemical interaction with the two excipients used.

Drug release

The drug release from the pellets prepared was found to be slow and sustained (Figure 6). But the release rate is different in various pellet formulations depending on the percentage of almond gum or gelucire employed. Almond gum and gelucire were employed at 3 different levels. As their proportion of increased, drug release rate decreased. A 2 factor 3 level factorial design was employed to study the influence of these two variables. In F1 and F2 formulations, though the release was slow, all the drug was completely released by the end of 6^{th} hour. In F3 and F4, the release is slightly more retarded but completed by 8^{th} hour. An interesting observation is that in F3 and F4 pellets, the release was almost the same, even though the almond gum was 50% less in F4. This is probably because gelucire's percentage in F4 is 50% more than in F3. So, this higher gelucire compensates for the less almond gum in controlling the release. But in pellets of F5 and F6 formulations with the same gelucire amount as F4, the release is slower, this is because the almond gum is higher. This confirms that, while gelucire contributes to the retarding effect of the drug, increased amounts of almond gum play an important role in retarding the release.

The theoretical desired release rate required from diltiazem hydrochloride is calculated from its pharmacokinetic parameters.[32] The biological half-life of diltiazem is 3.5 h. The normal conventional IR dose of diltiazem is 30 mg. The following equations were used to calculate the SR dose and the desired release rate for 12 h.

D_I= Immediate release normal dose= 30 mg

$t_{1/2}$= Biological half-life= 3.5 h

K_E= Elimination rate constant= 0.693/3.5 = 0.198 hr 1

K_0= Desired release rate for sustained dose= D_I x K_E= 30 x 0.198= 5.94 mg hr^{-1}

$D_I = K_0/K_E = D_S/K_E$ x T (because $K_0 = D_S/T$)

Therefore, $D_S = D_I$ x K_E x T= 30 x 0.198 x 12= 71.28 mg

D_I*= Corrected initial dose= $D_I - (t_p \times D_I \times K_E)$,

where t_p is the time for the peak plasma concentration

So corrected initial dose= 30 - (2 x 30 x 0.198)= 30 - 11.88= 18.12 mg

Total dose= $D_I + D_S$= 18.12 + 71.28= 89.4 ~ 90 mg

The desired release rate= 5.94 mg hr^{-1}

Of the various pellets, F6 formulation exhibited a release profile close to the theoretical desired release. In products F7 to F9, the release becomes much slower and is incomplete because of higher amounts of gelucire and almond gum. In spite of almond gum quantity being higher in F9 than in F8, the release profiles are almost the same in F8 and F9. This is probably because gelucire at higher levels (being same in F8 and F9) has a significant retarding effect on the release. Thus, it is evident from the release profiles that with the changes in the proportion of gelucire and almond gum in the pellets, the release rates varied. This observation is further confirmed in the statistical analysis that is conducted on the data obtained (discussed below).

To know the drug-release mechanism, the drug release data are analyzed as *per* first-order, Higuchi[33] and Korsmeyer et al.[34] models. The r^2 values in various models are given in Table 3. The various values of release rate constants and the "n" values of Peppas plot suggest that the drug release from the pellets is by non-Fickian anomalous diffusion.

Data analysis of percent release in 6 h

The regression equation that predicts the percentages released is given below:

Y (percent released)= 150.611 - 2.7 X_1 - 0.817 X_2

The observed value for percent release for all 9 formulations (F1-F9) varied from 39.45% to 100% among the formulations. Correlation coefficient value was found to be 0.949 and can be considered a good measure of the quality of the prediction of the dependent variable using the model employed. Negative signs of coefficients of X_1 and X_2 in regression equation indicated retarding effect of independent variables on the response (drug

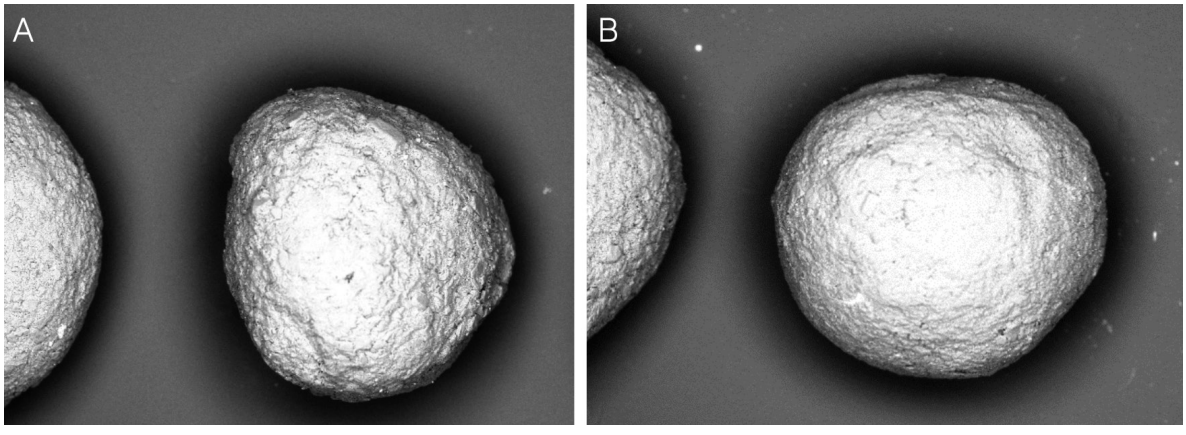

Figure 3. SEM photograph of pellets F9 (A) and F3 (B)

SEM: Scanning electron microscopy

release). The higher coefficient value of X_1 (gelucire) suggests the more retarding effect shown by gelucire on drug release than the other variable almond gum. This substantiates the earlier discussion made on the drug release.

Data analysis of size of pellets

The regression equation that predicts the size of pellets is given below:

Y (size of pellets)= 1106.667 - 24.1 X1 + 26.833 X_2

The observed values of size of pellets ranged from 1146 to 1458 µ. A negative sign on the coefficient for X_1 and a positive sign on the coefficient X_2 indicates that gelucire has an effect that reduces the size of the pellets, whereas almond gum has the opposite effect to resulting in pellets of higher size. A correlation coefficient value of 0.985 indicates a good level of prediction.

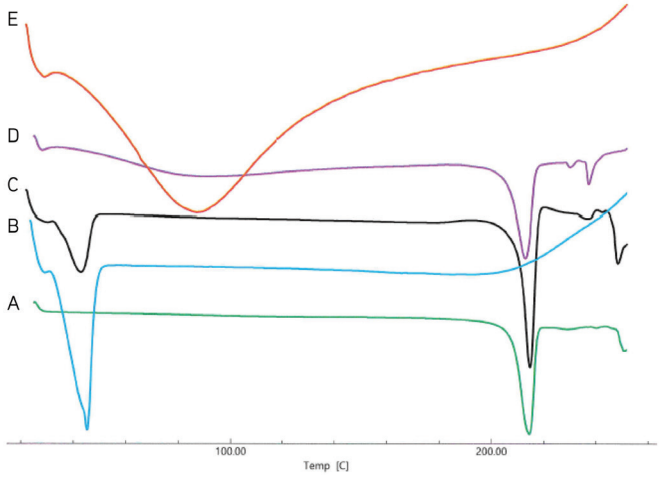

Figure 4. DSC thermograms of diltiazem (A), gelucire (B), diltiazem: Gelucire mixture (C), diltiazem: Almond gum mixture (D) and almond gum (E)

DSC: Differential scanning calorimetry

Data analysis in friability of pellets

The regression equation that predicts the friability of pellets is given below:

Y (percent friability)= 0.9116 + 0.114167 X_1 - 0.04055 X_2

A positive sign on the coefficient for X_1 and a negative sign on the coefficient of X_2 confirm the earlier discussion that higher amounts of gelucire in the pellet formula increase the friability, while almond gum reduces the friability.

The adequacy of the fitted model was verified by ANOVA and results are shown in Table 4. The various values from ANOVA tests indicate that the independent variables statistically significantly predict the dependent variables.

CONCLUSION

SR pellets of diltiazem hydrochloride could be prepared by extrusion and spheronization without the inclusion of MCC in pellet manufacture and by using almond gum as the extrusion and spheronization agent and matrix former for the SR. Dispersion of the drug in gelucire before it was converted to pellets resulted in extended release of the drug. A 3^2 factorial study and the multiple regression analysis helped investigate the effect of two independent variables, almond gum and gelucire, on the characteristics of the prepared pellets and the drug release. The flow properties, size, and friability of the pellets are affected by the proportions of almond gum and

Table 3. Drug release characteristics

Formula	Correlation coefficient (r^2)			K_1 (hr^{-1})	K_H ($mg.hr^{-1/2}$)	Korsmeyer-Peppas (n value)
	First order	Higuchi	Korsmeyer-Peppas			
F1	0.9719	0.9974	0.9944	0.5918	43.14	0.5017
F2	0.9948	0.9980	0.9974	0.4168	41. 53	0.5167
F3	0.9608	0.9888	0.9903	0.3767	39.96	0.5217
F4	0.9672	0.9824	0.9888	0.3984	40.04	0.5325
F5	0.9512	0.9913	0.9985	0.2885	33.24	0.6303
F6	0.9863	0.9961	0.9954	0.2601	33.64	0.7355
F7	0.9907	0.9840	0.9986	0.1612	32.01	0.8641
F8	0.9888	0.9885	0.9970	0.1133	27.71	0.8725
F9	0.9879	0.9749	0.9947	0.1087	25.38	0.8861

Table 4. Results of the regression analysis

Dependent variable	R	R^2	Adjusted R^2	F value	*p* value
Drug release	0.974	0.949	0.932	55.79	<0.001
Size of pellet	0.993	0.985	0.981	202.494	<0.001
Friability	0.983	0.967	0.956	88.43	<0.001

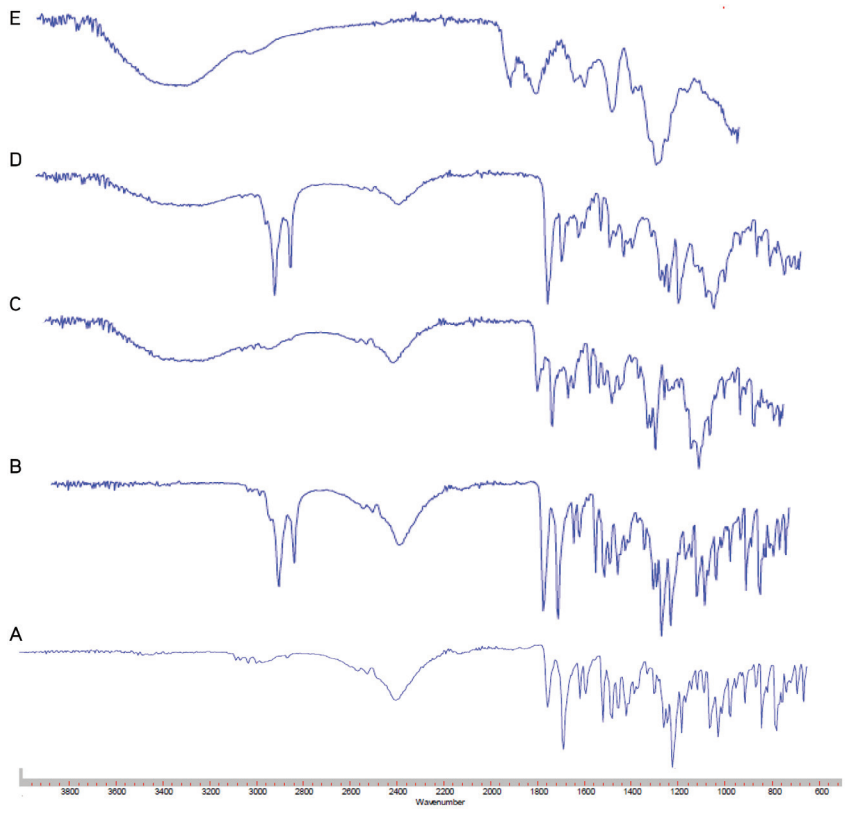

Figure 5. FTIR spectra of diltiazem hydrochloride (A), diltiazem: Gelucire mixture (B), diltiazem: Almond gum mixture (C), gelucire (D) and almond gum (E)
FTIR: Fourier-transform infrared

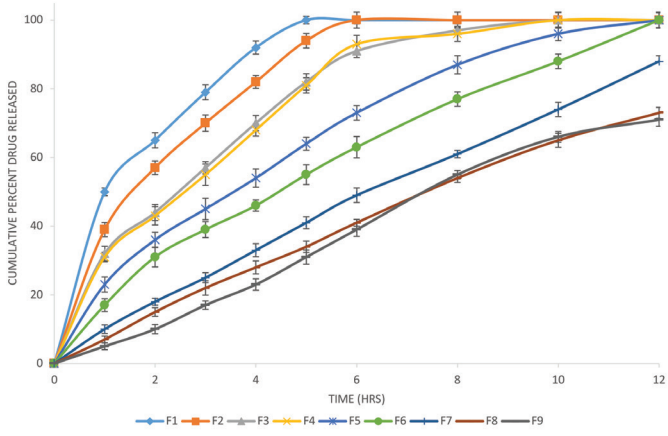

Figure 6. Drug release profiles from different pellet formulations

gelucire. The drug release rate changed with the changes in the proportion of the pellet composition. The results of the study suggest that employing gelucire (43/01) in the preparation of pellets is a useful approach in the design of SR products of highly water-soluble drug such as diltiazem hydrochloride.

ACKNOWLEDGMENTS

The authors express their gratitude to the President of RAK Medical and Health Sciences University (UAE) and Dean of RAK College of Pharmaceutical Sciences for their encouragement and support in conducting the research.

Ethics

Ethics Committee Approval: The study was approved by the RAK Medical and Health Sciences University Ethics Committee (approval no: RAKMHSU-REC-021-202/21-F-P).

Informed Consent: There was no investigation carried out using human volunteers.

Peer-review: Externally peer-reviewed.

Authorship Contributions

Concept: R.V.K., Design: R.V.K., O.S., H.Y., J.B., Data Collection or Processing: R.V.K., O.S., H.Y., J.B., Q.I., Analysis or Interpretation: R.V.K., O.S., H.Y., J.B., Literature Search: R.V.K., O.S., H.Y., J.B., Writing: R.V.K., O.S., H.Y.

Conflict of Interest: No conflict of interest was declared by the authors.

Financial Disclosure: The authors declared that this study received no financial support.

REFERENCES

1. Goonoo N, Bhaw-Luximon A, Ujoodha R, Jhugroo A, Hulse GK, Jhurry D. Naltrexone: a review of existing sustained drug delivery systems and emerging nano-based systems. J Control Release. 2014;183:154-166.
2. Junyaprasert VB, Manwiwattanakul G. Release profile comparison and stability of diltiazem-resin microcapsules in sustained release suspensions. Int J Pharm. 2008;352:81-91.

3. Thakur G, Singh A, Singh I. Chitosan-montmorillonite polymer composites: formulation and evaluation of sustained release tablets of aceclofenac. Sci Pharm. 2015;84:603-617.
4. He W, Wu M, Huang S, Yin L. Matrix tablets for sustained release of repaglinide: preparation, pharmacokinetics and hypoglycemic activity in beagle dogs. Int J Pharm. 2015;478:297-307.
5. Chen T, Li J, Chen T, Sun CC, Zheng Y. Tablets of multi-unit pellet system for controlled drug delivery. J Control Release. 2017;262:222-231.
6. Javed I, Ranjha NM, Mahmood K, Kashif S, Rehman SM, Usman F. Drug release optimization from microparticles of poly (E-caprolactone) and hydroxypropyl methylcellulose polymeric blends: formulation and characterization. J Drug Deliv Sci Techol. 2014;24:607-612.
7. Mahrous GM, Ibarhim MA, El-Badry M, Al-Anazi FK. Indomethacin sustained release pellets prepared by extrusion-spheronization. J Drug Deliv Sci Techol. 2010;20:119-125.
8. Alshora DH, Ibrahim MA, Ezzeldin E, Iqbal M. Optimized flurbiprofen sustained-release matrix pellets prepared by extrusion/spheronization. J Drug Deliv Sci Techol. 2020;59:101902.
9. Sriamornsak P, Nunthanid J, Luangtana-anan M, Weerapol Y, Puttipipatkhachorn S. Alginate-based pellets prepared by extrusion/spheronization: effect of the amount and type of sodium alginate and calcium salts. Eur J Pharm Biopharm. 2008;69:274-284.
10. Chatchawalsaisin J, Podczeck F, Newton JM. The preparation by extrusion/spheronization and the properties of pellets containing drugs, microcrystalline cellulose and glyceryl monostearate. Eur J Pharm Sci. 2005;24:35-48.
11. Al-Nimry SS, Assaf SM, Jalal IM, Najib NM. Adsorption of ketotifen onto some pharmaceutical excipients. Int J Pharm. 1997;149:115-121.
12. Torres Suárez AI, Gil Alegre ME, Camacho Sánchez MA. Solid-state interactions of two new antineoplastic drugs (mitonafide and amonafide) and common tablet excipients in preformulation studies. Eur J Pharm Biopharm. 1994;40:41-43.
13. Bornhöft M, Thommes M, Kleinebudde P. Preliminary assessment of carrageenan as excipient for extrusion/spheronisation. Eur J Pharm Biopharm. 2005;59:127-131.
14. Steckel H, Mindermann-Nogly F. Production of chitosan pellets by extrusion/spheronization. Eur J Pharm Biopharm. 2004;57:107-114.
15. Almeida Prieto S, Blanco Méndez J, Otero Espinar FJ. Starch-dextrin mixtures as base excipients for extrusion-spheronization pellets. Eur J Pharm Biopharm. 2005;59:511-521.
16. Singh R, Poddar SS, Chivate A. Sintering of wax for controlling release from pellets. AAPS PharmSciTech. 2007;8:E74.
17. Maboos M, Yousuf RI, Shoaib MH, Nasiri I, Hussain T, Ahmed HF, Iffat W. Effect of lipid and cellulose based matrix former on the release of highly soluble drug from extruded/spheronized, sintered and compacted pellets. Lipids Health Dis. 2018;17:136.
18. Panigrahi KC, Patra Ch.N, Jena GK, Ghose D, Jena J, Panda SK, Sahu M. Gelucire: a versatile polymer for modified release drug delivery system. Future J Pharm Sci. 2018;4:102-108.
19. Bouaziz F, Ben Romdhane M, Boisset Helbert C, Buon L, Bhiri F, Bardaa S, Driss D, Koubaa M, Fakhfakh A, Sahnoun Z, Kallel F, Zghal N, Ellouz Chaabouni S. Healing efficiency of oligosaccharides generated from almond gum (*Prunus amygdalus*) on dermal wounds of adult rats. J Tissue Viability. 2014;23:98-108.
20. Sarojini A, Kunam DS, Manavalan R, Jayanthi B. Effect of natural almond gum as a binder in the formulation of diclofenac sodium tablets. Int J Pharm Sci Res. 2010;1:55-60.
21. Rezaei A, NAsirpour A. Evaluation of release kinetics and mechanisms of curcumin and curcumin-β-cyclodextrin inclusion complex incorporated in electrospun almond Gum/PVA nanofibers in simulated saliva and simulated gastrointestinal conditions. Bionanoscience. 2019;9:438-445.
22. Ramesh KVRNS, Walayat FS, Usman S, Sarheed O, Kumar MV. Design and evaluation of sustained release matrix tablets of indomethacin by employing gelucires and badam gum. Asian J Pharm. 2015;9:234-242.
23. Ramesh KVRNS, Yadav HKS, Usman S, Elmarsafawy TS. Studies on the influence of formulation and processing factors on the drug release from multiparticulate systems. Asian J Pharm. 2020;14:17-25.
24. Gerald KM. American Society of Health System Pharmacists. AHFS Drug Information, Bethesda, Maryland. 2018;2012-2019.
25. Abdullah EC, Geldart D. The use of bulk density measurements as flowability indicators. Powder Technol. 1999;102:151-165.
26. Carr RL. Evaluating flow properties of solids. Chem Eng. 1965;72:163-168.
27. Reynolds AD. A new technique for the production of spherical particles. Manuf Chem Aerosol News. 1970;41:40-43.
28. Malinowski HJ, Smith WE. Use of factorial design to evaluate granulations prepared by spheronization. J Pharm Sci. 1975;64:1688-1692.
29. Agrawal AM, Howard MA, Neau SH. Extruded and spheronized beads containing no microcrystalline cellulose: influence of formulation and process variables. Pharm Dev Technol. 2004;9:197-217.
30. Podczeck F, Newton JM. The evaluation of a three dimensional shape factor for the quantitative assessment of the sphericity and surface roughness of pellets. Int J Pharm. 1995;124:253-259.
31. Rowe RC, York P, Colbourn EA, Roskilly SJ. The influence of pellet shape, size and distribution on capsule filling--a preliminary evaluation of three-dimensional computer simulation using a Monte-Carlo technique. Int J Pharm. 2005;300(:32-37.
32. Mazzo, DJ, Obetz CL, Shuster J. In: Harry GB (ed). Analytical profiles of drug substances and excipients. 1994;23:53-98.
33. Higuchi T. Mechanism of sustained action medication. Theoretical analysis of rate of release of solid drugs dispersed in solid matrices. J Pharm Sci. 1963;52:1145-1149.
34. Korsmeyer RW, Gurny R, Doelker E, Buri P, Peppas NA. Mechanisms of solute release from porous hydrophilic polymers. Int J Pharm. 1983;15:25-35.

Turk J Pharm Sci 2022;19(5):530-542
DOI: 10.4274/tjps.galenos.2021.35020

ORIGINAL ARTICLE

Stability Indicating RP-HPLC and Spectrophotometric Methods for Simultaneous Estimation of Sodium Benzoate and Cefdinir in the Presence of its Degradation Products-Application to Blank Subtraction Method

Mahmoud Abdelfettah MOHAMED[1], Mohamed El-Kassem Mohamed HASSOUNA[2]*

[1]Hikma Pharmaceutical Company, Quality Control, Beni-Suef, Egypt
[2]Beni-Suef University, Faculty of Science, Department of Chemistry, Beni-Suef, Egypt

ABSTRACT

Objectives: Empower 3 software is important in modeling, optimization, and reducing the time of manual calculation of related substance by subtracting the baseline of a blank chromatogram from the unknown sample automatically; so, the major objective of the developed method is to introduce a new, selective, and economical high performance liquid chromatography (HPLC) and spectrophotometric method for simultaneous estimation of sodium benzoate (SDB) and cefdinir (CFR) in the presence of its degradation products.

Materials and Methods: Chromatographic separation is optimized and adjusted using two methods; method (I) is characterized for separation of active pharmaceutical ingredient (CFR) in pure and dosage forms using Atlantis dC18 column [4.6 mm x 250 mm (5 µm particle size or equivalent)] with a mobile phase consisting of methanol: 0.02 M phosphate buffer solution pH 3.0 (40:60 v/v) at a flow rate of 1.0 mL/minute, injection volume 10 µL and wavelength 254 nm. Method (II) is identified for related substances in a Hichrom C18 column (15 x 0.46 cm), 5 µm particle size or equivalent, using a binary gradient consisting of solution A [0.1% tetramethylammonium hydroxide solution (pH: 5.5) with 0.1 M EDTA (1000:0.4 v/v)] and solution B (0.1% tetramethylammonium hydroxide solution (pH 5.5): acetonitrile: methanol : 0.1 M EDTA (500:300:200:0.4 v/v) using injection volume 10 µL for reversed-phase HPLC with a wavelength equals to 254 nm and flow rate 1.0 mL/min. Two ecofriendly spectrophotometric methods were successfully used to resolve the spectral overlap of drugs.

Results: Method A, the first derivative of ratio spectra spectrophotometric method (1stDD) where CFR was determined at two wavelengths 283.5 nm, 313.4 nm and SDB was determined at 216.7 nm, 235.5 nm. Method B, ratio subtraction method is performed to overcome the interference between CFR and the preservative SDB. The ultraviolet spectrum of the laboratory mixture is divided by that of CFR (20 µg/mL) as a divisor then subtracting the amplitudes in the plateau region at 250-315 nm (the constant) from that of the ratio spectrum. The zero-order spectra of SDB were obtained at 225 nm by multiplying the resulting ratio spectra by the divisor (CFR), zero order of CFR was been estimated at a wavelength value of 283 nm after multiplication of the divisor by the obtained constant.

Conclusion: The optimized method was adjusted and validated as *per* International Conference on Harmonization guidelines and could be easily utilized by quality control laboratories and for laboratory-prepared mixtures.

Key words: Empower 3 software, RP-HPLC-UV, spectrophotometric methods, blank subtraction method, cefdinir, sodium benzoate

***Correspondence:** mhassouna47@hotmail.com; mohamed.hassouna@science.bsu.edu.eg, **Phone:** +2 01223861504, **ORCID-ID:** orcid.org/0000-0002-4158-7667
Received: 13.07.2021, **Accepted:** 22.10.2021

INTRODUCTION

The application of blank subtraction method in related substances and degradation products has been widely applied in the quality control lab in the pharmaceutical industries to optimize, achievement and decrease number of experimental trials of a chromatographic system for manual calculations by using the empowered software. Empower 3 software photodiode array (PDA) detector can subtract mobile phase effects of a standard or sample. The possibility of blank subtraction is useful when the application is affected by gradient runs, in which least a solvent contains a ultraviolet (UV)-absorbing compound, system peaks and contaminants in the mobile phase. The blank subtraction removes the chromatographic tool from the dataset, resulting in a 3D chromatographic scheme corrected to the baseline. In fact, this 3D chromatogram is the difference between the blank and the standard or the sample at the specific wavelengths. Blank baseline subtraction procedure improves the chromatogram scheme in these ways; baseline closer to 0 absorbance units means, no additional peaks, less drift and peaks are easier to integrate.[1]

Cefdinir (CFR) in omnicef capsules and powder for granule suspension is referred to for the treating of patients with minor to major infections resulting from micro-sensitive strains. CFR is an extended group of semi-synthetic cephalosporins. CFR compound A is a combination of four isomers called CFR open ring lactones a, b, c, and d. Its molecular formula is $C_{14}H_{15}N_5O_6S_2$ and its molecular weight is 413.43. The molecular formula for CFR-related compound B is $C_{14}H_{14}N_4O_4S_2$ and its molecular weight is 366.41 (Figure 1a-m) for CFR and their related substances.[2] Sodium benzoate (SDB) is chemically known as sodium benzenecarboxylate ($C_7H_5NaO_2$), (Figure 1n). The ingredient is used as an excipient; treatment of hyperammonemia due to urea cycle disorders and treatment of non-ketotic hyperglycinemia.[3]

CFR and SDB are formally announced in the European and British Pharmacopeias that illustrated chromatographic method for CFR and a titration one for SDB,[3] while United States Pharmacopeia (USP) prescribed a chromatographic method for each.[4] Some new articles were published for the determination of CFR and its impurities using liquid chromatography-tandem mass spectrometry methods,[5-9] high performance liquid chromatography (HPLC) method.[10,11] Only one HPLC and ultra-high performance liquid chromatography (UPLC) method has been reported for simultaneous quantitation of CFR and SDB in their dosage forms, but this method is not indicated for the determination of impurities and there is no spectrophotometric method for simultaneous optimization of the laboratory mixture of CFR and SDB in their dosage forms,[12] thin layer chromatography,[13,14] and spectrophotometric.[15-21]

The novelty of the proposed method is lying in its ability to detect, identify, and separate all related substances to CFR while the previous published methods cannot separate most related substances in CFR. Besides, it overcomes the overlapping of the binary mixture by using a spectrophotometric method without the need of sophisticated application. A unique advantage of the proposed method is the reduction of waste time in manual calculation of impurities through the application of the blank subtraction method, in which Empower PDA software can subtract the effects of the mobile phase on a standard or sample and peaks will be easier to integrate. Therefore, the main objective of this method is to identify and separate CFR and SDB in the presence of CFR's degradation products using blank subtraction method and solve the interference of the binary mixture using a simple spectrophotometric method.

MATERIALS AND METHODS

Experimental and reagents

CFR and SDB were provided by Hikma Pharmaceutical Industries which is located in Beni-Suef governorate, Egypt. Reference standards of related CFR (compound A and B) were purchased from USP store (USA, Rockville, MD). All HPLC- and analytical grades were purchased from (Fisher Scientific, USA).

Instrumentation and data processing

Waters UHPLC system (Waters Corporation, USA), equipped with an LC quaternary pump with PDA detector, autosampler and quaternary solvent management, has the potential for multiple uses and flexibility to move from HPLC and UPLC and is provided with Empower™ 3 Software for processing methods.

UV 1900 (Shimadzu-Japan) provided with UV probe (2.7.1) software for processing data.

Chromatographic method

Chromatographic separation of CFR and its preservative SDB was accomplished using an Atlantis dC18 column [4.6 mm x 250 mm (5 µm particle size or equivalent)] with a mobile phase consisting of methanol: 0.02 M phosphate buffer solution pH 3.0 (40:60 v/v) at a flow rate of 1.0 mL/minute, injection volume 10 µL and wavelength 254 nm. Also, a binary gradient consisting of solution A [0.1% tetramethyl ammonium hydroxide solution (pH 5.5) with 0.1M EDTA (1000:0.4 v/v)] and solution B [0.1% tetramethyl ammonium hydroxide solution (pH 5.5): acetonitrile: methanol: 0.1M EDTA (500:300:200:0.4 v/v) with Hichrom C18 column (15 x 0.46 cm, 5 µm or equivalent, 150 Å pore size) at flow rate 1.0 mL/min, using injection volume 10 µL for reversed-phase-HPLC and wavelength at 254 nm with auto sampler temperature 4.0°C, column temperature 40.0°C and gradient program following the scheme: (i) 0-8 min: 95% (A), 5% (B) isocratic; (ii) 8-28 min: 75% (A), 25% (B); (iii) 28-43 min: 50% (A), 50% (B)] and (iv) 43-64 min: 95% (A), 5% (B) for separation of related substances, no statistical analysis data was used in the chromatographic method.

Solution preparations

A) For analysis of laboratory-prepared mixture

Solvent preparation: methanol: 0.02 M phosphate buffer solution pH 3.0 (50:50 v/v).

CFR solution: Accurately weighed about 10 mg CFR working standard, transferred to a 100 mL volumetric flask, added some

solvent, dissolved by sonication, allowed to cool and made up to the mark with solvent.

Sodium benzoate solution: Accurately weigh about 10 mg SDB, transfer to 100 mL volumetric flask and proceed similarly.

Resolution solution: 10.0 mL of both stock solutions of the above prepared drugs were pipetted into 100 mL volumetric flask, completed to the mark with solvent and the chromatogram is drawn as displayed in Figure 2a.

B) For related substances

Solution (1): Weigh about 14.2 g of anhydrous dibasic sodium phosphate transfer it to 1000 mL flask and dissolve in deionized water.

Solution (2): Weigh about 27.2 g of monobasic potassium phosphate and dissolve in 2.0 L of deionized water.

Buffer preparation: Combine the suitable quantities of solutions 1 and 2 (about 2:1) to get a solution having the pH value of 7.0 ± 0.1.

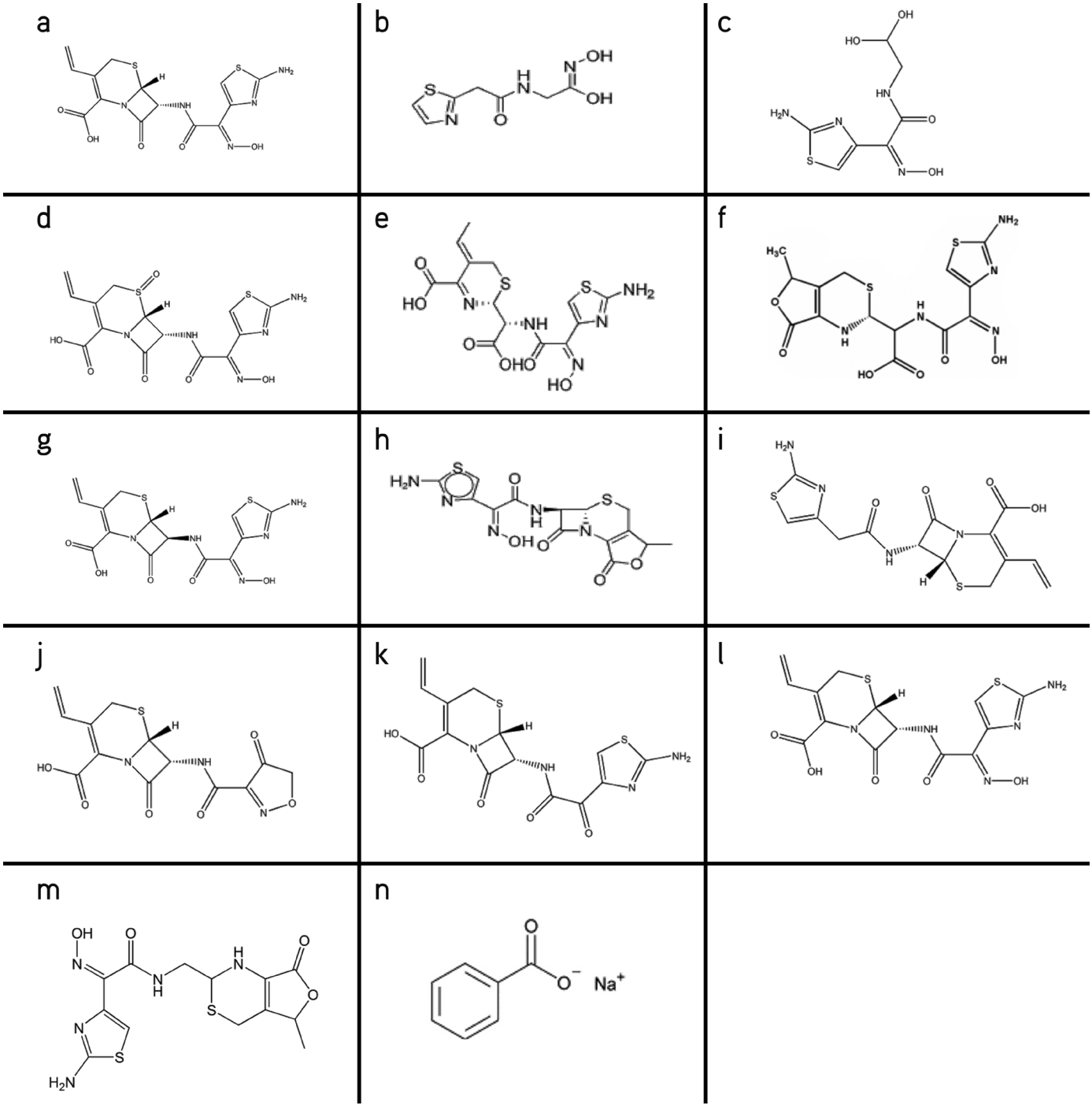

Figure 1. Chemical structures of (a-m) CFR and their related substances, and (n) SDB

CFR: Cefdinir, SDB: Sodium benzoate

Solvent preparation: Dilute 8 mL of tetramethylammonium hydroxide (25% in water) to 2000 mL with deionized water; adjust pH to 5.5 ± 0.1 using diluted appropriate acid.

Resolution solution preparation

Stock solution (A): Weigh about 10.0 mg of USP related CFR compound A transfer it quantitatively to a 250 mL volumetric flask using an appropriate volume of solvent, sonicate to complete dissolution, then complete to volume with a solvent to get a concentration of 0.04 mg/mL.

Stock solution (B): Weigh about 10.0 mg of USP related CFR compound B and proceed similarly to stock solution (B) to get a concentration of 0.04 mg/mL.

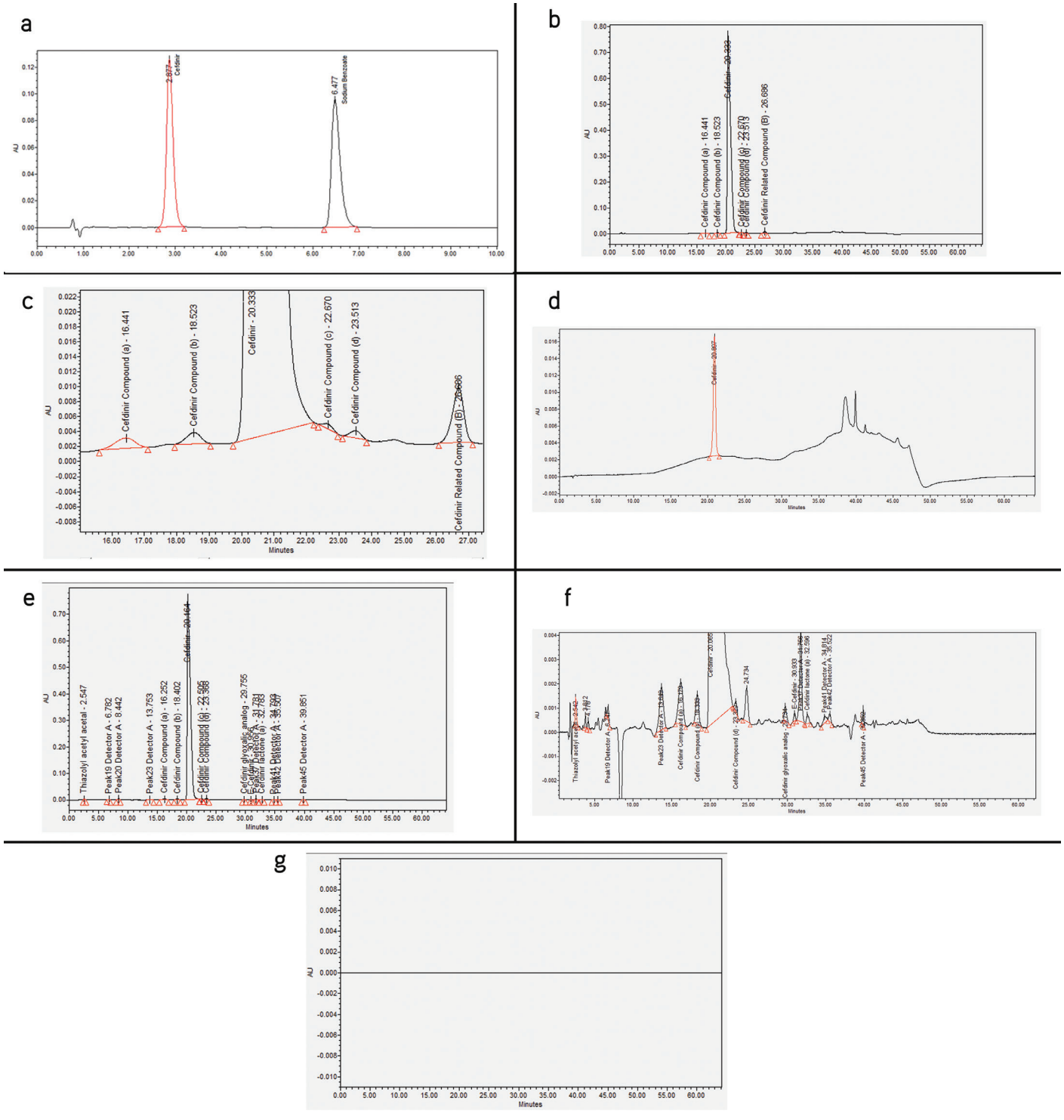

Figure 2. HPLC chromatograms of (a) 10 µg/mL of laboratory prepared mixture of CFR and SDB, (b, c) 1500 µg/mL of system suitability solution of [CFR and related compound (A, B)], (d) 15 µg/mL of standard solution of (CFR), (e, f) sample solution of omnicef, and (g) blank subtraction

CFR: Cefdinir, SDB: Sodium benzoate, HPLC: High performance liquid chromatography

Working resolution solution: Weigh about 37.5 mg of CFR convey quantitatively to 25 mL volumetric flask using 10 mL buffer. Sonicate until dissolution, complete to volume using buffer. Posteriorly, add 5.0 mL from each solution of related compounds (A and B) and makes up for the marks with solvent. Mix well and filter through 0.45 µm nylon membrane, then inject in the HPLC. The HPLC chromatogram is presented in Figure 2b, c.

CFR standard solution preparation: Weigh about 37.5 mg of CFR in 50 mL volumetric flask and complete to volume with buffer. Of the resulting solution, an aliquot of 2 mL was diluted to 100 mL with solvent, mix, and filter through the nylon membrane, then inject into the HPLC. The HPLC chromatogram is shown in Figure 2d.

Sample solution preparation: Constitute omnicef as directed in the product label and leaflet. Transfer accurately about the equivalent to 150 mg CFR in 100 mL volumetric flask using 30 mL buffer and completely to the mark with solvent. Similarly, mix, filter, and inject Figure 2e, f.

Calculations

Identify any peak for solvent and placebo by the processing method to be excluded.

Consider any peak that present in the chromatogram other than solvent, placebo, known impurities, and CFR as unknown impurities.

The percentage of each impurity in CFR portion of the oral suspension powder can be calculated by the equation given below:

Result= (Pt/PS) x (Ds/Dt) x (100/F) where

Pt= Peak area of individual impurity in the test solution

PS= Peak area of CFR standard solution

Ds= Actual concentration of CFR (mg/mL)

Dt= Nominal concentration of CFR in the test solution (mg/mL)

F= FRR (factor of relative response)

C) For UV spectroscopic methods

Solvent: Use methanol HPLC grade.

Standard solutions of CFR and SDB: Precisely weigh 10 mg of each CFR and SDB in two 100 mL volumetric flasks, add 70 mL of the solvent and sonicate to dissolve and complete to the mark with the same solvent and mix well.

Laboratory prepared mixture: Prepare mixtures of CFR and SDB containing different ratios from their working standard solutions (100 µg/mL) into a series of 10 mL volumetric flasks.

Procedures

Derivative ratio method (DD^1)

The absorption spectra of CFR were divided by a divisor of SDB (5 µg/mL), and the first derivative values caused by ratio spectra were registered. The linear curves for maximum and minimum amplitudes at 283.5 nm and 313.4 nm are established *versus* the congruous concentrations of CFR to calculate the regression equation. Alternatively, the scanned absorption spectra of SDB were divided by a CFR divisor (10 µg/mL) and the first derivative (D^1) was stored. As well, the linear curve for maximum and minimum amplitudes at 216.7 nm and 235.5 nm were dotted against the congruous concentrations of SDB to construct the regression equation.

Ratio subtraction method

The spectra of the bilateral mixture were divided by the advisor of CFR (10 µg/mL), then the amplitudes were subtracted in the plateau region at λ 250-315 nm (the constant) from that ratio spectrum. The zero order spectra of SDB were resolved by multiplying the resulting ratio spectra by the divisor (CFR). The concentration of SDB was computed through the congruous regression equation at 225 nm.

RESULTS AND DISCUSSION

Methods development and optimization

Blank subtraction

Before it is decided to proceed 3D blank baseline subtraction in empower 3 software, it should be considered whether these types of issues with your chromatography exist: Incapable of properly integrating the standard or sample due to small-noise peaks or a drifting noisy baseline. The blank chromatogram includes characteristics that are worth subtracting (for example; small noise peaks). The blank chromatogram does not change from run to run and 3D blank baseline subtraction does not improve the signal-to-noise ratio of the signal. Blank baseline subtraction removes only the background signal and may increase the noise. After that, select alter sample in the sequence or sample set, then labeling the blank injection with a special mark as "B", open the method set used to obtain the data, then press the top of derived channels and select to create a new derived channel. In the first tab, "first (only) channel", press the channel drop-down list and select "DAD", in the second tab, choose the operator "-" and "DAD" from the channel drop-down list and check box form injection labeled and write down "B", write a name for the new-derived channel "Blank Subtraction" press ok, edit the processing method and change channel from "DAD" to "Blank Subtraction," then save method set and process the data with the method set, the blank chromatogram will subtracted from the sample automatically,[22] as clarified in Figure 2g.

Detection of wavelengths

Various wavelengths are checked and scanned at (200-400 nm) for 20 µg/mL of each mixture member of both pure CFR and SDB drugs and in their dosage forms to accomplish the best selectivity wavelength at 254 nm with minimum noise (Figure 3).

Optimization of temperature and flow rates

To achieve the best resolution and separation, many trials were performed at column temperatures of (35, 40, and 45°C), in addition to changes in flow rates (0.7, 1.0, and 1.3 mL/min); the flow rates of 1.0 mL/min and 40°C were the best couple for a system with good selectivity.

Stationary phase

Preparatory experiments had been performed by trying various columns with different lengths and particle sizes, including Thermo® C18 column (15 x 0.46 cm, 5.0 µm), Agilent ZORBAX -C18 column (15 x 0.46 cm, 5.0 µm) and Hichrom C18 column (0.46 x 15 cm, 5.0 µm, 150 Å pore size) and the last column is the best better selectivity and resolution for peaks of all impurities.

Optimization of gradient programs

The binary gradient program is experimented using various systems: (1) (i) 0-2 min: 20% (B), 80% (A); (ii) 2-20 min: 30% (B), 70% (A); (iii) 20-35 min: 50% (B: A), (iv) 35-55 min: 80% (A), 20% (B). (2) (i) 0-2 min: 10% (B), 90% (A); (ii) 2-20 min: 30% (B), 70% (A); (iii) 20-35 min: 50% (A, B), (iv) 35-55 min: 90% (A), 10% (B). The followed binary gradient proved to the best system for selectivity and resolution: (i) 0-8 min: 95% (A), 5% (B) isocratic; (ii) 8-28 min: 75% (A), 25% (B); (iii) 28-43 min: 50% (A), 50% (B); and (iv) 43-64 min: 95% (A), 5% (B).

Derivative ratio method (DD^1)

The method was verified for simultaneous estimation of the compounds to resolve the interference in binary mixtures. DD^1 spectrophotometric method was established to increase the selectivity of the analysis of CFR without interference from SDB. To adjust DD^1 method, many concentrations of the SDB as a divisor were tried including 1, 2, 4, and 5 µg/mL of SDB and optimum results were achieved by applying 5 µg/mL of SDB as a divisor. The obtained ratio spectra are distinguished as *per* the used wavelength, and DD^1 values showed good selectivity at the maximum 283.5 nm and a minimum of 313.4 nm (Figure 4). For the estimation of SDB in the presence of CFR, many concentrations of CFR are tried including, 2, 5, 10, and 15 µg/mL of CFR, and the best results were achieved when using CFR as a divisor with a concentration of 10 µg/mL. The obtained ratio spectra were recorded for maximum and minimum amplitudes at 216.7 nm and 235.5 nm, respectively (Figure 5).

Ratio subtraction method

This method was selected for estimating binary mixtures in which the spectrum of one component is more extended than that of the other one. It was applied to solve the overlapping spectra of the mixture of CFR and SDB to get the extended (SDB) in zero order. The method involves dividing of the spectrum of the mixture in the zero-order by divisor of CFR (10 µg/mL). The resulted ratio spectrum is a new graph representing the plateau region. By subtracting this constant (plateau in 250-315 nm), after that multiplying the new graph with the divisor, the original spectrum of SDB in the mixture can be obtained at 225 nm. Thus, the interference of the CFR was removed (Figure 6). Also, the same procedure is repeated to gain the extended (CFR) in the zero order by subtracting the constant which is found in the plateau region (205-230 nm) and multiplying the new graph with the divisor of SDB (5 µg/mL) consequently, the zero-order spectrum of CFR is obtained at λ_{max} 283 nm. These data are represented in (Figure 7).

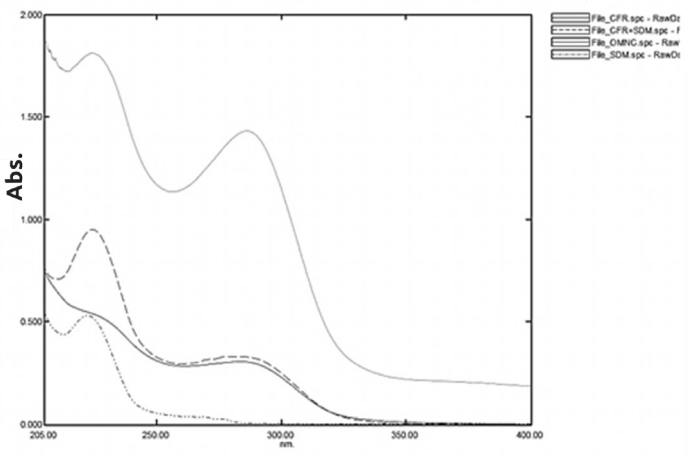

Figure 3. Zero order absorption spectra of 20 µg/mL of each of CFR, SDB, mix of CFR and SDB and omnicef 100 mg/5 mL using solvent as blank

CFR: Cefdinir, SDB: Sodium benzoate

Method validation

The proposed methods have been achieved and fully validated by following the guidelines of International Conference on Harmonization (ICH) recommended for method validation.[23] Then the applied USP pharmacopeia method was verified regarding system suitability testing, limit of quantification, and precision.[4]

I) Method (A) for active pharmaceutical ingredient (API)

Linearity and range

Linearity ranges, *e.g.* (0.003-0.075 mg/mL) and (0.002-0.050 mg/mL) were evaluated for CFR and SDB, respectively, with a correlation coefficient of regression >0.9999, Y-intercept of level 100% response of CFR equal to 0.4%. After running each preparation in triplicate, the relative standard deviations (RSD) percentage of the peak area of 3 injections for each level ≤2.0%. All the parameters of the regression analysis of the developed methods are presented in Table 1.

Limit of detection and composition

The quantitation limit refers to the lowest quantity of analytical material in a sample that can be quantified with appropriate accuracy. The obtained results for the limit of detection and limit quantitation are shown in Table 1.

Precision

System precision (repeatability)

The obtained results for six preparations were tabulated with RSD% <2.0%, as listed in Table 1.

Method precision

Method precision was evaluated by analyzing three different concentrations of the drugs being studied, each in triplicate on different days, performed by different analysts and equipment and RSD% was calculated, see Table 2 for ruggedness-related substance results.

Stability of analytical solutions

This method was been carried out by analyzing the assay of standard solution during three consecutive days at room temperature and in a fridge and comparing them with corresponding fresh results. The recovery results of the stability of the analytical solution are displayed in Table 2 with

RSD <2.0%.

Accuracy and recovery

The accuracy is estimated using three different concentrations (50%, 100% and 150%) with replicates and RSD between six injections from the same concentration <2.0% and recovery results between 98 and 102% as shown in Table 3.

Specificity and selectivity

If interference is observed (due to placebo, blank, diluent, *etc.*), it must not exceed 2.0% of the main peak target concentration limit. Placebo preparation was proceeded as under test preparation and (Figure 8a) confirmed that the API does not interfere with the placebo and solvent.

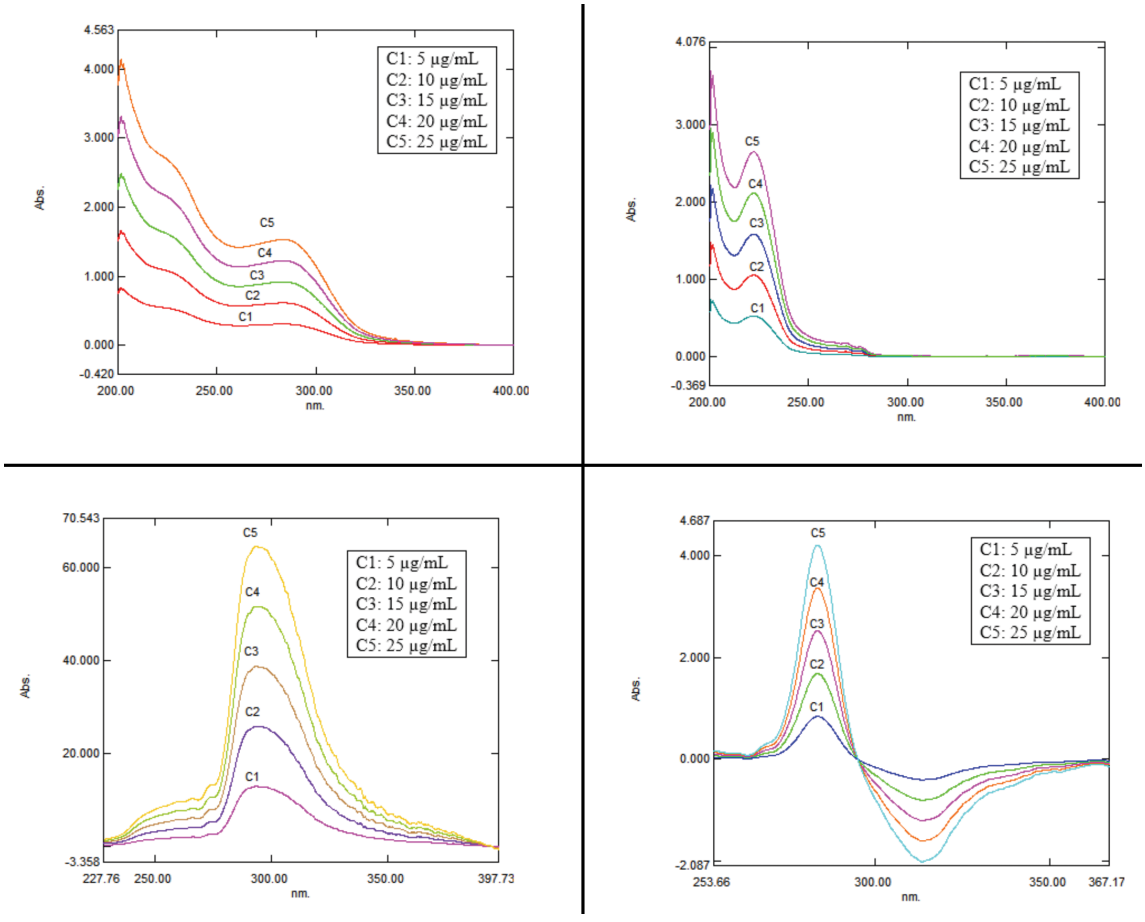

Figure 4. Ratio spectra and first derivative of the ratio spectra of standard solution of CFR using 5 µg/mL of SDB as a divisor and solvent as a blank
CFR: Cefdinir, SDB: Sodium benzoate

Table 1. Regression and validation parameters

Parameter	HPLC		DD[1]		RSM	
	CFR	SDB	CFR	SDB	CFR	SDB
Wavelength	254 nm	254 nm	283.5 nm	216.7 nm	283 nm	225 nm
Range (µg/mL)	3-75	2-50	5-25	5-25	5-25	5-25
Slope	18651283	1850.2	0.0705	0.3150	0.0563	0.3234
Intercept	988.5	1093.6	0.028	0.400	0.0063	0.0250
Correlation coefficient	0.9999	0.9999	0.9996	0.9997	0.9995	0.9996
Repeatability	0.2	0.1	0.3	0.2	0.4	0.2
LOD[a] (µg/mL)	0.41	0.42	0.73	0.36	0.33	0.30
LOQ[a] (µg/mL)	1.22	1.29	2.20	1.11	1.03	0.92

[a]LOD: Limit of detection (3.3 x σ/slope) and LOQ: Limit of quantitation (10 x σ/slope)
HPLC: High performance liquid chromatography, RSM: Ratio subtraction method, CFR: Cefdinir, SDB: Sodium benzoate

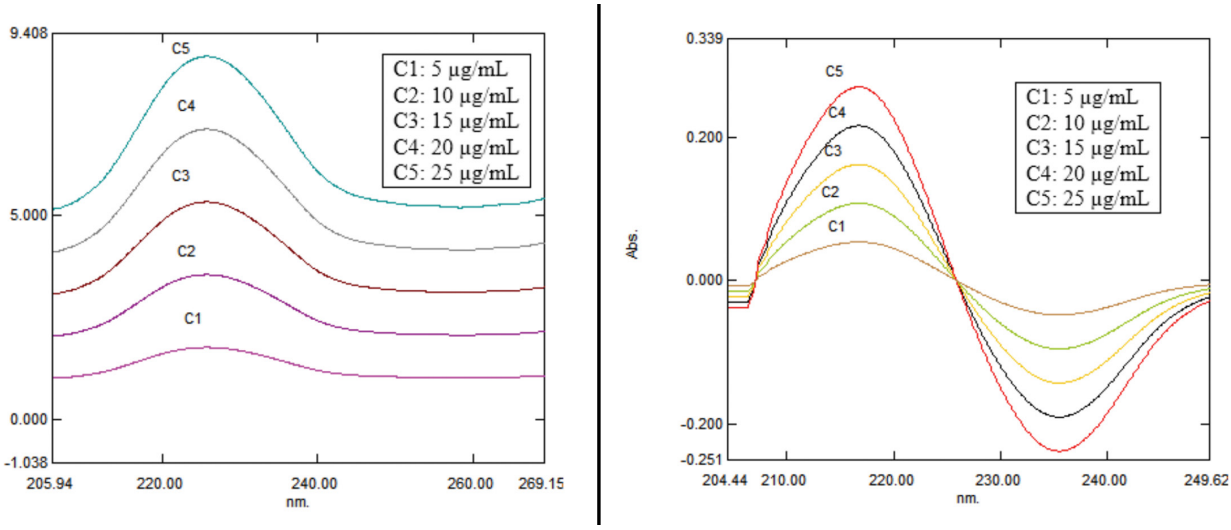

Figure 5. Ratio spectra and first derivative of the ratio spectra of standard solution of SDB using 10 µg/mL of CFR as a divisor and solvent as a blank
CFR: Cefdinir, SDB: Sodium benzoate

Table 2. Ruggedness, robustness, and stability of analytical solution of the proposed methods

Parameter	HPLC		UV		Limit %
	CFR	SDB	CFR	SDB	
Day to day	0.80	0.75	0.70	0.64	
Analyst to analyst	1.22	1.13	0.90	0.74	
Column to column	0.77	0.79	-	-	
Flow rate change (± 0.1 mL/min)	0.71	0.85	-	-	
pH changes of mobile phase (± 0.2)	0.88	0.79	-	-	RSD ≤2.0%
Wavelength change (254 ± 2.0 nm)	0.80	0.78	0.76	0.57	
Column temperature change (30, 25°C)	0.93	0.82	0.89	0.59	
Fresh sample	0.12	0.14	0.19	0.22	
Stored sample in fridge	0.66	0.47	0.54	0.49	
Stored sample at room temperature	0.89	0.94	0.83	0.77	

HPLC: High performance liquid chromatography, UV: Ultraviolet, CFR: Cefdinir, SDB: Sodium benzoate, RSD: Relative standard deviation

Forced degradation

The forced degradation of CFR was performed under different acid, base, oxidative, thermal, photolytic and neutral conditions. To establish the stability indicating capability of the related substance test method for omnicef, standard solution of CFR was separately subjected to the above-mentioned conditions. All degradants of CFR are well resolved and do show any interference with CFR peaks. CFR peak was found to be pure under all forced degradation conditions since that the peak purity angle match for CFR under all conditions was found to be less than the purity threshold as displayed in Table 4 and Figure 8.

II) Method (B) for UV spectroscopic method

Linearity and range

Linearity range (0.005-0.025 mg/mL) was evaluated for CFR and SDB for spectrophotometric methods with a correlation coefficient of regression >0.999, RSD percentage for each level ≤2.0%. All the parameters of the regression analysis of the developed methods are presented in Table 1.

Limit of detection and composition

The quantitation limit refers to the lowest quantity of analytical material in a sample that can be quantified with appropriate accuracy. The obtained results for limit of detection and limit quantitation are shown in Table 1.

i) Acid hydrolysis		
Transfer 10 mL of the standard stock solution	3 mL of 1 N HCl, sonicate for 20 min and mix well, store at room temperature for 2 h ----------> Add 50 mL solvent	Complete to 100 mL volumetric flask with solvent
İİ) Basic hydrolysis		
Applied to 10 mL standard stock solution	3 mL of 1 N NaOH, sonicate for 20 min and mix well, store at room temperature for 2 h ----------> Add 50 mL solvent	Complete to 100 mL volumetric flask with solvent
iii) Oxidation		
Transfer 10 mL of the standard stock solution	3 mL of 30% H_2O_2, sonicate for 20 min and mix well, store at room temperature for 2 h ----------> Add 50 mL solvent	Complete with solvent in 100 mL volumetric flask
iv) Thermal decomposition		
Applied to 10 mL of the standard stock solution	Heat for 2 h at 85°C in water bath ----------> Add 50 mL solvent	Complete to 100 mL volumetric flask with solvent
v) Light decomposition		
Applied to 10 mL of the standard stock solution	Keep in light for 2 h ----------> Add 50 mL solvent	Complete to 100 mL with a solvent

Precision

System precision (repeatability)

The obtained results for six preparations were tabulated with RSD% <2.0%, as listed in Table 1.

Method precision

Method precision was evaluated by analyzing three different concentrations of the drugs under study, each in triplicate on different days, performed by different analysts and equipment and RSD% was calculated, see Table 2 for ruggedness-related substance results.

Stability of analytical solutions

This method will be determined by analyzing the assay of standard solution during three consecutive days at room temperature and in a fridge and calculated it corresponding to fresh results. The recovery results of stability of the analytical solution are displayed in Table 2 with RSD <2.0%.

III) Method (C) for related substances

System suitability testing

System suitability of the analytical method is determined by preparing a standard solution of impurities and analyzed at least 6 times with RSD ≤2.0%, resolution not less than 1.5 between CFR and the third peak of USP CFR related compound A, tailing factor not more than 1.5 for CFR related compound B. All system suitability parameters are tabulated in Table 5.

Limit of detection and composition

The quantitation limit refers to the lowest quantity of analytical material in a sample that can be quantified with appropriate accuracy. The obtained results for limit of detection and limit quantitation are shown in Table 1.

System precision (repeatability)

The related substances obtained results for six preparations were tabulated and the average of the 12 preparations with RSD% <2.0% was calculated as listed in Table 1.

Specificity and selectivity

If interference is observed (due to placebo, blank, diluent, *etc.*), it must not exceed 10.0% of the impurity peak at the specification limit.

CONCLUSION

Efficient and novel stability indicated that HPLC and spectrophotometric methods have been validated and

Table 3. Accuracy and recovery of CFR in the proposed method

Concentration	Test	Result (%)	Average result (%)	RSD (%)
50%	T1 inj-1	99.98%	99.88%	0.18%
	T1 inj-2	99.76%		
	T2 inj-1	99.72%		
	T2 inj-2	99.68%		
	T3 inj-1	100.12%		
	T3 inj-2	99.98%		
100%	T1 inj-1	99.66%	99.49%	0.10%
	T1 inj-2	99.53%		
	T2 inj-1	99.48%		
	T2 inj-2	99.49%		
	T3 inj-1	99.40%		
	T3 inj-2	99.36%		
150%	T1 inj-1	99.93%	99.75%	0.13%
	T1 inj-2	99.88%		
	T2 inj-1	99.63%		
	T2 inj-2	99.73%		
	T3 inj-1	99.74%		
	T3 inj-2	99.60%		

CFR: Cefdinir, RSD: Relative standard deviation

Table 4. Stability indicating capability of the related substances

Cefdinir			
Condition	**Peak area**	**% Degradation**	**Peak purity match**
Normal	290534	-	Pass
Thermal	283365	2.47%	Pass
Light	283087	2.56%	Pass
Acidic	279986	3.63%	Pass
Basic	283603	2.39%	Pass
Oxidative	19087	93.43%	Pass

Table 5. System suitability testing parameters of the developed methods

Item	HPLC	Reference values
	CFR	-
Tailing factor	0.92	T ≤1.5
Injection precision	0.17	RSD ≤1%
Number of theoretical plates (N)	4850	N >2000
Resolution	3.0	R_s >1.5
Retention time (R_t)	0.10	RSD ≤1%

HPLC: High performance liquid chromatography, CFR: Cefdinir, RSD: Relative standard deviation, Rs: Resolution

developed for simultaneous quantification of the CFR and SDB in the presence of its degradants. As for the chromatographic methods, it was developed and validated as *per* ICH guidelines using the blank subtraction method on empower PDA software that reduces waste time in manual calculation of impurities. Two spectrophotometric methods were developed, the first derivative of ratio spectra spectrophotometric method (1^{st}DD) and the second is ratio subtraction method, which were used to resolve the interference between CFR and SDB. Based on peak purity results, which have obtained from selectivity and forced degradation analysis, we can confirm that the proposed method is selective and sensitive, and it can be used as stability indicating one for assay and related substances for CFR in QC labs. The proposed method was demonstrated to achieve a shorter time, high sensitivity, and cost effective of analysis and consumable reagents.

ACKNOWLEDGMENTS

The authors appreciate the possibilities provided by Hikma Company during performing this work.

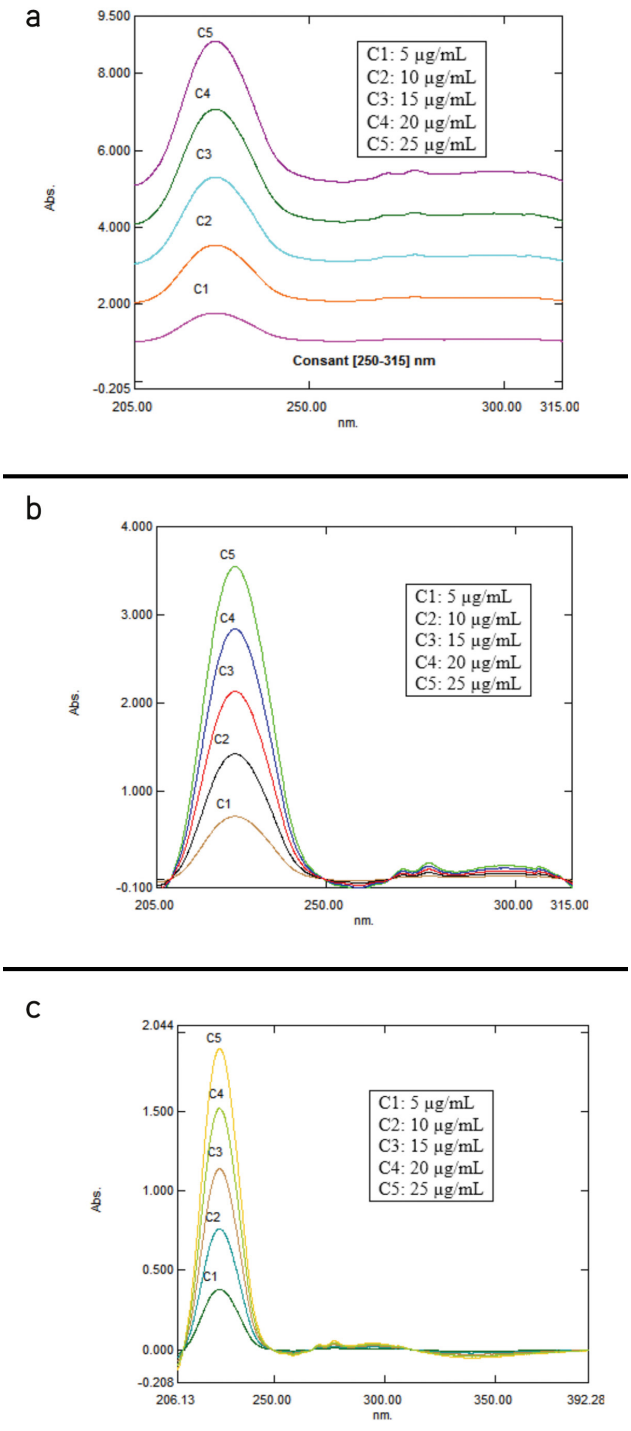

Figure 6. (a) Ratio spectra of a mixture of CFR and SDB using CFR (10 µg/mL) as a divisor. (b) Subtracting the value of the constant from the ratio spectra (c) the obtained SDB spectrum in zero order

CFR: Cefdinir, SDB: Sodium benzoate

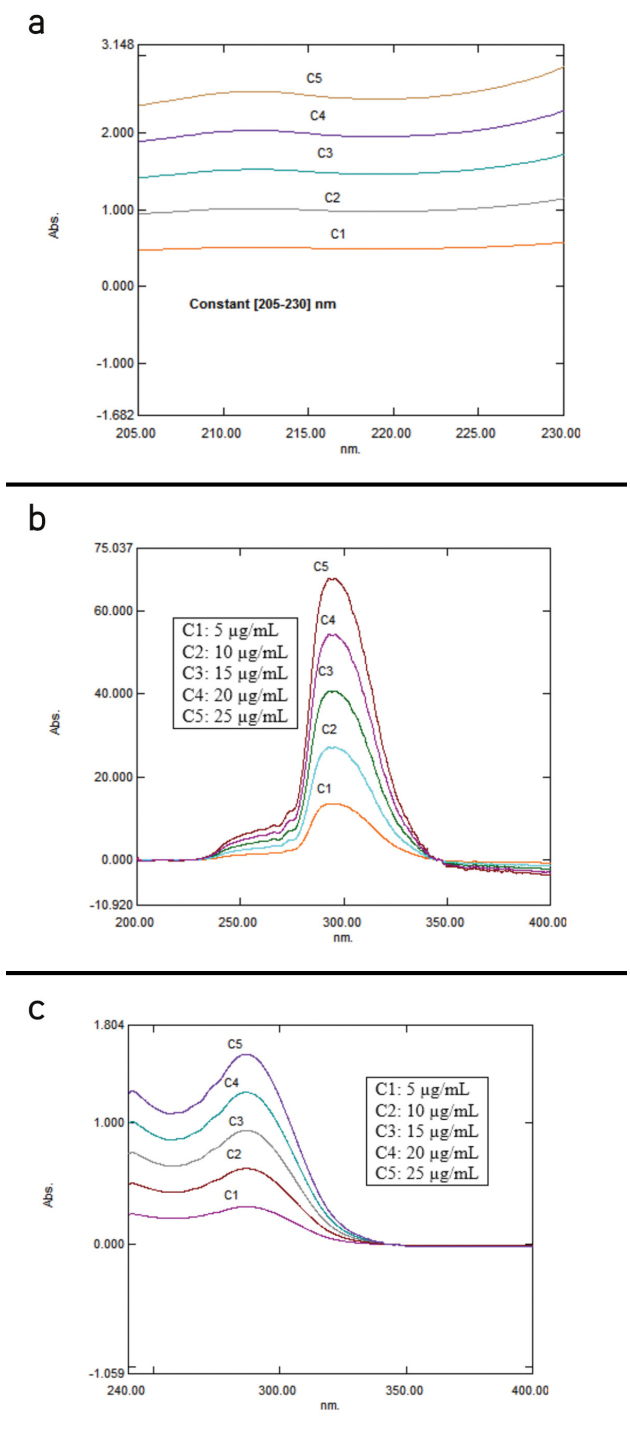

Figure 7. (a) Ratio spectra of a mixture of CFR and SDB using SDB (5 µg/mL) as a divisor. (b) Subtracting the value of the constant from the ratio spectra (c) the obtained CFR spectrum in zero order

CFR: Cefdinir, SDB: Sodium benzoate

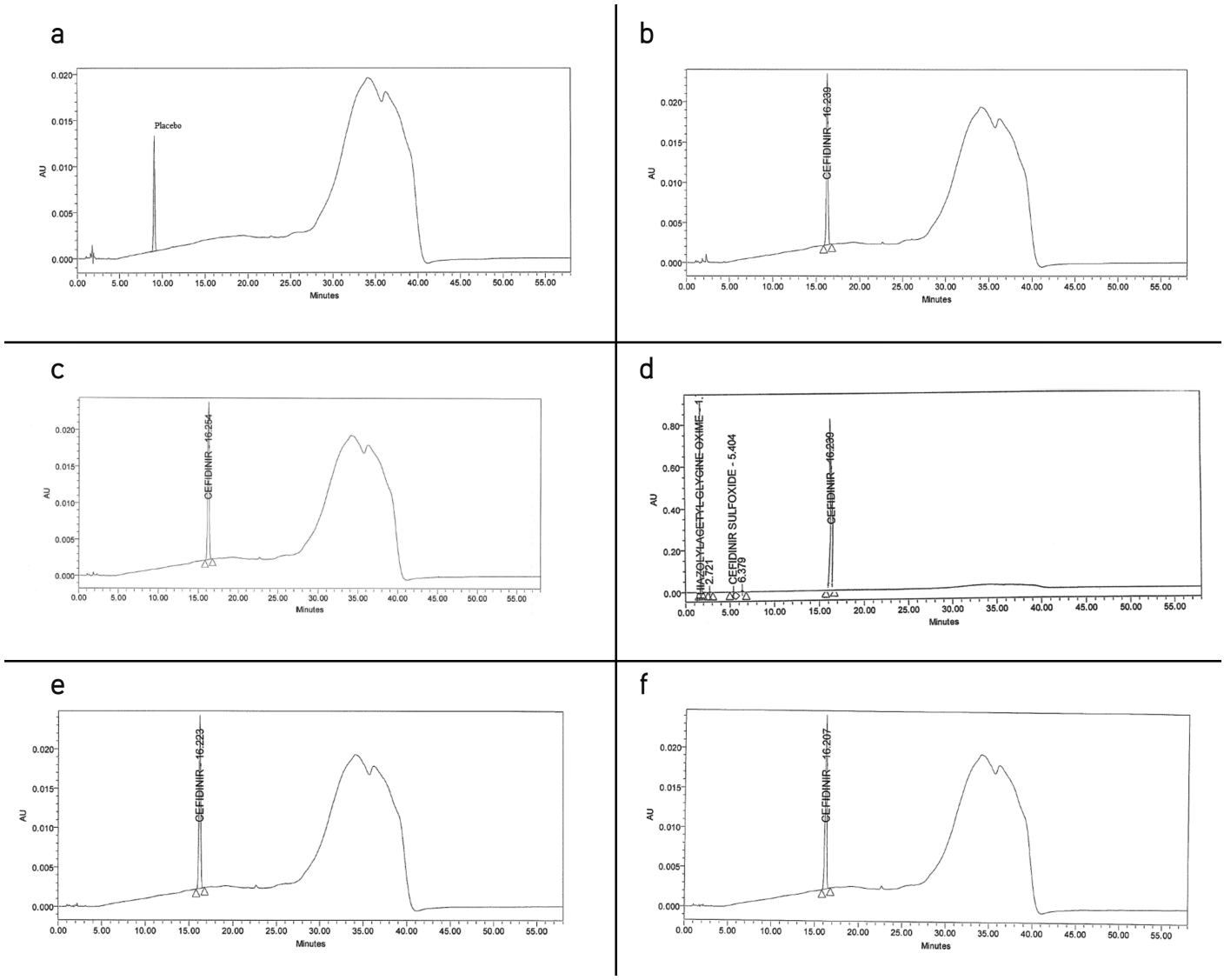

Figure 8. Chromatograms of (a) placebo, (b) acid hydrolyzed degraded sample, (c) base hydrolyzed-degraded sample, (d) oxidative-degraded sample, (e) thermal degraded sample, (f) sun light degraded sample

Ethics

Ethics Committee Approval: Not applicable.

Informed Consent: Not applicable.

Peer-review: Externally peer-reviewed.

Authorship Contributions

Concept: M.A.M., M.E.K.M.H., Design: M.A.M., M.E.K.M.H., Data Collection or Processing: M.A.M., Analysis or Interpretation: M.E.K.M.H., Literature Search: M.A.M., M.E.K.M.H., Writing: M.A.M., M.E.K.M.H.

Conflict of Interest: No conflict of interest was declared by the authors.

Financial Disclosure: The authors declared that this study received no financial support.

REFERENCES

1. 3D blank subtraction in Empower Waters, Milford, Massachusetts. 2018. Available from: https://support.waters.com/KB_Inf/Empower_Breeze/WKB8213_How_to_perform_3D_blank_subtraction_in_Empower
2. Al-Badr AA, Alasseiri FA. Cefdinir. Profiles of Drug Substances, Excipients and Related Methodology. In: Brittain H eds. 2014;39:41-112.
3. British Pharmacopoeia Stationary Office, Medicines and Healthcare Products Regulatory Agency. 2022;2:1019.
4. U.S. Pharmacopoeia, United States Pharmacopoeia Convention Inc. 2022;43:3761.
5. Rao KVVP, Rani A, Reddy AVR, Bharathi CH, Dandala R, Naidu A. Isolation, structural elucidation and characterization of impurities in cefdinir. J Pharm Biomed Anal. 2007;43:1476-1482.
6. Mashelkar UC, Renapurkar SD. A LCMS compatible stability-indicating HPLC assay method for cefdinir. Int J Chem Tech Res. 2010;2:114-121.

7. Chen ZZ, Zhang DS, Wang N, Feng F, Hu CQ. Identification of impurity peaks in the HPLC chromatogram by LC-MS and two-dimensional chromatographic correlation spectroscopy. Yao Xue Xue Bao. 2012;47:492-497.
8. Jin L, Li-Xin W, Shang-Chen Y, Chang-Qin H. Characterization of impurities in cefdinir bulk material by online column-switching liquid chromatography and tandem mass spectrometry. Curr Pharm Anal. 2013;9:145-158.
9. Al Bayyari MA, Abu Ajjour RS. Determination of antibiotic drug cefdinir in human plasma using liquid chromatography tandem mass spectroscopy. Am J Anal Chem. 2015;6:239-245.
10. Okamoto Y, Itoh K, Namiki Y, Matsushita J, Fujioka M, Yasuda T. Method development for the determination of cefdinir and its related substances by high-performance liquid chromatography. J Pharm Biomed Anal. 1996;14:739-748.
11. Hashem H, Gouda AA, Hassan W. Development and validation of a rapid stability indicating chromatographic determination of cefdinir in bulk powder and dosage form using monolithic stationary phase. J Liq Chromatogr Relat Technol. 2012;35:1638-1648.
12. Hassouna MEM, Mohamed MA. Application of lean six sigma methodologies and *in vitro* dissolution studies for simultaneous determination of cefdinir and sodium benzoate by RP-HPLC and UPLC methods in their dosage forms. Biomed J Sci Technol Res. 2019;16:1-13.
13. Abdel-Aziz O, Farouk M, Nagi R, Abdel-Fattah L. Simple spectrophotometric and HPTLC-densitometric methods for determination of cefdinir in bulk powder and pharmaceuticals, and in presence of its hydrolytic degradation products. J App Pharm Sci. 2014;4:129.
14. Popović G, Čakar M, Agbaba D. Simultaneous determination of loratadine and preservatives in syrups by thin-layer chromatography. Acta Chromatogr. 2007;19:161-169.
15. Gouda AA, Hashem H, Hassan W. Spectophotometric methods for determination of cefdinir in pharmaceutical formulations *via* derivatization with 1,2-naphthoquinone-4-sulfonate and 4-chloro-7-nitrobenzo-2-oxa-1, 3-diazole. Drug Test Anal. 2012;4:991-1000.
16. Baş E, Özdemir S, Çaglayan MG, Palabıyık İM, Onur F. Determination of cefixime and cefdinir in pharmaceutical preparations. Turk J Pharm Sci. 2013;10:321-328.
17. El Sheikh R, Amin AS, Gouda AA, Zahran D. Validated spectrophotometric methods for determination of cefdinir in pure and dosage forms through charge transfer complexation using alizarin derivatives. Int J Res Pharm Sci. 2017;2:11-18.
18. Hassouna MEM, Abdelrahman MM, Mohamed MA. Novel spectrophotometric methods for simultaneous determination of cefixime trihydrate and sodium benzoate in powder for oral suspension dosage form. Glob J Otolaryngol. 2017;12:69-79.
19. Kompany-Zareh M, Mirzaei S. Spectrophotometric resolution of ternary mixtures of pseudoephedrine hydrochloride, dextromethorphan hydrobromide, and sodium benzoate in syrups using wavelength selection by net analyte signals calculated with hybrid linear analysis. Anal Chim Acta. 2004;526:83-94.
20. Boltia SA, Algmaal SE, Mostafa NM, El Saharty YS. Development and validation of a spectrofluorimetric method for the determination of cefdinir *via* its degradation products. Appl Spectrosc. 2021;88:336.
21. Hassan MJM, Mizher OQ. Cloud point extraction for the spectrophotometric determination of cefdinir. Al-Mustansiriyah Journal of Science. 2019;30:85-93.
22. Create a derived channel in Empower, Waters, Milford, Massachusetts. 2018. Available from: https://support.waters.com/KB_Inf/Empower_Breeze/WKB16590_How_to_create_a_derived_channel_in_Empower where the wavelength switches at a given time
23. ICH: validation of analytical procedures: text and methodology, Q2 (R1), the International Council on Harmonisation of technical requirements for registration of pharmaceuticals for human use. 2005;1-17.

Turk J Pharm Sci 2022;19(5):543-551
DOI: 10.4274/tjps.galenos.2021.96603

ORIGINAL ARTICLE

Potential Drug Interactions in Adults Living in Manaus: A Real-World Comparison of Two Databases, 2019

Tayanny Margarida Menezes Almeida BIASE[1], Giulia Sartori BRUNIÉRI[1], Marcus Tolentino SILVA[2], Taís Freire GALVÃO[1]*

[1]State University of Campinas, School of Pharmaceutical Sciences, Graduate Program of Pharmaceutical Sciences, São Paulo, Brazil
[2]University of Sorocaba, Graduate Program of Pharmaceutical Sciences, São Paulo, Brazil

ABSTRACT

Objectives: Drug information systems are commonly used by professionals to assist in the identification of drug interactions and to ensure the safe use of medications. Real-world evidence about the comparison of different drug interaction sources is scarce. We aimed to compare two drug interaction databases to identify interactions in a population-based survey.

Materials and Methods: This is a cross-sectional study based on a previous survey performed in the city of Manaus, Brazil, in 2019. We included adults aged 18 years and over, who used two or more medicines 15 days before the interview. To assess potential drug interactions, we searched Micromedex and UpToDate databases. The primary outcome was the prevalence of potential drug interactions in each database. Weighted Kappa statistics were calculated to assess agreement on the presence of drug interaction, documentation and severity.

Results: A total of 752 participants were included in the study. The prevalence of drug interactions was 43.8% [95% confidence interval (CI): 40.2, 47.3%] in UpToDate and 30.2% (95% CI: 26.9, 33.5%), in Micromedex. The agreement related to drug interactions between the two databases was fair (Kappa: 0.631). For severity (Kappa: 0.398) and documentation (Kappa: 0.311), the agreement was poor.

Conclusion: Agreement among compared databases was sub-optimal. Better quality and transparency of evidence available in drug interaction sources are needed to support informed healthcare professionals' decision.

Key words: Drug interactions, software, documentation, classification, population health

INTRODUCTION

Proper identification of drug interactions is essential to ensure the safety and effective use of medications.[1] Pharmacists play a significant role in guiding drug therapy and the rational use of medicines in different levels of health care.[2-4] Clinical decision support software systems are commonly used in hospitals and in the community to assist pharmacists in identifying drug interactions of clinical significance.[5] These systems that are used by pharmacists and other health professionals to identify interactions have evolved to integrate computerized screening banks for drug interactions, clinical information, and other drug-related problems.[6-8]

Although these software tools can increase the ability of pharmacists to detect clinically significant interactions, these systems are far from fail-safe.[5,9] Optimal clinical decision support software should have a balance between low and high-risk alerts.[10,11] Excessive warnings can cause tiredness and suppression of clinically significant interactions, while the warning shortage can increase the risk of ignoring possible damage and decrease the user's perception in relation to the reliability and usefulness of the system.[12]

Searching for drug interaction is not a trivial step, as there is a wide variety of search sources, from package inserts to medicines, scientific literature and various databases and websites. This diversification of sources makes the search difficult, when looking for reliable information about drug interactions and ensuring patients receive safe drug therapy. Assessments of software performance to identify potential

*Correspondence: taisgalvao@gmail.com, Phone: +55 (19) 3521-7149, ORCID-ID: orcid.org/0000-0003-2072-4834
Received: 24.06.2021, Accepted: 25.10.2021

drug interactions mainly focus on hospital environment or are based on theoretical scenarios,[13-17] involving patients with multimorbidity, in polypharmacy and old age.[18] This highly selected population, usually from hospitals[19] may not reflect the reality of multiple drug use and possible interactions by the general population. A limited number of studies have investigated the prevalence of potential drug interactions in the general population. Further assessments and comparisons of sources for assessing potential drug interactions in the community can add valuable information, especially in less developed settings.[18,20] We compared two systems of drug interaction for a population-based survey.

MATERIALS AND METHODS

Study design

This is a cross-sectional study based on a previous survey performed in the city of Manaus (Brazil) from April to June 2019.[21]

Setting

The study setting was Manaus, the city capital of the State of Amazonas, with an estimated population of 2.219.580 people in 2020.[22]

Participants who had taken two or more medications in the previous 15 days were assessed for the presence of potential drug interactions.

Participants

The adults, who were included in the study were those at the age and over 18 years who self-reported using two or more medicines 15 days before the interview. In the original survey, the participants were selected by probabilistic sampling carried out in three stages: (1) Draw of the census tracks of the city, (2) systematic selection of households, and (3) random selection of the individual interviewed based on sex and age quotas.[21] The sample size was calculated as 2.300 participants for the main study - unrestricted to individuals who took at least two medicines - considering 20% of healthcare usage, confidence level of 95%, absolute precision of 2%, design effect of 1.5, and 2.106.355 in habitants aged ≥18 years living in Manaus.[21] Based on the results in the present analysis, *post-hoc* sample size was calculated.

Variables

The primary outcome was the prevalence of potential drug interactions. For clarity, in this study, we use "drug interactions" as a synonym of "potential drug interaction". The independent variables were sex (men, women), age (in years, categorized as: 18-24, 25-34, 35-44, 45-59, ≥60), economic classification (A/B, C, D/E, according to the 2018 Brazilian Economic Classification Criteria, in which A is the wealthiest and E is the poorest class),[23] education (higher education or beyond, high school, elementary school, below elementary school), health status (good, fair, poor), chronic diseases (yes, no), number of drugs used in the last 15 days (2, 3-4, ≥5).

Data sources and measurements

Experienced interviewers visited the participants' households in this study. The interviews were georeferenced, and the data collected were stored in e-devices. The use of medicines was assessed by the question: "Have you taken any medications in the last 15 days (two weeks)?" and its possible answers: "Yes" or "No". If yes, the name of the medication was registered as informed by the participant and could be confirmed by checking the medication packages and/or available medical prescriptions. The data were compiled in the Microsoft Excel® 2010 software and the drugs were coded according to the Brazilian Common Denomination and, subsequently, according to the World Health Organization's (WHO) Anatomical Therapeutic Classification System (ATC). Ineligible drugs or without an ATC code were classified as "uncoded".[24] From February to March 2021, we searched IBM Micromedex® Drug Interaction Checking[25] and Lexicomp® Drug Interaction from UpToDate®[26] to identify the drug interactions. These databases are commonly used to investigate drug interactions in clinical practice and subscription was available for research team, allowing present investigation.

All ATC-coded drugs were assessed in each database to verify drug interactions. If positive for drug interactions, the combination of drugs, severity and documentation was recorded according to the classification of the database used. Commercial combinations of drugs unavailable as an association in the database were searched by including each substance separately and interaction was recorded if occurred between the association and the other medicine. Both databases classify drug interactions according to severity and documentation. Micromedex classify severity of drug interactions as: contraindicated (medications are contraindicated for concomitant use), major (the interaction may be life-threatening and/or require medical intervention to reduce or avoid serious adverse effects), moderate (the interaction may result in the health problem exacerbation and/or require treatment change), and minor (the interaction would result in limited clinical effects).[25] In this database, documentation is categorized into the following: excellent (interaction confirmed from controlled studies), good (the interaction exists, but there is absence of properly controlled studies), and fair (the available documentation is unsatisfactory, but pharmacological considerations lead clinicians to suspect the existence of the interaction).

UpToDate database defines severity as: major (effects may result in death, hospitalization, permanent injury, or therapeutic failure), moderate (medical intervention needed to treat effects, effects do not meet criteria as major), and minor (effects would be considered tolerable in most cases, no need for medical intervention). Documentation reliability is defined as excellent, good, fair, and poor. It also assigns a risk rating, which is a rapid indicator regarding how to respond to the interaction: A (unknown interaction), B (minor, no action required), C (moderate, monitor therapy), D (main, consideration to modify therapy) or X (contraindicated, avoid combination).[26]

To allow comparability of the databases, "contraindicated" severity category from Micromedex was regrouped in "major"; "poor" documentation from UpToDate were rated "fair"; and

interactions of risk "A" from UpToDate were disregarded (considered as no drug interaction).

Bias

The data were collected by a team of experienced and trained interviewers.[21] The participant could optionally present the medicine package mentioned in the interview to confirm the data and avoid misclassifications. To ensure the encoding of all medicines according to the ATC, herbal, and homeopathic products were excluded from the research.

Ethics approval

This study was approved by the Ethics Committee of the Federal University of Amazonas (opinion no: 3,102,942), on December 28, 2018 (Certificate of Presentation for Ethical Appreciation 04728918.0.0000.502020). All participants signed a term of free and informed consent.

Statistical analysis

Participants were described statistically according to independent variables. Frequency of drug interactions, severity, and documentation classifications in each database were described, as well as more relevant disagreements on interactions between them (major severity or excellent documentation in one database was not considered a drug interaction in the other).

Weighted Kappa statistics were calculated to assess agreement on drug interaction, documentation, and severity classifications between both databases. Kappa values >0.75 were considered excellent agreement beyond chance, between <0.75-0.40 represented fair agreement, and values <0.40 denoted poor agreement beyond chance.[27]

RESULTS

From 2.321 interviewed, 752 participants were taking two or more medicines and were included in the study. Most participants were women (58.6%), aged 45-59 years (27.3%), belonged to economic classification C (low middle class, 54.5%), had higher (49.2%), self-reported good health status (49.7%), had chronic diseases (76.2%) and used only two drugs (49.3%; Table 1). The prevalence of drug interactions in UpToDate was 43.8% [95% confidence interval (CI): 40.2, 47.3%] and in Micromedex, 30.2% (95% CI: 26.9, 33.5%).

A total of 344 unique participants was reported with the presence of drug interactions in one or in both databases. More patients had drug interactions according to UpToDate (n: 329) Micromedex (n: 227); and 212 patients with drug interactions were identified by both databases (Figure 1).

The agreement on drug interactions between the two databases was fair (Kappa: 0.631). Using UpToDate, over half of the interactions were classified as moderate severity (61.2%), while Micromedex classified most as major severity (62.6%). Between the databases, the agreement on the severity classification was evaluated as poorly with a Kappa value of 0.398. In both databases, more than half of the interactions were based on fair documentation (UpToDate: 70.6%; Micromedex: 61.4%) and documentation agreement was poor (kappa: 0.311) (Table 2). The *post-hoc* minimum sample size based on this agreement would be 94 patients.

Among the more relevant classification disagreements identified between the databases, 27 different discordant drug interactions were reported with major severity or with excellent documentation in one database and not detected in the other (Table 3). Out of these discrepant classifications, 20 were present only in UpToDate (13 with major severity, 7 with excellent documentation), and seven present only in Micromedex (6 with major severity, 1 with excellent documentation). Most frequent drug interactions shown in UpToDate were related to major severity interactions: Carisoprodol-orphenadrine (n:

Table 1. Main characteristics of participants taking two or more medicines (n: 752)

Variables	n	%
Sex		
Male	311	41.4
Female	441	58.6
Age (years)		
18-24	108	14.4
25-34	168	22.3
35-44	147	19.6
45-59	205	27.3
≥60	124	16.5
Economic classification		
A/B	108	14.4
C	410	54.5
D/E	234	31.1
Education		
Higher education or beyond	60	8
High school	370	49.2
Elementary school	125	16.6
Below elementary school	197	26.2
Health status		
Good	374	49.7
Fair	292	38.8
Poor	86	11.4
Chronic diseases		
No	179	23.8
Yes	573	76.2
Number of medicines		
2	371	49.3
3-4	304	40.4
≥5	77	10.2

10), chlorpheniramine-orphenadrine (n: 8), and ciprofloxacin-ibuprofen (n: 3); and in Micromedex, acetylsalicylic acid-hydrochlorothiazide (n: 3). The paracetamol-tramadol interaction (n: 3) presented excellent documentation and minor severity in UpToDate. All major severity drug interactions were related to fair documentation, according to UpToDate and, based on Micromedex, the major severity interactions were fair (n: 4) and good documentation (n: 2). The drug interaction of excellent documentation (minor severity) was amitriptyline-estradiol (n: 1), according to Micromedex and not present in UpToDate. Drug interactions with excellent documentation ranged from minor (n: 7) to moderate (n: 1) severities, in UpToDate and not present in Micromedex. Most major severity interactions in UpToDate belonged to X risk classification (9 of 13), and minor severity interactions were classified as B risk (6 of 7) (Data not shown in Tables).

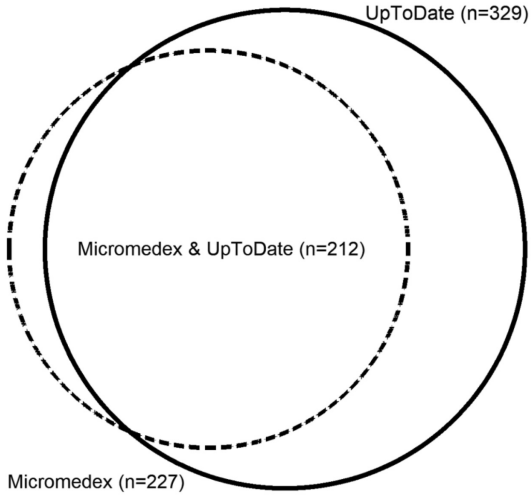

Figure 1. Agreement of drug interactions between UpToDate and Micromedex

Table 2. Agreement of drug interaction between the databases

Variable	UpToDate		Micromedex		Kappa
	n	%	n	%	
Interaction[a]					
No	423	56.3	525	69.8	0.631
Yes	329	43.8	227	30.2	
Severity[b]					
Minor	61	9.1	10	2.2	0.398
Moderate	411	61.2	161	35.2	
Major	200	29.8	286	62.6	
Documentation[b]					
Fair	473	70.6	282	61.4	0.311
Good	169	24.93	87	19.4	
Excelent	30	4.48	88	19.2	

[a]n: 752 patients, [b]n: 672 interactions in UpToDate; n: 457 interactions in Micromedex

In UpToDate, orphenadrine appeared in seven different drug interactions that were not similarly regarded in Micromedex. Moreover, it was the most frequent drug involved in these discordant interactions (Table 3). Non-steroidal anti-inflammatory drugs were the main ones in the drug interactions, present in nine different drug interactions, and additive effects between medicines were the main mechanism of the interactions (n: 10).

DISCUSSION

Drug interactions were present in 3 to 4 people among 10 adults living in Manaus, according to the consulted databases, showing a higher frequency in UpToDate than Micromedex. Agreement on the identification of drug interactions between the databases was considered fair, while severity and documentation classifications of these interactions were poor agreements. Depending on the source used, a lot of work may result from screening drug interaction in the population setting.

Due to the cross-sectional nature of this study, participants were not monitored over time to confirm the occurrence of adverse events due to drug interactions. Based on a list of self-reported medicines used by the participants 15 days before the interview, we assessed drug interactions and did not clinically investigate these interactions. This limitation can make our results prone to memory and information biases. The databases are periodically updated and may have undergone changes during or after the study, also potentially affecting our results.

In agreement with our findings, a higher prevalence of drug interactions was observed, when UpToDate was the reference for interactions. In the United States, an assessment performed in 2012 by screening 240 patients' medication profiles showed almost twice as many drug interactions using Micromedex.[28] In Türkiye, a study with 80 renal transplant recipients observed similar results, presenting almost twice the drug interactions identified in UpToDate in compared to Micromedex.[29] The use of different databases shows the lack of agreement on the number of possible drug interactions in different investigations, including ours, which raises concerns about the clinical relevance of checking multiple sources. Excessive alerts in clinical practice can lead to high workloads for healthcare professionals and mask important alerts.[30,31]

Micromedex and UpToDate had a fair agreement on the identification of drug interactions. Similar results were observed in previous studies that investigated agreement on multiple sources of drug interactions in clinical practice, including drugs for metabolic disorders, antiretrovirals, antimicrobials, and psychiatric drugs.[13,16,32,33] A study involving common therapeutic combinations of drugs for bipolar disorder tested 125 pairs of drug interactions in six databases in 2019, showing low agreement among the databases assessed.[16] Assessment of drug interactions in an Indian hospital using Epocrates and Medscape presented a significant discrepancy between the severity categories of drug interactions in 2015.[34] A retrospective analysis in an intensive care unit in Germany, including prescriptions for transplant patients, used five

Table 3. Characteristics of discordant drug interactions

Drug combination	n	Severity	Documentation	Management	Potential outcome	Mechanism	Database
Carisoprodol, orphenadrine	10	Major	Fair	Concurrent use should be avoided	CNS[a] depressants may enhance orphenadrine effects	Additive CNS[a] depression	UpToDate
Chlorpheniramine, orphenadrine	8	Major	Fair	Concurrent use should be avoided	CNS[a] depressants may enhance orphenadrine effects	Additive CNS[a] depression	UpToDate
Acetylsalicylic acid, hydrochlorothiazide	3	Major	Good	Monitor worsening renal function signs and assure diuretic efficacy	Reduced diuretic effectiveness and possible nephrotoxicity	Decreased production of renal prostaglandins	Micromedex
Ciprofloxacin, ibuprofen	3	Major	Fair	They considered an increased risk of seizure	Increased seizure-potentiating effect of quinolones	Enhanced central GABA-A[b] inhibition increased epileptogenic potential of the quinolone	UpToDate
Paracetamol, tramadol	3	Minor	Excellent	No action required	Decreased paracetamol absorption	Impairment in gastric motility	UpToDate
Ciprofloxacin, dipyrone	2	Major	Fair	They considered an increased risk of seizure	Increased seizure-potentiating effect of quinolones	Enhanced central GABA-A[b] inhibition increased epileptogenic potential of the quinolone	UpToDate
Loratadine, orphenadrine	2	Major	Fair	Concurrent use should be avoided	CNS[a] depressants may enhance orphenadrine effects	Additive CNS[a] depression	UpToDate
Scopolamine, orphenadrine	2	Major	Fair	Concurrent use should be avoided	CNS[a] depressants may enhance orphenadrine effects	Additive CNS[a] depression	UpToDate
Acebrophylline, caffeine	1	Major	Fair	Should not be coadministered	Enhanced stimulatory effect of CNS[a] stimulants	Not informed	UpToDate
Amitriptyline, orphenadrine	1	Major	Fair	Concurrent use should be avoided	CNS[a] depressants may enhance orphenadrine effects	Additive CNS depression	UpToDate
Amlodipine, calcium carbonate	1	Moderate	Excellent	Monitor decreased therapeutic effects	Decreased therapeutic effect of amlodipine	Not informed	UpToDate
Amlodipine, ibuprofen	1	Minor	Excellent	No action required	Decreased antihypertensive effect of amlodipine	Unknown	UpToDate
Budesonide, diclofenac	1	Major	Fair	Monitor bleeding signs	Increased risk of gastrointestinal ulcers or bleeding	Additive effects	Micromedex

Table 3. Continued

Drug combination	n	Severity	Documentation	Management	Potential outcome	Mechanism	Database
Budesonide, dipyrone	1	Major	Fair	Monitor bleeding signs	Increased risk of gastrointestinal ulcers or bleeding	Additive effects	Micromedex
Budesonide, ibuprofen	1	Major	Fair	Monitor bleeding signs	Increased risk of gastrointestinal ulcers or bleeding	Additive effects	Micromedex
Bupropion, desvenlafaxine	1	Major	Fair	Low-dose started treatment and gradually increase	Lower seizure threshold	Unknown	Micromedex
Calcium carbonate, gliclazide	1	Minor	Excellent	No action needed	Increased gliclazide absorption	Not informed	UpToDate
Carbamazepine, dipyrone	1	Major	Fair	Avoid the concurrent use of dipyrone with myelosuppressive agent	Enhanced toxic effect of myelosuppressive agents	Use of dipyrone is associated with a risk of agranulocytosis and pancytopenia, but mechanism is unknown	UpToDate
Dexchlorpheniramine, orphenadrine	1	Major	Fair	Concurrent use should be avoided	CNS[a] depressants may enhance orphenadrine effects	Additive CNS[a] depression	UpToDate
Esomeprazole, omeprazole	1	Minor	Excellent	Standard clinical care measures	Increased serum concentration of omeprazole	Inhibition of CYP2C19[c], responsible for omeprazole metabolism	UpToDate
Gliclazide, vildagliptin	1	Major	Fair	Consider a decrease in gliclazide dose and monitor patients for hypoglycemia	Enhanced hypoglycemic effects of gliclazide	Not informed	UpToDate
Lithium carbonate, promethazine	1	Major	Good	Monitor signs of toxicity or extrapyramidal symptoms	Weakness, dyskinesias, increased extrapyramidal symptoms, encephalopathy and brain damage	Unknown	Micromedex
Morphine, orphenadrine	1	Major	Fair	Concurrent use should be avoided	CNS[a] depressants may enhance orphenadrine effects	Additive CNS[a] depression	UpToDate
Morphine, paracetamol	1	Minor	Excellent	No action required	Decreased paracetamol absorption	Impairment in gastric motility	UpToDate
Naproxen, nifedipine	1	Minor	Excellent	No action required	Decreased antihypertensive effect of amlodipine	Unknown	UpToDate

Table 3. Continued

Drug combination	n	Severity	Documentation	Management	Potential outcome	Mechanism	Database
Amitriptyline, estradiol	1	Minor	Excellent	Dose adjustments	Possible attenuation of antidepressant effectiveness and tricyclic toxicity	Inhibition of hepatic metabolism of the antidepressant	Micromedex
Phenytoin, losartan	1	Major	Fair	Consider an alternative, monitor losartan decreased effects	Decreased losartan effect (CYP3A4[c] substrate)	CYP3A4[c] inducers may increase the metabolism of CYP3A4[c] substrates	UpToDate

[a]CNS: Central nervous system, [b]Gamma aminobutyric acid, [c]Cytochrome P450

databases to identify drug interactions and only 9% interactions were identified by all of them, showing discrepancies in the overall performance of these tools.[35]

When comparing the documentation and the severity classifications, the agreement between Micromedex and UpToDate was poor. Based on Micromedex, the interactions identified were more frequently rated major severity, whereas, based on UpToDate, they were more frequently rated minor or moderate. Most drug interactions relied on fair documentation in both databases. The assessment of drug interactions involving 78 patients from an Australian hospital in 2018 was compared using three databases: Stockley's Drug Interactions, Micromedex and YouScript. The results were low agreement on the severity classification of the consulted interactions.[36] Cross-sectional systematic comparative study using drug pairs, conducted in the United Arab Emirates in 2020, identified disagreements on the severity and documentation of drug interactions between eight databases: Micromedex reported a greater number of interactions related to major severity compared to other databases (Portable Electronic Physician Information Database, UpToDate, Medscape, Drugs.com, Stockley's Drug Interactions, Drug Interactions Analysis & Management: Facts and comparisons and British National Formulary).[37]

Most of the drugs involved in discordant drug interactions were over-the-counter, such as ibuprofen, diclofenac, paracetamol, and dipyrone. Drugs for treatment of chronic diseases, such as hypertension, heart disease, and diabetes were also frequent. Among the discordant drug interactions between the two databases analyzed, most were identified from UpToDate. More frequent management showed that simultaneous use should be avoided, and the potential result of the interactions consisted mainly of enhancing or decreasing therapeutic effects with mostly unknown mechanisms of action. Mostly, the alerts were based on minor severity and fair documentation, promoting alerts that were not considered clinically relevant by the health team.

Healthcare professionals are under constant pressure to provide appropriate care by making clinical decisions daily, with the help of drug information databases. The choice of the database can impact patient care and its outcomes.[38] Such sources, usually provided on a subscription-basis, should be periodically reviewed to improve relevant information based on high-quality evidence from real-world data.

Investments on well-designed studies to determine the incidence, outcomes, and risk factors related to the patients affected by drug interactions are needed to support the provided recommendations. Algorithms to define systematic and clear evidence assessment processes to assess the risk and severity of drugs should ideally be integrated into these electronic systems.[39] This low quality of evidence potentially overestimates the severity of drug interactions and leads to overriding warnings when they are considered less serious, which can gradually neglect serious drug interactions.[33] These disagreements disadvantage healthcare professionals when making clinical decisions in cases of drug interactions in which the patient's condition justifies the use of both drugs that interact with each other, especially when there are no alternatives available.[33,37]

We also observed that the search for drugs available as commercial combinations may interfere with the result of drug interactions in the database, such as those including dipyrone and orphenadrine, commonly used combined in Brazil. Since these sources are based on developed settings, these fixed combinations are usually not included in the databases and may represent a higher burden in searching for interaction. Professionals should also be aware, when searching for the active ingredients separately, because it is possible to find interactions between active ingredients contained in a combination.

CONCLUSION

As for the identification of drug interactions, slight agreement was observed between UpToDate and Micromedex in this real-world analysis, indicating poor agreement on severity and documentation of drug interactions. Consulting multiple databases to identify drug interactions may increase healthcare professionals' workload as well as undetermined clinical outcomes for patients. Better-qualified sources for obtaining drug information are in need so that they can provide better support for health professionals and patients.

Ethics

Ethics Committee Approval: This study was approved by the Ethics Committee of the Federal University of Amazonas (Opinion No. 3,102,942), on December 28, 2018 (Certificate of Presentation for Ethical Appreciation 04728918.0.0000.502020).

Informed Consent: All participants signed a term of free and informed consent.

Peer-review: Externally peer-reviewed.

Authorship Contributions

Concept: T.F.G., M.T.S., Design: T.F.G., M.T.S., Data Collection or Processing: T.M.M.A.B., G.S.B., Analysis or Interpretation: T.M.M.A.B., G.S.B., T.F.G., M.T.S., Literature Search: T.M.M.A.B., G.S.B., Writing: T.M.M.A.B., G.S.B., T.F.G., M.T.S.

Conflict of Interest: No conflict of interest was declared by the authors.

Financial Disclosure: This work was supported by the National Council for Scientific and Technological Development (grants no: 404990/2013-4 and 448093/2014-6). TFG receives a productivity scholarship from CNPq (grant no: 310238/2020-0).

REFERENCES

1. Nguyen T, Liu X, Abuhashem W, Bussing R, Winterstein AG. Quality of evidence supporting major psychotropic drug-drug interaction warnings: a systematic literature review. Pharmacotherapy. 2020;40:455-468.
2. Zaal RJ, den Haak EW, Andrinopoulou ER, van Gelder T, Vulto AG, van den Bemt PMLA. Physicians' acceptance of pharmacists' interventions in daily hospital practice. Int J Clin Pharm. 2020;42:141-149.
3. Ravn-Nielsen LV, Duckert ML, Lund ML, Henriksen JP, Nielsen ML, Eriksen CS, Buck TC, Pottegård A, Hansen MR, Hallas J. Effect of an in-hospital multifaceted clinical pharmacist intervention on the risk of readmission: a randomized clinical trial. JAMA Intern Med. 2018;178:375-382.
4. Ylä-Rautio H, Siissalo S, Leikola S. Drug-related problems and pharmacy interventions in non-prescription medication, with a focus on high-risk over-the-counter medications. Int J Clin Pharm. 2020;42:786-795.
5. Bagri H, Dahri K, Legal M. Hospital pharmacists' perceptions and decision-making related to drug-drug interactions. Can J Hosp Pharm. 2019;72:288-294.
6. Peabody J, Acelajado MC, Robert T, Hild C, Schrecker J, Paculdo D, Tran M, Jeter E. Drug-drug interaction assessment and identification in the primary care setting. J Clin Med Res. 2018;10:806-814.
7. Peabody J, Tran M, Paculdo D, Schrecker J, Valdenor C, Jeter E. Clinical utility of definitive drug-drug interaction testing in primary care. J Clin Med. 2018;7:384.
8. Warholak TL, Hines LE, Saverno KR, Grizzle AJ, Malone DC. Assessment tool for pharmacy drug-drug interaction software. J Am Pharm Assoc. (2003). 2011;51:418-424.
9. Saverno KR, Hines LE, Warholak TL, Grizzle AJ, Babits L, Clark C, Taylor AM, Malone DC. Ability of pharmacy clinical decision-support software to alert users about clinically important drug-drug interactions. J Am Med Inform Assoc. 2011;18:32-37.
10. Coleman JJ, van der Sijs H, Haefeli WE, Slight SP, McDowell SE, Seidling HM, Eiermann B, Aarts J, Ammenwerth E, Slee A, Ferner RE. On the alert: future priorities for alerts in clinical decision support for computerized physician order entry identified from a European workshop. BMC Med Inform Decis Mak. 2013;13:111. Erratum in: BMC Med Inform Decis Mak. 2013;13:122. Ferner, Robin E [corrected to Slee, Ann]; Slee, Ann [corrected to Ferner, Robin E].
11. Metzger J, Welebob E, Bates DW, Lipsitz S, Classen DC. Mixed results in the safety performance of computerized physician order entry. Health Aff (Millwood). 2010;29:655-663.
12. Hedna K, Andersson ML, Gyllensten H, Hägg S, Böttiger Y. Clinical relevance of alerts from a decision support system, PHARAO, for drug safety assessment in the older adults. BMC Geriatr. 2019;19:164.
13. Suriyapakorn B, Chairat P, Boonyoprakarn S, Rojanarattanangkul P, Pisetcheep W, Hunsakunachai N, Vivithanaporn P, Wongwiwatthananukit S, Khemawoot P. Comparison of potential drug-drug interactions with metabolic syndrome medications detected by two databases. PLoS One. 2019;14:e0225239.
14. Riu-Viladoms G, Carcelero San Martín E, Martín-Conde MT, Creus N. Drug interactions with oral antineoplastic drugs: the role of the pharmacist. Eur J Cancer Care (Engl). 2019;28:e12944.
15. Ramos GV, Guaraldo L, Japiassú AM, Bozza FA. Comparison of two databases to detect potential drug-drug interactions between prescriptions of HIV/AIDS patients in critical care. J Clin Pharm Ther. 2015;40:63-67.
16. Monteith S, Glenn T, Gitlin M, Bauer M. Potential drug interactions with drugs used for bipolar disorder: a comparison of 6 drug interaction database programs. Pharmacopsychiatry. 2020;53:220-227.
17. Fung KW, Kapusnik-Uner J, Cunningham J, Higby-Baker S, Bodenreider O. Comparison of three commercial knowledge bases for detection of drug-drug interactions in clinical decision support. J Am Med Inform Assoc. 2017;24:806-812.
18. Kardas P, Urbański F, Lichwierowicz A, Chudzyńska E, Czech M, Makowska K, Kardas G. The prevalence of selected potential drug-drug interactions of analgesic drugs and possible methods of preventing them: lessons learned from the analysis of the real-world national database of 38 million citizens of Poland. Front Pharmacol. 2020;11:607852.
19. Mousavi S, Ghanbari G. Potential drug-drug interactions among hospitalized patients in a developing country. Caspian J Intern Med. 2017;8:282-288.
20. Burato S, Leonardi L, Antonazzo IC, Raschi E, Ajolfi C, Baraghini M, Chiarello A, Delmonte V, Di Castri L, Donati M, Fadda A, Fedele D, Ferretti A, Gabrielli L, Gobbi S, Lughi S, Mazzari M, Pieraccini F, Renzetti A, Russi E, Scanelli C, Zanetti B, Poluzzi E. Comparing the prevalence of polypharmacy and potential drug-drug interactions in nursing homes and in the community dwelling elderly of Emilia Romagna Region. Front Pharmacol. 2021;11:624888.
21. Silva MT, Nunes BP, Galvao TF. Use of health services by adults in Manaus, 2019: protocol of a population-based survey. Medicine (Baltimore). 2019;98:e15769.
22. Instituto Brasileiro de Geografia e Estatística. Cidades@. Manaus. IBGE. Accessed August 25, 2021. Available from: https://cidades.ibge.gov.br/brasil/am/manaus/panorama
23. Brazilian Association of Research Companies. [Brazil's Economic Classification Criteria 2018]. ABEP. Accessed May 11, 2019. Available from: http://www.abep.org/criterio-brasil
24. WHO Collaborating Centre for Drug Statistics Methodology (WHOCC). ATC/DDD Index. Norwegian Institute of Public Health. Accessed 13

December 2019, 2019. Available from: https://www.whocc.no/atc_ddd_index/?code=J&showdescript

25. Micromedex. Drug Interactions. Truven Health Analytics. Available from: https://www.micromedexsolutions.com/micromedex2/librarian
26. Uptodate. Lexicomp. Drugs & Drug Interaction. Available from: https://www.uptodate.com/home/drugs-drug-interaction
27. Fleiss JL, Levin B, Paik MC. The Measurement of interrater agreement. Statistical Methods for Rates and Proportions. 3 ed. Wiley; 2003:598-626.
28. Smithburger PL, Kane-Gill SL, Seybert AL. Drug-drug interactions in the medical intensive care unit: an assessment of frequency, severity and the medications involved. Int J Pharm Pract. 2012;20:402-408.
29. Tecen-Yucel K, Bayraktar-Ekincioglu A, Yildirim T, Yilmaz SR, Demirkan K, Erdem Y. Assessment of clinically relevant drug interactions by online programs in renal transplant recipients. J Manag Care Spec Pharm. 2020;26:1291-1296.
30. Nanji KC, Seger DL, Slight SP, Amato MG, Beeler PE, Her QL, Dalleur O, Eguale T, Wong A, Silvers ER, Swerdloff M, Hussain ST, Maniam N, Fiskio JM, Dykes PC, Bates DW. Medication-related clinical decision support alert overrides in inpatients. J Am Med Inform Assoc. 2018;25:476-481.
31. Muhič N, Mrhar A, Brvar M. Comparative analysis of three drug-drug interaction screening systems against probable clinically relevant drug-drug interactions: a prospective cohort study. Eur J Clin Pharmacol. 2017;73:875-882.
32. Vivithanaporn P, Kongratanapasert T, Suriyapakorn B, Songkunlertchai P, Mongkonariyawong P, Limpikirati PK, Khemawoot P. Potential drug-drug interactions of antiretrovirals and antimicrobials detected by three databases. Sci Rep. 2021;11:6089.
33. Liu X, Hatton RC, Zhu Y, Hincapie-Castillo JM, Bussing R, Barnicoat M, Winterstein AG. Consistency of psychotropic drug-drug interactions listed in drug monographs. J Am Pharm Assoc (2003). 2017;57:698-703.e2.
34. Kannan B, Nagella AB, Sathia Prabhu A, Sasidharan GM, Ramesh AS, Madhugiri V. Incidence of potential drug-drug interactions in a limited and stereotyped prescription setting - comparison of two free online pharmacopoeias. Cureus. 2016;8:e886.
35. Amkreutz J, Koch A, Buendgens L, Trautwein C, Eisert A. Clinical decision support systems differ in their ability to identify clinically relevant drug interactions of immunosuppressants in kidney transplant patients. J Clin Pharm Ther. 2017;42:276-285.
36. Meslin SMM, Zheng WY, Day RO, Tay EMY, Baysari MT. Evaluation of clinical relevance of drug-drug interaction alerts prior to implementation. Appl Clin Inform. 2018;9:849-855.
37. Shariff A, Belagodu Sridhar S, Abdullah Basha NF, Bin Taleth Alshemeil SSH, Ahmed Aljallaf Alzaabi NA 4th. Assessing consistency of drug-drug interaction-related information across various drug information resources. Cureus. 2021;13:e13766.
38. Clauson KA, Marsh WA, Polen HH, Seamon MJ, Ortiz BI. Clinical decision support tools: analysis of online drug information databases. BMC Med Inform Decis Mak. 2007;7:7.
39. Hines LE, Malone DC, Murphy JE. Recommendations for generating, evaluating, and implementing drug-drug interaction evidence. Pharmacotherapy. 2012;32:304-313.

Turk J Pharm Sci 2022;19(5):552-559
DOI: 10.4274/tjps.galenos.2021.25664

ORIGINAL ARTICLE

Effects of Some Interferon-Related Proteins on Influenza A Viruse RNA Polymerase Activity

Elif ÇAĞLAYAN[1], Kadir TURAN[2]*

[1]University of Health Sciences Türkiye, Kartal Koşuyolu High Speciality Educational and Research Hospital, Department of Medical Microbiology, İstanbul, Türkiye
[2]Marmara University, Faculty of Pharmacy, Department of Basic Pharmaceutical Sciences, İstanbul, Türkiye

ABSTRACT

Objectives: Interferons (IFNs) are one of the most important components of innate immunity against viruses, especially those carrying the RNA genomes such as influenza viruses. Upon viral infection, the IFNs are rapidly secreted, inducing the expression of several genes in the target cells and establishing an antiviral state. In this study, the effects of proteins encoded by some IFN-related genes on influenza A virus RNA-dependent RNA polymerase enzyme were investigated. We evaluated the importance of these proteins in the pathogenesis of different influenza A virus types.

Materials and Methods: The IFN-related genes were amplified by polymerase chain reaction from the HEK293 cDNA library and cloned into pCHA expression vector. The expression of genes and subcellular localizations of the proteins were determined by Western blotting and immunofluorescence staining, respectively. The effects of IFNs-related proteins on virus RdRP enzyme were determined by influenza A virus mini-replicons.

Results: The study revealed that the influenza A virus infections significantly altered the transcript level of the IFN-related *CCL5*, *IFIT1*, *IFIT3*, *IFITM3*, and *OAS1* genes in HEK293 cells. It was determined that the alteration of the gene expression was also related to the virus type. The mini-replicon assays showed that the transient expression of *CCL5*, *IFI27*, *OAS1*, *IFITM3*, *IFIT1*, and *IFIT3* have inhibitory effects on WSN and/or DkPen type virus RdRP enzymes. We observed that the proteins except OAS1 inhibited WSN type RdRP enzyme at a higher level than that of DkPen enzyme.

Conclusion: It was concluded that influenza A virus infection significantly alters the IFN-related gene expression in the cells. Most of the proteins encoded from these genes showed an inhibitory effect on the virus RdRP enzymes in the HEK293 cells. The inhibition of the influenza virus RdRP with IFN-related proteins may be the result of direct or indirect interactions between the host proteins and the viral enzyme subunits.

Key words: Influenza A virus interferon response, PCR array, influenza RdRP

INTRODUCTION

Influenza A viruses are enveloped viruses classified in the Orthomyxoviridae family. These viruses have a genome consisting of single-stranded, negative-sense RNA molecules. Influenza A viruses can be easily transmitted from person to person and cause upper respiratory disease. The high mutation rate and reassortment of the viral genome make it necessary to develop new prevention and treatment methods.[1] In this context, it is critical to identify the viral and cellular protein factors that play a role in virus-host interactions. However, innate and acquired immunity are of great importance in terms of the severity of influenza A virus infections. Interferons (IFNs) are among the most important actors of innate immunity.[2,3] The IFNs bind to specific receptors on the target cells, triggering several biochemical reactions within the cell and obstructing or completely inhibiting the virus replication. This occurs because of interactions between IFN-related host proteins and viral replication processes. The IFNs secreted from the infected cells stimulate the transcription of the genes carrying the ISRE control elements by transmitting signals to other cells through both paracrine and endocrine pathways. These proteins, which are synthesized because of the stimulation of IFNs, act as barriers to prevent viral replication in the cells by different mechanisms.

The influenza A virus RNA polymerase enzyme, consisting of PB2, PB1, and PA subunits, is the target of some host cellular proteins stimulated by IFNs. Among these proteins, Mx proteins inhibit influenza A virus RNA polymerase enzymes by direct

*Correspondence: kadirturan@marmara.edu.tr, Phone: +90 533 499 73 69, ORCID-ID: orcid.org/0000-0003-4175-3423
Received: 22.07.2021, Accepted: 01.11.2021

interaction or indirect mechanisms.[4,5] Additionally, the viral RNA polymerase enzyme plays an important role in controlling the host's anti-viral mechanisms by binding to cellular proteins such as IPS-1 or inhibiting IFNβ production.[6] In this study, how the expression levels of some genes related to the IFN response were affected in cells infected with influenza A viruses was evaluated. The effects of the proteins encoded by these genes on the viral RdRP enzyme activity were investigated with a mini-replicon assay.[5]

MATERIALS AND METHODS

Cells

Human cervical cancer cells (HeLa) and human embryonic kidney cells (HEK293) were used for viral infections and transient transfection assays. The cells were cultured in Dulbecco's Modified Eagle's Medium (DMEM) medium supplemented with 10% of heat-inactivated fetal calf serum (Gibco Laboratories, Gaithersburg, MD, USA, #11573397), 100 IU/mL penicillin, 100 µg/mL streptomycin, and 2 mM glutamine. The cultures were incubated at 37°C in an atmosphere of more than 95% humidity and 5% carbon dioxide.

Viruses

Influenza A/WSN/33/H1N1 (WSN) and low pathogenic avian influenza A/Duck/Pennsylvania/10,218/84/H5N2 (DkPen) viruses were used to infect the HEK293 cells. The viruses were obtained from infectious biology (virology) laboratory of Tsukuba University (Japan). Viruses were propagated in Madin-Darby canine kidney cells and titrated with a standard plaque formation assay.[7]

Plasmid vectors

Some plasmids were constructed within the scope of this work whereas others were constructed in previous studies. For protein expression in transiently transfected HEK293 and HeLa cells, the IFN-related chemokine (C-C motif) ligand 5 (*CCL5*), IFN, alpha-inducible protein 27 (*IFI27*), IFN-induced protein with tetratricopeptide repeats 1 (*IFIT1*), IFN-induced protein with tetratricopeptide repeats 3 (*IFIT3*), IFN-induced transmembrane protein 3 (*IFITM3*), and 2'-5'-oligoadenylate synthetase 1 (*OAS1*) genes were cloned in pCHA plasmid[8] derived from pCAGGS.[9] The cDNAs were prepared with reverse transcription of the HEK293 cell RNA. A 500 ng of RNA and 50 pmol oligo-dT primer were added to a 1.5 mL plastic tube, and the volume was increased to 12.5 µL with nuclease free-water. After denaturation of the RNA molecules at 65°C for 10 min, 4 µL 5x reaction buffer, 0.5 µL (40 U/µL) RNase inhibitor (Biotechrabbit GmbH, Hennigsdorf, Germany, #BR0400901), 2 µL (10 mM) dNTP mixture, and 1 µL (200 U/µL) reverse transcriptase enzyme (Biotechrabbit GmbH, Hennigsdorf, Germany, #BR0400601) were added to the samples. The reaction was carried out at 45°C for 60 min and then held at 80°C for 10 min to inactivate the reaction. The cDNAs of the *CCL5*, *IFI27*, *IFIT1*, *IFIT3*, *IFITM3*, and *OAS1* genes were amplified by polymerase chain reaction (PCR) by using gene-specific primer pairs phosphorylated with T4 polynucleotide kinase (New England Biolabs Ltd., Hitchin, UK, #M0201S). The primers given in Table 1 were designed from reference gene sequences of the genes (*CCL5*/NCBI reference sequence: NM_002985.3, *IFI27*-v.1/NCBI reference sequence: NM_001130080.3, *IFIT*-v.1/NCBI reference sequence: NM_001548.5, *IFIT3*/NCBI reference sequence: NM_001549.6, *IFITM3* -v.1/NCBI reference sequence, and *OAS1*/NCBI reference sequence: NM_016816.4). The PCR-amplified cDNAs were cloned into pCHA plasmid digested by EcoRV (New England Biolabs Ltd., Hitchin, UK, #R095S), and the resultant plasmid vectors were designated as pCHA-*CCL5*, pCHA-*IFI27*, pCHA-*IFIT1*, pCHA-*IFIT3*, pCHA-*IFITM3*, and pCHA-*OAS1*.

The construction of plasmids sets of the influenza A virus mini-replicon (pCAGGS-PB2/WSN, pCAGGS-PB1/WSN, pCAGGS-PA/WSN, pCAGGS-NP/WSN, pCAGGS-PB2/DkPen, pCAGGS-PB1/DkPen and pCAGGS-PA/DkPen, pCAGGS-NP/DkPen and pHH21-vNS-Luc) has been described previously.[5,10] For normalization of firefly luciferase, the pRL (Promega, Madison, USA, #E289B) plasmid encoding *Renilla reniformis* luciferase was used.

Infections of HEK293 cells with viruses and total RNA extraction

The HEK293 cells were seeded in 12 well plates (5 x 10^5 cells/well) and incubated in standard culture conditions (37°C, 5% CO_2 and >95% humidity) for 24 h. After incubation, the media of the cultures were removed, and the cells were washed with serum-free DMEM medium. 200 µL of influenza A virus (WSN or DkPen) samples diluted at an average of 1 moi in 1% BSA were added to the cell monolayers. Plates were kept for 30 min at 37°C with gentle mixing at 5 minute intervals for virus attachment. The virus suspensions were removed, and 1 mL of OPTI-MEM (Gibco Laboratories, Gaithersburg, MD, USA, #31600-083) was added to the cells. Infected cultures were incubated for 8 h, and then the RNA was extracted from the cells. The total RNA extraction was carried out with a commercial RNA extraction kit

Table 1. Oligonucleotide primers used in PCR amplification of human *CCL5*, *IFI27*, *IFIT1*, *IFIT3*, *IFIM*3, and *OAS1* genes

Primer name	Nucleotide sequence
CCL5 for	5'-*ATCATGAAGGTCTCCGCGGCAGC*-3'
CCL5 rev	5'-*ATCTAGCTCATCTCCAAAGAGTTG*-3'
IFI27 for	5'-*ATCATGGAGGCCTCTGCTCTCAC*-3'
IFI27 rev	5'-*ATCTAGTAGAACCTCGCAATGAC*-3'
IFIT1 for	5'-*ATCATGAGTACAAATGGTGATGA*-3'
IFIT1 rev	5'-*ATCATAAGGACCTTGTCTCACAG*-3'
IFIT3 for	5'-*ATCATGAGTGAGGTCACCAAGAATTC*-3'
IFIT3 rev	5'-*ATCAGTTCAGTTGCTCTGAGTTAGAG*-3'
IFITM3 for	5'-*ATC ATGAATCACACTGTCCAAAC*-3'
IFITM3 rev	5'-A*TCTATCCATAGGCCTGGAAGAT*-3'
OAS1 for	5'-*ATCATGATGGATCTCAGAAATACCCC*-3'
OAS1 rev	5'-*ATCAGAGGATGGTGCAGGTCCAGT*-3'

PCR: Polymerase chain reaction

(New England Biolabs Ltd., Hitchin, UK, #T2010S), according to the manufacturer's instructions.

Quantification of IFN-related gene transcripts in virus - infected cells with qPCR

The cDNAs of IFN-related genes from the total RNA of virus-infected cells were prepared as described above. The 96 well "RT^2 Profiler PCR Array" (PAHS-016ZD-6) plates developed by Qiagen (Qiagen, Hilden, Germany) was used for quantitation of *CCL5*, *IFI27*, *IFIT1*, *IFIT3*, *IFITM*3, and *OAS1* gene transcripts in the cDNAs with quantitative real-time qPCR. Equal amounts of ×2 SYBR Green Master Mix (Roche, Mannheim, Germany, #4673484001) were added to each PCR tube containing 2.5 µL cDNA and 5 µL primer mix. The cycle conditions were applied as an initial denaturation step at 95˚C for 10 min, followed by 45 cycles of amplification for 15 s at 95˚C and 1 min at 60˚C. The relative quantities of the transcripts were normalized by the amount of signal transducer and activator of transcription 3 transcript level. The relative expression values of each gene were revealed, and the results were given as a bar graph and heat map.

Transfection

Polyethyleneimine (PEI) was used for transfection of plasmid DNA into the HEK293 cells.[11] The cells were seeded in 12 well culture plates (1x10^5 cells/well) and incubated at standard culture conditions for 24 h. The plasmid DNAs diluted in Opti-MEM (Gibco, USA, #31600-083) at a concentration of 20 ng/µL were mixed with equal volumes of the PEI solution (50 ng/µL). The mixtures were maintained at room temperature for 5-10 minutes for complex formation and added to the cultures. Forty-eight hours after transfection, the cells were harvested for Western blotting or luciferase enzyme assays.

Western blotting

The expression of human *CCL5, IFI27, IFIT1, IFIT3, IFITM3,* and *OAS1* genes in transiently transfected HEK293 cells was analyzed by Western blotting. Plasmid DNA (1-2 µg) was transfected into HEK293 cells as described above. After 48 h, the cells were harvested in an SDS-sample loading buffer. The proteins in the cell lysates were separated with SDS-PAGE and transferred to the polyvinylidene difluoride membrane. After blocking with 5% skim milk, the membrane was first treated with mouse monoclonal anti-HA (Santa Cruz, #sc-7392) followed by horseradish peroxidase-conjugated second antibody [anti-mouse IgG-HRP (invitrogen, #31420). The proteins were visualized with an ECL detection kit (GE Healthcare, Italy, #RPN3004).

Immunofluorescence assay

The HeLa cells were seeded on coverslips in a 12 well palate (7.5x10^4 cells/well) and incubated in standard culture conditions for 24 h. Then the cells were transfected with 1.5 µg of the plasmid DNA encoding *CCL5*, *IFI27*, *IFIT1*, *IFIT3*, *IFITM*3 or *OAS1* proteins as described above. After 40 h transfection, the cells were rinsed in PBS and fixed with 3% *para*-formaldehyde. The cells were permeabilized with 0.1% NP-40, washed in PBS, treated with 1% skim milk for 30 min, and incubated with mouse monoclonal anti-HA for 60 min. After washing with PBS, the cells were treated with Alexa-488-conjugated goat anti-mouse IgG (at 1:300 dilutions in 1% skim milk) for 60 min. The nuclei of the cells were stained with DAPI. The coverslips were mounted in a medium (0.1% *p*-phenylenediamine and 80% glycerol), and the cells were visualized using a fluorescence microscope.

RdRP activity assay

The effects of IFNs-related proteins on the influenza A virus RdRP enzyme were investigated with the influenza A virus mini-replicon system.[5] The HEK293 cells were seeded in 24 well plates (5x10^4 cells/well) and incubated under standard culture conditions for 24 h. The plasmids encoding IFNs-associated proteins were mixed with a set of mini-replicon plasmids (pHH21-vNS-luc, pCAGGS-PB1, pCAGGS-PB2, pCAGGS-PA, and pCAGGS-NP). The pRL plasmid was used for normalization. The total amount of plasmid DNA for each well was adjusted to 250 ng with the pCAGGS plasmid. Then, the plasmid DNAs were transfected with PEI as described above. After 48 h transfection, the cells were lysed in a lysis buffer (Promega, Madison, USA, # E1531), and luciferase activity was detected with commercial kits (for firefly luciferase, #E1483; for *Renilla* luciferase, #Z3051, Promega, Madison, USA) according to the manufacturer's instructions.

Statistical analysis

The statistical significance of differences between experimental groups was evaluated using analysis of variance (one-way ANOVA with Newman-Keuls *post-test*) in the SPSS. *P* values less than 0.05 were considered statistically significant.

RESULTS

Quantifications of IFN-related gene transcript in virus-infected cells

In our previous study, the expression profiles of 84 IFN and IFN-related genes were determined in the cells infected with influenza A viruses.[12] Here, the *CCL5, IFI27, IFIT1, IFIT3, IFITM3,* and *OAS1* genes, which are thought to be important in viral replication, and the effects of proteins encoded by these genes on influenza A viral RdRP enzymes were evaluated. The transcript levels of the genes in HEK293 cells infected with two types of influenza A virus were determined by the qPCR technique (Figure 1).

The results showed that *CCL5* gene expression is up-regulated in the HEK293 cells infected with both influenza A virus types (p<0.01). It was observed that up-regulation was more pronounced in the cells infected with WSN type viruses compared with the DkPen type viruses. No significant change was detected in the *IFI27* gene transcript level in the virus-infected cells. The profiles of the *IFIT1* and *OAS1* gene transcripts in the virus-infected cells were found to be similar to the changes in the *CCL5* gene transcript levels. A significant increase in the transcript level of these two genes was detected in the cells infected with WSN type

viruses compared with uninfected cells ($p<0.01$). In contrast, *IFIT3* gene was up-regulated in WSN-type virus-infected cells, while it was significantly down-regulated in the cells infected with DkPen type viruses. While some decrease in *IFITM3* gene transcript was observed in DkPen type virus-infected cells, there was no statistically significant change in the *IFITM3* gene transcript level in WSN virus-infected cells.

Expression and subcellular localization of the IFN-related proteins

To identify the effects of proteins encoded by the IFN-related genes on the influenza A virus RdRP enzymes, the genes were cloned into the pCHA mammalian expression vector. Expression of the genes and subcellular localization of the encoded proteins were determined by Western blotting and immunofluorescence techniques, respectively (Figures 2 and 3). Western blotting revealed that the genes cloned into the pCHA plasmid were expressed at different levels in the HEK293 cells. The expected band sizes were detected based on the size of the protein: ~46 kDa for *OAS1*, ~55 kDa for *IFIT1*, ~56 kDa for *IFIT3*, ~15 kDa for *IFITM3*, and ~12 kDa for *IFI27* (Figure 2A). The CCL5 protein (~10 kDa) could not be detected with Western blotting in transiently transfected HEK393 cells. The expression levels of *OAS1*, *IFIT1*, and *IFIT3* proteins were found to be higher than that of *IFITM3* and *IFI27* proteins in transiently transfected HEK293 cells (Figure 2B).

We have examined the subcellular localizations of the IFN-related proteins in the HeLa cells with an immunofluorescence assay. HeLa cells were transiently transfected with plasmids coding the HA-tagged proteins. The cells were fixed 44 h after transfection and stained with mouse monoclonal anti-HA antibodies (Figure 3). The results showed that all genes cloned into the pCHA plasmid were expressed in the cells. It was observed that all proteins except the *OAS1* were dominantly localized in the cytosol. The presence of *CCL5* and *IFITM3* proteins as granules in the cytoplasm indicated that these proteins were localized in the organelles. The *OAS1* protein was observed more intensely in the cell nucleus. However, *OAS1* protein was found to be present in significant amounts in the cytoplasm.

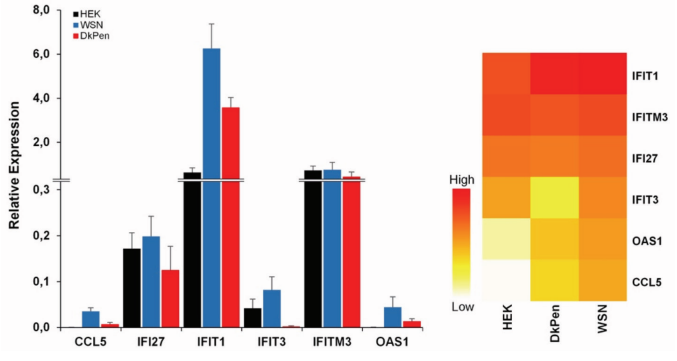

Figure 1. Expression profiles of interferon-related genes in HEK293 cells infected with influenza A viruses (WSN or DkPen) and uninfected HEK293 cells

Effects of IFN-related proteins on the influenza A virus RNA polymerase enzyme

The influenza A virus RdRP enzyme consists of three subunits-PB2, PB1, and PA-that performs transcription and replication of the viral genome. This enzyme, which is vital for virus replication, interacts with many cellular events and proteins. These interactions may be necessary for the functions of the RdRP enzyme or may cause the enzyme inhibition. Therefore, the effects of *CCL5*, *IFI27*, *IFIT1*, *IFIT3*, *IFITM3*, and *OAS1* proteins, which are thought to be important for influenza A virus replication, were tested in the viral RdRP enzymes in the HEK293 cells by using the mini-replicon assays.[5,10] The HEK293 cells were co-transfected with a certain number of minireplicon plasmids and increasing number of plasmids encoding IFNs-related proteins. The reporter luciferase activity normalized with *Renilla* luciferase in transfected HEK293 cells is shown in Figure 4. The results showed that the proteins, except OAS1, negatively affected both types of influenza A virus RdRP enzymes at different levels. We observed that the proteins had a higher inhibition on the WSN type virus RdRP enzyme than

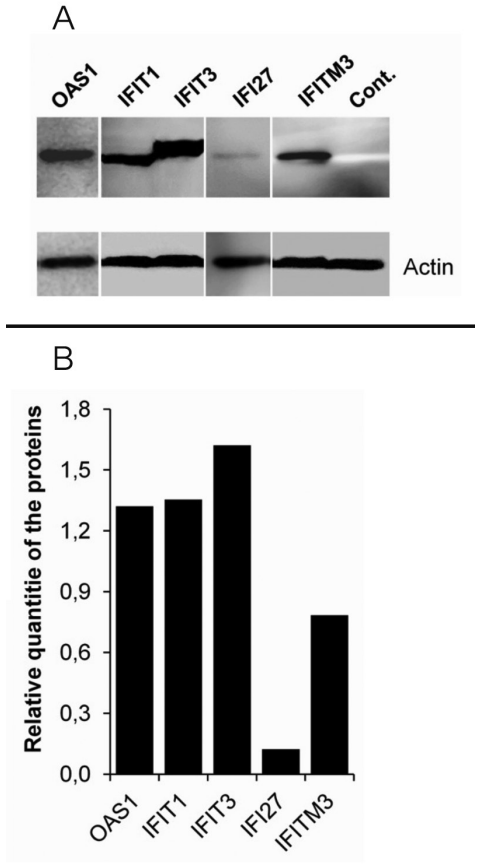

Figure 2. Western blot analysis of the interferon-related proteins encoded from the plasmid vectors in the HEK293 cells transiently transfected. A) The bands of *OAS1*, *IFIT1*, *IFIT3*, *IFI27*, *IFITM3* and actin beta proteins. B) Relative quantity of the proteins compared to the actin beta. A total of 15 µL cell lysate was loaded into each well of 10% polyacrylamide gel. Electrophoresis was performed under a constant voltage of 40 V/gel for 15 minutes and then 80 V/gel for 75 minutes. The relative quantity of the proteins was determined by using ImageJ software. Cont: Untransfected-HEK293 cell lysate

that of DkPen in the HEK293 cells. In contrast, the *OAS1* protein did not have a significant effect on the WSN type virus RdRP in the cells while it had a negative effect on the DkPen type virus enzyme.

DISCUSSION

Among the host defense mechanisms against the viral infections, the IFN-related pathways of host cells are of great importance. Influenza infection causes rapid synthesis and secretion of type I IFNs after the appearance of viral components in infected cells. The binding of these proteins to the specific receptors on the cell surface causes up-regulation of hundreds of IFN-stimulated genes, which creates an "antiviral state" that will limit the further proliferation and spread of the viruses.[13] In this study, the expression profiles of some genes related to the IFN pathway in virus-infected cells and the effects of the proteins encoded from these genes on the influenza A virus RNA polymerase enzyme were investigated. Several proteins in the IFN pathway interact with influenza A viruses, some of which have negative regulatory effects on viral replication and some of which have stimulating effects.[5,14-19] However, the expression profiles of various genes in the cells infected with the viruses

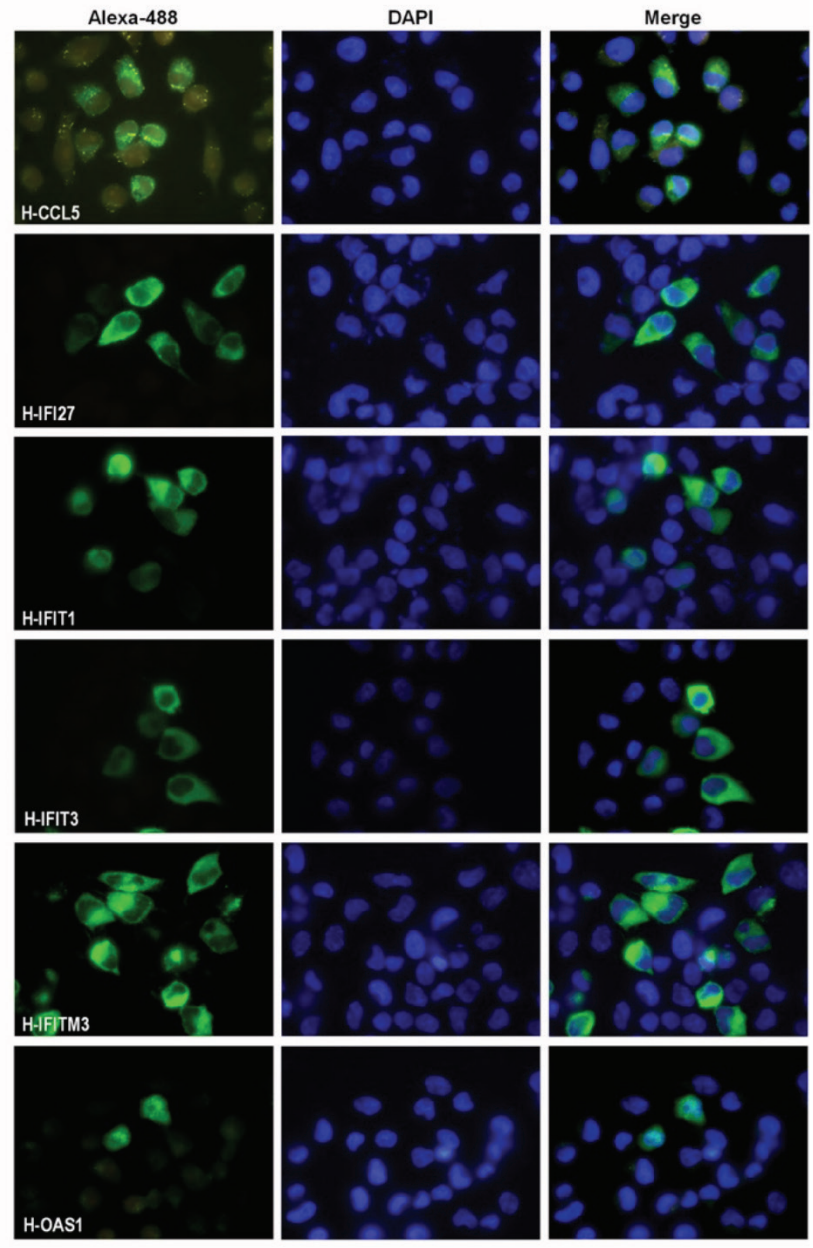

Figure 3. Subcellular localizations of interferon-related proteins encoded by plasmids in HeLa cells. HeLa cells were transiently transfected with plasmids encoding HA-tagged *CCL5*, *IFI27*, *IFIT1*, *IFIT3*, I*FITM3*, and *OAS1* proteins. The cells were fixed 44 h after transfection and stained with mouse monoclonal anti-HA antibodies. Alexa 488 conjugated anti-mouse IgG antibody (1/300 dilution) was used as the secondary antibody. The cell nuclei were stained with DAPI

HeLa: Human cervical cancer cell, IgG: Immunoglobulin

are altered at different levels and in different directions. It was observed that *IFIT3* gene expression was up-regulated in cells infected with WSN-type virus but down-regulated in DkPen-type virus-infected cells (Figure 1). Genes other than *IFI27* were more up-regulated in the cells infected with WSN-type viruses than those of DkPen. The results showed that the transcript levels of genes except *IFI27* were higher in the cells infected with WSN type viruses. In some studies, it has been reported that DkPen-type viruses have a lower replication efficiency in the mammalian cells.[20-22] Although this seems to contradict the fact that the DkPen-type virus infection up-regulates the expression of some IFN-related genes less than WSN type viruses; this may be a result of the DkPen virus RdRP enzyme inhibiting the host cell gene expression more than the WSN type virus enzyme.[12]

The influenza A virus RdRP enzymes are targets of some IFN-related proteins. In this study, the HEK293 cells were co-transfected with certain number of minireplicon plasmids and increasing number of the plasmids encoding IFN-related proteins, and the viral RdRP enzyme activities were measured

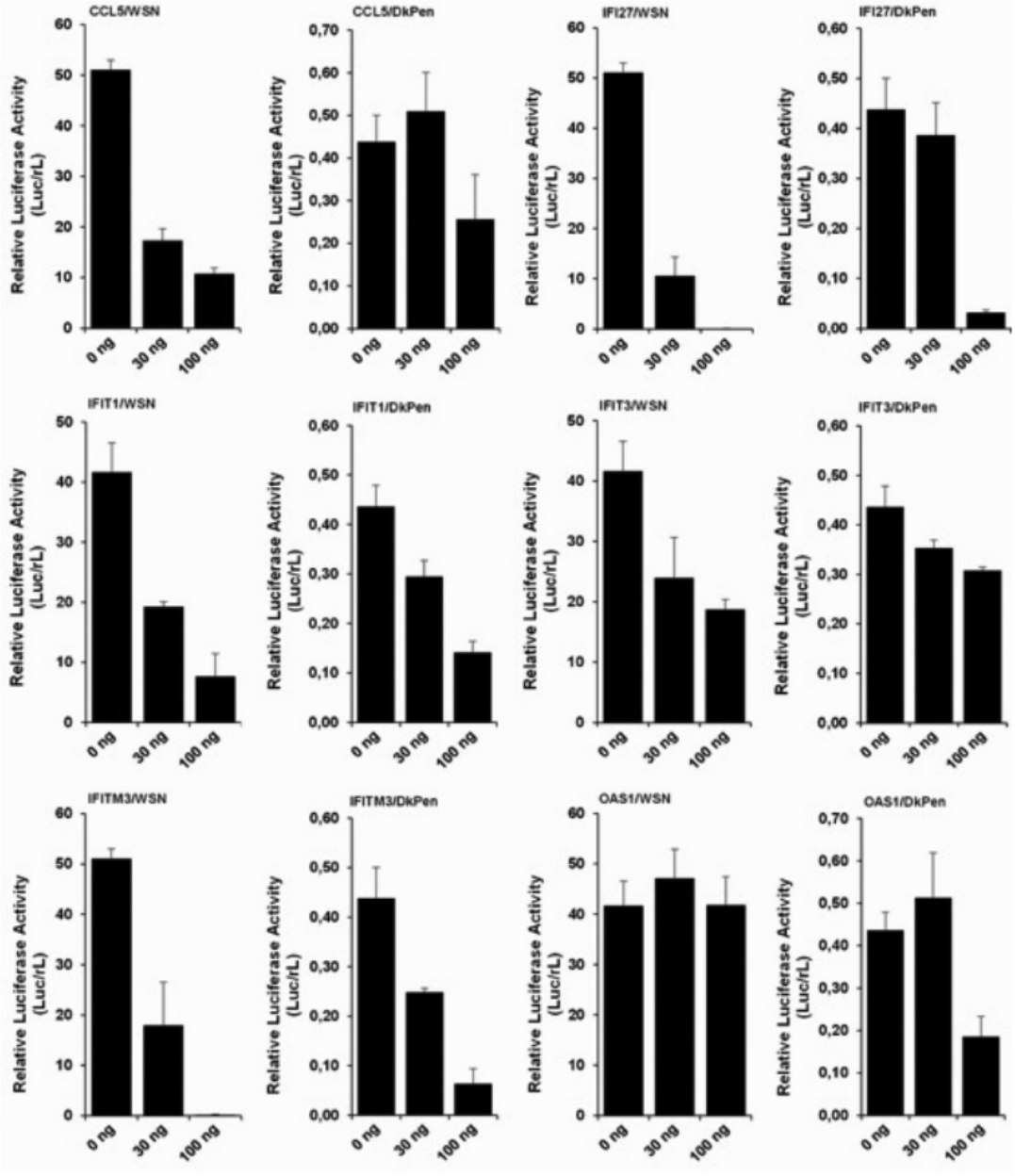

Figure 4. The effects of interferon-related *CCL5*, *IFI27*, *IFIT1*, *IFIT3*, *IFITM3*, and *OAS1* proteins on WSN- and DkPen-type virus RdRP enzymes in the HEK-293 cells. The cells were grown in 24 well plates, and co-transfected with a protein coding-plasmid (30/well or 100 ng/well), and a certain amount of minireplicon plasmids [WSN: pCAGGS-PB2/W (3 ng/well), pCAGGS-PB1/W (3 ng/well), pCAGGS-PA/W (1 ng/well), pCAGGS-NP/W (10 ng/well), pHH21-vNS-luc (5 ng/well), pRL (2 ng/well), DkPen: pCAGGS-PB2/D (10 ng/well), pCAGGS-PB1/D (10 ng/well), pCAGGS-PA/D (3 ng/well), pCAGGS-NP/D (10 ng/well), pHH21-vNS-luc, (5 ng/well) pRL (2 ng/well)]. After 48 hours transfection, the cells were lysed, and reporter luciferase and *Renilla* luciferase activities were measured with luciferase assay kits

via the luciferase reporter enzyme activity. The results showed that the expression of IFN-related proteins *CCL5*, *IFI27*, *IFITM3*, *IFIT1*, and *IFIT3* have inhibitory effects on both WSN and DkPen-type virus RdRP enzymes. *OAS1* protein showed a negative effect only on the DkPen virus RdRP (Figure 4). The *CCL5* gene encodes a G-protein-coupled receptor protein carrying 7 transmembrane domains. The *CCL5* protein, along with the *CCL3* and *CCL4* receptors, belongs to the C-C chemokine family.[23] It was reported that the *CCL5* gene, whose transcript level is up-regulated in HEK293 cells infected with influenza A viruses, negatively affects the virus replication, and mutant mice with this gene were found to be very susceptible to virus infection.[24] In this study, it was determined that the *CCL5* gene transcript level increased in HEK293 cells infected with both the WSN- and DkPen-type viruses. Furthermore, the *CCL5* gene expression was increased approximately 5 times more with the WSN-type virus infection compared to the DkPen viruses. This difference may be important for influenza A virus host specificity.

No significant change was detected in the transcript level of the *IFI27* gene in virus-infected HEK293 cells. However, the high inhibition of influenza RdRP enzymes by the IFI27 protein in HEK293 cells reveals the importance of this protein for viral replication. Remarkable increases in the expression level of this gene in virus-infected organisms have been reported.[25] Tang et al.[26] demonstrated that IFI27 is an important diagnostic marker in the differentiating of influenza and bacterial infections.

One of the IFN-related genes whose transcript levels were increased in HEK293 cells infected with the influenza A virus is the OAS1. The *OAS1* gene expression in WSN-infected cells was also found to be higher than that of DkPen viruses. The human *OAS1* gene belongs to the *OAS* gene family, which includes the *OAS2*, *OAS3*, and *OASL* genes.[27] These genes encode the 2'-5' oligoadenylate synthetase enzymes that catalyzing the formation of 2'-5' oligoadenylate, which activates RNase L enzymes.[28,29] The active RNase L enzyme inhibits the protein synthesis by breaking down both viral and cellular RNA molecules.[30-32] Although there was a significant increase in the *OAS1* transcript level in cells infected with influenza A viruses, it was observed that this protein did not cause an inhibition of the WSN-type virus RdRP enzyme (Figure 4). In contrast, it was observed that the *OAS1* expression partially inhibited the DkPen virus RdRP enzyme. The negative effect of *OAS1* on the DkPen virus RdRP enzyme can be considered a reason for the slow replication of this virus type in the mammalian cells.

IFITM3 belongs to the *IFITM*. These proteins get the fusion of viral and endosomal membranes difficult and prevent the release of virus genomes inside the cell.[14,15,17] No significant change in the transcription of this gene was observed in the WSN virus-infected cells (Figure 1). However, both viral RdRP enzymes were strongly inhibited by *IFITM3* expression (Figure 4).

IFIT proteins (*IFIT1* and *IFIT3*) related to the IFNs defense mechanism have negative regulatory effects on viral replication. These proteins specifically inhibit the viral replication by binding directly to the viral nucleic acids or disrupting the function of eukaryotic initiation factor 3.[33] Both of these proteins showed a negative effect on the influenza A virus RdRP enzyme. However, while the *IFIT3* gene transcription was up-regulated in WSN virus-infected cells, the down-regulation of the cells infected with DkPen viruses remains to be elucidated.

CONCLUSION

In conclusion, most IFN-related proteins focused on in this study showed inhibitory effects on the virus RdRP enzymes in the HEK293 cells. However, the possible interactions of these proteins with the RdRP enzyme subunits have not been considered. Therefore, it is uncertain that these proteins directly inhibit influenza A virus RdRP enzymes in minireplicons by direct interaction with the subunits. The inhibition of the influenza virus RdRP enzymes with IFN-related proteins in transfected HEK293 cells may also be the result of the indirect interactions.

Ethics

Ethics Committee Approval: Not necessary.

Informed Consent: Not necessary.

Peer-review: Externally peer-reviewed.

Authorship Contributions

Concept: E.Ç., K.T., Design: E.Ç., K.T., Data Collection or Processing: E.Ç., K.T., Analysis or Interpretation: E.Ç., K.T., Literature Search: E.Ç., K.T., Writing: E.Ç., K.T.

Conflict of Interest: No conflict of interest was declared by the authors.

Financial Disclosure: This work was supported by a grant from the Marmara University Research Foundation (grant no: SAG-C-DRP-250919-0291).

REFERENCES

1. Chao DL, Bloom JD, Kochin BF, Antia R, Longini IM Jr. The global spread of drug-resistant influenza. J R Soc Interface. 2012;9:648-656.
2. Pitini V, Arrigo C, Altavilla G. How cells respond to interferons. J Clin Oncol. 2010;28:e439; author reply e440.
3. Stark GR. How cells respond to interferons revisited: from early history to current complexity. Cytokine Growth Factor Rev. 2007;18:419-423.
4. Verhelst J, Parthoens E, Schepens B, Fiers W, Saelens X. Interferon-inducible protein Mx1 inhibits influenza virus by interfering with functional viral ribonucleoprotein complex assembly. J Virol. 2012;86:13445-13455.
5. Turan K, Mibayashi M, Sugiyama K, Saito S, Numajiri A, Nagata K. Nuclear MxA proteins form a complex with influenza virus NP and inhibit the transcription of the engineered influenza virus genome. Nucleic Acids Res. 2004;32:643-652.
6. Iwai A, Shiozaki T, Kawai T, Akira S, Kawaoka Y, Takada A, Kida H, Miyazaki T. Influenza A virus polymerase inhibits type I interferon induction by binding to interferon beta promoter stimulator 1. J Biol Chem. 2010;285:32064-32074.
7. Turan K, Nagata K, Kuru A. Antiviral effect of *Sanicula europaea* L. leaves extract on influenza virus-infected cells. Biochem Biophys Res Commun. 1996;225:22-26.

8. Nagata K, Saito S, Okuwaki M, Kawase H, Furuya A, Kusano A, Hanai N, Okuda A, Kikuchi A. Cellular localization and expression of template-activating factor I in different cell types. Exp Cell Res. 1998;240:274-281.

9. Niwa H, Yamamura K, Miyazaki J. Efficient selection for high-expression transfectants with a novel eukaryotic vector. Gene. 1991;108:193-199.

10. Pham PTV, Turan K, Nagata K, Kawaguchi A. Biochemical characterization of avian influenza viral polymerase containing PA or PB2 subunit from human influenza A virus. Microbes Infect. 2018;20:353-359.

11. Longo PA, Kavran JM, Kim MS, Leahy DJ. Transient mammalian cell transfection with polyethylenimine (PEI). Methods Enzymol. 2013;529:227-240.

12. Çağlayan E, Turan K. Expression profiles of interferon-related genes in cells infected with influenza A viruses or transiently transfected with plasmids encoding viral RNA polymerase. Turk J Biol. 2021;45:88-103.

13. Randall RE, Goodbourn S. Interferons and viruses: an interplay between induction, signalling, antiviral responses and virus countermeasures. J Gen Virol. 2008;89:1-47.

14. Brass AL, Huang IC, Benita Y, John SP, Krishnan MN, Feeley EM, Ryan BJ, Weyer JL, van der Weyden L, Fikrig E, Adams DJ, Xavier RJ, Farzan M, Elledge SJ. The IFITM proteins mediate cellular resistance to influenza A H1N1 virus, West Nile virus, and dengue virus. Cell. 2009;139:1243-1254.

15. Desai TM, Marin M, Chin CR, Savidis G, Brass AL, Melikyan GB. IFITM3 restricts influenza A virus entry by blocking the formation of fusion pores following virus-endosome hemifusion. PLoS Pathog. 2014;10:e1004048.

16. Haller O, Arnheiter H, Lindenmann J, Gresser I. Host gene influences sensitivity to interferon action selectively for influenza virus. Nature. 1980;283:660-662.

17. Li K, Markosyan RM, Zheng YM, Golfetto O, Bungart B, Li M, Ding S, He Y, Liang C, Lee JC, Gratton E, Cohen FS, Liu SL. IFITM proteins restrict viral membrane hemifusion. PLoS Pathog. 2013;9:e1003124.

18. Pavlovic J, Haller O, Staeheli P. Human and mouse Mx proteins inhibit different steps of the influenza virus multiplication cycle. J Virol. 1992;66:2564-2569.

19. Xiao H, Killip MJ, Staeheli P, Randall RE, Jackson D. The human interferon-induced MxA protein inhibits early stages of influenza A virus infection by retaining the incoming viral genome in the cytoplasm. J Virol. 2013;87:13053-13058.

20. Slepushkin VA, Staber PD, Wang G, McCray PB Jr, Davidson BL. Infection of human airway epithelia with H1N1, H2N2, and H3N2 influenza A virus strains. Mol Ther. 2001;3:395-402.

21. Wille M, Holmes EC. The Ecology and evolution of influenza viruses. Cold Spring Harb Perspect Med. 2020;10:a038489.

22. Zhang H, Hale BG, Xu K, Sun B. Viral and host factors required for avian H5N1 influenza A virus replication in mammalian cells. Viruses. 2013;5:1431-1446.

23. Soria G, Ben-Baruch A. The inflammatory chemokines *CCL2* and *CCL5* in breast cancer. Cancer Lett. 2008;267:271-285.

24. Tyner JW, Uchida O, Kajiwara N, Kim EY, Patel AC, O'Sullivan MP, Walter MJ, Schwendener RA, Cook DN, Danoff TM, Holtzman MJ. *CCL5-CCR5* interaction provides antiapoptotic signals for macrophage survival during viral infection. Nat Med. 2005;11:1180-1187.

25. Chen Y, Jiao B, Yao M, Shi X, Zheng Z, Li S, Chen L. ISG12a inhibits HCV replication and potentiates the anti-HCV activity of IFN-α through activation of the Jak/STAT signaling pathway independent of autophagy and apoptosis. Virus Res. 2017;227:231-239.

26. Tang BM, Shojaei M, Parnell GP, Huang S, Nalos M, Teoh S, O'Connor K, Schibeci S, Phu AL, Kumar A, Ho J, Meyers AFA, Keynan Y, Ball T, Pisipati A, Kumar A, Moore E, Eisen D, Lai K, Gillett M, Geffers R, Luo H, Gul F, Schreiber J, Riedel S, Booth D, McLean A, Schughart K. A novel immune biomarker *IFI27* discriminates between influenza and bacteria in patients with suspected respiratory infection. Eur Respir J. 2017;49:1602098.

27. Hovanessian AG. On the discovery of interferon-inducible, double-stranded RNA activated enzymes: the 2'-5'oligoadenylate synthetases and the protein kinase PKR. Cytokine Growth Factor Rev. 2007;18:351-361.

28. Kodym R, Kodym E, Story MD. 2'-5'-Oligoadenylate synthetase is activated by a specific RNA sequence motif. Biochem Biophys Res Commun. 2009;388:317-322.

29. Melchjorsen J, Kristiansen H, Christiansen R, Rintahaka J, Matikainen S, Paludan SR, Hartmann R. Differential regulation of the *OASL* and *OAS1* genes in response to viral infections. J Interferon Cytokine Res. 2009;29:199-207.

30. Castelli JC, Hassel BA, Wood KA, Li XL, Amemiya K, Dalakas MC, Torrence PF, Youle RJ. A study of the interferon antiviral mechanism: apoptosis activation by the 2-5A system. J Exp Med. 1997;186:967-972.

31. Chakrabarti A, Ghosh PK, Banerjee S, Gaughan C, Silverman RH. RNase L triggers autophagy in response to viral infections. J Virol. 2012;86:11311-11321.

32. Zhou A, Paranjape J, Brown TL, Nie H, Naik S, Dong B, Chang A, Trapp B, Fairchild R, Colmenares C, Silverman RH. Interferon action and apoptosis are defective in mice devoid of 2',5'-oligoadenylate-dependent RNase L. EMBO J. 1997;16:6355-6363.

33. Diamond MS, Farzan M. The broad-spectrum antiviral functions of *IFIT* and *IFITM* proteins. Nat Rev Immunol. 2013;13:46-57.

Turk J Pharm Sci 2022;19(5):560-571
DOI: 10.4274/tjps.galenos.2021.45945

ORIGINAL ARTICLE

Nasotransmucosal Delivery of Curcumin-Loaded Mucoadhesive Microemulsions for Treating Inflammation-Related CNS Disorders

Mukeshkumar Shamalbhai PATEL[1]*, Snigdha Das MANDAL[2], Surjyanarayan MANDAL[3], Shital FALDU[4], Jayvadan PATEL[5]

[1]Wockhardt USA LLC/Morton Grove Pharmaceuticals, Inc., Senior Process Engineer, Morton Grove, United States of America
[2]Parul University, Department of Pharmacy, Gujarat, India
[3]AGIO Pharmaceuticals Ltd., Gujarat, India
[4]Smt. R.D. Gardi B. Pharmacy College, Gujarat, India
[5]Sankalchand Patel University, Faculty of Pharmacy, Department of Pharmacy, Gujarat, India

ABSTRACT

Objectives: This investigation was aimed at designing an effective mucoadhesive microemulsion system to accomplish higher brain uptake of curcumin through intranasal route.

Materials and Methods: Mucoadhesive microemulsion of curcumin (MMEC) was developed using screened oil, surfactant, and co-surfactant by Box-Behnken design and was evaluated for mucoadhesion, stability, and naso-ciliotoxicity study. Comparative brain uptake of curcumin after nasal administration of MMEC and polycarbophil curcumin gel and intravenous administration of plain curcumin solution was studied by performing bio-distribution study in Swiss albino rats.

Results: The results showed that all formulation variables *i.e.*, the amount of capmul MCM (X1), S_{mix} (accenon CC: transcutol P) (X2) and percentage of aqueous. Polycarbophil (X3) had a significant effect ($p<0.05$) on the responses. The developed MMEC was stable and non-ciliotoxic with 66.74 ± 3.46 nm and 98.58% ± 1.21 as average globule size and drug content, respectively. Polydispersibility index (0.133 ± 0.17) data and transmission electron microscopy study depicted the narrow size distribution of MMEC. Furthermore, following a comparative investigation of the brain uptake of curcumin among MMEC, plain drug gel and intravenous administration at 2.86 mg/kg, more brain uptake of curcumin was demonstrated for MMEC over intravenous application. Moreover, curcumin uptake in olfactory bulb after nasal administration of MMEC (31.11 ± 1.6) was than 9.44 times higher than intravenous injection of curcumin solution (3.25 ± 1.01). Area under curve represents the ratio of 2.86 mg/kg in brain tissue to plasma acquired afterward(s) the intranasal injection of MMEC (and it) was essentially greater than after the intravenous administration of curcumin solution.

Conclusion: Findings of the investigation revealed that optimal MMEC and intranasal route may be considered to be promising and an alternative approach for brain targeting of curcumin.

Key words: Intranasal delivery, microemulsion, brain-targeting, MMEC, mucoadhesion, TEM, curcumin

INTRODUCTION

Brain targeting through the nasal route has become a fruitful research platform, and in recent times, it is attracting a lot of attention around the globe. Drug delivery through the nasal route offers numerous benefits like quick bioavailability of the drug, circumvention of liver first-pass metabolic rate and better-delivering drug to the brain through the olfactory region (OR).[1] The olfactory part of the nasal route has a large surface area, *i.e.*, 10 cm^2 and acts as a relatively more vital region of drug-carrying to the central nervous system (CNS) and cerebrospinal fluid. The connective tissue of the olfactory area is known as lamina propria that comprises blood vessels and axons.[2] Several studies have reported literature the brain target drugs insoluble in water *via* nasal route.[3] However, the intranasal administration of drug is connected to numerous intrinsic problems. The fundamental problem is its adequate

*Correspondence: mspatel25@gmail.com, Phone: +1-706-449-4590, ORCID-ID: orcid.org/0000-0003-4594-5510
Received: 10.07.2021, Accepted: 03.11.2021

nasal volume in humans, which is ≤400 µL (200 µL *per* nose), that is undeniably a challenge for the formulators to develop a suitable formulation for poorly water-soluble drugs.[4] Secondly, the rapid proliferation of the nasal mucosal layer (every 10 to 15 min) and ciliary movement facilitate the drug molecules clear from the nasal cavity.[2] Naso-ciliary clearance as a natural defense mechanism instead decreases the adhesion of the preparation to the nasal mucosa over a longer period.[5]

Curcumin is a bioactive constituent present in the rhizomes of *Curcuma longa* L. Curcumin exhibits pharmacologic effects such as anti-inflammatory, anticancer, antibacterial, antirheumatic, antimalarial, antioxidant, cardioprotective, nephroprotective, neuroprotective, and hepatoprotective effects.[6] But curcumin is a a phytoconstituent, which is absorbed, when given through the oral route leading to very poor oral bioavailability (less than 4%), which in fact is due to its poor aqueous solubility and erratic dissolution.[2,3] Further, its incomplete oral absorption and high first-pass metabolism make it difficult to enter the brain due to *P*-glycoprotein overexpression limit its clinical usefulness.[7-9] Therefore, we have tried herein to improve the brain targeting of curcumin by developing a new formulation through the nasal route of administration.

A microemulsion (ME) is an anisotropically precise and thermodynamic stable liquid formulation with a globule size <200 nm. It is composed of oil and water phases, stabilized by a concrete mixture of surfactant and co-surfactant (S_{mix}).[10-14] Several studies in the literature revealed the application of ME for intranasal, topical, and parenteral, transdermal, and oral drug delivery systems.[7,15] Additionally, o/w ME is a better choice for drug incorporation with low water solubility due to its solution-like feature, which provides uniform of dose. But, the ME used for intranasal administration becomes the future area for the CNS targetting.[16,17] The addition of a suitable mucosal adhesive (polycarbophil) such as a polyelectrolyte polymer helps overcome the difficulties associated with the nasal route of drug delivery by retaining the ME formulation on the nasal mucosa for a more extended period. The tissue appropriation and blood-cerebrum (CRB) obstruction entrance information. The kinetics of tissue distribution and blood-brain barrier penetration data revealed that curcumin and nanoformulation were efficient enough for brain targeting.[3,17,18] Moreover, used a quality by design approach was to develop a suitable ME formulation for intranasal delivery, which ultimately maximizes brain targeting.[2-4,16-20]

Therefore, this research aimed to develop an optimal mucoadhesive microemulsion system (MMEC) and perform a comparative brain distribution study of curcumin following intranasal and intravenous administration in the rat. It is thought that MMECs can effectively distribute curcumin in the brain due to the unique connection between the brain and the nose, and the controlled release capability of the developed formulation.[2-4,18-20] Thus, it can provide an innovative method for treating inflammatory diseases of the CNS.

It is thought that MMEC might be effective enough to distribute curcumin within and into the brain due to the unique nose-brain connection and the controlled release capability of the formulation.[2-4] It can provide an innovative approach for treating inflammation-related CNS disorders.

MATERIALS AND METHODS

Curcumin and emodin were acquired from Arjuna Natural Pvt. Ltd. (Kerala, India). Capex, Capmul MCM, Cremophor EL, accenon CC, and transcutol P was obtained from ABITEC Corporation (Columbus, USA). Polycarbophil was received from Lubrizol India Pvt. Ltd., (Navi Mumbai, India). Labral M 1944CS and labrafac CC were acquired from Gattefosse, Navi Mumbai, isopropyl myristate, PEG 400, tween-80, PEG 600, glycerol, isopropyl alcohol, tween-60, oleic acid, and isobutyl alcohol, were procured from Sigma-Aldrich (Bangalore, India). Propranolol was obtained from Torrent Pvt. Ltd. (Ahmedabad, India). Hexane, diethyl ether, NaH_2PO_4, Na_2HPO_4, *p*-phenyl phenol, and acetonitrile [high performance liquid chromatography (HPLC) grade] were acquired from Merck Life Science Pvt (Bengaluru, India). All the reagents used were of analytical grade. Double distilled pure water was used in the present research.

Experimental method

Animals

All animal experiments were performed using (National Institute of Health instructions for the care and use of laboratory animals publishing # 85-23, revised 1996). The Institutional Animal Ethical Committee approved the animal experiment (CPCSEA no: 984/14/11/CPCSEA) (New Delhi, India). Albino rats (230-270 g) were obtained from Zydus Cadila Healthcare Ltd., Moriya, and Ahmedabad, India. The rats were fasted for approximately 12-18 hours with free access to water and quality food through research. The rats were maintained at constant room temperature (25 ± 2°C) and air humidity (50 ± 10%) with a light/dark cycle of 12 h.

Pre-formulation study

The selection of oil as internal phase and core phases for intranasal o/w MME was mainly made on drug solubility in nasomucosal compatible oils.[3] The solubility of the drug in various screened oils such as labrafil M 1944CS, isopropyl myristate, capmul MCM, labrafac CC, and oleic acid for the intranasal drug delivery was determined through saturation solubility technique. Surfactants such as tween-60, tween-80, captex-355, accenon CC, and cremophor RH 40 with hydrophilic-lipophilic balance (HLB) values ranging between 12 and 16, were screened for curcumin solubility. Screening of co-surfactants was based on their ability to form stable and transparent MEs at a minimum concentration, and few reported co-surfactants like PEG 400, PEG 600, propylene glycol, glycerol, isobutyl alcohol, isopropyl alcohol, and transcutol P were screened.[7,21] Excess of curcumin was added to each cap vial containing 5 mL of each selected vehicle. After sealing, mixtures were shaken with a shaker at 37°C for 24 h. After reaching equilibrium, centrifuged each vial was kept at 8000 rpm for 15 min, and excess insoluble curcumin was separated by filtering the supernatant by

Whatman filter (0.45 µm). Solubilized drug concentration from the supernatant was quantified by ultraviolet-visible (UV-VIS) spectrophotometer (Shimadzu UV-1800)[2,5]

Preparation of MMEC

Amount of oil and surfactant-cosurfactant ratio (S_{mix}) was selected from pseudo-ternary phase diagram data. MME was then prepared by water titration method using the screened formulation compositions and was optimized by Box-Behnken design of Design-Expert® software (Stat-Ease, Inc., Minneapolis, Minnesota, USA, V 7.1.0).[7,11] Three independent factors such as percentage amount of capmul MCM (X1), S_{mix} (accenon CC: transcutol P, X2), and percent measure of polycarbophil (X3, as far as % w/v in water) with their three levels. It is taken from preliminary experiments.[8] A total of 15 formulation compositions of MMEC were obtained. The polynomial model and equation were experimentally interpreted based on significant terms ($p<0.05$) and non-significant lack of fit data as provided by Design-Expert® software to define the influence of independent variables on the responses.[22,23] The experimental design was quadratic and details of the three levels taken are demonstrated in Table 1. MMECs were prepared experimentally using the compositions of all model MMECs as summarized in Table 1. S_{mix}, *i.e.*, a mixture of accenon CC and transcutol P (3:1), was mixed well with drug-dissolved capmul MCM solution. The above mixture was then titrated with different aqueous polycarbophil concentrations with gentle and continuous stirring at room temperature using a magnetic stirrer.[10,21,23] Finally, it was decided on standard droplet size, flux, retention time, and drug release (%) to be measured experimentally for all fifteen batches. Flux was estimated from the *ex vivo* permeation study. Plain curcumin dispersed polycarbophil gel [polycarbophil curcumin gel (PCG) 3.0 mg/mL] was prepared by dispersing 30 mg curcumin to the already prepared 0.5% aqueous-based plain polycarbophil-based gel with continuous stirring.

Optimization of MMEC

Responses like average globule size, flux, mucoadhesive potential, and drug release (%) were selected for numerical and graphical optimization. It was decided to choose the maximum flux and drug release (%), while having a minimum average globule size with suitable mucoadhesive potential to obtain an optimized formulation. From the overlay plot, the best composition as MMEC was visually selected. Finally, for verification, checkpoint batches were prepared experimentally and predicted values of all four responses were compared with the observed value. The best-suited composition was considered an optimized batch and was used for further study.

Table 1. Details of variables with levels, compositions and responses of MMEC model formulations provided by Box-Behnken design

Batch	X_1	X_2	X_3	Globule size (nm)	Flux (µg/cm² h)	RT (min)	Drug release (%)
F1	0.10	1.55	0.50	59.62	13.8	17.6	96.1
F2	0.50	1.55	0.50	76.36	18.3	21.5	83.1
F3	0.10	1.65	0.50	55.82	16.3	23.4	80.0
F4	0.50	1.65	0.50	62.59	14.2	22.1	86.2
F5	0.10	1.60	0.25	56.44	15.4	16.2	90.4
F6	0.50	1.60	0.25	68.74	17.5	21.8	76.4
F7	0.10	1.60	0.75	79.22	14.6	24.7	86.2
F8	0.50	1.60	0.75	90.13	16.1	27.8	79.3
F9	0.30	1.55	0.25	60.64	16.4	21.5	85.8
F10	0.30	1.65	0.25	56.54	24.2	23.7	90.4
F11	0.30	1.55	0.75	71.89	12.4	23.2	87.3
F12	0.30	1.65	0.75	63.33	22.0	23.1	85.7
F13	0.30	1.60	0.50	64.12	25.9	22.6	88.3
F14	0.30	1.60	0.50	62.89	25.8	22.5	88.6
F15	0.30	1.60	0.50	63.75	25.6	22.4	88.1
Variables					**Low**	**Medium**	**High**
X_1= Capmul MCM (oil)					0.1 mL	0.3 mL	0.5 mL
X_2= Accenon CC: Transcutol P (S_{mix})					1.55	1.60	1.65
X_3= % aqueous polycarbophil					0.25%	0.5%	0.75%

Amount of curcumin: 30 mg; total volume of MMEC= 10 mL

RT: Retention time (time required for formulations to separate from the agar plates), MMEC: Mucoadhesive microemulsion in curcumin, S_{mix}: Mixture of surfactant and co-surfactant

Evaluation of dependent variables

Droplet size, zeta potential, and polydispersity index (PDI)

The droplet size, zeta potential, and PDI of optimized MMEC were determined by Zetasizer (nano Z.S.; Malvern Instruments Inc, Malvern, U.K.). Therefore, to identify the type of ME formed, a dilutability test was carried out by dispersing 1 g formulation in 100 mL of distilled water and was evaluated for phase separation.[22]

The mucoadhesive potential

The mucoadhesive potential, indicated by the residence time of developed nasal formulations, was evaluated as *per* reported method.[23-25] Briefly, 100 mg MMEC was kept on the focal point of the different agar plates at room temperature at (1% w/w, prepared in phosphate buffer solution, pH 6.4). After 10 min, the agar plates were linked with the USP disintegration test equipment and moved up and down at a speed of 30 ± 2 times in phosphate-buffered saline at 37 ± 1°C.The time taken by the formulations to isolate from the agar plates was noted outwardly as the residence time of the formulations.[22]

Flux

Flux was quantified as the amount of permeated curcumin from the unit area of the nasal mucosa. For this study, a Franz diffusion cell with an effective diffusion area of 7.06 cm^2 and volume 30 mL was used.[26-29] The sheep nasal mucosa with the same thickness was collected from slater house in formalin, prepared, and mounted on the receptor compartment with 30 mL of phosphate buffer (pH: 6.4) as diffusion medium. The donor compartment was amassed to it and was stacked with 1 mL MMECs, PCG, and plain curcumin solution (PCS) (≈ 3 mg curcumin). Diffusion was done at 37 ± 1°C and 50 rpm. At predetermined intervals of 10 mins, an aliquot of 0.5 mL diffusion medium was drawn from the receptor medium and was dissected by UV-VIS spectrophotometer at 422 nm. The results are obtained three times and the mean value is considered.

In vitro drug diffusion study

In vitro drug diffusion study of MMEC was conducted in a modified dissolution apparatus containing 400 mL of dissolution media, *i.e.*, phosphate buffer saline (PBS), pH 6.4.[30-35] The temperature was maintained at 37 ± 1°C and set rpm at 50. The dialysis membrane of cut-off weight 10.000 D was soaked in PBS (pH: 6.4) overnight before the experiment. Different formulations of MMEC, PCG, and PCS equivalent to 30 mg curcumin were placed in separate diffusion bags tied to both ends. Aliquots (5 mL) were withdrawn at an interval of 30 min for the first one hour and then 1 h intervals for the rest of the study period, *i.e.*, 10 h, and supplanted with a similar measure of new phosphate-buffered saline. After proper dilution with dilution media, samples were evaluated at 422 nm by UV-VIS spectrophotometer.[30-34] The results were obtained thrice and the mean value was considered.

pH

pH of the optimal MMEC was measured using a digital pH meter (Welltonix digital pH meter PM100). One g of MMEC was accurately weighed and dispersed in 10 mL of purified water. The calibrated pHmeter electrode was inserted into the sample 10 min before reading at room temperature. pH value was measured in triplicate and the mean value was calculated.[32]

The content analysis of drug

For drug content, 0.5 g equivalent weight of curcumin was placed in a 100 mL volumetric flask and dissolved in 50 mL of ethanolic phosphate buffer (70 mL ethanol and 30 mL PBS- pH: 6.4). The volumetric flask was maintained for 2 h and shaken well in a shaker to mix it properly. It was diluted appropriately and analyzed on a UV-VIS spectrophotometer (Shimadzu UV 1800) at 422 nm.

Spreadability

For MMEC gel spreadability study, 0.5 g MMEC was placed on the glass plate within a premarked circle of 10 mm diameter. A second plate was put over this first petridish, and 50 g weight was permitted to rest on the upper petridish.[2,26] Spreading of the gel with respect to the increase in the diameter was noted.

Viscosity

Viscosity of the developed MMEC was measured in triplicate at 25 ± 1°C by brookfield viscometer (model HVT).[2,32] The prepared MMEC 50 g was placed in a container and permitted to equilibrate for 5 min prior to estimation dial measurements using TC shaft spindle #64 at 20 rpm.

Transmission electron microscopy (TEM)

Morphology of the emulsion droplet for the optimal MMEC was observed using TEM (JEM 1010, JEOL Ltd., Tokyo, Japan) with an acceleration voltage of 80 Kv. The optimal MMEC was diluted with water (1:1000). One drop of the sample was directly plain matrix with has a cross-section size of 300, discolored to 2% weight by volume tungstic acid for 2 min, after drying the MMEC. It was extra dried at retention time (RT) and then inspected using TEM. The interaction was determined at the image was intensified 1, 50.000 times at 8.000 times.[2,32]

Nasal ciliotoxicity

The nasal ciliary toxicity study was conducted using extracted sheep nasal mucosa to evaluate the ingredients' safety to the mucosal layer used in the formulation. In a briefly, the nasal mucosa of the sheep except the diaphragm was collected from the slaughterhouse in phosphate buffered saline (pH: 6.4). At that point, three different parts of the nasal mucosa (NP1, NP2, NP3) having an equal thickness were mounted on a Franz dispersion cell and then were exposed to 2 mL MMEC (test sample, 2860 µg/mL curcumin), PBS (pH 6.4) (negative control) and isopropyl alcohol, a serious nasal mucociliary toxicity agent (positive control)[23,26] for 2 h, respectively. All three nasal samples were washed with purified water after 2 h and the cross-section of the mucociliary was examined with an optimal microscope (Nikon Fx35A, Japan) then the sample was stained with hematoxylin and eosin.[23,26,30]

Animal experiment

The rats were maintained at temperature (25 ± 2˚C) and humidity (45 ± 5%) and were supplied with standard laboratory diet and water *ad libitum* on a 12 h light/dark cycle. The rats were assigned to five groups with six animals in each group.

Group I: Saline treated (normal control).

Group II: Intranasal administration of optimized MMEC at 2860 µg/kg of body weight at two-hour intervals was administered through intraperitoneal route for two weeks.

Group III: Animals treated animal PCG 2860 µg/kg body weight at two-hour intervals were administered through intraperitoneal route for two weeks.

Group IV: Animals were first treated with MMEC 2860 µg/kg in the same above method followed by intranasal applied plain drug solution at 2860 µg/kg of curcumin/kg of body weight for two weeks.

Group V: Animals were treated with 2860 µg/kg of curcumin/kg of body weight for two weeks.

In brief, the animals were anesthetized using intraperitoneal pentobarbital injection (40 mg/kg of body weight) and were maintained their body temperature by keeping them on a heating pad set at 37°C. 40 µL MMEC and PCG containing curcumin equivalent to 2.86 mg/kg each were administered through the intranasal route with the assistance of a micropipette (200 µL) connected to low-density polyethylene tubing with 0.1 mm inner measurement at the delivery site. For intravenous administration, 0.5 mL PCS was delivered (portion comparable to 2.86 mg/kg) through the femoral vein. At 5, 15, 30, 60, 120, 180, 240, and 360 min after the portion, blood was gathered in the anesthetized condition by cardiac puncture in heparinized eppendorf tube (Eppendorf India Pvt. Ltd., Bangalore). Blood samples were then centrifuged at 6000 rpm and -4°C for 15 min to obtain plasma. At each time point, the animals have sacrificed by euthanasia. At that point, the skull was cut open, and the olfactory bulb (OB), olfactory plot (OT), CRB, and cerebellum (CEB) were carefully excised. All four excised brain tissues were rinsed with saline followed by blotting up with channel paper to take out blood spoil and plainly visible veins as much as could reasonably be expected. After gauging, the CRB tissue was homogenized independently with 5 mL saline in a tissue homogenizer (BD-144 tissue homogenizer, India). All tissue samples, such as aliquots of plasma and CRB tissue homogenates, were put away in a freezer (-20°C) until HPLC analysis. Measurements of curcumin were made using 3 rats at each time point.

Pharmacokinetic data analysis

A non-compartmental pharmacokinetic analysis method was used to investigate the pharmacokinetic behavior of curcumin. Microsoft Excel was used to calculate the pharmacokinetic parameters from the experiments. The total area under the plasma concentration-time curve was determined by the trapezoidal rule using plasma curcumin concentration *vs.* time data from time zero to the last sampling time, *i.e.* 6 h plus the extrapolated area (from the last experimental time to infinity). The relative bioavailability of the representative MMEC to control was calculated as follows:

Relative bioavailability %= $[(AUC_{MMEC} \times Dose_{control}) / (Dose_{MMEC} \times AUC_{control})]$

where;

Area under curve$_{MMEC}$ (AUC_{MMEC}) means the area under the plot of plasma concentration of a drug *versus* time after MMEC gives insight into the extent of exposure to a MMEC and its clearance rate from the body.

The AUC control represents the total exposure to the curcumin solution across time.

The clear elimination half-life ($t_{1/2}$) was calculated from the estimated elimination rate constant (kel) by linear regression of the log of the plasma concentrations as in $0.693/_{kel}$. The elimination rate constant (kel) can be calculated directly from those parameters using the equation kel equals clearance divided by the volume of distribution. The maximum plasma concentration and time to maximum concentration after oral administration were determined directly from the concentration *versus* time curve.

Analytical method

Curcumin in plasma and brain tissue was quantified by HPLC method.[27] Curcumin was extracted from plasma by protein precipitation method.[28,36] To 0.2 mL of processed plasma samples, 10 µL emodin (suitably diluting in methanol) was added as an internal standard and was sonicated in a bath sonicator for foe 120 seconds. The HPLC system consisted of an LC-10AD VP HPLC pump (Shimadzu, Japan) equipped with a UV detector with lab-solution software. The column used was an agilent C18 column (Inertsil, 250 mm x 4.6 mm, particle size 5 µ, USA). Chromatographic analysis were carried out at 1 mL/min flow rate of the mobile phase *i.e.*, acetonitrile - 5% acetic acid (75:25, v/v). The mobile phase was prepared by mixing acetonitrile and 5% acetic acid and was further filtered by a 0.22 µ membrane filter, followed by degassing by sonication before use. Elution of the drug was identified at 425 nanometers. 80-400 µL of brain tissue homogenates, 30 µg/mL of emodin was added and stirred for 2 min. At this point of centrifugation at 10.000 rpm for 10 min, the drug was removed from the supernatant by adding 0.7 mL of *n*-hexane and diethyl ether (1:1). Next, the separated organic phase was evaporated at 40˚C until dryness. The residue reconstituted in 100 µL mobile phase, and afterward, 20 µL was injected onto the HPLC framework. The residue was reconstituted in 100 µL mobile phase, and then 20 µL was implemented into an HPLC framework.[2] The blood samples were analyzed using the same mobile phase and chromatographic conditions.

The RT was 5.8 min for curcumin and 3.2 min for the interior standard (*i.e.* emodin). The linear range of curcumin is 40-600 ng/mL, and the linear range of plasma and brain tissue is 20-400 ng/g. Extraction recoveries of curcumin from plasma and tissue homogenates were more than 86.7% and 82.6%, respectively.[33]

Stability study

The stability of MMEC was carried out as *per* the International Conference on Harmonization guidelines (Q1A, R2) for 6 months[30,36] the optimal ME was stored at cold temperature (4-8°C, 45% RH ± 5), (25 ± 2°C, and 60% RH ± 5) and at accelerated temperature (40 ± 2°C, 75% RH ± 5). After each 3 months for half year, MMEC was analyzed for droplet size, particle size distribution, mucoadhesion, and percent drug content. Since curcumin is reported to light-sensitive, the formulation was kept in an amber-colored container.[37]

Statistical analysis

All data were displayed as mean ± standard deviation (SD), and the distinctions between the groups were tested using the student's *t*-test at the significance level of $p<0.05$. More than two groups were compared using ANOVA and differences greater at $p<0.05$ were considered significant.

RESULTS AND DISCUSSION

Pre-formulation study

Capmul MCM is a compatible hydrophobic vehicle to the nasal mucosa, which exhibiting maximum curcumin-dissolving volume (42.17 ± 3.12 mg/mL) compared to other screened oils to develop a ME system. Therefore, it was designated as the oil phase. However, accenon CC, which has an HLB value of 15.6, was chosen as the surfactant and has relatively low drug solubility compared to other surfactants. The selection of capmul was MCM was based on more reservoirs and a more negligible effect partitioning effect of curcumin. Because curcumin remains in the core phase as a dissolved state, curcumin is less soluble in accenon CC, which leads to sustained drug release.[7,30] The longer retention time of curcumin may be due to the loading of curcumin in MME as a reserve source for sustained release of curcumin in brain tissue. The results from the release studies confirm this controlled release. The accumulation of curcumin in the brain may be due to the microsizes of the particles and the presence of surfactant on MME surfaces, which may cause the brain uptake reduction of lipid carriers by the reticuloendothelial system. The predicted result can be compared to data obtained from the literature.[20] In his results, Bashara specified the controlled release of buspirone and high concentration of the same buspirone in the brain, which approving the transport of blunt nasal passages to the brain after an intranasal loading ME of buspirone.[30]

Results of the pseudo-ternary phase study showed that accenon CC and transcutol P (S_{mix}) revealed no significant changes in the existing ME region from 2:1, 2.5:1, and 3:1. For developing ME, S_{mix} of 2.5:1 was chosen since another two proportions (2:1 and 3:1) have more surfactant, which may not help the supply the reservoir properties of the formulation. Then, at that point, we obtained an appropriate ME, which did not aggravate the nasal mucosa, S_{mix} having relatively less surfactant was not selected. Pseudo-ternary phase diagram is shown in Figure 1. These data can be compared to the findings of the results in the literature.[30-32]

Optimization of MMEC

To develop the best MMEC and to observe the effect of independent variables on the responses, such as normal droplet size, flow rate, and retention time as mucosal adhesion possible and drug release (%), three independent variables (X1, X2, and X3) is based on response surface method to Design Expert® programming[14] and the consequences of various regression analysis are summed up in Table 2. Additionally, as shown in Table 1, we also see that the normal droplet size, transition, retention time, and curcumin drug discharge (%) are significantly affected by the independent factors described in polynomial equations 1 to 4.

The evaluation of the responses showed the suitability of the quadratic model ($p<0.05$). Final conditions for all responses, *i.e.*, mean droplet size, movement, hold time, and drug discharge (%) in terms of their respective coded values, were obtained by running ANOVA as follows.

$$\text{Droplet size} = +77.88 + 3.47 \times A - 2.63 \times B + 3.89 \times C - 0.64 \times (A \times B) + 1.12 \times (B \times C) + 2.54 \times (A \times C) + 1.52 \times A^2 - 1.67 \times B^2 + 2.37 \times C^2 \quad \text{equation (1)}$$

Equation 1 showed that the average droplet size of MMEC was generally influenced by capmul MCM, accenon CC: transcutol P concentration ratio and polycarbophil with their interactions. For developing a suitable intranasal drug delivery system, droplet size plays a vital role as it affects the *in vivo* absorption of the drug from the formulations.[4,24] The droplet size of the ME formulation is a key factor because it affects the release rate of the drug and the *in vivo* profile of the drug. In this way, the experiment of optimizing a ME with a droplet size usually smaller confirms that the rapid penetration through mucous layers is an objective of this research. The observed droplet size of the formulations ranged between 55.82 nm and 90.13 nm (Table 1). The results showed that the increase in the oil volume from 0.1 mL to 0.5 mL and the concentration of the mucosal adhesion polymer from 0.25-0.75% caused a significant increase in globule size of ME formulation. This could be because it did not diminish the interfacial tension among the oil and the external phase with maximum concentration with a similar mix. Additional, at higher S_{mix} concentration, the lipophilic property of oil was well masked, resulting in low interfacial tension, and therefore, droplet size reduces.[23] Mucoadhesive polymer also shows to upsurge the droplet size, which may be because it was capable of absorbing water and swell, which in turn disturbed the HLB of the system.

$$\text{Flux} = +88.46 + 2.47 \times B - 1.83 \times C + 0.58 \times (A \times B) - 1.67 \times (A \times C) + 1.55 \times C^2 \quad \text{equation (2)}$$

Capmul MCM due to its reservoir action and polycarbophil due to the viscosity enhancing property showed a negative effect on the release rate. Therefore, the drug concentration gradient across the permeation barrier (nasal mucosa) is not high and hence the flux. The results obtained in this study indicated that oil concentration (X1) and mucoadhesive polymer concentration (X3) have significant effects on the flux through sheep nasal

mucosa (p-0.0001). However, S_{mix} showed a positive effect on flux because both surfactant and cosurfactant are capable of altering the permeation behavior of the membrane by changing the fluidization of lipid enabling the drug molecule to permeate through rapidly.

Retention time= + 47.37 + 3.55 × C + 2.79 × (A × C) + 0.88 × (B × C) - 0.76 × B^2 + 1.04 × C^2 equation (3)

Polycarbophil, due to its mucoadhesive property along with viscosity enhancing property, showed a noticeably positive effect on the retention time of MMEC on the nasal mucosa, while oil and S_{mix} showed non-significant effects as shown in equation 3. The mucoadhesive nature of the polymer may be because of the presence of a high density of hydrogen bonding groups, which could combine with mucin more strongly, as shown in equation 3 (p-0.0021).[37]

Drug release (%)= + 93.87 - 1.89 × A + 2.01 × B - 3.11 × C + 0.88 × (A × B) - 1.95 × (A × C) - 1.89 × (B × C) + 0.51 × A^2 - 0.67 × B^2 - 1.34 × C^2 equation (4)

Drug release from MMEC was inversely affected by capmul MCM and polycarbophil concentration, while a mixture of accenon CC and transcutol P was found to facilitate the release of curcumin from the developed formulation, as revealed in equation 4. Drug release from the model MMEC batches after 8 h ranged from 79% to 96%, as given in Table 1. Capmul MCM showed to retard

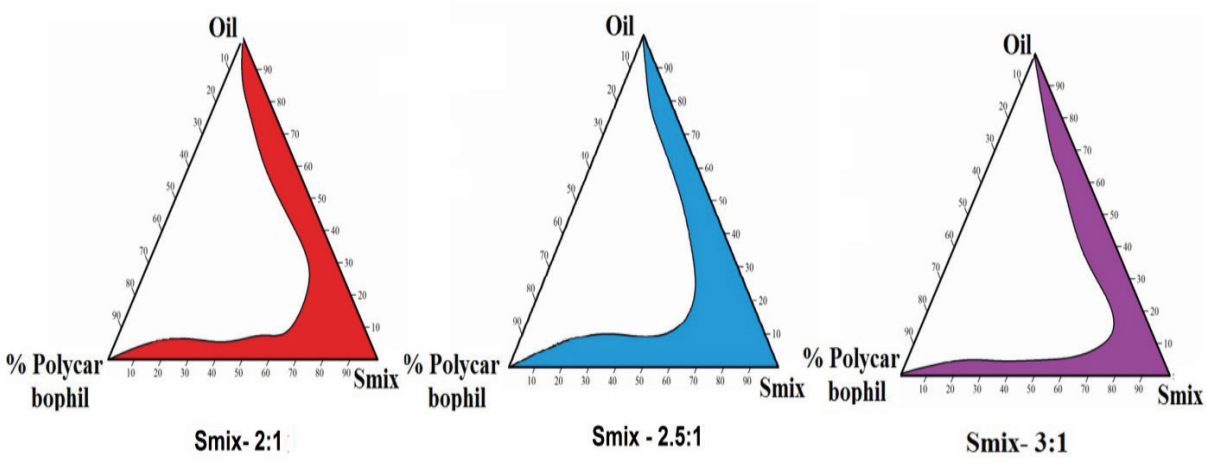

Figure 1. Pseudo-ternary phase diagram of MMEC showing microemulsion existing region with 2.5:1 S_{mix}
MMEC: Mucoadhesive microemulsion in curcumin

Table 2. Statistical parameter of responses determined by multiple regression analysis

Regression coefficient	Coefficient estimate			
	Globule size (nm)	Flux (µg/cm² h)	Rt (min)	Drug release (%)
A- Capmul MCM (X1)	3.47	-0.47	0.39	-1.89
B- S_{mix} (X2)	-2.63	2.47	-0.21	2.01
C- % aqueous polycarbophil (X3)	3.89	-1.83	3.55	-3.11
AB (X1 X2)	-0.64	0.58	0.35	0.88
AC (X1 X2)	2.54	-1.67	2.79	-1.95
BC (X1 X2)	1.12	-0.43	0.88	-1.89
A^2	1.52	-0.45	0.37	0.51
B^2	-1.67	0.43	-0.76	-0.67
C^2	2.37	1.55	1.04	-1.34
Model (p value)	0.0002	0.0003	0.0021	0.0002
Coefficient of variation	0.991	0.999	0.962	0.999
R^2	0.973	0.998	0.976	0.997
Adjusted R^2	0.6710	0.2891	0.8771	0.0580
Lack of fit (p value)	3.47	-0.47	0.39	-1.89

Rt: Retention time, S_{mix}: Mixture of surfactant and co-surfactant

the drug release from the formulation due to its partitioning and reservoir properties, while polycarbophil because of its viscosity enhancing property, kinetics of the drug molecule reduced leading to the slow release. However, S_{mix} (accenon CC and transcutol P mixture) increased curcumin release because it increased the water solubility of curcumin by reducing the interfacial tension. This increase in drug release may be further be due to nanoglobule size with a narrow size distribution.

The rationale of optimization through factorial design was to obtain the ranges of all independent factors, establish their influence on responses, and find a robust composition for intranasal delivery of curcumin. In this study, globule size, viscosity, and retention time (Rt indicating the mucoadhesive property) were set to the maximum without affecting release, while flux and release were set to maximum. Confirming the desirability of the optimized nasal formulations, three MMECs, so obtained from the overlay plot were prepared experimentally, and all responses were evaluated as given in Table 3. It was observed that experimentally found data matched the predicted responses for all three MMECs, and hence, the optimization process was verified.[32-34]

MMEC characterization

MMEC with 0.5% w/v polycarbophil, 0.3 mL capmul MCM, 3.70 mL S_{mix} (2.5: 1 ratio) exhibited the smallest droplet size (55.82-90.12 nm); the highest flux and drug release (80-96.1%) are demonstrated in Table 3 and are closer to the observed results than predicted. Therefore, was considered the optimal formulation. The average globule size was 66.74 ± 3.46 nm with PDI equivalents to 0.133 ± 0.017, as revealed in Figure 2. Besides, the PDI value (<0.3) showed the monodisperse property of the formulation.[38]

Zeta potential of MMEC was -21.4 mV ± 4.11 as shown in Figure 3. These data depict neither the stability of the formulation, which might be because moderate negative surface charges neither result in strong aggregation nor repulsion of the globules.[7] So, individual nanoglobules increased the surface area, which in turn helped in the nasal absorption of the drug and hence the stability of formulation and brain targeting. TEM data further support the nanosize with narrow size distribution, as illustrated in Figure 4.

Curcumin content was discovered to be 97.82 ± 0.44%, 98.11 ± 0.51% and 99.32 ± 0.22% for MMEC, PCG and PCS individually. The pH (6.7 ± 0.18), thickness, and mucoadhesive strength data showed the appropriateness for the nasal application of MMEC. The stability studies showed no significant changes in droplet size; size distribution, retention time, and phase separation over six months were observed from the stability study. Hence, developed mucoadhesive nasal formulation of curcumin was considered physically stable for 6 months.

Optical microscopic pictures showed no mucociliary damage by MMEC as shown in Figure 5C, which revealed non-ciliotoxicity profile of developed MMEC while complete cilia destruction was observed in the isopropyl-treated mucosa. Hence, developed MMEC was considered suitable for nasal application. This may be because all formulation compositions were of GRAS and had no interaction.

The prepared gel produces excellent spreadability and mucoadhesive strength. The drug content of the MMEC was found to be 98.67 ± 0. 44% and pH was found to be 6.58 ± 0. 29. The viscosity of the gel was found to be 18.7 ± 2.11 Ps at 10 rpm. Spreadability, pH, viscosity, and mucoadhesive strength data show the suitability for intranasal application of MMEC. From the stability study, as shown in Table 4, no significant changes in globule size, size distribution, Rt, and phase separation over a period of 6 months were observed. Hence, developed mucoadhesive nasal formulation of curcumin was considered physical stable for 6 months.

Pharmacokinetic study

Curcumin concentration in plasma and brain tissue concentrations after nasal administration of MMEC and PCG and intravenous administration of PCS at 2.86 mg/kg body weight of rat was estimated. The pharmacokinetic parameters

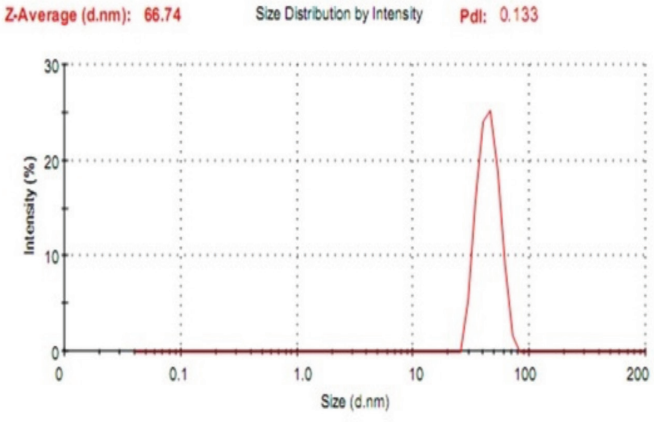

Figure 2. Result of globule size with size distribution indicating the nano size range of optimal MMEC

MMEC: Mucoadhesive microemulsion in curcumin

Table 3. Obtained predicted data and observed data of size, flux, retention time and drug release (%) of MMEC

No	Components			Globule size (nm)		Flux (μg/cm² h)		Rt (min)		Drug release (%)	
	O	S_{mix}	p	Pre.	Obs.	Pre.	Obs.	Pre.	Obs.	Pre.	Obs.
1	0.30	3.80	0.50	48.6	47.4	24.0	23.9	22.9	22.2	93.9	95.6
2	0.31	3.80	0.52	48.4	47.5	24.7	23.8	22.8	22.0	89.8	93.0
3	0.30	3.70	0.50	46.7	46.3	25.4	25.8	22.9	22.8	94.1	94.8

MMEC: Mucoadhesive microemulsion in curcumin, S_{mix}: Mixture of surfactant and co-surfactant, Rt: Retention time, O: Oil, Pre.: Predicted, Obs.: Observed

obtained by non-compartmental pharmacokinetic analysis (n: 3; mean ± SD) are given in Table 5.

Following the IV administration of PCS, plasma curcumin fixations arrived at the maximum level before 15 min and then decreased rapidly over time, as shown in Figure 6. After intranasal administration of MMEC, maximum concentration of curcumin was achieved even before 30 min in OB, while 60-120 min in other brain parts like OT, CRB and CEB. Curcumin content differed considerably in different brain regions. The highest concentration was observed in the OB (the peak drug level was 1109.1 ± 56.4 ng/g), followed by OT, then the CEB and finally in CRB as shown in Figure 6. These findings support the existence of a nose-brain direct pathway following the intranasal administration. As shown in Table 5, curcumin concentration, particularly in the OB, was noticeably higher than in other tested parts of the brain following nasal administration of MMEC.

AUC0→360 for MMEC was 2.81 times (56449 ± 3113 ng min/g) more that obtained after *i.v.* injection of PCS (20088 ± 1241 ng min/g). However, PCG showed comparatively less curcumin uptake than that of MMEC, which was a clear indication of only mucoadhesive property was not sufficient for nasal delivery to the brain.

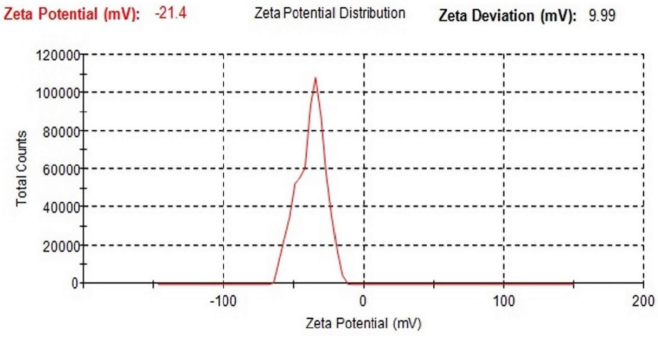

Figure 3. Zetapotential data representing the physical stability of MMEC

MMEC: Mucoadhesive microemulsion in curcumin

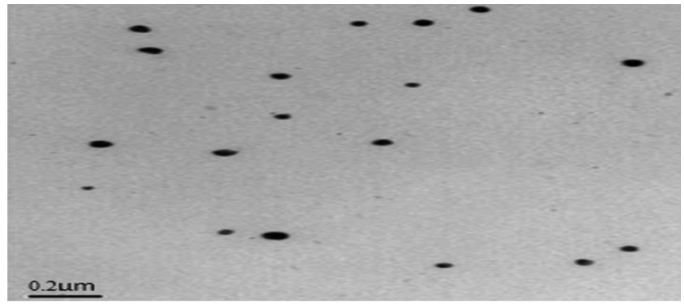

Figure 4. TEM result of the optimized MMEC indicating the narrow particle size with uniform distribution

TEM: Transmission electron microscopy, MMEC: Mucoadhesive microemulsion in curcumin

Table 4. Results indicating the stability of developed nasal formulation in three different storage conditions

Temperature and relative humidity	Evaluated parameters of MMEC							
	Globule size (nm)		Retention time (min)		PDI		Phase separation	
	3rd month	6th month	3rd month	6th month	3rd month	6th month	3rd month	6th month
2 - 8°C 45 + 5%	75.5 ± 4.2	83.3 ± 3.7	19.8 ± 2.2	22.3 ± 1.9	0.31 ± 0.02	0.36 ± 0.07	No	No
25 + 2°C 60 + 5%	62.7 ± 4.8	69.6 ± 5.3	22.5 ± 1.27	22.8 ± 1.85	0.201 ± 0.02	0.217 ± 0.03	No	No
45 + 2°C 75 + 5%	63.9 ± 4.9	61.8 ± 4.4	18.9 ± 1.87	20.1 ± 1.37	0.364 ± 0.21	0.343 ± 0.017	No	Yes

(Result= mean ± SD, n: 3). MMEC: Mucoadhesive microemulsion in curcumin, PDI: Polydispersity index, SD: Standard deviation

Table 5. Pharmacokinetic parameters of curcumin after transnasal and intravenous application of MMEC and PCS respectively (n: 3)

Parameters and routes	Plasma	OB	OT	CBR	CEB
C_{max} (ng/mL g) (intranasal)	112.3 ± 21.5	956.8 ± 71.2	345.6 ± 101.6	256.7 ± 21.2	2037 ± 19.8
C_{max} (ng/mL g) (intravenous)	954.5 ± 56.4	3087.8 ± 72.5	2807.7 ± 87.3	2857.9 ± 99.7	464.7 ± 169.3
$AUC_{0\rightarrow360}$ (ng min//mL g) (intranasal)	21311 ± 871	62458 ± 1867	8876.1 ± 928	6542.8 ± 298.7	3894.2 ± 228.6
$AUC_{0\rightarrow360}$ (ng min/mL g) (intravenous)	72561 ± 4427	26857 ± 971	13241.2 ± 366	19288.1 ± 558	14389.6 ± 237
% ($AUC_{i.n.}$/$AUC_{i.v.}$)	29.36	232.56	67.03	33.92	27.06

(Result; mean ± SD, n: 3). C_{max}: Maximum peak plasma concentration, SD: Standard deviation, MMEC: Mucoadhesive microemulsion in curcumin, PCS: Plain curcumin solution, OB: Olfactory bulb, OT: Olfactory tract, CBR: Cerebrum, CEB: Cerebellum, AUC: Area under curve, *i.v.*: Intravenous, *i.n.*: Intranasal

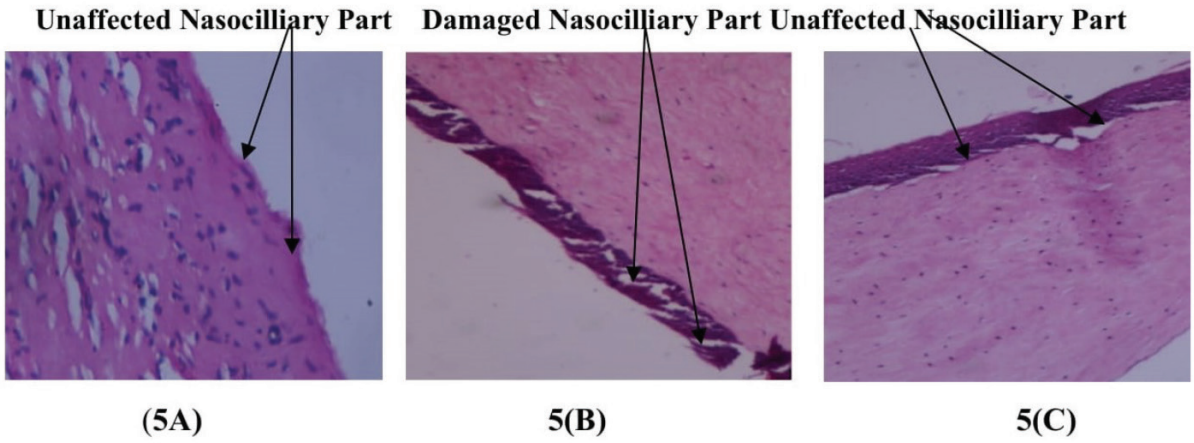

Figure 5. Result of naso-ciliotoxicity study displaying the non-toxicity of developed MMEC. 5(A), 5(B), and 5(C) are representative of PBS (pH: 6.4), propranolol and developed MMEC treated naso mucosal part individually

MMEC: Mucoadhesive microemulsion in curcumin, PBS: Phosphate buffer saline

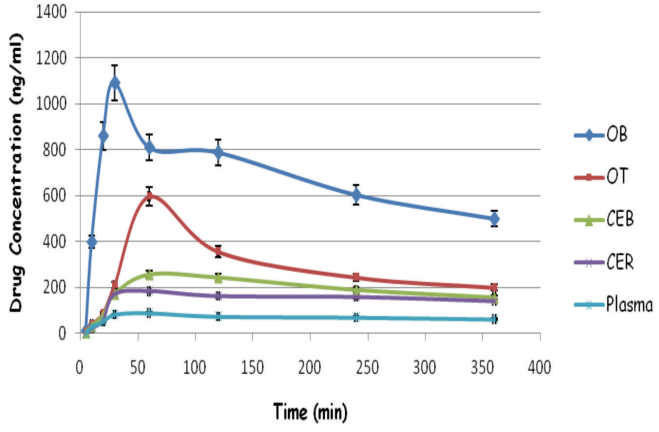

Figure 6. Curcumin concentration in different parts of brain and blood after intranasal delivery (n: 3; mean ± SD)

SD: Standard deviation, OB: Olfactory bulb, OT: Olfactory tract, CER: Cerebrum, CEB: Cerebellum

Curcumin uptake in other brain parts (OT, CRB, and CEB) after nasal dosing of MMEC was lower than OB (n: 3; mean ± SD) as shown in Table 5 and Figure 6, which may be due to its anatomical position from the nasal turbinates.[33,35] After nasal dosing of MMEC, curcumin transport from the nasal turbinates into the OR may occur through three pathways, *i.e.*, transcellular between the sustentacular cells by endocytosis, paracellularly through tight junctions between the sustentacular cells, and intracellular axonal transport *via* the olfactory nerve pathway following endocytosis or pinocytosis into the OB. MMEC increased the aqueous solubility of lipophilic curcumin, enhancing the drug permeation through the nasal cells by combining all three above described methods and reaching the therapeutic area.[37,38]

Curcumin uptake into other brain regions like OT, CBR, and CEB, after nasal dosing of MMECs was lower than *i.v.* dosing of PCS, as shown in Table 5 and Figure 6. These may be attributed to the comparative lower plasma levels from MMEC, which might reduce curcumin distribution in the brain. In contrast to CBR and CEB, the mass of the OB is small. The distribution of higher curcumin from OB into other brain regions could be counteracted by its small masses, thus leading to a significant increase in curcumin content in different brain tissue (olfactory pathway). Due to the controlled release of curcumin from MMEC and mucoadhesive nature, prolonged curcumin absorption was observed, indicating the nose-direct brain transport. These obtained data were also similar to the data given in the literature[36-38] showing a unique nasal mucosa-brain connection. To evaluate the brain targeting through nasal delivery of MMEC, the brain-to-plasma curcumin AUC ratios at 10, 30, and 360 min following intravenous and intranasal routes were calculated. Results showed that the ratio of AUC in brain tissue to that in plasma after intranasal application of MMEC was significantly higher ($p<0.05$) than those after intravenous injection of PCS and PCG. For instance, in 10 min after nasal dosing, the AUC ratio was 5.83 times higher than that after intravenous dosing (19.85 ± 1.5 v/s 3.4 ± 1.1) in OB, as shown in Figure 7A.

Similarly, 9.17 times (60.41 ± 2.8 v/s 6.58 ± 1.3) and 9.56 times (31.11 ± 1.6 v/s 3.25 ± 1.01) increment of curcumin concentration in OB following *i.n.* and *i.v.* delivery at the time points 30 min and 360 min (n: 3; mean ± SD) respectively as shown in Figure 7B, C. Following intranasal administration, 87.22% of curcumin was transported to the brain *via* the olfactory pathway in six hours.[37,38] It can be concluded that the nasal route of administration and mucoadhesive formulation may help curcumin enhance its brain uptake.

CONCLUSION

Results confirmed that polycarbophil-based MME system including capmul MCM (3% v/v), accenon CC (26% v/v), and transcutol P (9% v/v) was optimal for transnasal delivery of curcumin. The developed ME system was non-ciliotoxic, physical stable at ambient conditions for 6 months and was suitable for controlled curcumin delivery to the brain. Results of a brain distribution study confirmed that a fraction of

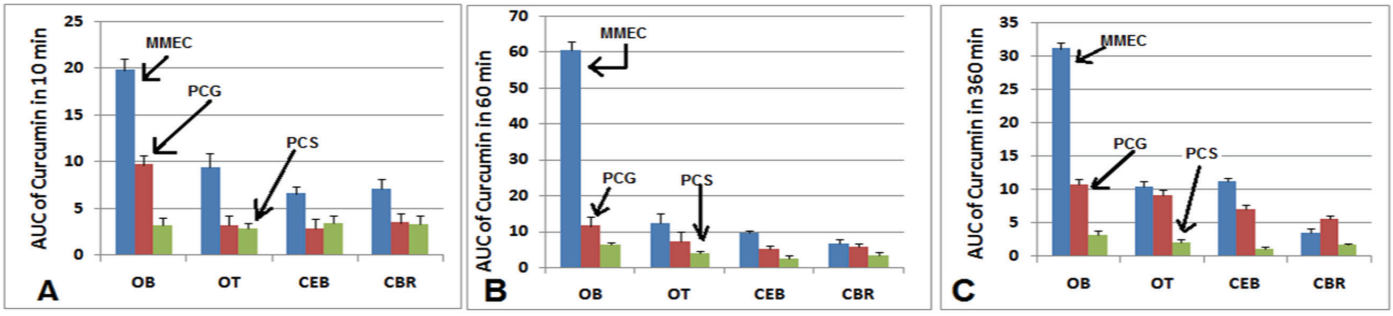

Figure 7. Plasma curcumin concentration and in different parts of brain after intranasal administration of MMEC, PCG and intravenous dosing of PCS after 10 min (A), 30 min (B), and 360 min (C) respectively (n: 3; mean ± SD)

MMEC: Mucoadhesive microemulsion in curcumin, PCG: Polycarbophil gel, PCS: Plain curcumin solution, SD: Standard deviation, OB: Olfactory bulb, OT: Olfactory tract, CBR: Cerebrum, CEB-Cerebrellum

curcumin could be transported directly into the brain after nasal delivery, which may decrease the dose and frequency of dosing and hence maximize its therapeutic index. However, clinical benefits to risk ratio of this mucoadhesive formulation so developed in this investigation will decide its effectiveness in the clinical practice.

Ethics

Ethics Committee Approval: The animal experiment was approved by the Institutional Animal Ethical Committee (CPCSEA No. 984/14/10/CPCSEA New Delhi, India) and registration no: 1244/08/ CPCSEA, India.

Informed Consent: Not necessary.

Peer-review: Externally peer-reviewed.

Authorship Contributions

Surgical and Medical Practices: J.P., Concept: S.D.M., J.P., S.M., Design: S.D.M., S.M., Data Collection or Processing: S.M., S.F., S.D.M., Analysis or Interpretation: S.F., Literature Search: M.S.P., S.D.M., S.M., S.F., J.P., Writing: M.S.P.

Conflict of Interest: No conflict of interest was declared by the authors.

Financial Disclosure: The authors declared that this study received no financial support.

REFERENCES

1. Romeo VD, deMeireles J, Sileno AP, Pimplaskar HK, Behl CR. Effects of physicochemical properties and other factors on systemic nasal drug delivery. Adv Drug Deliv Rev. 1998;29:89-116.
2. Mandal S, Mandal SD, Chutani K, Subudhia BB. The mucoadhesive microemulsion of ibuprofen: design and evaluation for brain targeting efficiency through intranasal route. Braz J Pharma Sci. 2015:51:721-731.
3. Mandal SD, Mandal S, Patel J. Brain targeting efficiency of curcumin loaded mucoadhesive microemulsion through intranasal route. J Pharm Investig. 2016;46:179-188.
4. Pathak R, Dash RP, Misra M, Nivsarkar M. Role of mucoadhesive polymers in enhancing delivery of nimodipine microemulsion to brain *via* intranasal route. Acta Pharm Sin B. 2014;4:151-160.
5. Aggarwal BB, Harikumar KB. Potential therapeutic effects of curcumin, the anti-inflammatory agent, against neurodegenerative, cardiovascular, pulmonary, metabolic, autoimmune and neoplastic diseases. Int J Biochem Cell Biol. 2009;41:40-59.
6. Lawrence MJ, Rees GD. Microemulsion-based media as novel drug delivery systems. Adv Drug Deliv Rev. 2000;45:89-121.
7. Tenjarla S. Microemulsions: an overview and pharmaceutical applications. Crit Rev Ther Drug Carrier Syst. 1999;16:461-521.
8. Mandal S, Mandal SD. Design and development of carbamazepine mucoadhesive microemulsion for intranasal delivery: an *ex-vivo* study. Int J Pharm Sci Rev Res. 2010;3:56-60.
9. Mandal SD, Mandal S, Patel J. Development of curcumin loaded microemulsion drug delivery system for improving its dissolution profile. IJPFA. 2013;4:101-107.
10. Himesh S, Sharan PS, Mishra K, Govind N, Ak S. Qualitative and quantitative profile of curcumin from ethanolic extract of *Curcuma longa*. Int Res J Pharm. 2011;2:180-184.
11. Bitter C, Suter-Zimmermann K, Surber C. Nasal drug delivery in humans. Curr Probl Dermatol. 2011;40:20-35.
12. Stevens J, Ploeger BA, van der Graaf PH, Danhof M, de Lange EC. Systemic and direct nose-to-brain transport pharmacokinetic model for remoxipride after intravenous and intranasal administration. Drug Metab Dispos. 2011;39:2275-2282.
13. Md S, Khan RA, Mustafa G, Chuttani K, Baboota S, Sahni JK, Ali J. Bromocriptine loaded chitosan nanoparticles intended for direct nose to brain delivery: pharmacodynamic, pharmacokinetic and scintigraphy study in mice model. Eur J Pharm Sci. 2013;48:393-405.
14. Paradkar A, Ambike AA, Jadhav BK, Mahadik KR. Characterization of curcumin-PVP solid dispersion obtained by spray drying. Int J Pharm. 2004;271:281-286.
15. Dhuria SV, Hanson LR, Frey WH 2nd. Intranasal delivery to the central nervous system: mechanisms and experimental considerations. J Pharm Sci. 2010;99:1654-1673.
16. Jeffrey P, Summerfield S. Assessment of the blood-brain barrier in CNS drug discovery. Neurobiol Dis. 2010;37:33-37.
17. Tsai YM, Chien CF, Lin LC, Tsai TH. Curcumin and its nano-formulation: the kinetics of tissue distribution and blood-brain barrier penetration. Int J Pharm. 2011;416:331-338.
18. Shah B, Khunt D, Bhatt H, Misra M, Padh H. Application of quality by design approach for intranasal delivery of rivastigmine loaded solid lipid nanoparticles: effect on formulation and characterization parameters. Eur J Pharm Sci. 2015;78:54-66.

19. Swamy NGN, Abbasb Z. Mucoadhesive *in situ* gels as nasal drug delivery systems: an overview. Asian J Pharm Sci. 2012;7:168-180.

20. Wang X, Chi N, Tang X. Preparation of estradiol chitosan nanoparticles for improving nasal absorption and brain targeting. Eur J Pharm Biopharm. 2008;70:735-740.

21. Mandal SD, Mandal S, Patel J. Intranasal mucoadhesive microemulsion for the neuroprotective effect of curcumin in MPTP induced Parkinson model. Braz J Pharm Sci. 2017;53:e15223.

22. Aqil M, Kamran M, Ahad A, Imam SS. Development of clove oil-based nanoemulsion of olmesartan for transdermal delivery: Box-Behnken design optimization and pharmacokinetic evaluation. J Mol Liq. 2016;214:238-248.

23. Thakkar H, Patel A, Chauhan N. Formulation and optimization of mucoadhesive microemulsion containing mirtazapine for intranasal delivery. Chron Young Sci. 2014;4:25-32.

24. Joshi HM, Bhumkar DR, Joshi K, Pokharkar V, Sastry M. Gold nanoparticles as carriers for efficient transmucosal insulin delivery. Langmuir. 2006;22:300-305.

25. Kan P, Chen ZB, Kung RY, Lee CJ, Chu IM. Study on the formulation of o/w emulsion as carriers for lipophilic drugs. Colloids Surf B: Biointerfaces. 1999;15: 117-125.

26. Acharya SP, Pundarikakshudu K, Panchal A, Lalwani A. Preparation and evaluation of transnasal microemulsion of carbamazepine. Asian J Pharm Sci. 2013;8:64-70.

27. Kumar M, Misra A, Babbar AK, Mishra AK, Mishra P, Pathak K. Intranasal nanoemulsion based brain targeting drug delivery system of risperidone. Int J Pharm. 2008;358:285-291.

28. Li J, Jiang Y, Wen J, Fan G, Wu Y, Zhang C. A rapid and simple HPLC method for the determination of curcumin in rat plasma: assay development, validation and application to a pharmacokinetic study of curcumin liposome. Biomed Chromatogr. 2009;23:1201-1207.

29. Wang D, Hu J, Lv L, Xia X, Liu J, Li X. Enhanced inhibitory effect of curcumin *via* reactive oxygen species generation in human nasopharyngeal carcinoma cells following purple-light irradiation. Oncol Lett. 2013;6:81-85.

30. Bshara HN, Ahmed RO, Holayel SM, El-Shamy AEH. Improvement of the bioavailability of buspirone HCl using intranasal delivery systems. Az J Pharm Sci. 2012;45:86-102.

31. Karasulu HY, Sanal ZE, Sözer S, Güneri T, Ertan G. Permeation studies of indomethacin from different emulsions for nasal delivery and their possible anti-inflammatory effects. AAPS PharmSciTech. 2008;9:342-348.

32. Kaur P, Kim K. Pharmacokinetics and brain uptake of diazepam after intravenous and intranasal administration in rats and rabbits. Int J Pharm. 2008;364:27-35.

33. Rao J, McClements DJ. Formation of flavor oil microemulsions, nanoemulsions and emulsions: influence of composition and preparation method. J Agric Food Chem. 2011;59:5026-5035.

34. Dey S, Mahanti B, Mazumder B, Malgope A, Dasgupta S. Nasal drug delivery: an approach of drug delivery through nasal route. Der Pharmacia Sinica. 2011;2:94-106.

35. Vyas TK, Babbar AK, Sharma RK, Singh S, Misra A. Preliminary brain-targeting studies on intranasal mucoadhesive microemulsions of sumatriptan. AAPS PharmSciTech. 2006;7:E8.

36. Mandal S, Mandal SD, Chuttani K, Dharamsi A, Subudhi BB. Transnasomucosal mucoadhesive microemulsion of zaltoprofen: a comparative brain distribution study. J Drug Deliv Sci Technol. 2017;39:237-246.

37. Chen X, Zhi F, Jia X, Zhang X, Ambardekar R, Meng Z, Paradkar AR, Hu Y, Yang Y. Enhanced brain targeting of curcumin by intranasal administration of a thermosensitive poloxamer hydrogel. J Pharm Pharmacol. 2013;65:807-816.

38. Tian XH, Lin XN, Wei F, Feng W, Huang ZC, Wang P, Ren L, Diao Y. Enhanced brain targeting of temozolomide in polysorbate-80 coated polybutylcyanoacrylate nanoparticles. Int J Nanomedicine. 2011;6:445-452.

Turk J Pharm Sci 2022;19(5):572-582
DOI: 10.4274/tjps.galenos.2021.43678

ORIGINAL ARTICLE

Fabrication and Evaluation of Matrix Type Novel Transdermal Patch Loaded with Tramadol Hydrochloride

Shankhadip NANDI[1]*, Saptarshi MONDAL[2]

[1]Eminent College of Pharmaceutical Technology, Department of Pharmaceutics, Kolkata, West Bengal, India
[2]Bengal School of Technology, Department of Pharmaceutics, Chinsurah, West Bengal, India

ABSTRACT

Objectives: Transdermal drug delivery as a novel drug delivery system has become a major research interest to the scientists for its controlled drug release and improved patient compliance. This study was conducted to develop an optimized transdermal patch of tramadol hydrochloride using an appropriate amount of suitable polymers. It was also planned to control the drug permeation rate from the device to achieve a sustained release pattern.

Materials and Methods: Several numbers of formulations were prepared by altering the amount of excipients. Physicochemical and biopharmaceutical parameters were checked to get the optimized formulation with desired characteristics.

Results: Fourier transform infrared spectroscopy results displayed no abnormal peaks and hence concluded that the drug and polymers were compatible with each other. The minimum standard deviation values of different physicochemical parameters assured that the method of preparation was skilled to develop patches with least intra-batch variability. A higher percentage of hydroxypropyl methylcellulose (HPMC) resulted in the greater tensile strength, moisture content and water vapor transmission rate of the patches. A high folding endurance value (>200) indicated the flexibility of the prepared patches and their integrity to the skin. The transdermal patches coded as F26 containing only HPMC polymer demonstrated the desired drug permeation rate (65.51%) within 12 hours through *ex vivo* permeation studies.

Conclusion: The formulation coded as F26 was found to be the most optimized patch as it exhibited sustained drug permeation rate followed by higuchi diffusion kinetics, that also confirmed the capability of the formulation to exhibit matrix type drug delivery.

Key words: Optimized transdermal patch, tramadol hydrochloride, *ex vivo* permeation studies, higuchi diffusion kinetics, matrix type drug delivery

INTRODUCTION

In the recent few years, a research interest has been evolved to design a wide variety of novel drug delivery systems (NDDS) using the existing drug molecules.[1] Currently, transdermal drug delivery is considered as one of the most promising approaches for the implementation of NDDS.[2] Topical dosage forms containing one or more therapeutic agents that can produce a systemic effect of the agent is termed as transdermal drug delivery system (TDDS).[3] There are several advantages of TDDS like controlled release of the drug, steady blood-level profile, minimized systemic side effects, bypassing first-pass hepatic metabolism, self-administration, enhanced patient compliance, improved efficacy over any other conventional dosage forms.[1] Transdermal system has been designed for delivering an effective amount of drug across the intact skin to accomplish both the local and systemic effects.[4] Pain, hypertension, motion sickness, angina, nicotine addiction are the diseases which can be treated by the aid of transdermal delivery of drugs. Latest example of successfully using this system is healing of urinary incontinency and contraception.[5] Transderm SCOP approved by Food and Drug Administration (FDA) in 1979, was the first transdermal system which was used to inhibit nausea and vomiting associated with motion sickness.[1] Creams, ointments, pastes, gels, lotions, sprays, and patches are the most common transdermal formulations available in the market.

*Correspondence: shankhadipnandi@gmail.com, Phone: +91-9804344736, ORCID-ID: orcid.org/0000-0002-7673-7645
Received: 26.07.2021, Accepted: 03.11.2021

A transdermal patch is a user friendly, convenient and extensively accepted medicated adhesive device that distributes the drug through the skin for systemic effects in a controlled and programmed manner.[6] Exposing of patch application site should be avoided from the external heat sources such as hot water bottles, hot water bags *etc.* A higher body temperature may also elevate the rate of drug release. Here, the patch must be removed immediately.[1] Restricting nature of skin is one of a significant drawbacks for passive delivery of drugs through transdermal patches.[7] Transdermal patches are classified into three types as the drug (i) in a reservoir system, (ii) in adhesive, (iii) in matrix.

The drug in matrix systems are developed by dispersing or dissolving the active pharmaceutical ingredient in a polymer matrix followed by adding an adhesive layer if desired. The polymer matrix regulates the rate of drug delivery.[8,9] The selection of a polymer depends upon its physicochemical properties, compatibility with drug, optimization of the drug loaded into the matrix with other ingredients, skin contact, mode of drug release, and stability.[10,11] Ideal drug candidates for transdermal patch that can readily permeate to the skin must have a low molecular weight, high therapeutic potency, be moderately lipophilic and being non-allergenic, and non-irritating.[7] Tramadol hydrochloride is a 4-phenyl-piperidine analogue of the opioid drug codeine, 2-(dimethyl amino)-methyl)-1-(3′-methoxyphenyl) cyclohexanol hydrochloride, which was first synthesized in 1962.[12] The drug is categorized as an analgesic and can be used to relieve from moderate to severe acute and chronic (cancer and non-cancer) pain, osteoarthritis. For treating dental pain, osteoarthritis flare pain, and chronic back pain, tramadol provides rapid onset and prolonged action along with acetaminophen.[13] It has been evidenced that at small dosages, tramadol hydrochloride is an effective and safe treatment protocol for premature ejaculation, a common sexual disorder.[14] The study out by Chandak and Verma[15] indicated that the matrix type transdermal patches of tramadol fabricated with different grades and altered ratios of hydroxypropyl methylcellulose (HPMC) embraced adequate potential for transdermal delivery owing to controlled release pattern of drug from the patches and on the aegis of their *in vitro* and pharmacokinetic results. Recent experimental studies have demonstrated that the transdermal patch containing HPMC as a polymer in higher concentrations caused an increased drug release.[16] This work focused on the development of an optimized sustained release transdermal patch of tramadol hydrochloride with suitable physicochemical properties and desired release kinetics.

MATERIALS AND METHODS

Tramadol hydrochloride was purchased from Emmennar Pharma Pvt. Ltd. (Visakhapatnam, India). Potassium dihydrogen orthophosphate, sodium hydroxide, triethyl citrate, HPMC E15, ethyl cellulose (EC), polyvinyl alcohol, potassium bromide, potassium chloride, polyethylene glycol (PEG) 400, *n*-octanol, calcium chloride (fused) were procured from Loba Chemie Pvt. Ltd. (Mumbai, India). HPMC E5 was provided by Colorcon Asia Pvt. Ltd. (Goa, India). Glycerol, propylene glycol, methanol was purchased from Merck Specialities Pvt. Ltd. (Mumbai, India). All these ingredients used were of analytical grade except *n*-octanol (high performance liquid chromatography grade) and potassium bromide [infrared (IR) spectroscopy grade].

Identification of drugs

Many monographic tests (Table 1) were employed as *per* IP[17] to identify tramadol hydrochloride, which was used as the drug candidate for designing the formulations.

Table 1. Specifications required for identification of drug[17]

Tests	Specification
Solubility	
In water	Freely soluble
In methanol	Freely soluble
In acetone	Very slightly soluble
Appearance of solution	
A 5.0% (w/v) solution of tramadol hydrochloride	Clear and colorless
Acidity	
0.2 mL of methyl red solution and 0.2 mL of 0.01 M hydrochloric acid were added to 10 mL of 5.0% (w/v) solution of tramadol hydrochloride	Solution will be red
A specified amount of 0.01 M sodium hydroxide was added to change the colour from red to yellow	Not more than 0.4 mL
Loss on drying	
1.0 g tramadol hydrochloride was dried in a hot air oven at 105°C for 3 h	Not more than 0.5%
Sulfated ash	Not more than 0.1%
Assay	
0.18 g of tramadol hydrochloride was dissolved in 25 mL of anhydrous acetic acid and 10 mL of acetic anhydride. Then, it was then titrated with 0.1 M perchloric acid. The end point was determined potentiometrically. A blank titration was carried out (1 mL of 0.1 M perchloric acid is equivalent to 0.02998 g of tramadol hydrochloride)	-

Compatibility of the drug with polymers

Compatibility between the drug and polymers was examined using fourier transform IR spectroscopy (FT-IR) spectrophotometer. The IR spectra were recorded under a wave range between 4000-400 cm^{-1}.[18,19]

Preparation of backing membrane

To prepare the backing membrane, 3 g of polyvinyl alcohol was dissolved in 100 mL of distilled water warmed at a temperature 40˚C. After filtering the solution, 2 mL filtrate was transferred to each glass mold. It was then placed in a tray dryer at 60˚C for 6 hours to get dried.[20]

Formulation of matrix type transdermal patches

A total 26 batches (F1-F26) of matrix type transdermal patches were fabricated using different ratios of HPMC and EC as a rate regulatory polymers (Table 2). PEG 400, glycerol, and triethyl citrate were used as plasticizers. Propylene glycol was added as an anti-crystalizing agent. The polymers and other excipients in different ratios (Table 2) were dissolved in methanol. Tramadol hydrochloride (50 mg) was added slowly to the polymeric solutions of individual batch and stirred on a magnetic stirrer until a uniform mixture was obtained. The mixture was then poured on the glass mold, which was covered with a glass funnel of appropriate size to govern evaporation

Table 2. Composition of matrix type transdermal patches (F1-F26)

Patches	Quantity/patch (mg)								
	Tramadol HCl	HPMC E5	HPMC E15	EC	PEG 400	Glycerol	Propylene glycol	Triethyl citrate	Total weight (mg)
F1	50	-	-	50	10	-	-	10	120
F2	50	-	-	100	10	-	-	10	170
F3	50	-	-	100	10	10	-	-	170
F4	50	-	-	100	20	10	-	-	180
F5	50	-	-	100	30	10	-	-	190
F6	50	-	-	100	20	20	-	-	190
F7	50	-	-	150	20	20	-	-	240
F8	50	-	-	200	20	20	-	-	290
F9	50	100	-	-	20	20	-	-	190
F10	50	150	-	-	20	20	-	-	240
F11	50	200	-	-	20	20	-	-	290
F12	50	100	-	100	20	20	-	-	290
F13	50	150	-	100	20	20	-	-	340
F14	50	200	-	100	20	20	-	-	390
F15	50	200	100	-	20	20	-	-	390
F16	50	200	200	-	20	20	-	-	490
F17	50	200	125	-	20	20	-	-	415
F18	50	200	125	-	20	20	10	-	425
F19	50	200	125	-	20	20	20	-	435
F20	50	200	125	-	20	20	15	-	430
F21	50	200	125	-	-	20	10	-	405
F22	50	200	125	-	-	30	10	-	415
F23	50	200	125	-	-	40	10	-	425
F24	50	200	125	-	-	50	10	-	435
F25	50	200	150	-	-	50	10	-	460
F26	50	250	190	-	-	50	10	-	550

HPMC: Hydroxypropyl methylcellulose, EC: Ethyl cellulose, PEG: Polyethylene glycol

rate of the solvent. The casting solvent was subsequently permitted to evaporate overnight at 40˚C for attaining the dried patches.[21] After drying, the patches were cut from the glass mold. Backing membrane was affixed with suitable adhesive and dried at the room temperature. The patches were then kept between sheets of wax paper and stored in desiccators for their evaluation followed by optimization.[22,23]

Evaluation of matrix type transdermal patches

Planned patches were evaluated for different physicochemical parameters such as thickness, drug content, moisture content, moisture uptake, flatness, tensile strength, water vapor transmission (WVT) rate, folding endurance, *etc*.[1,6,21]

Thickness

Thickness was measured using a digital screw gauge at five distinct portions of the patches from each batch and the mean value including standard deviation was calculated.[24]

Weight variation

Randomly selected ten patches from each batch were subjected to weight variation test. A specified area of the individual patch was cut into different parts and weighed. Average weight and standard deviation were calculated from the weights measured individually.[25]

Drug content

An accurately weighed (100 mg) section of transdermal patch was dissolved in 100 mL of phosphate buffer (pH 7.4) and the solution was then shaken continuously for 24 hours in a shaker incubator followed by sonication for about 15 min. After subsequent filtration and suitable dilution, the drug content in the solution was assessed using a ultraviolet (UV)-visible spectrophotometer at a wavelength of 275 nm.[25,26]

Moisture content

The patches from the individual batch were weighed individually and stored in a dessicator installed with activated *silica* at room temperature for 24 hours. The patches were then weighed repeatedly until a constant weight was found. Percentage moisture content was measured using the following formula.[25,27]

$$\text{Percentage moisture content} = \frac{\text{Initial weight - Final weight}}{\text{Final weight}} \times 100$$

Moisture uptake

A transdermal patch was weighed and placed in a dessicator containing a saturated solution of potassium chloride at room temperature for 24 hours. After the completion of the period, the patch was weighed repeatedly until a constant weight was found. Percentage moisture uptake was measured using the following formula.[25]

$$\text{Percentage moisture uptake} = \frac{\text{Final weight - Initial weight}}{\text{Initial weight}} \times 100$$

Flatness

A flatness test was performed to confirm that the developed patches retain a smooth surface and will not constrict with time. One longitudinal strip was cut from the center and two from either end of the patches which were individually measured. The variation in length caused by non-uniformity in flatness was checked by determining the percent constriction. Zero percent constriction is considered as equivalent to 100 percent flatness. Percentage constriction was calculated using the following formula.[25,26]

$$\text{Percentage constriction} = \frac{\text{Initial length of strip - Final length of strip}}{\text{Initial length of strips}} \times 100$$

Folding endurance

Folding endurance of the patches was estimated by repeatedly folding a small section of the patch (2×2 cm) at the same place until it cracked. The number of times through which the patch could be folded at the same place without producing any crack line presented the folding endurance value. Three patches from each batch were considered for performing the test.[28]

Tensile strength

Transdermal patches were cut into 1 cm^2 size and placed between two clamps of the tensilometer. Weight was gradually added so that the increasing pulling force could break the film. The force needed to break the patch was recognized as tensile strength expressed in the unit kg/cm^2.[25]

Water vapor transmission rate

The quantity of moisture transmitted through unit area of patch in unit time is expressed as the WVT rate. Glass vials of equal diameter and volume were used as transmission cells, which were washed thoroughly. After drying the vials in a hot air oven, about 1 g of anhydrous fused calcium chloride was taken in each vial, and the patch was affixed over the edge of the vial using a suitable sticking plaster. The weight of the vial was noted and kept in a desiccator comprising a saturated solution of potassium chloride for maintaining 84% relative humidity. These cells were removed from the desiccators after 24 hours and re-weighed. The water vapor transmission rate was determined as follows:[28]

$$\text{WVT rate} = \frac{\text{Weight of water vapor transmitted x Thickness of patch}}{\text{Surface area exposed in square meters}}$$

In vitro permeation studies

Modified Franz diffusion cell was employed to conduct *in vitro* permeation studies. Mixed cellulose ester membrane was used as a dialysis (barrier) membrane which was previously soaked in distilled water for 24 hours. The transdermal patches were adhered to the dialysis membrane and the membrane was tied firmly to the donor compartment of the diffusion cell. The receptor compartment of the diffusion cell was filled with 85 mL of phosphate buffer (pH 7.4). The donor compartment

was lowered to the receptor compartment in such a way that the dialysis membrane only touched the media of the receptor compartment. This assembly was constructed on a magnetic stirrer with a heater. Temperature of the receptor compartment was maintained at 37 ± 2°C. The content of the diffusion cell was continuously stirred using a teflon-coated bead at a constant speed of 600 rpm. Samples were taken at specified intervals of time and the same amount of phosphate buffer (pH 7.4) was added to maintain the sink condition. After suitable dilution, the samples were examined for percent drug content using UV-visible spectrophotometer at a wavelength of 275 nm.[21] *In vitro* permeation study was conducted for 6 hours.[29,30]

Ex vivo skin permeation studies

In *ex vivo* skin permeation studies, goat skin was used as a dialysis (barrier) membrane which was obtained from a local slaughterhouse. The skin was thoroughly cleaned with running tap water followed by eliminating full thickness and non-dermatome skin using a scalpel.[31] It was then soaked in an isotonic solution for 30 min. *Ex vivo* permeation study was conducted for 12 hours. Procedure mentioned for *in vitro* permeation studies was followed for performing these studies.[32]

Drug release kinetics study

Data obtained from *in vitro* and *ex vivo* permeation studies were fitted to different mathematical models such as zero order, first order, and Higuchi release kinetics to define the kinetics and pattern of drug release.[33] Statistical analysis was not used in this study.

RESULTS AND DISCUSSION

Identification of drugs

Several monographic tests were performed (Table 3) to check the identity of tramadol hydrochloride. Obtained results matched satisfactorily with their corresponding specification required.[17] Hence, monographic tests confirmed the identity of tramadol hydrochloride.

Fourier transform infrared spectroscopy

The drug and polymeric materials were found to be physically compatible with each other. The characteristic absorption peak obtained from FT-IR spectra of tramadol hydrochloride (Figure 1) resembled almost the same with the spectra of standard sample of that. It was evidently manifest that the individual characteristics bands of tramadol hydrochloride (Figure 1), and the polymers HPMC E5 (Figure 2), HPMC E15 (Figure 3), EC (Figure 4) at the particular wavenumbers were also present in the FT-IR spectra analyzed for the physical mixtures of the drug along with these polymers (Figure 5, Table 4). Interpretation from the FT-IR studies directed that the drug was pure and chemically compatible with the polymers used. HPMC, as a hydrophilic polymer and EC, as a water insoluble polymer were used in the formulations.

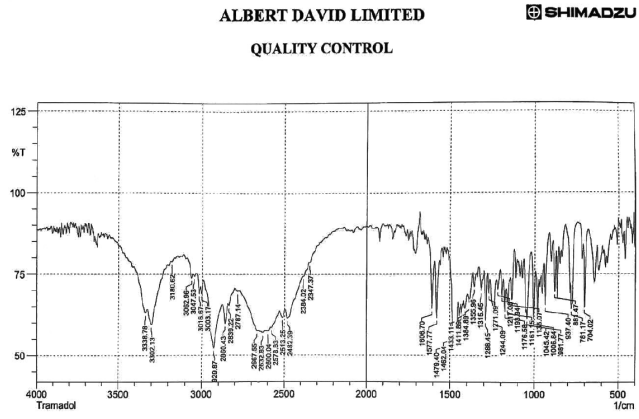

Figure 1. FT-IR spectra of tramadol hydrochloride
FT-IR: Fourier transform infrared spectroscopy

Table 3. Identification of drug by performing several monographic tests

Tests	Obtained result
Solubility	
In water	Freely soluble
In methanol	Freely soluble
In acetone	Very slightly soluble
Appearance of solution	
A 5.0% (w/v) solution of tramadol hydrochloride	Clear and colorless
Acidity	
0.2 mL of methyl red solution and 0.2 mL of 0.01 M hydrochloric acid were added to 10 mL of 5.0% (w/v) solution of tramadol hydrochloride	Red color solution was formed
A specified amount of 0.01 M sodium hydroxide is added to change the colour from red to yellow	A yellow color appeared after adding 0.3 mL
Loss on drying	
1.0 g Tramadol hydrochloride was dried in a hot air oven at 105°C for 3 h	0.3%
Sulfated ash	0.087%
Assay	
0.18 g of tramadol hydrochloride was dissolved in 25 mL of anhydrous acetic acid and 10 mL of acetic anhydride. Then, it was titrated with 0.1 M perchloric acid. The end point is determined potentiometrically. A blank titration was then carried out (1 mL of 0.1 M perchloric acid is equivalent to 0.02998 g of tramadol hydrochloride)	98.13%

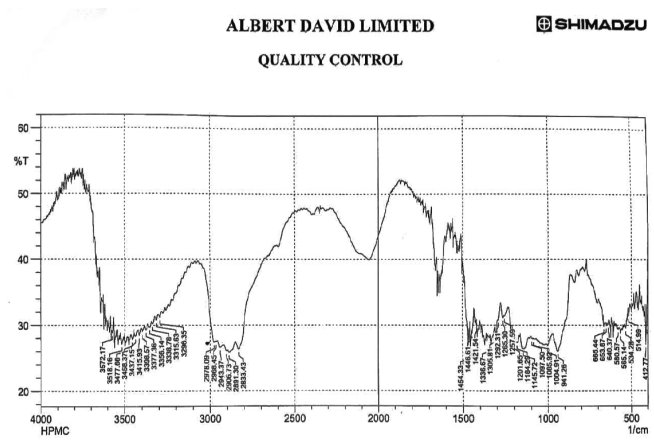

Figure 2. FT-IR spectra of HPMC E5

HPMC: Hydroxypropyl methylcellulose, FT-IR: Fourier transform infrared spectroscopy

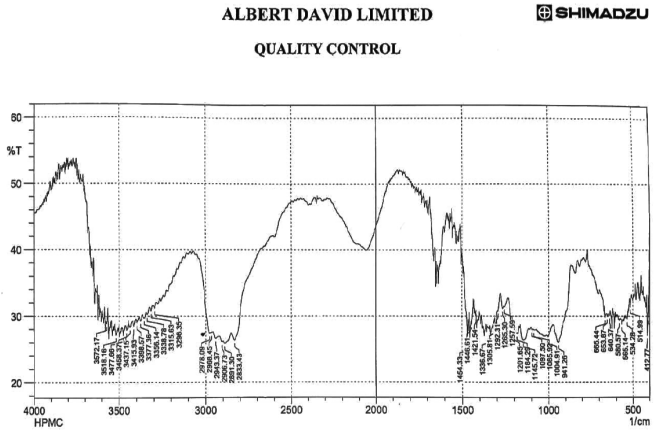

Figure 3. FT-IR spectra of HPMC E15

HPMC: Hydroxypropyl methylcellulose, FT-IR: Fourier transform infrared spectroscopy

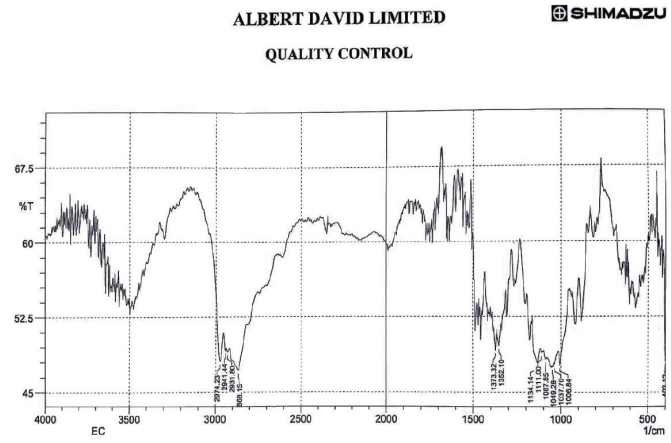

Figure 4. FT-IR spectra of EC

FT-IR: Fourier transform infrared spectroscopy, EC: Ethyl cellulose

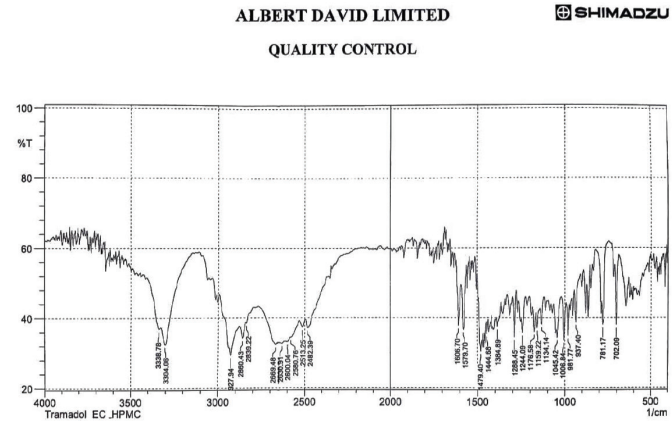

Figure 5. FT-IR spectra of tramadol hydrochloride along with polymers used

FT-IR: Fourier transform infrared spectroscopy

Table 4. Interpretation of FT-IR spectrum

Wave number of tramadol hydrochloride (cm^{-1})	Wave number of HPMC E5 (cm^{-1})	Wave number of HPMC E15 (cm^{-1})	Wave number of EC (cm^{-1})	Wave number of drugs along with polymers (cm^{-1})	Interpretation
3047.53	3077.60	3079.41	3080.51	3081.61	C-H stretching (aromatic)
1577.77	1575.03	1578.36	1579.76	1579.70	C-C stretching
1479.40	1478.10	1479.08	1479.38	1479.40	$-CH_3$ bending
2839.22	2833.43	2833.91	2838.82	2839.22	C-H stretching
1741.31	1740.22	1741.32	1741.02	1741.52	C=O stretching
1240.51	1241.02	1240.43	1241.53	1240.58	C-O stretching

FT-IR: Fourier transform infrared spectroscopy, HPMC: Hydroxypropyl methylcellulose, EC: Ethyl cellulose

Evaluation of matrix type transdermal patches

Based on the observations found from the physical appearance of all batches (F1-F26) of transdermal patches (Table 5), only eleven batches were nominated for evaluation.

Physicochemical parameters

Thickness of the patches ranged from 0.47 to 0.57 mm (±0.003 to ±0.007) while the average weight of the patches varied from 289.89 to 558.16 mg (±0.40 to ±0.48) (Table 6). These minimum SD values assured that the method of preparation was skilled to develop patches with least intrabatch variability. Satisfactory

percentage of drug content with minimum SD value (Table 6) was found throughout all patches. Table 6 displays that increased amounts of HPMC caused an increase in the percentage of moisture content and moisture uptake of the transdermal patches due to hydrophilic properties of HPMC. Patel et al.[23] reported that a higher percentage of HPMCs results in a higher moisture content. However, lower percentage of moisture content of the batches was capable of prevent the patches from microbial contamination and retarding their bulkiness. Flatness of the transdermal patches shown in Table 6 indicated a minimum level constriction just close to zero percent.[1] Folding endurance value was found to be greater than 200 in all batches with minimum SD value (±0.51 to ±0.58) (Table 7) which proved that the prepared transdermal patches were flexible enough, able to withstand mechanical pressure and proficient to retain the integrity with skin folding after its application. From Tables 6 and 7, it was reported that decreasing in the thickness of the patches accomplished a higher folding endurance value. The patches containing higher amounts of HPMC showed greater tensile strength, whereas an increasing amount of EC lowered the strength. Limpongsa and Umprayn[34] also reported that the addition of EC resulted in the lower tensile strength. Due to the hydrophilic properties of HPMC, the films containing a higher proportion of HPMC showed greater WVT rate and addition of EC lowered it.

In vitro and ex vitro permeation studies

Because of their long-term release pattern, only F14, F18, F23, and F26 batches were selected (Table 8) for *ex vivo* skin permeation and kinetics study. The results obtained from *in vitro* permeation studies showed controlled drug release as the concentration of EC decreased. The formulation F26 containing the higher amounts of HPMC E5, HPMC E15 as polymers

Table 5. Physical appearance of the planned transdermal patches (F1-F26)

Formulation code	Observation	Remarks
F1	Patch was not formed	Rejected
F2	Patch was formed, but became brittle on drying	Rejected
F3	Patch was brittle; crystallization occurred on drying	Rejected
F4	Patch was not formed	Rejected
F5	Showed crystallization and enhanced brittleness	Rejected
F6	Crystallization has occurred	Rejected
F7	Patch was formed firmly	Selected
F8	Patch was formed firmly	Selected
F9	Patch was not formed	Rejected
F10	Patch was formed, but crystallization occurred	Rejected
F11	Better than F10, crystallization occurred in negligible amounts	Selected
F12	Better than F10, crystallization occurred in negligible amounts	Selected
F13	Patch was not formed	Rejected
F14	Better than F11 and F12	Selected
F15	Patch was formed firmly	Selected
F16	Patch was formed, but enhanced crystallization was found	Rejected
F17	Patch was formed, but slightly brittle	Rejected
F18	Patch was formed firmly	Selected
F19	Patch was sticky	Rejected
F20	Patch was sticky	Rejected
F21	Patch was more brittle than F17	Rejected
F22	Patch was more brittle than F17	Rejected
F23	Patch was formed firmly	Selected
F24	Patch was formed firmly	Selected
F25	Better patch from all respects	Selected
F26	Better patch from all respects	Selected

Table 6. Evaluation of physicochemical parameters of the selected transdermal patches

Formulation code	Thickness[a] (mm) ± SD	Weight variation[b] (mg) ± SD	Drug content[a] (%) ± SD	Moisture content[b] (%) ± SD	Moisture uptake[b] (%) ± SD
F7	0.49 ± 0.006	289.89 ± 0.41	99.23 ± 0.79	1.19 ± 0.07	2.29 ± 0.07
F8	0.57 ± 0.003	299.42 ± 0.41	99.33 ± 0.61	1.18 ± 0.05	2.28 ± 0.05
F11	0.51 ± 0.004	299.91 ± 0.48	98.93 ± 0.77	1.29 ± 0.07	4.42 ± 0.03
F12	0.51 ± 0.006	300.18 ± 0.40	99.13 ± 0.65	1.22 ± 0.07	4.34 ± 0.03
F14	0.48 ± 0.006	398.77 ± 0.41	98.91 ± 0.78	1.81 ± 0.06	4.94 ± 0.03
F15	0.55 ± 0.005	399.60 ± 0.43	99.09 ± 0.84	2.19 ± 0.04	6.76 ± 0.03
F18	0.50 ± 0.003	434.47 ± 0.47	99.27 ± 0.81	2.56 ± 0.09	6.94 ± 0.03
F23	0.56 ± 0.007	434.50 ± 0.43	99.40 ± 0.72	2.59 ± 0.05	6.97 ± 0.01
F24	0.51 ± 0.006	443.53 ± 0.46	98.96 ± 0.76	2.58 ± 0.06	6.98 ± 0.02
F25	0.53 ± 0.007	468.28 ± 0.47	99.02 ± 0.82	3.08 ± 0.06	7.81 ± 0.08
F26	0.47 ± 0.004	558.16 ± 0.42	99.41 ± 0.60	3.52 ± 0.04	9.94 ± 0.03

All values are expressed as mean SD, [a]n: 10, [b]n: 5, SD: Standard deviation

Table 7. Evaluation of physicochemical parameters of selected transdermal patches

Formulation code	Flatness[a] (%) ± SD	Folding endurance[b] ± SD	Tensile strength[a] (kg/cm^2) ± SD	WVT studies[b] (g/m^2/24 h) ± SD
F7	99.87 ± 0.002	202 ± 0.54	0.51 ± 0.03	1.84 ± 0.02
F8	99.88 ± 0.004	200 ± 0.55	0.46 ± 0.05	1.81 ± 0.01
F11	100.03 ± 0.004	201 ± 0.52	0.63 ± 0.08	1.93 ± 0.05
F12	99.91 ± 0.001	200 ± 0.58	0.52 ± 0.02	1.85 ± 0.07
F14	99.97 ± 0.003	205 ± 0.52	0.57 ± 0.03	1.91 ± 0.04
F15	100.07 ± 0.002	200 ± 0.56	0.68 ± 0.01	2.21 ± 0.08
F18	99.93 ± 0.001	201 ± 0.55	0.70 ± 0.05	2.29 ± 0.07
F23	99.89 ± 0.004	200 ± 0.57	0.69 ± 0.04	2.33 ± 0.08
F24	99.96 ± 0.002	200 ± 0.51	0.69 ± 0.03	2.31 ± 0.05
F25	100.00 ± 0.003	200 ± 0.57	0.73 ± 0.06	2.73 ± 0.04
F26	100.01 ± 0.001	207 ± 0.58	0.87 ± 0.08	3.12 ± 0.08

All values are expressed as mean SD, [a]n: 10, [b]n: 5, SD: Standard deviation, WVT: Water vapor transmission

Table 8. *In vitro* permeation study of matrix type transdermal patches

Time (min)	Percentage cumulative drug release										
	F7	F8	F11	F12	F14	F15	F18	F23	F24	F25	F26
0	0	0	0	0	0	0	0	0	0	0	0
30	49.51	26.74	49.76	31.46	27.22	36.62	29.68	34.57	40.21	32.36	21.46
60	85.43	41.87	91.48	68.63	38.64	51.62	40.12	42.55	48.19	45.62	30.26
120	98.52	69.49	90.13	88.67	52.58	68.32	54.54	61.31	66.95	62.74	42.10
240	97.78	86.31	-	87.31	69.83	87.82	72.46	80.35	83.56	85.12	60.28
360	-	93.78	-	-	78.24	101.87	83.22	88.77	94.41	99.63	71.96

showed a rate regulatory drug-release pattern compared to the other formulations. As a plasticizer, effect of glycerol was most satisfactory with increased concentration of HPMC in the formulation F26, which showed the controlled *in vitro* drug release.

The effect of polymers and plasticizers on the results of *ex vivo* permeation studies was the same as the ingredients that influenced the results of *in vitro* permeation studies. Percentage cumulative drug release from the formulations was found to be more than 60% after 12 hours (Table 9), which was considered satisfactory. *In vitro* (Table 8) and *ex vivo* drug release profiles (Table 9) of the mentioned batches were fitted into different kinetic models (Figures 6 and 7). The data obtained from Table 10 explained that the selected batches except F23 were best fitted to Higuchi release kinetics for *in vitro* permeation studies. The rate of permeation of the drug through goat skin was slower and in a sustained manner compared to *in vitro* release profile. This could be explained by comparing the thickness of the goat skin membrane with that of dialysis membrane used. However, the data obtained from Table 11 clarified that the selected batches were best fitted to Higuchi release kinetics for *ex vivo* permeation studies.

Table 9. *Ex vivo* permeation study of matrix type transdermal patches

Time (min)	Percentage cumulative drug release			
	F14	F18	F23	F26
0	0	0	0	0
30	11.15	15.87	19.67	12.78
60	20.88	24.83	28.56	18.42
120	34.82	35.78	45.71	29.25
240	52.07	52.776	58.51	42.17
360	60.48	63.98	69.87	50.11
480	68.61	72.66	80.78	57.26
720	71.98	75.87	83.71	65.51

Table 10. Values of correlation coefficient of different kinetics models for *in vitro* permeation study

Release kinetics	Correlation coefficients (R^2)			
	F14	F18	F23	F26
Zero order	0.840	0.849	0.827	0.905
First order	0.964	0.980	0.984	0.983
Higuchi	0.986	0.990	0.981	0.999

Table 11. Values of the correlation coefficient of different kinetics model for *ex vivo* permeation study

Release kinetics	Correlation coefficients (R^2)			
	F14	F18	F23	F26
Zero order	0.837	0.845	0.825	0.887
First order	0.924	0.937	0.947	0.961
Higuchi	0.969	0.978	0.973	0.993

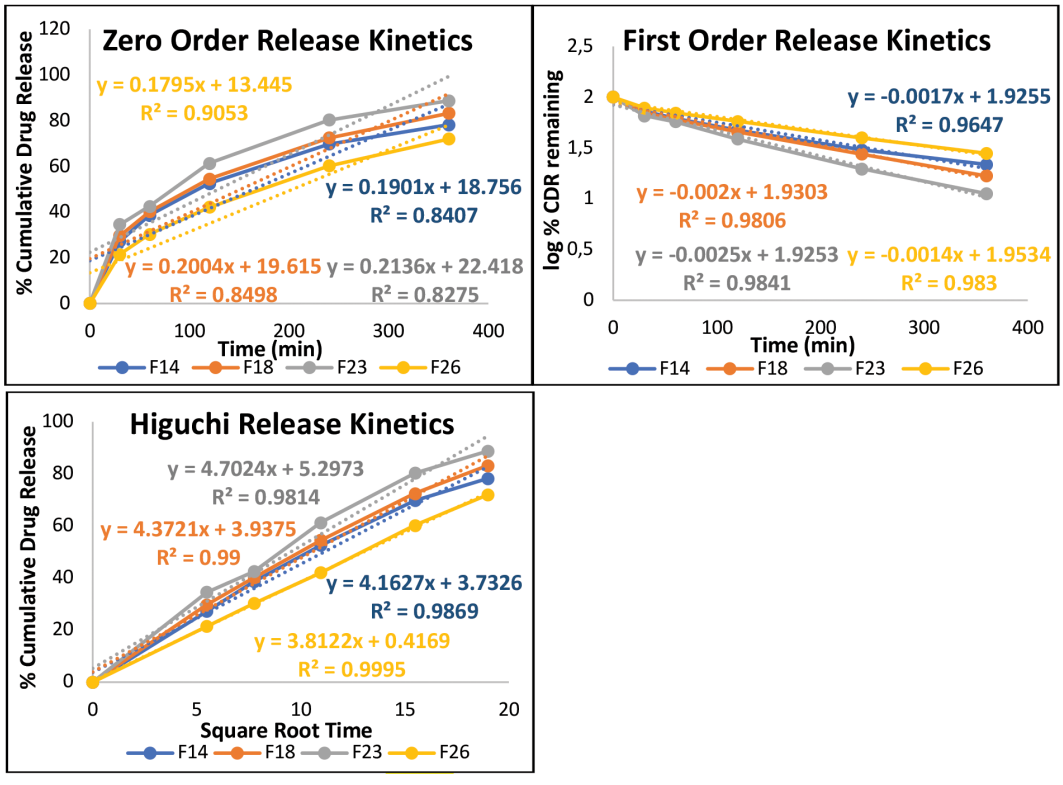

Figure 6. Fitting the data obtained from *in vitro* permeation study to a different kinetics model

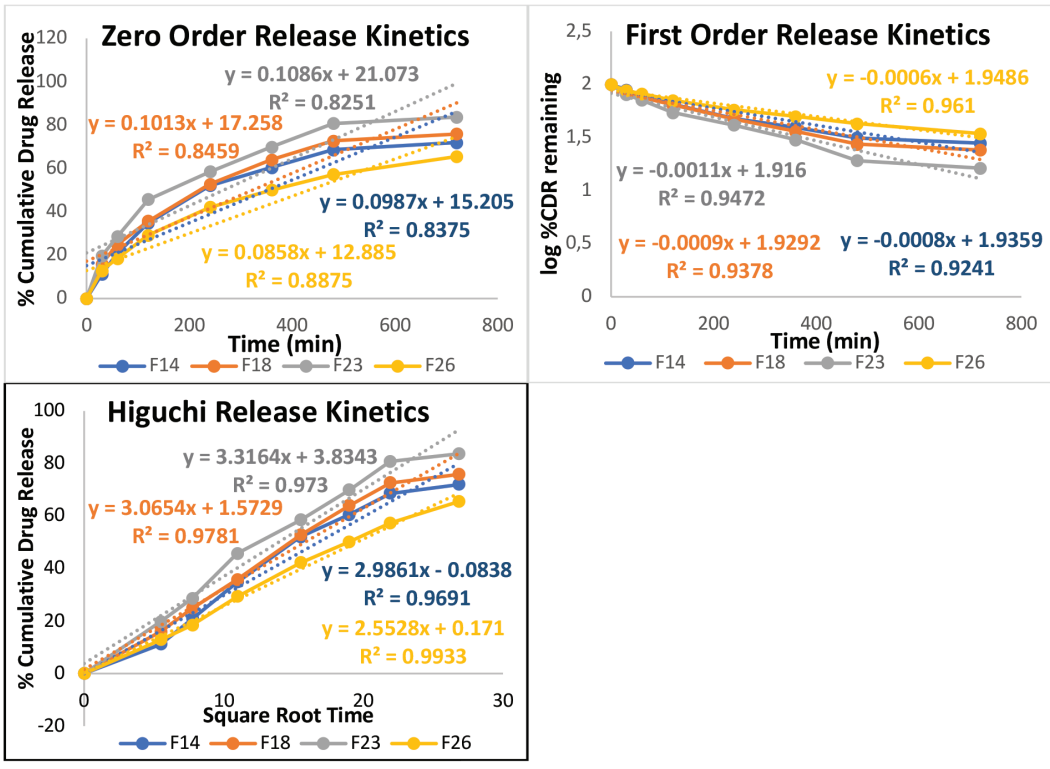

Figure 7. Fitting the data obtained from *ex vivo* permeation study to a different kinetics model

Depending upon the results obtained from physicochemical evaluations performed and particularly based on the sustained release profile, F26 was designated as the optimized formulation. For this formulation, the best kinetics model was the Higuchi equation, whereas the plots exposed great linearity with highest R^2 values (Figures 6 and 7), suggesting the process of diffusion. Hence, it was confirmed that the formulation was capable of exhibiting matrix type drug delivery.

CONCLUSION

To achieve better bioavailability and improved patient compliance, optimized matrix type novel transdermal patches containing tramadol hydrochloride were developed with higher amounts of HPMC as rate regulating polymer. As *per ex vivo* drug release, the concern was that the optimized formulation permeated only 65.51% drug through goat skin within 12 hours (Table 9). This indicated a window for using a permeation enhancer in the formulation to improve the drug permeation rate through the goat skin. However, further *ex vivo* permeation studies must be conducted to determine the suitable permeation enhancer.

ACKNOWLEDGEMENTS

The authors acknowledge their gratitude to the management of Albert David Limited, Kolkata, West Bengal, for providing their R&D laboratory facility to conduct the necessary research work. Authors would also like to thank Mr. Souvik Ghatak, Senior Chemist, R&D Department, Albert David Limited, Kolkata for his esteemed guidance to complete this research work.

Ethics

Ethics Committee Approval: Not applicable.

Informed Consent: Not applicable.

Peer-review: Externally peer-reviewed.

Authorship Contributions

Surgical and Medical Practices: S.M., Concept: S.M., Design: S.N., S.M., Data Collection or Processing: S.N., S.M., Analysis or Interpretation: S.N., S.M., Literature Search: S.N., Writing: S.N.

Conflict of Interest: No conflict of interest was declared by the authors.

Financial Disclosure: The authors declared that this study received no financial support.

REFERENCES

1. Tanwar H, Sachdeva R. Transdermal drug delivery system: a review. Int J Pharm Sci Res. 2016;7:2274-2290.
2. Rani S, Saroha K, Syan N, Mathur P. Transdermal patches a successful tool in transdermal drug delivery system: an overview. Der Pharmacia Sinica. 2011;2:17-29.
3. Zaman M, Khalid U, Raja MAG, Siddique W, Sultana K, Amjad MW, Ur Rehman A, Khan MA. Fabrication and characterization of matrix type transdermal patches loaded with ramipril and repaglinide *via* cellulose based hydrophilic and hydrophobic polymers: *in-vitro* and *ex-vivo* permeation studies. Polymer-Plastics Technology and Engineering. 2017;56:1713-1722.
4. Alexander A, Dwivedi S, Ajazuddin, Giri TK, Saraf S, Saraf S, Tripathi DK. Approaches for breaking the barriers of drug permeation through transdermal drug delivery. J Control Release. 2012;164:26-40.

5. Thomas BJ, Finnin BC. The transdermal revolution. Drug Discov Today. 2004;9:697-703.
6. Nair RS, Ling TN, Shukkoor MSA, Manickam B. Matrix type transdermal patches of captopril: *ex vivo* permeation studies through excised rat skin. J Pharm Res. 2013;6:774-779.
7. Suksaeree J, Thuengernthong A, Pongpichayasiri K, Maneewattanapinyo P, Settharaksa S, Pichayakorn W. Formulation and evaluation of matrix type transdermal patch containing silver nanoparticles. J Polym Environ. 2018;26:4369-4375.
8. Pichayakorn W, Suksaeree J, Boonme P, Amnuaikit T, Taweepreda W, Ritthidej GC. Deproteinized natural rubber latex/hydroxypropylmethyl cellulose blending polymers for nicotine matrix films. Ind Eng Chem Res. 2012;51:8442-8452.
9. Wokovich AM, Prodduturi S, Doub WH, Hussain AS, Buhse LF. Transdermal drug delivery system (TDDS) adhesion as a critical safety, efficacy and quality attribute. Eur J Pharm Biopharm. 2006;64:1-8.
10. Sugibayashi K, Morimoto Y. Polymers for transdermal drug delivery systems. J Control Release. 1994;29:177-185.
11. Valenta C, Auner BG. The use of polymers for dermal and transdermal delivery. Eur J Pharm Biopharm. 2004;58:279-289.
12. Subedi M, Bajaj S, Kumar MS, Yc M. An overview of tramadol and its usage in pain management and future perspective. Biomed Pharmacother. 2019;111:443-451.
13. Dhillon S. Tramadol/paracetamol fixed-dose combination: a review of its use in the management of moderate to severe pain. Clin Drug Investig. 2010;30:711-738. Erratum in: Clin Drug Investig. 2010;30:866.
14. Eassa BI, El-Shazly MA. Safety and efficacy of tramadol hydrochloride on treatment of premature ejaculation. Asian J Androl. 2013;15:138-142.
15. Chandak AR, Verma PRP. Development and evaluation of HPMC based matrices for transdermal patches of tramadol. Clin Res Regul Aff. 2008;25:13-30.
16. Garala KC, Garala RJ, More HN, Shinde AJ. Effect of cross-linking agent on the release of drug from the transdermal matrix patches of tramadol hydrochloride. Res J Pharm and Tech. 2008;1:187-192.
17. Government of India, Ministry of Health & Family Welfare. Indian Pharmacopoeia. The Indian Pharmacopoeia Commission, Ghaziabad. 6th ed. 2010. Ghaziabad, India.
18. Amrutkar JR, Gattani SG. Chitosan-chondroitin sulfate based matrix tablets for colon specific delivery of indomethacin. AAPS PharmSciTech. 2009;10:670-677.
19. Biswas GR, Chakraborty S, Das U, Majee SB. Insight into the release kinetics of amoxicillin trihydrate from buccoadhesive tablets with a natural gum. Res J Pharm Biol Chem. 2014;5:772-785.
20. Asija R. Gupta A, Maheshwari BS. Formulation and evaluation of transdermal patches of torasemide. Int J Adv Sci. 2015;1:38-44.
21. Shinde AJ, Garala KC, More HN. Development and characterization of transdermal therapeutics system of tramadol hydrochloride. Asian J Pharm Sci. 2008;2:265-269.
22. Wahid A, Sridhar BK, Shivakumar S. Preparation and evaluation of transdermal drug delivery system of etoricoxib using modified chitosan. Indian J Pharm Sci. 2008;70:455-460.
23. Patel MN, Bharadia PD, Patel MM. Formulation & evaluation of matrix type transdermal patches based on composite polymers. Int J Pharm Res. 2012;4:53-58.
24. Palanisamy P, Jaykar B, Venkateswarlu BS, Chandira RM, Suriyan D. A review on transdermal drug delivery system. Indian J Nat Sci. 2020;10:27035-27056.
25. Sachan R, Bajpai M. Transdermal drug delivery system: a review. Int J Res Dev Pharm Life Sci. 2013;3:748-765.
26. Parivesh S, Sumeet D, Abhishek D. Design, evaluation, parameters and marketed products of transdermal patches: a review. J Pharma Res. 2010;3:235-240.
27. Gannu R, Vishnu YV, Kishan V, Rao YM. Development of nitrendipine transdermal patches: *in vitro* and *ex vivo* characterization. Curr Drug Deliv. 2007;4:69-76.
28. Singh A, Bali A. Formulation and characterization of transdermal patches for controlled delivery of duloxetine hydrochloride. J Anal Sci Technol. 2016;7:25.
29. Ng SF, Rouse JJ, Sanderson FD, Meidan V, Eccleston GM. Validation of a static Franz diffusion cell system for *in vitro* permeation studies. AAPS PharmSciTech. 2010;11:1432-1441.
30. Salamanca CH, Barrera-Ocampo A, Lasso JC, Camacho N, Yarce CJ. Franz Diffusion cell approach for pre-formulation characterisation of ketoprofen semi-solid dosage forms. Pharmaceutics. 2018;10:148.
31. Gupta V, Trivedi P. *Ex vivo* localization and permeation of cisplatin from novel topical formulations through excised pig, goat, and mice skin and *in vitro* characterization for effective management of skin-cited malignancies. Artif Cells Nanomed Biotechnol. 2015;43:373-382.
32. Marwah H, Garg T, Rath G, Goyal AK. Development of transferosomal gel for trans-dermal delivery of insulin using iodine complex. Drug Deliv. 2016;23:1636-1644.
33. Nandi S, Deb P, Banerjee J, Reza KH. Formulation and evaluation of enteric coated elementary osmotic pump (ECEOP) tablets of diclofenac sodium. Int J Pharm Sci Res. 2020;11:5703-5711.
34. Limpongsa E, Umprayn K. Preparation and evaluation of diltiazem hydrochloride diffusion-controlled transdermal delivery system. AAPS PharmSciTech. 2008;9:464-470.

Turk J Pharm Sci 2022;19(5):583-588
DOI: 10.4274/tjps.galenos.2021.09216

ORIGINAL ARTICLE

Analgesic and Sedative-Hypnotic Potentiality of Crude Methanolic Extract of *Gomphandra tetrandra* (Wall.) Sleumer Leaves

N. M. Mahmudul Alam BHUIYA[1], Md. Forman HOSSEN[1], Md. Monirul ISLAM[2], Moynul HASAN[1]*

[1]Jagannath University, Department of Pharmacy, Dhaka, Bangladesh
[2]Northern University Bangladesh, Department of Pharmacy, Dhaka, Bangladesh

ABSTRACT

Objectives: *Gomphandra tetrandra* (Wall.) Sleumer (leaves) belonging to the family Stemonuraceae was investigated for preliminary phytochemical screening and evaluating their pharmacological activities in various pharmacological models.

Materials and Methods: The crude methanolic extract was screened with different chemical reagents for the qualitative detection of different phytochemical groups. The peripheral analgesic function was determined using the acetic acid-induced writhing procedure and sedative-hypnotic behaviors were assessed using hole-board, open field, and hole-cross tests using different doses of the extract (200 mg/kg and 400 mg/kg body weight).

Results: Phytochemical screening revealed that methanolic extract of *G. tetranda* leaves contains steroids, gums, mucilages, phytosterols, carbohydrates, and flavonoids. The crude methanolic extract at 200 mg/kg and 400 mg/kg doses showed statistically significant activity in acetic acid-induced writhing inhibition test with 60% ($p<0.01$) and 76.47% ($p<0.01$) inhibition, respectively, compared to control. The extract also had dose-dependent substantial ($p<0.01$) sedative-hypnotic activities compared with diazepam in the hole-board, open field, and hole-cross tests.

Conclusion: It may be assumed that the methanolic leaf extract of *G. tetrandra* possesses a strong possibility of having analgesic and sedative-hypnotic activity due to the presence of bioactive compounds in its leaves. Moreover, observed results have opened a new era of in-depth research to discover the possible mechanism of analgesic and sedative-hypnotic activity.

Key words: *Gomphandra tetrandra*, methanolic extract, analgesics, sedative-hypnotic activity

INTRODUCTION

The use of plants in all major systems of medicine, regardless of the underlying philosophical premise, illustrates their universal function in treating diseases.[1] Plant species are being depleted at a rapid rate; they cannot be botanically registered or chemically & pharmacologically studied. Thus, it is essential to create an increased effort toward conserving gene pools.[2]

Natural sources are credited for the excellent revolution in modern medicine, and since the beginning, medicinal plants have played a crucial role in the field of drug discovery. Bangladesh is a well-known source of medicinal plants.[3] Today, several medicines, such as morphine from *Papaver somniferum* L. and atropine from *Atropa belladonna* L., are extracted from medicinal plants.[4,5] Secondary metabolites (potential drug sources) are present in significant amounts in medicinal plants. Medicinal plants are in high demand in both developing and developed countries because of these factors.[6] In Bangladesh's rural and tribal communities, medicinal plants play a vital role in the socio-cultural, spiritual, and therapeutic spheres.

A survey conducted by the World Health Organization (WHO) in 1993 depicts that traditional practitioners treat about 80% of patients in India, 85% in Burma, and 90% in Bangladesh. The use of plants for medicinal purposes dates back to 4000-5000 B.C., and the Chinese were the first to use natural herbal preparations as medicines. Also, about 25% of all modern pharmacopeial drugs are plant-derived and many other

*Correspondence: moynul_47@yahoo.com, Phone: +8801730593893, ORCID-ID: orcid.org/0000-0002-1488-3516
Received: 24.04.2021, Accepted: 08.11.2021

synthetic analogs based on prototype compounds isolated from plants.[7]

Gomphandra tetrandra (Wall.) Sleumer is a herbaceous plant species found in the forest, which belongs to the family Stemonuraceae (formerly Icacinaceae). This family has had a popular medicinal history for a long time in many countries globally, especially in the evergreen forest, tropical, and subtropical regions.[8,9] Various pharmacological investigations have already been conducted on different plants of this family. For example, *Mappianthus iodoides* Hand.-Mazz. is used to treat hepatitis, jaundice, rheumatalgia, and arthralgia.[10] Other studies revealed the hepatoprotective and hypoglycemic activity of *Lasianthera africana* P.Beauv. (Icacinacaeae/Stemonuraceae) in animal models.[11,12] *L. africana* leaves also showed potent *in vitro* antioxidant activity in DPPH free radical scavenging test.[13] In this study, we tried to explore the analgesic and neuropharmacological potential of the methanolic leaf extracts of *G. tetrandra*.

MATERIALS AND METHODS

Collection of the plant

G. tetrandra was collected from the Moulvibazar District, Bangladesh, for this study. One of the professional taxonomists at the Bangladesh National Herbarium, Mirpur, Dhaka, Bangladesh, identified the plant, and a voucher was deposited there for future reference with the plant identification number 51332. The desired plant parts (leaves) were separated from unwanted materials, plants or plant parts. Then, they were then allowed to dry for a week under light. Using a suitable grinder, the sun-dried leaves were converted into coarse powder. An airtight container was used to store the coarse powder. The container was kept in a cool, dark, and dry place till analysis was initiated.

Preparation of G. tetrandra leaf extracts

Approximately 400 g of powdered plant material was soaked in 2100 mL of 80% methanol in a clean, flat-bottomed glass vessel. The glass vessel was properly sealed and stored for seven days with periodic shaking and stirring. After that, the mixture was filtered twice, using a piece of clean cotton material and a cotton plug. The filtrate was evaporated until absolutely dry using a ceiling fan and a water bath. It produced a sticky material with a reddish-black color that was identified as crude methanol extract.

Chemicals and solvents

Different chemicals and solvents of analytical grade were used in this study, including methanol and acetic acid. They were purchased from a local supplier and were used directly. Eskayef Pharmaceuticals Ltd. (Bangladesh) and Orion Infusion Limited, Tejgaon (Dhaka, Bangladesh) supplied diclofenac sodium and 0.9% NaCl solution, respectively. Incepta Pharmaceuticals Ltd. provided the diazepam, which was used as standard in neuropharmacological activity tests.

Phytochemical screening of methanol extracts of G. tetrandra leaf

The primary phytochemical studies include testing of various chemical groups present in the extract. Different chemical tests were accomplished to ensure the presence of carbohydrates (using Molisch reagent), tannins (using bromine water), alkaloids (using Wagner's reagent), saponins (foam formation by olive oil), flavonoids (using NaOH), phenols (using $FeCl_3$ solution), anthraquinone glycosides, cardiac glycosides, proteins, and gums & mucilage (swelling properties).[14]

Test animals

Swiss-albino mice were obtained from the Jahangirnagar University's animal house, which were of both sexes, 4-5 weeks old and 20-30 g weight. They were held in a controlled environment and served ICDDR, B developed rodent food as well as water (*ad libitum*). During the experiments, the mice were chosen randomly and irrespective of sex and divided into different groups following the standard procedures.[15] Since these mice are susceptible to habitat changes, they are held in the experimental condition for at least 3-4 days before the test. This study strictly adheres to globally recognized principles for standard use of experimental animal models developed by the International Council for Laboratory Animal Science and National Institutes of Health[16,17] and finally approved by the Local Ethics Committee (ref. no: DoP/RC/EC/2020/06/02).

Evaluation of analgesic activity by acetic acid-induced writhing test

The writhing test is an experimental procedure for inducing peripheral pain in mice by administering irritants such as acetic acid. The test compound's analgesic efficacy is determined by a reduction in the number of writings.[18] Twenty Swiss albino mice (weighing 20-30 g) were randomly taken and divided into four groups, each with five mice. Group I mice were given normal saline (10 mL/kg *per* body weight, orally), group II mice were given diclofenac sodium (50 mg/kg *per* body weight, orally) as a standard drug. In contrast, groups III and IV received methanolic extract (200 and 400 mg/kg *per* body weight, orally) as the sample. One hour after this treatment, 0.1 mL of 0.6% (v/v) acetic acid was administered intraperitoneally. The animal's abdominal muscle writhing characterized by stretching with a twitch at the back limb was taken as writhing movement, which is an indicator of pain response. The number of writhing motions in individual mice was counted for 15 min after the acetic acid administration. The percentage inhibition of writhing was counted from the following equation:

$$Inhibition\ (\%) = \frac{Average\ writhing\ of\ control - Average\ writhing\ of\ sample}{Average\ writhing\ of\ control} \times 100\%$$

Healthy Swiss albino mice of both sexes, 4-5 weeks old and 20-30 g weight, were used for the test. A positive control group was treated with diazepam (1 mg/kg *i.p.*), and the negative control group was administered with vehicle (10 mL/kg, normal saline orally). The test groups (groups II and III) received two different doses (200 and 400 mg/kg, respectively) of *G.*

tetrandra leaf extract by oral administration. The following three methods evaluated the sedative-hypnotic activity:

i) Hole-board test

Studying the exploratory activities of mice, this test is widely recognized as a way to assay potential sedative and anxiolytic effects of any compound. The equipment contained 16 equal size and evenly spaced holes. Normal saline (0.1 mL/mice, *p.o.*) and diazepam (1 mg/kg, *i.p.*) were given to the control and standard groups, respectively. It was established that the animals' head-dipping activity is directly relevant to their emotional situation.[19] The mice were put on the perforated flat platform after a period of 30 min in the case of the control and crude extract, and 15 min in the case of the standard, and the head dips' number in a period of five minutes was registered.

ii) Open field test

It is performed to evaluate exploratory behavior and anxiety along with to evaluate anxiolytic, anxiogenic, and non-pharmacological treatment. The test was performed to assess the anxiolytic activity of the test compound in mice central nervous system (CNS) as described by Gupta et al.[20] The open field apparatus consisted of a half-square-meter square wooden field with a series of squares painted in black and white alternately. The apparatus also contained a 30 cm high wall and was kept in a dimly lit place. The experimental animals were treated with vehicle, extract or diazepam and were held in the open field's center. After the treatment, the number of squares crossed by the animals was counted for 3 min at 30, 60, 90, and 120 min.

iii) Hole cross test

In this experiment, a cage with a dimension of 30×20×14 cm was used, with a fixed partition in the middle with a hole of 3 cm in diameter.[21] Mice received either a negative control, standard or an extract before being allowed pass the hole from one chamber to the next. The animals were observed for 3 min and the number of passages was counted at 30, 60, 90, and 120 min after the treatments.

In all three methods, the percent inhibition (%) value was calculated as follows:

$$Inhibition\ (\%) = \frac{Reaction\ time\ (control) - Reaction\ time\ (sample)}{Reaction\ time\ (control)} \times 100\%$$

Statistical analysis

One-way ANOVA followed by Dunnett's *t*-test was used to determine statistically significant differences between means. Results were considered significant at $p<0.05$. All the data analysis and statistical analysis were done using Microsoft Excel version 13.0 and Statistical Package for Social Sciences version 22.0.

RESULTS

Phytochemical screening

A series of chemical reactions were performed for the qualitative assessment of phytochemicals present in the crude methanolic extract of *G. tetrandra* leaves. Table 1 summarizes the results of different chemical tests used to detect and identify chemical constituents.

Acetic acid-induced analgesic activity

According to the statistical analysis, the extract in both doses exerted a dose-dependant analgesic activity in mice (Table 2). In this experiment, the reference drug (diclofenac sodium) 50 mg/kg and *G. tetrandra* leaf extract at 200 and 400 mg/kg significantly reduced the mean number of abdominal constrictions or writhes.

Sedative-hypnotic activity

(i) Hole board test

The effect of the plant extract as a sedative on mice using the hole board test is summarized in Table 3. The observed results suggest that the leaf extract of *G. tetrandra* possesses the significant potential to having a sedative-hypnotic activity compared to the standard.

Table 1. Phytochemical screening of methanolic extract of *Gomphandra tetrandra* leaves

Phytochemicals	Outcomes
Phytosterols	++
Steroids	+++
Carbohydrates	+++
Saponins	-
Gums and mucillages	+++
Soluble starch	-
Cardiac glycosides	-
Anthraquinone glycosides	-
Tannins	-
Flavonoids	++
Proteins	-
Terpenoids	-

(+): Detected, (-): Not detected

Table 2. Analgesic activity of methanolic extract of *Gomphandra tetrandra* leaf in the acetic acid-induced writhing test

Group	No of writhing	% of inhibition functions
Control	21.25 ± 2.87	-
Standard	3.75 ± 0.96	82.35***
Extract (200 mg/g)	8.5 ± 1.00	60.00**
Extract (400 mg/kg)	5 ± 0.82	76.47***

The number of writhing is expressed as a mean + SEM (n: 5), and significance of the percentage of inhibition writhing is determined compared to the control group, where **$p<0.01$, ***$p<0.001$, SEM: Standard error of mean

(ii) Open field test

The observed result reveals that the extracts substantially ($p<0.05$) decreased the mice's locomotion in the open field examination. The suppressive effect began after 30 min and lasted until 120 min, after the extract was administered. The impact of the plant extract on the animal model using the open field test is summarized in Table 4. This suggested that the extract at both doses has significant activity.

(iii) Hole cross test

The effect of the plant extract as a sedative-hypnotic using the hole cross test is summarized in Table 5. This suggested that the extract at both doses has significant activity compared to the standard.

DISCUSSION

The findings of this study demonstrated that the extract of *G. tetrandra* leaf possessed analgesic activity evident in the model, which suggests the presence of peripherally mediated mechanisms. The acetic acid-induced writhing response is a commonly used method for determining the peripheral analgesic function of any plant component. In an animal model, acetic acid is a primary pain inducer.[22] Several studies revealed that the pain response induced by acetic acid involves peritoneal mast cells and prostaglandin pathways.[23,24] The intraperitoneal administration of acetic acid has enriched the release of some inflammatory mediators, including histamine, serotonin, substance P, prostaglandins, and bradykinin. The release of these inflammatory mediators produces further abdominal constriction or discomfort.[25] Deraedt et al.[26] reported accumulation of prostaglandins PGE2e PGF2 within 30 min of acetic acid injection. Jiang et al.[27] also found an elevated level of lipoxygenase enzyme in peritoneal fluid following intraperitoneal acetic acid injection. Various flavonoids, including rutin, quercetin, pectolinarin, and gossypin, have been shown to induce considerable analgesic activity in various pain tests in previous studies.[28] Therefore, the flavonoids' involvement in the extract could play a vital role in the observed analgesic activity as they may inhibit the release of these inflammatory mediators. These findings also provide scientific credence for the traditional use of the leaf of *G. tetrandra* as an analgesic.

The obtained results suggest that the methanolic leaf extract of *G. tetrandra* possesses significant neuropharmacological activity in the animal model. The sedative-hypnotic activity was carefully assessed based on motor activity and exploratory behavior in the hole board, open field, and hole cross test. The open field is the most popular observational approach for general motor function. The most significant advantage of assessing motor movement in the open field is that the trend

Table 3. Effect of the *Gomphandra tetrandra* leaf extract as sedative-hypnotics on hole board test

Treatment	Head dips mean ± SD	% Inhibition
Control	20.5 ± 0.58	-
Standard	4 ± 0.82	80.49***
Extract (200 mg/kg)	7.25 ± 0.96	64.63***
Extract (400 mg/kg)	2.75 ± 0.96	86.59***

Values are expressed in mean ± SD (n: 5), where, ***$p<0.001$. SD: Standard deviation

Table 4. Effect of the *Gomphandra tetrandra* leaf extract as an antidepressant in the open field test

Time interval (minute)	Mean ± SD value of four groups (number of square crossing)				% Inhibition		
	Control (10 mL/kg)	Standard (100 mg/kg)	Extract (200 mg/kg)	Extract (400 mg/kg)	Standard (100 mg/kg)	Extract (200 mg/kg)	Extract (400 mg/kg)
30	54 ± 1.83	17.75 ± 0.96	33.25 ± 2.75	22.25 ± 0.50	67.13***	38.43***	58.80***
60	56.75 ± 2.06	10.25 ± 1.26	31 ± 2.16	21 ± 1.83	81.94***	45.37***	63.11***
90	59.5 ± 1.29	7.5 ± 1.29	26.25 ± 2.50	16.25 ± 0.50	87.39***	55.88***	72.69***
120	56.5 ± 1.29	4.75 ± 0.50	31.5 ± 4.20	20.25 ± 0.96	91.59***	44.25***	64.16***

***$p<0.001$. SD: Standard deviation

Table 5. Effect of the *Gomphandra tetrandra* leaf extract as antidepressants on hole cross test

Time interval (minute)	Hole crossing Mean ± SD value of four groups				% Inhibition		
	Control (10 mL/kg)	Standard (100 mg/kg)	Extract (200 mg/kg)	Extract (400 mg/kg)	Standard (100 mg/kg)	Extract (200 mg/kg)	Extract (400 mg/kg)
30	10.75 ± 1.26	4.25 ± 0.96	7.75 ± 0.96	4.5 ± 1.29	60.47***	27.91*	58.14***
60	12.75 ± 0.50	3.5 ± 0.58	8 ± 0.82	4.5 ± 0.58	72.55***	37.25***	64.71***
90	12 ± 0.82	3.25 ± 0.50	7 ± 0.82	4 ± 0.82	72.92***	41.67***	66.67***
120	12.5 ± 1.73	2.75 ± 0.50	6.5 ± 0.58	3.75 ± 0.50	78***	48***	70***

Values are expressed in mean ± SD (n: 5), *$p<0.05$, *** $p<0.001$. SD: Standard deviation

and qualitative profile of action can be detected explicitly.[29] Moreover, the hole board test has also achieved wide acceptance to assess the sedative-hypnotic activity of any drugs in the rodent model. Hole-poking (also known as head-dipping) is a standard prepotent action proven to be highly responsive to drug effects.[30] There are many physiologic conditions that can potentiate insomnia and other sleep disorders. Nervousness, tension, and indecision, both of which are accompanied by physiological arousal, may exacerbate sleep disruptions.[31] Synaptic transmission inhibition is required in this case, and agonists of the γ-aminobutyric acid receptor type A ($GABA_A$) are commonly used to achieve this (*e.g.*, benzodiazepines).[32]

Furthermore, muscle fatigue, reduced ambulatory function, and sedation are well-known results of CNS depressant medications like benzodiazepines.[33,34] Plants containing flavonoids and tannins are well-known for their ability to treat various CNS disorders.[35] As a consequence, the extract's sedative-hypnotic properties are most likely attributed to the flavonoids coupling to the $GABA_A$-benzodiazepine complex.

CONCLUSION

Phytochemical screening revealed that the methanolic extract of *G. tetrandra* contains steroids, carbohydrates, phytosterols, gums, flavonoids, and mucilages. The leaf extract of *G. tetrandra is* endowed with the significant potential of having analgesic and sedative-hypnotic activity. It reduced the pain of mice, where acetic acid was injected intraperitoneally. The results of these *in vivo* experiments inspire us to investigate the animals' motor performance further to determine the potentiality of antinociceptive involvement in the central and peripheral nervous systems. However, the findings demand a more of-depth investigation in animal models to uncover the molecular mechanisms of action in analgesic and sedative-hypnotic activity.

Ethics

Ethics Committee Approval: Approved by the local Ethics Committee (ref. no: DoP/RC/EC/2020/06/02).

Informed Consent: Not applicable.

Peer-review: Externally peer-reviewed.

Authorship Contributions

Concept: N.M.M.A.B., Design: M.H., N.M.M.A.B., Data Collection or Processing: M.F.H., Analysis or Interpretation: N.M.M.A.B., M.M.I., Literature Search: N.M.M.A.B., M.H., Writing: N.M.M.A.B., M.M.I., M.H.

Conflict of Interest: No conflict of interest was declared by the authors.

Financial Disclosure: The authors declared that this study received no financial support.

REFERENCES

1. Farnsworth N, Soejarto D. Global importance of medicinal plants. In Akerele O, Heywood V, Synge H (eds.). Conservation of Medicinal Plants. 1991;25-52.
2. Samuelsson G, Bohlin L. Drugs of natural origin: a treatise of Pharmacognosy. CRC Press Inc.; 2017.
3. Ghani A. Medicinal plants of bangladesh: chemical constituents and uses. Asiatic Society of Bangladesh. 1998;467.
4. Dimitrov K, Metcheva D, Boyadzhiev L. Integrated processes of extraction and liquid membrane isolation of atropine from *Atropa belladonna* roots. Sep Purif Technol. 2005;46:41-45.
5. Ziegler J, Diaz-Chávez ML, Kramell R, Ammer C, Kutchan TM. Comparative macroarray analysis of morphine containing *Papaver somniferum* and eight morphine free *Papaver* species identifies an *O*-methyltransferase involved in benzylisoquinoline biosynthesis. Planta. 2005;222:458-471.
6. Kavishankar GB, Lakshmidevi N, Mahadeva Murthy S. Phytochemical analysis and antimicrobial properties of selected medicinal plants against bacteria associated with diabetic patients. Int J Pharm Biosci. 2011;2:509-518.
7. Tewari DN. Report of the task force on conservation and sustainable use of medicinal plants. Bulletin of Planning Commission, Government of India, New Delhi, India. Published online: 2000.
8. Byng JW, Bernardini B, Joseph JA, Chase MW, Utteridge TM. Phylogenetic relationships of Icacinaceae focusing on the vining genera. Bot J Linn Soc. 2014;176:277-294.
9. Ramesha BT, Suma HK, Senthilkumar U, Priti V, Ravikanth G, Vasudeva R, Kumar TR, Ganeshaiah KN, Shaanker RU. New plant sources of the anti-cancer alkaloid, camptothecine from the Icacinaceae taxa, India. Phytomedicine. 2013;20:521-527.
10. Fang D, Zuo D. Two new species of *Adinandra* and *Mappianthus* from Guangxi, China. Acta Bot Yunnan. 2002;24:709-711.
11. Nwidu LL, Teme RE. Hot aqueous leaf extract of *Lasianthera africana* (Icacinaceae) attenuates rifampicin-isoniazid-induced hepatotoxicity. J Integr Med. 2018;16:263-272.
12. Ekanem NG, Mbagwu HOC, Harry GI. Phytochemical screening and hypoglycaemic activity of *Lasianthera africana* Beauv. (Aquifoliales: Stemonuraceae) leaf extract on diabetic rats. Braz J Biol Sci. 2016;3:293-298.
13. Ekpo DE, Joshua PE, Ogidigo JO, Nwodo OF. High resolution UPLC-PDA-QTOF-ESI-MS/MS analysis of the flavonoid-rich fraction of *Lasianthera africana* leaves, and *in vivo* evaluation of its renal and cardiac function effects. Heliyon. 2020;6:e04154.
14. Goshwami D, Rahman MM, Muhit MA, Islam S. *In-vitro* evaluation of anthelmintic activity of *Lasia spinosa* leaves. Int J Curr Pharm Res. 2013;5:34-35.
15. Raka SC, Rahman A, Hussain F, Rahman SMA. Synthesis, characterization and *in vitro*, *in vivo*, *in silico* biological evaluations of substituted benzimidazole derivatives. Saudi J Biol Sci. 2022;29:239-250.
16. Demers G, Griffin G, De Vroey G, Haywood JR, Zurlo J, Bédard M. Harmonization of animal care and use guidance. Science. 2006;312:700-701.
17. Osborne N, Avey MT, Anestidou L, Ritskes-Hoitinga M, Griffin G. Improving animal research reporting standards: HARRP, the first step of a unified approach by ICLAS to improve animal research reporting standards worldwide. EMBO Rep. 2018;19:e46069.
18. Bhuiya NM, Hasan M, Mahmud ZA, Qais N, Kabir MS, Ahmed F, Uddin MM. *In vivo* analgesic, antipyretic and anti-inflammatory potential of leaf extracts and fractions of Eria javanica. J Complement Integr Med. 2017;14.

19. Crawley JN. Exploratory behavior models of anxiety in mice. Neurosci Biobehav Rev. 1985;9:37-44.

20. Gupta BD, Dandiya PC, Gupta ML. A psycho-pharmacological analysis of behavior in rats. Jpn J Pharmacol. 1971;21:293-298.

21. Takagi K, Watanabe M, Saito H. Studies of the spontaneous movement of animals by the hole cross test; effect of 2-dimethyl-aminoethanol and its acyl esters on the central nervous system. Jpn J Pharmacol. 1971;21:797-810.

22. Bhuiyan MMR, Bhuiya NMMA, Hasan MN, Nahar UJ. *In vivo* and *in silico* evaluation of antinociceptive activities of seed extract from the *Holarrhena antidysenterica* plant. Heliyon. 2020;6:e03962.

23. Ribeiro RA, Vale ML, Thomazzi SM, Paschoalato AB, Poole S, Ferreira SH, Cunha FQ. Involvement of resident macrophages and mast cells in the writhing nociceptive response induced by zymosan and acetic acid in mice. Eur J Pharmacol. 2000;387:111-118.

24. Vogel HG. Drug discovery and evaluation: pharmacological assays. Springer Science & Business Media; 2002.

25. Ikeda Y, Ueno A, Naraba H, Oh-ishi S. Involvement of vanilloid receptor VR1 and prostanoids in the acid-induced writhing responses of mice. Life Sci. 2001;69:2911-2919.

26. Deraedt R, Jouquey S, Delevallée F, Flahaut M. Release of prostaglandins E and F in an algogenic reaction and its inhibition. Eur J Pharmacol. 1980;61:17-24.

27. Jiang B, Huang X, Yao H, Jiang J, Wu X, Jiang S, Wang Q, Lu T, Xu J. Discovery of potential anti-inflammatory drugs: diaryl-1, 2, 4-triazoles bearing *N*-hydroxyurea moiety as dual inhibitors of cyclooxygenase-2 and 5-lipoxygenase. Org Biomol Chem. 2014;12:2114-2127.

28. Calixto JB, Beirith A, Ferreira J, Santos AR, Filho VC, Yunes RA. Naturally occurring antinociceptive substances from plants. Phytother Res. 2000;14:401-418.

29. Denenberg VH. Open-field behavior in the rat: what does it mean? Ann N Y Acad Sci. 1969;159:852-859.

30. Kelley AE. Locomotor activity and exploration. Techniques in the Behavioral and Neural Sciences. 1993:499-518.

31. Spielberger CD. State-trait anxiety inventory. The Corsini Encyclopedia of Psychology. Hoboken: Wiley. 2010;1.

32. Tobler I, Kopp C, Deboer T, Rudolph U. Diazepam-induced changes in sleep: role of the alpha 1 GABA(A) receptor subtype. Proc Natl Acad Sci U S A. 2001;98:6464-6469.

33. Farkas S, Berzsenyi P, Kárpáti E, Kocsis P, Tarnawa I. Simple pharmacological test battery to assess efficacy and side effect profile of centrally acting muscle relaxant drugs. J Pharmacol Toxicol Methods. 2005;52:264-73.

34. López-Rubalcava C, Hen R, Cruz SL. Anxiolytic-like actions of toluene in the burying behavior and plus-maze tests: differences in sensitivity between 5-HT(1B) knockout and wild-type mice. Behav Brain Res. 2000;115:85-94.

35. Adeyemi OO, Yemitan OK, Taiwo AE. Neurosedative and muscle-relaxant activities of ethyl acetate extract of Baphia nitida AFZEL. J Ethnopharmacol. 2006;106:312-316.

Turk J Pharm Sci 2022;19(5):589-594
DOI: 10.4274/tjps.galenos.2021.33733

ORIGINAL ARTICLE

Determination of Metoclopramide Hydrochloride in Pharmaceutical Formulations using *N*-Oxidation Caroate

Mykola BLAZHEYEVSKIY[1], Deghinmotei ALFRED-UGBENBO[2]*, Olena Oleksandrivna MOZGOVA[1], Valery Petrovich MOROZ[3]

[1]National University of Pharmacy, Department of Inorganic and Physical Chemistry, Kharkiv, Ukraine
[2]Bayelsa Medical University, Department of Pharmaceutical Chemistry, Yenagoa, Nigeria
[3]National University of Pharmacy, Department of Analytical Chemistry and Analytical Toxicology, Kharkiv, Ukraine

ABSTRACT

Objectives: To develop two (titrimetric and spectrophotometric) simple, rapid, sensitive and cost-effective methods for the determination of metoclopramide (MCP) in pharmaceutical dosage forms.

Materials and Methods: The titrimetric method (A) was based on the *N*-oxidation reaction involving the use of potassium hydrogen peroxymonosulfate and subsequent iodometric back titration of a known residual reagent. The spectrophotometric method (B) was based on derivatization of MCP with potassium hydrogen peroxymonosulfate in the presence of iodide to produce a chromogen (triiodide) with a wavelength of maximum absorption at 350 nm.

Results: Method "A" was applicable over the concentration range of 0.25-3.5 mg to end volume 10 mL. In method "B", Beer's law was obeyed over the concentration range of 0.3-3.5 µg/mL with molar absorptivity of 24600 L/mol cm. The limits of quantification were calculated to be 0.25 mg/10 mL (A) and 0.2 µg/mL (B), respectively.

Conclusion: The proposed methods were suitable for determination of MCP as a pure substance in tablets and injection.

Key words: Analytical method, metoclopramide, titrimetry, spectrophotometry

INTRODUCTION

Metoclopramide [(MCP), Reglan®, Clopra®, Gimoti® *etc.*] known as (4-amino-5-chloro-[*N*]-[2-(diethylamino) ethyl]-2-methoxybenzamide) (Figure 1) is primarily used as an antiemetic or a gastrointestinal prokinetic drug in adult and children medicine as well as for gastroparesis in patients with diabetes nausea, vomiting, a feeling of fullness satiety, and loss of zest.[1-4]

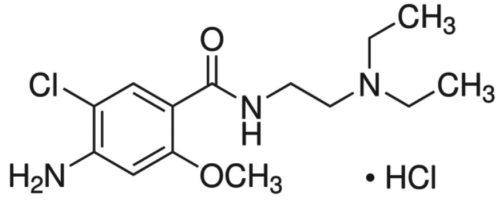

Figure 1. Structural formula of MCP
MCP: Metoclopramide

Because of having a wide application and a great therapeutic in empirical and clinical medicine, much study have concentrated on its determination in dosage forms. For the quantification of MCP in pharmaceutical products and biological fluids, several analytical methods have proposed such as high performance liquid chromatography (HPLC),[5,6] spectrofluorimetric,[7] electrochemical,[8-10] chemiluminescence,[11] tandem mass spectrophotometry.[12] Liquid chromatography is the official method for assay of MCP in the British Pharmacopoeia and United States Pharmacopoeia.[13,14] Several of these mentioned procedures are not simple for routine analysis, costly or complicated instruments, may require heating, or have relatively poor selectivity.

*Correspondence: audeghinmotei@gmail.com, Phone: +2348077868934, ORCID-ID: orcid.org/0000-0003-4835-1638
Received: 22.06.2021, Accepted: 12.11.2021

Titrimetry and visible spectrophotometry are perhaps the most widely techniques reported for the determination of MCP in pharmaceuticals.[15-22] Further, literature surveys revealed the use of spectrophometric method for estimation of MCP in the injection dosage form by direct ultraviolet (UV) spectroscopy at a wavelength of 270 nm with maximum absorbance using 0.1 M HCl as solvent.[23] Injections have little or no interference compared to other dosage forms such as tablets or suspensions since they contain almost no excipients. A stability indicating method has been developed for quantification of MCP in bulk by UV spectrophotometry in presence of its degradation products. The limit of detection (LOD) and limit of quantification (LOQ) values were found to be 3.26 μg/mL and 9.89 μg/mL, respectively.[24]

The redox titrimetric method of analysis is a possible alternative the various available analytical methods they are not only sensitive, precise, cost-effective; but relatively accurate.

This investigation develops simple, sensitive, and cost-effective methods for the determination of MCP in pure preparation, injection, and tablets using redox techniques.

The titrimetric method was based on the *N*-oxidation reaction involving the use of potassium hydrogen peroxymonosulfate as the titrant. A known excess of reagent is added and, after a specified time, the residual reagent is determined iodometrically. The spectrophotometric method depends upon the oxidation of MCP with Oxone® in alkali medium (pH: 9.9) followed by coupling with iodide in acidic medium (pH: 4.0) to give a yellow-brown colored chromogen (triiodide) with a wavelength of maximum absorption at 350 nm.

MATERIALS AND METHODS

Reagents

MCP hydrochloride, 98.8% ACROS Organics™; CAS 7232-21-5, $C_{14}H_{23}Cl_2N_3O_2$; melting point 171-173°C.

MCP was oxidized to a MCP hydrochloride *N*-oxide with the aid of potassium peroxymonosulfate ($KHSO_5$), a component in the commercial product called Oxone®; formula of Oxone®: $2KHSO_5 \cdot KHSO_4 \cdot K2SO_4$; CAS number. 70693-62-8, extra pure, min 4.5% active oxygen, ACROS Organics™; its formula weight is 614.78 g/mol. Moreover, it is considered "green"-oxidizing agent because of its nontoxic effects.

Standard drug solution

A stock standard solution of pure preparation containing 1 × 10^{-2} mol/L (3.363 mg/mL) MCP was prepared in double-distilled water and used in titrimetric method.

Injection: 2 mL «Polpharma» (Poland) N 5 injection containing active substance of MCP hydrochloride 10 mg;

Excipients: Sodium pyrosulfite 2 mg, sodium chloride 14 mg, water for injection up to 2 mL; and tablet containing MCP.

Tablet: Cerucal® 10 mg N50, AWD Pharma, manufactured «PLIVA Hrvatska» (Croatia). Each tablet contained active substance MCP hydrochloride monohydrate 10.54 mg (which corresponds to anhydrous MCP hydrochloride 10.00 mg);

Excipients: Potato starch 36.75 mg, lactose monohydrate 76.65 mg, gelatin 2.16 mg, silicon dioxide 2.60 mg, magnesium stearate 1.30 mg. According to the quality certificate, the quantitative content of MCP hydrochloride ($C_{14}H_{23}Cl_2N_3O_2$) was 9.9 mg. They were purchased from local commercial sources.

Apparatus: Unicam SP 800 instrument, Beckman DB spectrophotometer. 10 mL microburette. Air thermostat TS-80 m.

Solutions: $KHSO_5$, 1.73 x 10^{-2} mol/L from analytical-grade Oxone. Potassium iodide, 5% analytical-grade potassium iodide. Iodide, 1 mol/L from analytical-grade potassium iodide. Sulfuric acid, $c(H_2SO_4)$= 0.5 mol/L, volumetric solution. Sodium thiosulfate standard solution [$c(Na_2S_2O_3 \cdot 5H_2O)$= 0.1 mol/L].

Buffer solutions: 20 g/L of potassium hydrogen phthalate (pH: 4.0); 0.2 M solution potassium pyrophosphate with values of 8.6 and 9.3. For pH: 9.9: dissolve 28.62 g of sodium carbonate ($Na_2CO_3 \cdot 10H_2O$) and 8.40 g of sodium bicarbonate ($NaHCO_3$) in 1 L volume-distilled water.

Synthesis of MCP N-oxide

A mixture of MCP hydrochloride (0.71 g, 2 mmol), (0.76 g, 2.5 mmol) Oxone® ($2KHSO_5 \cdot KHSO_4 \cdot K_2SO_4$) and 20% aqueous solution of sodium carbonate (25 mL) and solution was stirred at room temperature until disappearance of the starting material. The solution was treated in an ultrasonic bath for 15 min. Water was removed from the mixture by evaporation under vacuum and the resulting solution was lyophilized at room temperature. The residue was taken up with ethyl acetate to give MCP *N*-oxide in quantitative yield as a colorless solid. Further information about maximization of yield is already published.[25]

Titrimetric assay

The procedure for quantitative determination of MCP in pure preparation

MCP (0.35404 g) dissolved in 100 mL of double distilled water. Using a pipette, volumes (10 mL) of a prepared solution were accurately transferred to 100 mL measuring flask, 10 mL of 0.02 mol/L previously prepared solution of the $KHSO_5$, pH: 9.9 buffer solution (75 mL) and water were added to make the final volume of a 100 mL solution. They were mixed to homogeneity (start stop clock). Within a chosen period (10-15 min), 20.00 mL was pipetted to the reaction mixture in a 150 mL conical flask. 4.0 mL of 0.5 mol/L sulfuric acid and 5 mL of 5% solution of potassium iodide were added while shaking. The formed iodine was titrated with 0.01 mol/L sodium thiosulfate using a micro buret until the mixture turned colorless. The blank titration was repeated, omitting MCP (control titration).

The MCP content in the pure preparation, % (*X*), was calculated using the following equation:

$$X = \frac{(V_0 - V_1) \times K \times T \times 100 \times 100 \times 100}{m \times V_a \times 10 \times (100 - w)} \times 100\%, \qquad \text{equation (1)}$$

where V_0 is 0.01 mol/L sodium thiosulfate volume used for titration in blank determination, mL;

V_1 is 0.01 mol/L sodium thiosulfate volume used for titration in procedure, mL;

K is correction factor of concentration of concentration 0.0100 mol/L sodium thiosulfate solution concentration;

T is a mass of a substance, which reacts with 1 mL of 0.01 mol/L sodium thiosulfate, g/mL;

100 is volumetric flask capacity, mL;

V_a is volume of reaction mixture taken for analysis, mL;

m is mass of a substance to be determined, g;

w is substance moisture content, %;

10 is volume of the pipette, which is used for measuring the solution aliquot, mL.

1.00 mL of standard 0.0100 mol/L sodium thiosulfate solution is equivalent to 0.0016813 g/mL of MCP, which should be 99-101% in the preparation terms of the anhydrous base.

Quantitative determination of MCP in tablets Cerucal® 10 mg

Twenty tablets containing MCP were weighed and ground into fine powder for methods A and B, and a weighed quantity of the crushed tablet equivalent to 200 mg MCP (2.5880 g) was transferred to a 100 mL flask and shaken with 60 mL water for about 20 min, then made up to the mark with water, mixed and filtered using a Whatman N42 filter paper. Transfer was carried using a pipette to accurately measure the volume (15 mL) of the prepared solution to 100 mL measuring flask. Same procedure as mentioned in the procedure for determination of MCP in pure preparation was repeated.

MCP content in one tablet, mg (*X*), has been calculated by the following equation:

$$X = \frac{(V_0 - V_1) \times K \times T \times 10 \times 100}{15 \times 20 \times 20} \quad \text{equation (2)}$$

where V_0 is 0.01 mol/L sodium thiosulfate volume used for titration in blank determination, mL;

V_1 is 0.01 mol/L sodium thiosulfate volume used for titration, mL;

K is the correction factor of concentration of concentration 0.0100 mol/L sodium thiosulfate solution concentration;

T is a mass of a substance, which reacts with 1 mL of 0.01 mol/L sodium thiosulfate, g/mL (1.6813 mg/mL MCP);

15 is the volume of a dosage form solution taken for analysis, mL; 20 is volume of the pipette, which is used for measuring the solution aliquot, mL; 100 is volume of flask used, mL; 20 is number of tablets taken for analysis.

1.00 mL of standard 0.0100 mol/L sodium thiosulfate solution corresponds to 0.0016813 g/mL of MCP, which should be 95-105% in the preparation in terms of the anhydrous base.[26]

Quantitative determination of MCP in 0.5% injection dosage form

Accurately measured volumes (10.0 mL) of solution for injection (content five-six ampoules) were transferred using a pipette to a 100 mL measuring flask and same procedure as for the determination of MCP in pure preparation was repeated. The titration was repeated without the addition of a buffer solution (pH: 9.9), the same volume of double distilled water was used in its place. For 0.1 mol/L hydrochloric acid solution, 2 mL instead of 10 mL was added (control titration).

MCP content in the solution for injection, g to 100 mL (*X*), was calculated using the following equation:

$$X = \frac{(V_0 - V_1) \times K \times T \times 10 \times 100}{10.00} \quad \text{equation (3)}$$

where V_0 is 0.01 mol/L sodium thiosulfate volume used for titration in blank determination, mL;

V_1 is 0.01 mol/L sodium thiosulfate volume used for titration in procedure, mL;

K is the correction factor of concentration of concentration 0.0100 mol/L sodium thiosulfate solution concentration;

T is a mass of a substance, which reacts with 1 mL of 0.01 mol/L sodium thiosulfate, g/mL;

10.00 is volume of a dosage form solution taken for analysis, mL;

100 is recalculation to 100 mL;

10 is dilution factor.

1.00 mL of standard 0.0100 mol/L sodium thiosulfate solution corresponds to 0.0016813 g/mL of MCP, which should be 90-110% in the preparation in terms of the anhydrous base.

Spectrophotometric assay

Procedure for obtaining results for calibration graph

Into 50 mL flask, an aqueous solution (standard) of MCP (0.5-5.0 mL) was added, and then 1.73 x 10^{-4} mol/L $KHSO_5$ solution (3.00 mL). The flask was washed with adequate water to increase the volume to 8.0 mL, to which the buffer solution (20 mL) was added and maintained for 10-15 min. Then 0.5 mol/L sulfuric acid solution (1 mL) was added and the volume adjusted to 45 mL with the solution containing 20 g/L of potassium hydrogen phthalate; 5 mL of 5% solution of potassium iodide was also added (5 mL). Prepared solutions were maintained for 60 s and the absorbance at 350 nm was measured against distilled water. A control measurement was carried out similar to the working experiment, with the difference that double-distilled water was used instead of the investigated drug solution. The difference in optical densities obtained in the control and working experiments, respectively (ΔA), was plotted *versus* the concentration of MCP.

Spectrophotometric determination of MCP in tablets Cerucal® 10 mg

Twenty tablets were weighed and pulverized. The equivalent to 200 mg MCP was dissolved in double distilled water and

filtered; the residue was rinsed, volume adjusted to 100 mL, and further diluted with same diluent to obtain the working concentration (1 x 10^{-4} mol/L). The prepared aqueous solution of MCP (2.00 mL) and 1.7 x 10^{-4} mol/L $KHSO_5$ solution (3.00 mL) were pipetted into a 50 mL graduated flask, and subsequent addition of reactants, diluents and buffers as in the above-written spectrophotometric procedure for obtaining results for calibration graph. The prepared solution was made up to 50 mL (after being kept for 60 seconds) and measured absorbance measured; the amount of MCP present in the sample was computed from the calibration curve.

Spectrophotometric determination of MCP in 0.5% injection dosage form

Accurately measured volumes (5.0 mL) of solution for injection were transferred using a pipette to a 100 mL measuring flask and brought to a final volume of 100 mL with water. Then, an aqueous solution of MCP (3.00 mL) was transferred to a 50 mL graduated flask and same procedure as further written in spectrophotometric determination of MCP in tablets Cerucal® 10 mg was carried out. For control measurement: In place of a sulfuric acid solution and a buffer solution with a pH of 9.9, double-distilled water was used.

Recovery studies

The recovery was calculated as the percentage of values obtained using standard pharmacopeial method as provided by the certificate of analysis from quality control laboratory.

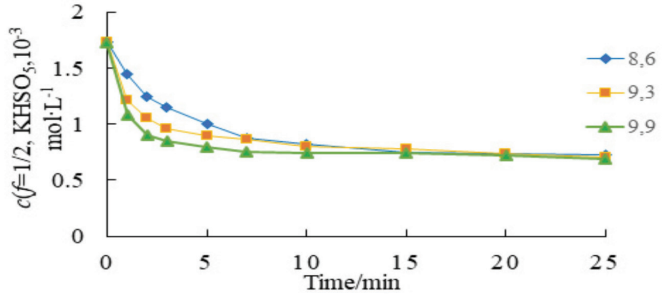

Figure 2. Concentration *versus* time plot of potassium hydrogen peroxymonosulfate during the oxidation of MCP. Concentration *versus* time plot of potassium hydrogen peroxymonosulfate during the oxidation of MCP. pH: 8.6; 9.3 and 9.9;. c (f= 1/2, $KHSO_5$)= 1.73 x 10^{-3} mol/L; c (MCP)= 1 x 10^{-3} mol/L

MCP: Metoclopramide

RESULTS AND DISCUSSION

The stoichiometry of the reaction for synthesis of MCP *N*-oxide was assessed and found to be 1:1 (MCP: $KHSO_5$). The study of kinetics showed that the optimal time of quantitative interaction is 10-15 min at pH: 9.9 (Figure 2).

The interaction of MCP with potassium hydroperoxy monosulfate can be represented by the scheme in Figure 3. During study of the influence of iodide concentration on the absorbance of the final solution, steady absorbance was obtained when the iodide concentration was 0.1 mol/L. The molar absorptivity at 350 nm was found to be 2.46 x 10^4 (Table 1, Figure 4). Calculations based on the association constant for tri-iodide (log*K*: 2.9) show that more than 97% of the iodine was found as tri-iodide in solutions containing >0.05 mol/L iodide; thus, a percentage of the reduction in molar absorptivity observed in lower iodide concentrations may be explained due to incomplete formation of tri-iodide. Notwithstanding, an explanation for the occurrence of such significant reduction in the presence of higher $KHSO_5$ concentrations may currently be difficult; as Nisli and Townshend[27] suggest, it may be due to incomplete $KHSO_5$-iodide reaction under these conditions.

These conditions were the basis for developing a new-oxidimetric method for the quantitative determination of MCP using potassium hydrogen peroxymonosulfate as an analytical reagent. In titrimetric method, when the reaction between the tertiary amine group present in MCP with $KHSO_5$ was completed, the excess $KHSO_5$ was detected iodometrically.

The results of MCP determination in pure substance by oxidimetry-using potassium hydrogen peroxymonosulfate (Oxone®) are shown in Table 2.

The results for both titrimetric and spectrophotometric determination of MCP in tablets and solution for injection dosage forms are presented in Table 2. Results of recovery studies show that in all cases that δ* was within the recommended limits. In spectrophotometric determination of MCP, LOQ (10S) is 4.61 x 10^{-7} mol/L.

CONCLUSION

Two simple methods for the determination of MCP in tablets and in injection were developed. These methods are based on *N*-oxidation reactions. This spectrophotometric method is the simplest method ever reported and the iodometric titration method is the first ever reported for the determination of

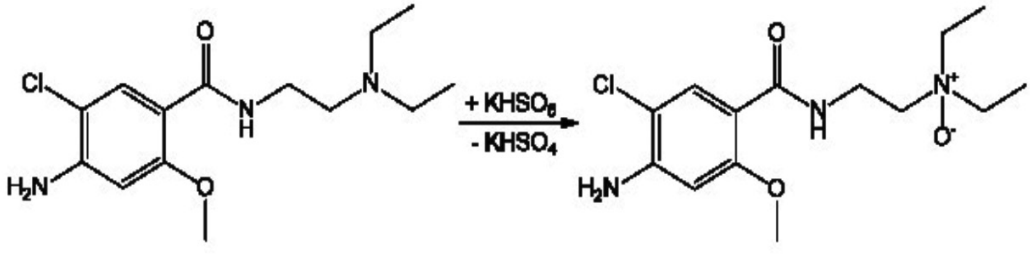

Figure 3. Scheme of interaction between MCP and potassium hydrogen peroxymonosulfate

MCP: Metoclopramide

Table 1. Characteristics of linear regression equation curve calibration graph

Characteristics	Parameters
Correlation coefficient (r)	0.9998
Linear regression equation (y= a + bx)	y= 24636x
Slope (b ± Δb)	24636 ± 543
Intercept (a ± Δa)	-0.0064 ± 0.0032
SD of slope (S_b)	195.5
SD of intercept (S_a)	0.0011
LOD (3S)	1.38 x 10^{-7} mol/L
LOQ (10S)	4.61 x 10^{-7} mol/L

LOD: Limit of detection, LOQ: Limit of quantification, SD: Standard deviation

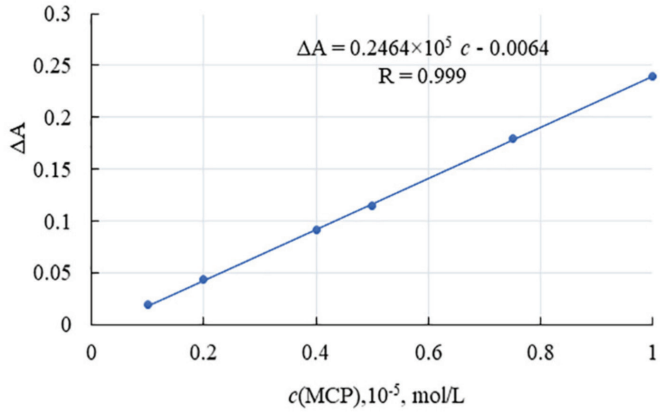

Figure 4. Calibration graph for the spectrophotometric determination of MCP

MCP: Metoclopramide

Table 2. Results of titrimetric and spectrophotometric determination of pure substance (i), tablets (ii), and injection (iii) dosage forms containing metoclopramide using Oxone

Statistical parameters	A. Titrimetric method					B. Spectrophotometric method		
	i. Pure substance (g)		ii. Tablets Cerucal® (mg/tablet)		iii. Injection «metoclopramide hydrochloride 0.5%» (g/*per* 100 mL)	ii. Tablets Cerucal® 10 mg/tablet		iii. Injection «metoclopramide hydrochloride 0.5%» (g/*per* 100 mL)
Found	%	99.10	mg	9.89	g 0.489	mg	10.11	g 0.482
		99.81		9.95	0.488		10.05	0.486
		98.72		10.11	0.494		9.95	0.491
		99.10		10.03	0.496		9.83	0.496
		98.20		9.92	0.498		9.72	0.503
Metrological characteristics (n: 5, p=0.95)	$\bar{x}$	98.99% (Re: 100.19%)		9.98 mg (Re: 100.81%)	0.493 g/*per* 100 mL (Re: 100.61%)	$\bar{x}$: 9.93 mg (Re: 100.30%)		0.492 g/*per* 100 mL (Re: 100.41%)
	S	0.59		$8.98 \cdot 10^{-2}$	0.44 x 10^{-2}	0.16		$8.3 \cdot 10^{-3}$
	$\Delta\bar{x}$	0.74		$1.08 \cdot 10^{-2}$	0.54 x 10^{-2}	0.20		0.010
	RSD (%)	0.60		0.90	0.88	1.60		1.68
	δ* (%)	+ 0.19		+ 0.81	+ 0.61	+ 0.30		+ 0.41

Max error, δ*: ($\bar{x}$-μ) 100%/μ; μ - content found by standard pharmacopoeial procedure.
ii: According to the quality certificate, the quantitative content MCP was 9.9 mg (98.7%).
iii: According to the quality certificate, the quantitative content MCP 1.0 mL of solution for injection contains 4.9 mg of MCP (0.49 g *per* 100 mL).
RSD: Relative standard deviation, MCP: Metoclopramide, Re: Recovery

MCP. The titrimetric method is applicable over wide linear dynamic ranges and was successfully applied to the tablets and injection. The statistical characteristics and recovery study information revealed the reproducibility and accuracy of the methods. Besides the simplicity and sensitivity of the procedures, the relative cheap cost of apparatus and reagents is also an advantage. The methods are also useful due to high tolerance limit for common excipients found in pharmaceutical formulations. These merits coupled with the use of simple and relatively inexpensive instruments and high selectivity of the methods suggest their possible application in routine quality control laboratories.

Ethics

Ethics Committee Approval: Not applicable.

Informed Consent: No part of this work was experimented on human or animals.

Peer-review: Externally peer-reviewed.

Authorship Contributions

Concept: M.B., Design: D.A.U., Data Collection or Processing: M.B., O.O.M., V.P.M., Analysis or Interpretation: M.B., D.A.U., O.O.M., V.P.M., Literature Search: D.A.U., O.O.M., Writing: M.B., D.A.U.

Conflict of Interest: No conflict of interest was declared by the authors.

Financial Disclosure: The authors declared that this study received no financial support.

REFERENCES

1. Vandenplas Y, Hauser B. An updated review on gastroesophageal reflux in pediatrics. Expert Rev Gastroenterol Hepatol. 2015;9:1511-1521.
2. Mashkovsky MD. Medicines (16th ed). Moscow: New Wave: Umerenkov, 2020.
3. Becker WJ. Acute migraine treatment in adults. Headache. 2015;55:778-793.
4. The American Society of Health-System Pharmacists. AHFS Drug Information-monograph of metoclopramide (1st ed). Maryland: American Society of Health-Systems Pharmacists, 2021.
5. Kahali N, Khanam J. A novel HPLC method validation based on analytical techniques of metoclopramide benzamide derivative (metoclopramide base) and its determination from solid dispersion by solvent evaporation method. J Appl Pharm Sci. 2018;8:018-026.
6. Khan A, Khan J, Irfan M, Naqvi SBS, Khan GM, Shoaib MH, Yousaf RI, Khan A. Validation and application of high performance liquid chromatographic method for the estimation of metoclopramide hydrochloride in plasma. Pak J Pharm Sci. 2017;30:143-147.
7. Elmansi H, Mohamed SAEA, Fathy M. Simultaneous determination of metoclopramide and aspirin by spectrofluorimetric technique: application to pharmaceutical formulations and human plasma. Anal Methods. 2016;8:1281-1292.
8. Al-Haideri AMA, Abdulla NI, Malih IK. Polymeric membrane sensors for the selective determination of metoclopramide hydrochloride and their applications to pharmaceutical analysis. Iraqi J Pharm Sci. 2017;21:70-77.
9. Patil SM, Pattar VP, Nandibewoor ST. Simultaneous electrochemical determination of acetaminophen and metoclopramide at electrochemically pre-treated disposable graphite pencil electrode. J Electrochem Sci Eng. 2016;6:265-276.
10. Ghonim OAAA. PVC membrane sensors for potentiometric determination of metoclopramide in pharmaceutical preparations and in presence of its degradate. Anal Bioanal Electrochem. 2014;6:296-307.
11. Hun X, Zhang Z. Electrogenerated chemiluminescence sensor for metoclopramide determination based on Ru (bpy) 3^{2+}-doped silica nanoparticles dispersed in Nafion on glassy carbon electrode. J Pharm Biomed Anal. 2008;47:670-676.
12. Lee HW, Ji HY, Kim HY, Park ES, Lee KC, Lee HS. Determination of metoclopramide in human plasma using hydrophilic interaction chromatography with tandem mass spectrometry. J Chromatogr B Analyt Technol Biomed Life Sci. 2009;877:1716-1720.
13. British Pharmacopeia. Monograph of metoclopramide (volume II). London: The Stationary Office Ltd; 2013.
14. USP 36-NF 31 Supplement 2. United States Pharmacopiea, 2013.
15. Naggar A, Elnasr TAS, Sayed Ali AS, Kotb A, El Sayed AAY. Determination of metoclopramide hydrochloride in pharmaceutical formulations using three different spectrophotometric methods. Pharm Anal Acta. 2017;8:2.
16. Devi OZ, Basavaiah K, Vinay K, Revanasiddappa HD. Sensitive spectrophotometric determination of metoclopramide hydrochloride in dosage forms and spiked human urine using vanillin. Arabian J Chem. 2016;9:64-72.
17. Thangamani A, Smith AA, Vedhapriya B. Development of analytical method for metoclopramide using UV-spectrophotometry. Inter J Pharm Chem Biol Sci. 2014;4:551-555.
18. Jawad A, Kadhim K. Spectrophotometric determination of metoclopramide hydrochloride in bulk and pharmaceutical preparations by diazotization-coupling reaction. Int J Pharm Pharm Sci. 2013;5:294-298.
19. Dudhane N, Vidhate SS, Borkar BH, Lohiya RT, Umekar MJ. Simultaneous UV spectrophotometric estimation of metoclopramide hydrochloride and paracetamol in solid dosage form. J Pharm Sci & Res. 2010; 2:48-52.
20. Al-Abbasi KM, Mohammed SA, Sarsam LA. Spectrophotometric determination of metoclopramide hydrochloride in pharmaceutical preparations using diazotization reaction. Rafidain J Sci. 2011;22:76-88.
21. Devi OZ, Basavaiah K, Vinay KB, Revanasiddappa HD. Determination of metoclopramide hydrochloride in pharmaceuticals and spiked human urine through diazotization reaction. J Food Drug Anal. 2012;20:454-463.
22. Khammas ZAA, Abdulkareem HM. A new visible spectrophotometric approach for mutual determination of amoxicillin and metoclopramide hydrochloride in pharmaceuticals after cloud point extraction. Sci J Anal Chem. 2016;4:66-76.
23. Basheer MY, Kashif AA, Aljaily A, Ibrahim MM, Osman HM. Development and validation of UV-spectroscopic method for assay of metoclopramide hydrochloride in bulk and injectable dosage form. Am J Res Commun. 2017;5:22-33.
24. Deokate UA, Gorde AM. A stability indicating UV spectrophotometric method for determination of metoclopramide hyrdrochloride. Int J Pharm Pharm Sci. 2014;6:394-397.
25. Maurich V, De Amici M, De Micheli C, Rossato P. Identification and full characterization of a new metabolite of metoclopramide. Eur J Med Chem. 1995;30:757-762.
26. Alfred Ugbenbo D, Zdoryk OA, Bevz NY, Georgiyants VA. Validation of the method for hydrochlorothiazide assay in extemporaneous preparations. J. Org Pharm Chem. 2017;15:12-17.
27. Nisli G, Townshend A. Spectrophotometric determination of some *vic*-diols. Talanta. 1968;15:1377-1384.

Turk J Pharm Sci 2022;19(5):595-602
DOI: 10.4274/tjps.galenos.2021.53050

ORIGINAL ARTICLE

Development and Evaluation of Floating Microspheres of Anticonvulsant Drug by 3^2 Full Factorial Design

Manish BHISE[1]*, Karunakar SHUKLA[2], Sourabh JAIN[2], Nitin BHAJIPALE[1], Suresh SUDKE[3], Pramod BURAKLE[4]

[1]Shri Gurudatta Shikshan Prasarak Sanstha Institute of Pharmacy, Department of Pharmaceutics, Akola, (MS), India
[2]College of Pharmacy, Dr. APJ Abdul Kalam University, Indore, (MP), India
[3]Satara College of Pharmacy, Department of Pharmaceutics, Satara, (MS), India
[4]Dr. Rajendra Gode College of Pharmacy, Department of Pharmaceutical Chemistry, Amravati, (MS), India

ABSTRACT

Objectives: Present study was to develop and evaluate gastroretentive microspheres by the solvent evaporation technique.

Materials and Methods: Gabapentin and HPMC K100 were used to develop the formulations. Gastroretentive microspheres were developed by the solvent evaporation technique from the preliminary batches of gabapentin microspheres batch FMG3 were selected for factorial study.

Results: Factorial batches showed the mean particle size of the floating microsphere formulations for gabapentin (FFMG1-FFMG9) was in the range of 185.63 ± 0.13 to 510.04 ± 0.09 µm. The percentage yields of formulations FFMG1 to FFMG9 for gabapentin ranged from 53.5 ± 0.95 to 96.64 ± 0.42. The buoyancy percentage was calculated for the formulations and found that all formulations could float on dissolution medium for 12 h. The drug loading in gabapentin microspheres was found 65.29 ± 0.46 to 84.3 ± 0.44. The swelling study was found to be 756.34 ± 1.48 to 890.46 ± 0.78 for gabapentin. Batch FFMG6 and FFMC2 showed better drug release 99.1% and 99.25% respectively. The optimized formulation FFMG6 for gabapentin showed an n value 0.8474 and R^2 value 0.9965.

Conclusion: Optimized formulation obeys Korsmeyer-Peppas release. Scanning electron microscopy images of microspheres were spherical, discrete, and freely flowing. ANOVA for the given formulations showed *p* value less than 0.0500. The stability study indicated no significant changes in the microspheres. In radiographic images, floating microspheres were retained in the stomach of rabbits for twelve hours.

Key words: Gastroretentive, anticonvulsant, radiographic, microspheres, rabbit

INTRODUCTION

Microspheres are tiny spherical particles of micrometer diameter range (usually between 1 µm and 1000 µm). Often, microspheres are called microparticles. Microspheres can be obtained from different natural and synthetic materials. Commercially available are ceramic microspheres, polymer microspheres and glass microspheres. Microspheres with solid and hollow densities vary drastically and, therefore, are used in various usages. Hollow microspheres are normally used as antioxidants to reduce material density.

Recent advances have resulted in the development of various types of microspheres (such as floating, mucoadhesive, radio-active, double-walled, and magnetic) to serve different purposes. For example; floating/mucoadhesive microspheres have been developed as gastroretentive delivery systems.[1]

MATERIALS AND METHODS

Materials

Gabapentin was obtained as a gift sample from Alkem Laboratories (Mumbai, India). The other excipients used were of analytical grade.

Preparation of microspheres

The solvent evaporation technique was employed to prepare gabapentin-loaded floating microspheres. HPMC K100 and cellulose acetate phthalate were dissolved in various ratios at

*Correspondence: manishbhise.patil@gmail.com, Phone: 08329407345, ORCID-ID: orcid.org/0000-0002-3848-2549
Received: 27.03.2021, Accepted: 12.11.2021

room temperature in a blend of ethanol and dichloromethane. Gabapentin was added to the above solution and was agitated to create a homogeneous solution on a magnetic stirrer. The above solution containing gabapentin was squeezed into 100 mL of water containing 0.01% tween 80 at room temperature and stirred for three hours. Finally, microspheres were filtered, separated and dried at room temperature. The formulation composition is provided in Tables 1 and 2.

Characterization of floating gastroretentive microspheres

Micromeritic evaluation

Bulk density: Bulk density= Bulk/mass volume

Tapped density: Tapped density= Tapped/mass volume

Carr's (compressibility) index:

$$\%\ \text{Compressibility index} = \frac{Tapped\ density\text{-}Bulk\ density\ X100}{Tapped\ density}$$

$$Hausner\ ratio: Hausner\ ratio = Bulk\ density/Tapped\ density$$

$$Angle\ of\ repose: \theta = Tan^{-1}(h/r)$$

Where h= pile height, r= pile radius, and θ= angle of repose

Particle size

The size of a particles of the blank and gabapentin-loaded microsphere was determined by optical microscopy method using a compound microscope (Olympus India) equipped with ocular and calibrated stage micrometers. After the calibration of an ocular micrometer by placing the ocularlens and following focusing on the object to be measured and determining the size in ocular units, then placing the samples on a slide and measuring the size of microspheres.[2-4]

$$One\ ocular\ unit = \frac{Divisions\ (mm)\ stage\ micrometer}{Ocular\ micrometer\ division}\ X100\ \mu m/mm$$

Percentage yield

The percentage yield of microspheres is ratio the of the weight of microspheres collected or recovered to the total weight of all solid contents taken. Dry microspheres collected were weighed to assess recovery:[5]

$$\%\ Yield = \frac{Mass\ of\ microspheres\ obtained\ (g)}{Theorotical\ mass\ of\ microspheres\ (g)}\ X100$$

Measurement of microspheres hydration

Hydration of the microspheres is described as the ratio of wet microspheres to dry microsphere's weight. The recovered microspheres were immediately weighed and depicted at the end of each microencapsulation phase (M1). When the microsphere is dry to a constant weight, it is again measured and shown as an (M2). It is expressed by the following equation:[6]

$$\%\ Microsphere's\ hydration = \frac{M1}{M2}X100$$

Determination of drug loading of microspheres

20 mg of hollow-loaded gabapentin microsphere samples were dissolved at room temperature by ultrasonication in 50 mL ethanol to determine to load. The liquid was then purified by a millipore (0.45 µm) filter. Ultraviolet (UV)-visible sensor (UV 1700-1800) (Shanghai Phoenix Optical Instrument Co., Ltd., Shanghai, China) was used to determine drug concentrations at 210 nm and 284 nm. The drug loading of gabapentin-loaded hollow microspheres was determined by the following equation.[7]

$$Drug\ loadingamount = \frac{Amount\ of\ FD\ in\ hollow\ microspheres}{Amount\ of\ hollow\ microspheres\ containing} \times 100$$

Drug entrapment efficiency

The entrapment efficiency of the microspheres was determined by extraction of drug from the microspheres. In a typical procedure, 50 mg of dried microspheres was ground in a pestle and mortar, and the fine microspheres dissolved in a few mL of ethanol and diluted with 50 mL of 0.1 N HCl for 24 h. After 24 h, the solution was moved over a 0.45 µm filter. The gabapentin present in the filtrate was evaluated spectrophotometrically at 210 nm using a UV-visible spectrophotometer (Shimadzu, UV-1800, Japan) using 0.1 N HCl as blank.[8,9]

Table 1. Formulation composition of floating microspheres of gabapentin preliminary batches

Formulation code	FMG1	FMG2	FMG3	FMG4	FMG5	FMG6
Gabapentin	200	200	200	200	200	200
HPMC K100: CAP	0.5 :0.50	0.5:0.75	0.5:1.00	0.5:0.25	0.75:0.5	1.00:0.25
Solvent ratio ethanol:dichloromethane (%v/v)	1:1	1.5:1	2:1	1:1	1: 1.5	1: 2

Table 2. Formulation composition of floating microspheres of gabapentin factorial batches

Formulation code	FFM G1	FFMG 2	FFM G3	FFMG 4	FFM G5	FFM G6	FFMG 7	FFMG 8	FFM G9
Gabapentin	200	200	200	200	200	200	200	200	200
HPMC K100: CAP	0.5:0.5	0.37:0.75	0.25:0.75	0.25:0.25	0.5:0.25	0.5:0.75	0.37:0.50	0.37:0.25	0.25:0.50
Solvent ratio ethanol:dichloromethane (%v/v)	1:1	1.5:1	2:1	1:1	1: 1.5	1: 2	1:1	1.5:1	2:1

$$Drug\ entrapment\ efficiency = \frac{Weight\ of\ drug\ in\ microspheres}{Weight\ of\ fed\ drug} X\ 100$$

Swelling measurement

The dissolution apparatus United State Pharmacopoeia (USP) type II, was used for the swelling analysis. The vessels that comprise simulated gastric fluid (SGF) were correctly weighed with gabapentin microsphere and allow to swell. The speed of rotation was adjusted at 50 rpm. The microspheres were removed and blocked-in filter paper at a pre-determined period to eliminate the excess water. The weight increases were calculated at various times before the full weight was increased. The index swelling was determined by the following equation:[10]

$$Swelling\ index\ (S): \frac{W_m - W_t}{W_t} X100$$

where W_m signifies the weight at equilibrium and W_t signifies the initial microsphere's weight.

In vitro buoyancy

Gabapentin-equipped microspheres were assessed for *in vitro* floating properties on a USP dissolution device 2 (paddle type). Fifty single microspheres were submerged in a vessel of 500 mL SGF from each formulation. The rotation of the paddle at 50 rpm, while maintaining the temperature at 37 ± 0.5°C. The number of microspheres floating was measured up to eight hours at hourly periods. *In vitro* buoyancy was represented as a percentage and the following equation was determined:[11]

$$F\% = \frac{Weight\ of\ floating\ microspheres}{Weight\ of\ initial\ microspheres} X100$$

In vitro drug release

Dose equivalent to 100 mg of floating microspheres of gabapentin was accurately weighed and dissolution studies were conducted using SGF (enzyme-free) (900 mL) at temperature 37 ± 0.5°C using USP type II apparatus. The rotation speed was maintained at 100 rpm. An aliquots of 5 mL of dissolution medium was removed at a fixed intervals until a period of 12 h and substituted with a fresh medium. The content of gabapentin microspheres was determined using a UV spectrophotometer (Spectro UV-2080, double beam, Analytical Technologies, India) at 210 nm against SGF as blank.[12]

Scanning electron microscopy (SEM)

Dry gabapentin microspheres were mounted on a gold-coated electron microscope in an ion sputter. The random scan of a stub took a view of the microsphere. The microspheres study was conducted using JEOL, JSM-670F Japan. At an accelerated voltage of 3.0, the microspheres were presented.[13]

Drug release kinetics

The drug release from various controlled-release preparations is more often measured using four kinetic models. The data obtained from *in vitro* release of the drug were measured using 5 models to identify the most suitable model. The release of zero-order kinetics is a drug-release mechanism that is not based on drug concentration. The zero-order release equation is:[6]

Zero-order kinetics: Ft= K0t

Here, F indicates the drug fraction released in time t and $K0$ denotes the zero-order release constant.

First-order kinetics: "Ln (1 - F) = -K1t"

Here F shows the drug release fraction in time t and $K1$denotes the Ist order release constant

Higuchi model: F= $K2$ $t1/2$

Here F signifies drug release fraction in period t &$K2$ denotes the "Higuchi constant".

Korsmeyer-Peppas model: $Mt/M\infty$= K3t^n

Here Mt denotes the drug amount released in time t, M∞ signifies the drug amount release at time infinity, $K3$ denotes the kinetic constant and n indicates the exponent defining the swelling mechanism.

Stability study[14]

The optimized formulation was kept for accelerated stability study according to the International Conference on Harmonization (ICH) guidelines for 3 months. Microspheres were packed in a laminated aluminum foil and kept in a stability chamber maintained at a temperature of 40 ± 2°C and 75.5% relative humidity. At the end of 0, 30, 60, 90 days, samples were withdrawn and examined for percentage buoyancy drug, entrapment efficiency and *in vitro* drug release.

In vivo study[15,16]

The *in vivo* radiographic studies were conducted on young and healthy four male albino rabbits weighing 2.0 to 2.2 kg to monitor the *in vivo* transit behavior of the prepared floating hollow microspheres. The animals were fasted for 12 h before the start of the experiment. The absence of radioopaque material in the gastro intestinal tract was confirmed by taking the first radiographic image of the animal. The optimized formulations, which showed good *in vitro* buoyancy and sustained-release behavior were selected for the study. The optimized formulation *i.e.* FFMG6 batch was administered to rabbits.

RESULTS AND DISCUSSION

Micromeritic evaluation of gabapentin microspheres

The designed formulations possessed an average particulate size between 198.55 ± 0.28 and 469.3 ± 0.09 µm. *Ci* values range from 2.62 ± 0.61 and 19.81 ± 0.93 that indicate poor to excellent microspheres flow. All the formulations exhibited *Hr* values below 1.25 that indicate good flow characteristics. Besides, angle of repose value less than 25 indicates good flow properties.

Evaluation of preliminary batches of gabapentin microspheres

The percentage yield was 54.5 ± 0.92 to 91.18 ± 0.24 and *in vitro* buoyancy 68.89 ± 0.44 to 92.41 ± 0.21 for preliminary batches prepared. Drug loading in all formulation batches was good and ranged from 7.778 ± 0.39 to 10.03 ± 0.05. The swelling study revealed the swelling properties of the polymers used and the swelling index was found between 675.0 ± 2.37 to 856.3 ± 0.19. The results are demonstrated in Table 3.

In vitro drug release

The SGF (pH 1.2) was used for *in vitro* drug release experiments. The drug release for batch FMG3 was highest among the preliminary batches 98.64%. The result is shown in Figure 1.

Evaluation of gabapentin microspheres factorial batches

Micromeritic evaluation of gabapentin factorial batches

The average particle size of the floating microsphere formulations (FFMG1-FFMG9) ranged from 185.63 ± 0.13 to 510.04 ± 0.09 µm. Formulations representing an increase in cellulose acetate phthalate and HPMC k15 concentrations demonstrated a rise in the size of the particle. This can be attributed to increased relative viscosity of cellulose acetate phthalate and HPMC k15, which takes great energy to cut droplets and is harder to spread by enhancing interfacial tension and reducing shearing ability, contributing to the formation of major droplets of floating microspheres when polymer solution is added. The bulk and tapped formulation densities were observed between 0.410 ± 0.11 to 0.875 ± 0.12 and 0.463 ± 0.14 to 0.91 ± 0.16, respectively. The Carr's index indicates how microsphere bridges are formed. The values of all formulations ranged from 0.25 ± 0.06 to 12.15 ± 0.28, which showed excellent microsphere flow and compression, except formulation FFMG7, which shows 35.21 ± 0.15. The Hausner ratio for the cohesion of microspheres particles was calculated. All formulations had values below 1.54, which indicates strong flow characteristics with simple handling during processing. The angle of repose values of formulations was below 21, suggesting microspheres free-flow characteristics. The stronger microspheres flow means that the development of floating microspheres was non-aggregated. The improved flow can be attributed to changes in the particle shape and size of the prepared microspheres, resulting in reduced friction.

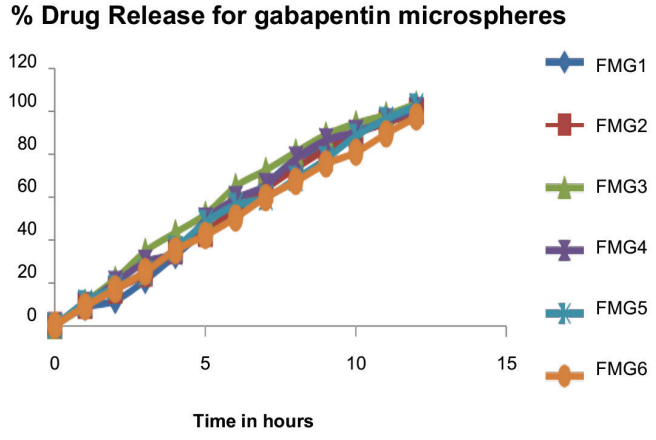

Figure 1. % drug release for gabapentin microspheres for preliminary batches

Evaluation of designed floating microspheres batches

To assess the polymer impact on the formulations, percentage yield of the floating microsphere was studied. The result indicates that the FFMG1 to FFMG9 percentage yields, as shown in Table 4, vary from 53.5 ± 0.95 to 96.64 ± 0.42. The rise in the polymer concentration contributed to an increase in percentage yield. This impact could be clarified by the fact that with the increasing concentration of alginate, the quantity of polymer is sufficient for gabapentin particles.

Drug trapping was linked to the permeation features of used polymers that would simplify the dissemination of a section of a medium stuck in floating microsphere preparation. With the polymer concentration, drug entrapment effectiveness improved. Table 4 presents the results. This is because the content of polymer has increased and more gabapentin particles are covered such that the encapsulation performance is improved.

The buoyancy percentage was studied and all formulations were observed to float for 12 h on the dissolution medium (0.1 N HCl, pH 1.2). The microspheres buoyancy percentage was observed to decline with a rise in cellulose acetate phthalate concentration (Table 4). This is due to the high viscosity of the polymer solution, which in turn leads to more dense microspheres and fewer pores besides cavities during preparation.

The drug loading in gabapentin microspheres was found to be 8.324 ± 0.23 to 11.843 ± 0.44. The swelling index was 756.34 ± 1.48 to 890.46 ± 0.78 indicating more swelling and hydration of microspheres. Besides, gastric residence time was also increased to a greater extent.

In vitro drug release for gabapentin factorial batches

The drug release was studied in SGF. The batch FFMG6 containing 0.5:0.75 polymer concentration exhibited maximum drug release (99.1%) relative to other batches. This indicates that batch FFMG6 contained the optimum concentration of

Table 3. Evaluation of preliminary batches of gabapentin microspheres

Formulation code	Percentage yield	Drug entrapment efficiency	*In vitro* buoyancy	Drug loading of microspheres	Swelling measurement
FMG1	54.5 ± 0.92	73.4 ± 0.07	80.22 ± 0.21	8.242 ± 0.40	789.4 ± 3.86
FMG2	67.07 ± 0.87	81.5 ± 0.05	76.12 ± 0.53	8.998 ± 0.34	840.0 ± 2.46
FMG3	91.18 ± 0.24	92.3 ± 0.04	92.41 ± 0.21	9.674 ± 0.22	856.3 ± 0.19
FMG4	72.88 ± 0.67	84.3 ± 0.15	68.89 ± 0.44	10.03 ± 0.05	810.2 ± 0.23
FMG5	84.2 ± 0.36	88.7 ± 0.09	70.17 ± 0.37	7.936 ± 0.46	675.0 ± 2.37
FMG6	69.3 ± 0.46	76.15 ± 0.11	72.21 ± 0.77	± 0.39	750.0 ± 0.70

polymer required for desired drug release. The drug release profiles of the designed batches are presented in Figure 2.

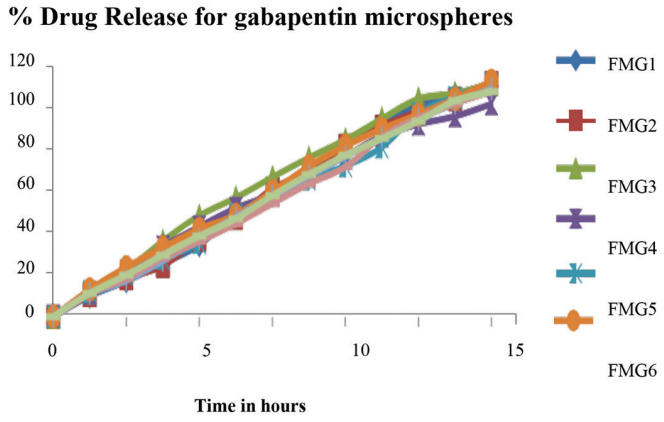

Figure 2. Drug release study for gabapentin microspheres

Scanning electron microscopy

The surface morphology of the microspheres was examined by SEM study. Figure 3 shows SEM images of microspheres taken in various magnifications. The SEM images showed the circular, isolated, and free-flowing microsphere. The surfaces were often slightly rough and drug crystals often existed on the microsphere surface. These drug crystals were liable for the explosion of the drug from the microspheres.

Drug release kinetics

To analysis, the gabapentin release mechanism *in vitro*, different release equations and kinetic models were fitted (zero order, first order, Korsmeyer-Peppas and Higuchi) for all selected batches. When the release profile was compared with the square root of time, a linear connection with the regression coefficient was observed nearly one. When *n* takes 0.5, it suggests diffusion-controlled release and indicates swelling-controlled release of medicines for value 1. A value of *n* within 0.5 to 1 represents the release mechanism by diffusion and swelling (anomalous transport). The optimized formulation FFMG6 shows an *n* value

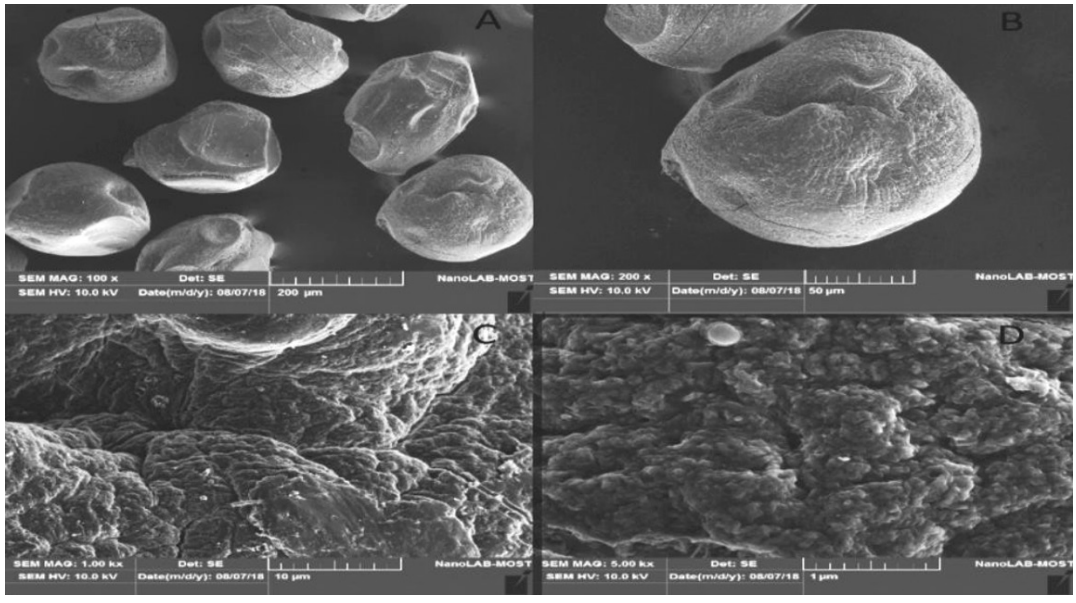

Figure 3. Surface analysis for gabapentin microspheres drug release kinetics

Table 4. Evaluation of designed floating microsphere formulation

Formulation code	Percentage yield	Drug entrapment efficiency	*In vitro* buoyancy	Drug loading	Swelling index
FFMG1	53.5 ± 0.95	74.28 ± 0.07	94.01 ± 0.21	8.324 ± 0.23	756.34 ± 1.48
FFMG2	65.09 ± 0.81	82.87 ± 0.05	93.18 ± 0.53	8.786 ± 0.56	855.23 ± 1.38
FFMG3	70.89 ± 0.64	86.28 ± 0.15	85.72 ± 0.44	9.557 ± 0.12	787.57 ± 0.16
FFMG4	90.23 ± 0.21	94.18 ± 0.04	90.43 ± 0.21	10.34 ± 0.10	816.49 ± 0.37
FFMG5	91.35 ± 0.34	90.18 ± 0.09	80.38 ± 0.37	8.945 ± 0.46	756.83 ± 2.46
FFMG6	96.64 ± 0.42	97.37 ± 0.11	95.25 ± 0.77	11.843 ± 0.44	890.46 ± 0.78
FFMG7	90.17 ± 0.23	93.18 ± 0.12	92.67 ± 0.69	9.475 ± 0.48	779.90 ± 3.16
FFMG8	89.27 ± 0.12	94.87 ± 0.36	90.89 ± 0.18	9.734 ± 0.59	798.90 ± 2.15
FFMG9	93.19 ± 0.44	92.81 ± 0.67	94.78 ± 0.16	9.285 ± 0.30	835.19 ± 0.23

of 0.8474 and an R^2 value of 0.9965. Hence, it can be concluded that the optimized formulation obeys the Korsmeyer-Peppas release kinetic model. The obtained results are demonstrated in Figure 4.

Statistical analysis and response surface study of factorial batches

The drug release and floating lag time were selected as dependent variables, and the effect of independent variables was studied on these responses. The ANOVA study showed that the selected independent variables HPMC K100 and cellulose acetate phthalate significantly affected the responses (p<0.05) (Table 5, Figure 5).

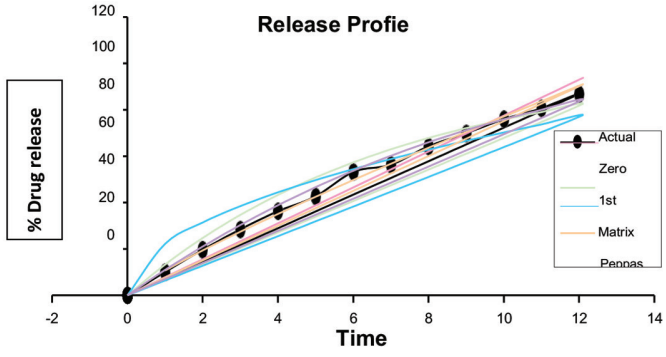

Figure 4. Drug release kinetics for gabapentin microspheres for batch FFMG6

Final equations in the terms of actual factors

Drug release= +96.17222 + 2.18833 HPMC K100 + 2.21833 cellulose acetate phthalate- 1.83000 HPMC K100 *Cellulose acetate phthalate (Table 6).

Final equations in the terms of actual factors

Floating lag time= +63.01111 + 2.55500 HPMC K100 + 9.95167

Cellulose acetate phthalate -1.6150 HPMC K100 * cellulose acetate

Phthalate +12.08833 HPMC K100² + 3.58833 cellulose acetate phthalate² (Figure 6)

Stability study

The stability study was conducted as *per* ICH guidelines and indicated that developed microspheres were stable. This was evident from the unchanged properties of the microspheres after the duration of the study.

In vivo study

After oral dosing, it was obvious to the stomach clearly the hard gelatin capsules comprising $BaSO_4$ loaded hollow floating microspheres. All microspheres were observed scattered inside the stomach in the radiographic image within an hour. Dense microsphere images were seen at first hours, but with time passing, the microsphere images became lighter. This may be due to the distribution and scattering in the GI area of the microsphere. The images showed that these floating hollow microspheres were successfully stored for up to 12 h in the stomach (Figure 7).

Table 5. Response 1. Drug release for 2FI model using ANOVA[12]

Source	Sum of squares	df	Mean square	F value	*p* value	
Model	71.65	3	23.88	66.57	0.0002	Significant
A- HPMC K100	28.73	1	28.73	80.08	0.0003	-
B- Cellulose acetate phthalate	29.53	1	29.53	82.29	0.0003	-
AB	13.40	1	13.40	37.34	0.0017	-
Residual	1.79	5	0.3588	-	-	-
Cor total	73.45	8	-	-	-	-

ANOVA for 2FI model

Table 6. Response 2. Floating lag time for quadratic model using ANOVA[12]

Source	Sum of squares	df	Mean square	F value	*p* value	
Model	961.82	5	192.36	31.69	0.0085	Significant
A- HPMC K100	39.17	1	39.17	6.45	0.0847	-
B- Cellulose acetate phthalate	594.21	1	594.21	97.90	0.0022	-
AB	10.43	1	10.43	1.72	0.2812	-
A^2	292.26	1	292.26	48.15	0.0061	-
B^2	25.75	1	25.75	4.24	0.1315	-
Residual	18.21	3	6.07	-	-	-
Cor total	980.03	8	-	-	-	-

ANOVA for quadratic model

CONCLUSION

The floating microspheres of gabapentin were prepared and evaluated by 3^2 factorial design using HPMC K100 and cellulose acetate phthalate as polymers. The micromeritic study showed that the designed microsphere formulation displays better bulk and flow properties with optimum particle size. Moreover, FFMG6 batch was optimized based on the maximum drug release (99.1%). The developed microsphere formulations possessed optimum evaluation parameters, as evident from the study. The optimized formulation obeyed Korsmeyer-Peppas

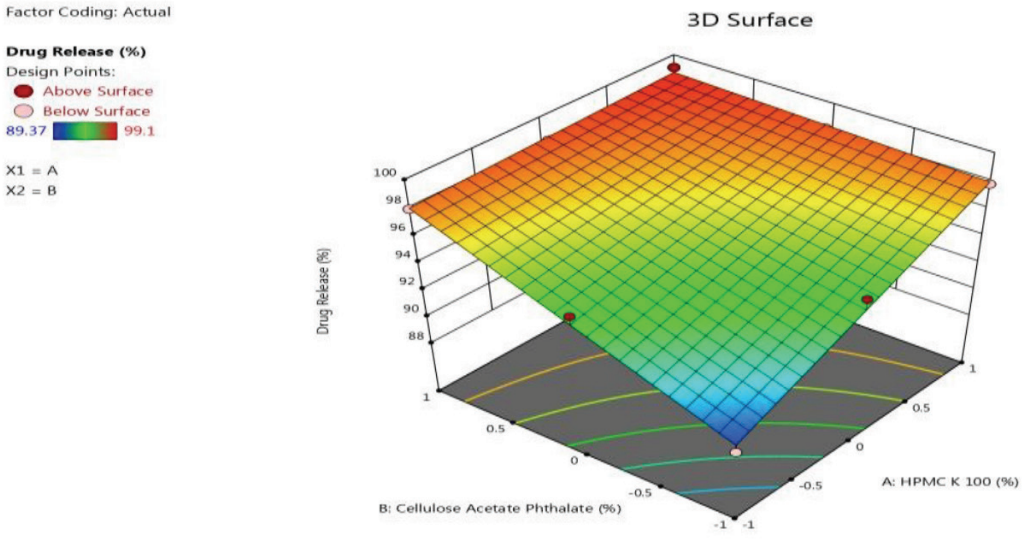

Figure 5. 3D plot for % drug release for factorial batches of gabapentin microspheres

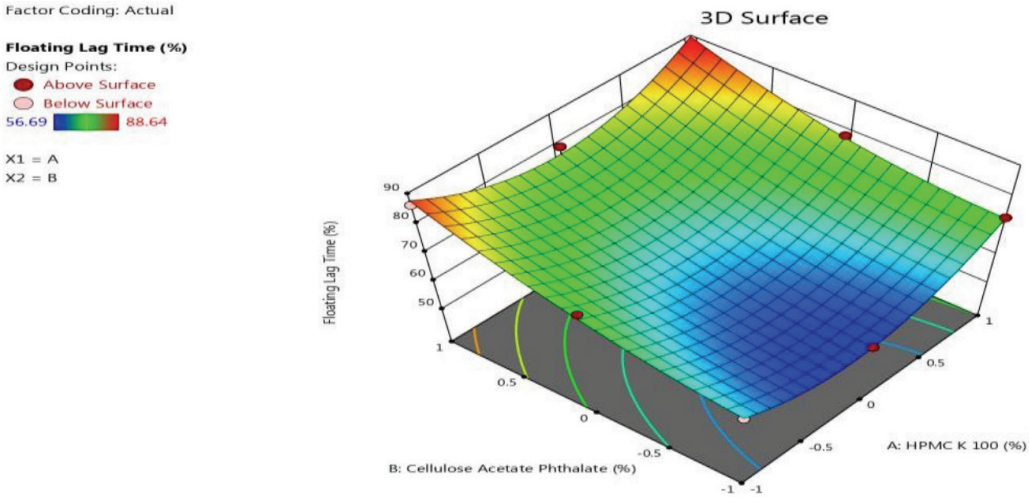

Figure 6. 3D plot for floating lag time for factorial batches of gabapentin microspheres

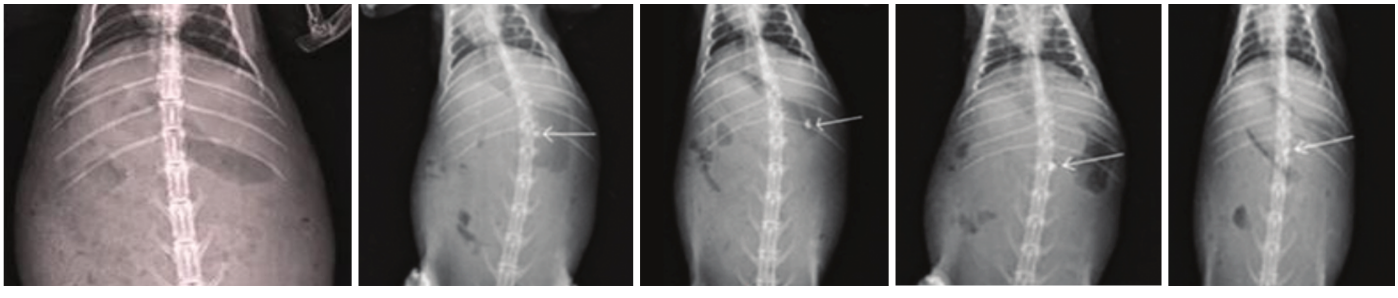

Figure 7. *In vivo* images for gabapentin microspheres (a) for 0 hrs (b) for 3 hrs (c) for 6 hrs (d) for 9 hrs (e) for 12 hrs

release kinetic model and SEM images showed spherical, discrete, and freely floating microspheres. Besides, floating hollow microspheres were successfully stored up to twelve hours in the stomach. The gastroretentive microspheres were stable under appropriate storage conditions. Therefore, the designed floating microspheres can be used for the delivery of the drugs like gabapentin.

Ethics

Ethics Committee Approval: The research article entitled "Development and evaluation of floating microspheres of anticonvulsant drug by 32 full factorial design" was carried out at IBSS College of Pharmacy, Malkapur (MS) India, and the has been approved by institutional ethical committee of this institute to carry out the experiment based on animals. Our CPCSEA establishment no: 1336/AC/10/CPCSEA.

Informed Consent: Not applicable.

Peer-review: Externally peer-reviewed.

Authorship Contributions

Surgical and Medical Practices: S.S., Concept: M.B., Design: M.B., Data Collection or Processing: M.B., K.S., S.J., N.B., Analysis or Interpretation: P.B., Literature Search: M.B., Writing: S.S., M.B.

Conflict of Interest: No conflict of interest was declared by the authors.

Financial Disclosure: The authors declared that this study received no financial support.

REFERENCES

1. Shukla P, Vaani V. Review article on microsphere. Int J Pharm Anal Res. 2015;4:291-301.
2. Abbas AK, Alhamdany AT. Floating microspheres of enalapril maleate as a developed controlled release dosage form: investigation of the effect of an ionotropic gelation technique. Turk J Pharm Sci. 2020;17:159-171.
3. Amoyav B, Benny O. Microfluidic based fabrication and characterization of highly porous polymeric microspheres. Polymers (Basel). 2019;11:419.
4. Kesharvani S, Jaiswal PK, Mukerjee A, Singh AK. Formulation and evaluation of metformin hydrochloride loaded floating microspheres. Int J Pharm Pharm Sci. 2019;12:74-82.
5. Mwila C, Walker RB. Improved stability of rifampicin in the presence of gastric-resistant isoniazid microspheres in acidic media. Pharmaceutics. 2020;12:234.
6. Farooq U, Khan S, Nawaz S, Ranjha NM, Haider MS, Khan MM, Dar E, Nawaz A. Enhanced gastric retention and drug release *via* development of novel floating microspheres based on Eudragit E100 and polycaprolactone: synthesis and *in vitro* evaluation. Des Monomers Polym. 2017;20:419-433.
7. Pi C, Feng T, Liang J, Liu H, Huang D, Zhan C, Yuan J, Lee RJ, Zhao L, Wei Y. Polymer blends used to develop felodipine-loaded hollow microspheres for improved oral bioavailability. Int J Biol Macromol. 2018;112:1038-1047.
8. Khattab A, Zaki N. Optimization and evaluation of gastroretentive ranitidine HCl microspheres by using factorial design with improved bioavailability and mucosal integrity in ulcer model. AAPS PharmSciTech. 2017;18:957-973.
9. Yang L, Wang S, Ma O, Song Z, Hou R, Huang S, Cheng D, Zhang Z. Fabrication of sulfoxaflor-loaded natural polysaccharide floating hydrogel microspheres against Nilaparvata lugens (Stal) in rice fields. Pest Manag Sci. 2020. Doi: 10.1002/ps.5855.
10. Amin ML, Ahmed T, Mannan MA. Development of floating-mucoadhesive microsphere for site specific release of metronidazole. Adv Pharm Bull. 2016;6:195-200.
11. Purohit KK, Garud N. Formulation and evaluation of floating microspheres of losartan potassium using sodium alginate and HPMC by solvent evaporation method. J Drug Deliv Ther. 2019;9: 60-66.
12. Bhavani J, Saloni S, Rajeshri D. Formulation and evaluation of floating microspheres using factorial design. Int J Recent Sci Res. 2019;10:36363-36370.
13. Maeng M, Choi S, Shahi NK, Dockko S. Experimental approaches for identifying the impact of enhanced flotation technology using hollow microspheres. J Environ Manage. 2020:253.
14. Ramadan AA, Elbakry AM, Sarhan HA, Ali SH. Silymarin loaded floating polymer(s) microspheres: characterization, *in-vitro*/*in-vivo* evaluation. Pharm Dev Technol. 2020;2:76-81.
15. Gadad AP, Naik SS, Dandagi PM, Bolmal UB. Formulation and evaluation of gastroretentive floating microspheres of lafutidine. Indian J Pharm Edu Res. 2016;50:S76-S81.
16. Gupta R, Prajapati SK, Pattnaik S, Bhardwaj P. Formulation and evaluation of novel stomach specific floating microspheres bearing famotidine for treatment of gastric ulcer and their radiographic study. Asian Pac J Trop Biomed. 2014;4:729-735.

Turk J Pharm Sci 2022;19(5):603-609
DOI: 10.4274/tjps.galenos.2021.29488

REVIEW

Hepcidin as a Potential Biomarker for the Diagnosis of Anemia

Zainab H. FATHI*, Jehan A. MOHAMMAD, Zaid M. YOUNUS, Sameer M. MAHMOOD

University of Mosul, College of Pharmacy, Department of Pharmacognosy and Medicinal Plants, Mosul, Iraq

ABSTRACT

There are several blood-based markers to assess iron stores, but they all have some limitations. Hepcidin, a low-molecular-weight peptide hormone, is produced mainly by the liver. It is the main regulator of iron homeostasis by preventing iron release into plasma from absorptive enterocytes and macrophages. This review aims to critically assess existing data on potential role of hepcidin in diagnosis, particularly the (pre) analytical implications of the hepcidin measurement. There is a well-known causative correlation between hepcidin and iron deficiency. Therefore, hepcidin is considered as a promising marker in the assessment of iron status, particularly in patients with a diagnostic dilemma, such as patients with chronic renal disease and infants. The clinical implications of this peptide hormone in diagnosis of other diseases have been expanded in the recent studies, including elevated hepcidin levels in neoplastic diseases, sepsis, and inflammation. The potential role of hepcidin in diagnosis is controversial in the various types of iron deficiency because data are conflicting (as in anaemia of chronic disease) or limited (as in infants), whereas in the case of hereditary haemochromatosis, it has been proposed that hepcidin may be used for stratification of molecular testing, or to improve the frequency of phlebotomy, however, this issue still needs to be investigated. Due to lack of a clinically approved test, the medical application of this peptide as a biomarker in diagnosis is restricted. Recently, assays have been developed to determine hepcidin levels in serum and urine, facilitating the future use of hepcidin in research and clinical practice.

Key words: Hepcidin, iron deficiency, anemia, peptide hormone

INTRODUCTION

Biologically important hemoproteins such as hemoglobin (Hb) and myoglobin contain iron as an essential element. Therefore, iron homeostasis is critical for normal erythropoiesis and other cellular processes.[1] As there is no regulatory mechanism for excreting iron from the body apart from losses due to menstruation and other bleeding processes, dietary iron uptake and status of internal iron stores are the major regulators of constant iron balance.[2] Anemia represents a worldwide public health problem with symptoms caused either by nutrient deficiency to hereditary changes in absorption and metabolism of iron.[3] Although different forms of enzymes and proteins have been involved in iron transporting, it was found that iron homeostasis is tightly controlled *via* a hepatic-produced hormone, *i.e.* hepcidin, by tightly affecting the production of erythrocytes. Therefore, discovery of hepcidin in 2001 changed our understanding of iron problems and its measurement should help with diagnosis and treatment.[4] High levels of hepcidin inhibit intestinal absorption and macrophage recycling of iron, resulting in iron-restricted erythropoiesis and anemia. In contrast, low levels of hepcidin stimulate the supply of iron to the bone marrow for Hb synthesis and production of erythrocytes.[5] Erythropoiesis, after erythropoietin therapy or hemorrhage, inhibits hepcidin by decreasing transferrin saturation and releasing of erythroblast and the hepcidin inhibitor (erythroferrone). However, decreased erythropoiesis, reducing iron consumption, increasing transferrin saturation and stimulating hepcidin transcription.[6]

Hepcidin acts by binding with a ferroprotein, a multipass membrane protein and thus inhibiting the iron efflux into the plasma.[7] Many studies have confirmed the relationship between hepcidin production and pathogenesis of iron-linked diseases.[8-10] Elevated hepcidin levels may be associated with anemia unresponsive to treatment with iron, while decreased plasma hepcidin may result in excess iron in the circulation with tissue-iron deposition.[10,11] Additionally,

*Correspondence: zainabh@uomosul.edu.iq, Phone: +009647738502141, ORCID-ID: orcid.org/0000-0003-0327-0914
Received: 10.04.2021, Accepted: 26.08.2021

higher hepcidin levels have been involved in many clinical conditions, such as inflammation, neoplastic diseases, and sepsis.[2,12,13] In future, the dependence on proven detection methods will enhance the possibility of hepcidin use as a novel biomarker in clinical practice.

Hepcidin synthesis and regulation

Hepcidin is a small cationic peptide of 25 amino acids and mass of 2.7 kDa. Because of its antifungal and antibacterial activities, hepcidin was first identified as a hepatic produced antimicrobial proteins.[14] Then, the antimicrobial activity and origin of hepcidin were found in the liver, reflecting its new official nomenclature. Although the major source of hepcidin synthesis is in the liver, recent findings also revealed extra-hepatic synthesis of hepcidin in the kidney, heart, retina, alveolar cells, bacteria-activated neutrophils, macrophages, pancreatic β-cells, and adipocytes.[15] However, substantially lower expression of hepcidin gene has been observed in these tissues compared to with hepatic production and its relative importance remains unknown.

Hepcidin peptide in humans is encoded by the *hepcidin antimicrobial peptide* gene that present in chromosome 19. Hepcidin is encoded as a preprohepcidin protein, a 84 amino acid precursor, which is subsequently converted to the bioactive hepcidin peptide by two sequential cleavages in the cytoplasm of hepatocyte and in the blood.[1] After hepatic production, hepcidin reaches blood circulation and provides widespread in the tissues. All hepcidin isoforms 20, 22, and 25 are excreted in urine. Hepcidin-20 and 22 are regarded as degradation byproducts of hepcidin.[2]

As indicated by nuclear magnetic resonance (NMR) spectroscopy studies, human hepcidin's molecular structure consists of one beta sheet in the peptide backbone, which has an eight cysteine loop formed by four disulfide bonding molecules. It is considered necessary to perform out biological activities with cysteine and *N*-terminal amino acids, which form the copper and nickel binding (ATCUN) motif.[14] Hepcidin works in three primary iron-metabolism target cell types, namely, enterocytes, hepatocytes, and reticuloendothelial macrophages, which are considered the three primary plasma iron sources (transferrin-Fe2+). Hb incorporated in the erythrocytes is attributed to approximately 66% iron in the human body. Macrophages ingest senescent erythrocytes, then releasing iron in blood or storing it as ferritin. Similarly, intestinal epithelial cells absorb all heme and non-heme iron, thus resulting in iron released in plasma or iron stored as ferritin. Endocytosis is used in cells expressing transferrin receptors to get transferrin from the bloodstream.[2] This iron is used for erythropoiesis by bone marrow erythroid cells, while it is used for storage by liver cells. Ferroportin is the iron exporter across membranes responsible for iron efflux from tissue to the circulation for use in erythropoiesis. Hepcidin binds with ferroportin and induces an adverse effect on erythropoiesis by stimulating the uptake and then degradation of ferroportin.[7,10,16]

Pathogenesis of iron metabolism disorders

Iron deficiency diseases are the first type of iron metabolism disease. Iron deficiency conditions are associated with reduction of ferritin, reduced serum iron and transferrin saturation, microcytosis, and hypochromia. However, in certain cases, like newborns, inflammatory diseases, or severe renal disorders using erythropoietin-stimulant medications, the diagnosis of iron deficiency diseases depending on these laboratory results is difficult. Therefore, hepcidin may be an important biomarker in these situations.

Hepcidin in clinical diagnosis

Plasma levels of hepcidin are well correlated with plasma ferritin in healthy persons. Moreover, serum hepcidin concentrations are significantly reduced in iron deficit patients.[17] Hepcidin is an acute phase protein of type II, with elevated hepcidin correlating with higher serum ferritin in severe inflammations.[18,19] In comparison with traditional biomarkers, hepcidin with ferritin has significant value in diagnosis of different forms of iron diseases.[20] In addition to importance of ferritin as a reliable biomarker for iron storage, the pathogenesis of many iron conditions like anemia of chronic disease (ACD) or haemochromatosis includes variations in hepcidin levels. Thus, hepcidin determination may provide an indicator on etiology of iron diseases and enable diagnosis before depletion of iron stores.[17] The diagnostic role of hepcidin in situations that have diagnostic difficulties with traditional biomarkers is outlined below.

Hepcidin in infants with iron deficiency anemia (IDA)

Infants with iron-deficient erythropoiesis or latent iron deficiency had difficulty in diagnosis with the conventional iron laboratory parameters. In these infants, ferritin is not an ideal indicator of anemia so that transferrin levels are often low in infants. Additionally, there is no diagnostic benefit for serum transferrin receptor (sTfR).[21] To avoid permanent changes of neurodevelopment, early diagnosis of iron deficiency in children is necessary.[22] The content of reticulocyte Hb (CHr) represented the availability of iron for incorporation in the bone marrow just a few days earlier. The best iron indicator for infants seems to be CHr,[23] but there is still limited availability of this test. Even before anemia occurs, hepcidin has been recommended to diagnose children with iron deficiency.[20]

Genetic diseases rarely result in IDA in children. Iron-refractory IDA (IRIDA) is a genetic disease marked by inherited hypochromic microcytic anemia, typically unresponsive to oral intake of iron, and partially improves with intravenous intake of iron. In IRIDA patients, mutations are heterogeneous, including splicing, frame-shift, nonsense and missense mutations in TMPRSS6, an encoding gene for matriptase-2. Normally, matriptase-2 suppresses the expression of hepcidin. Mutation in this gene contributes to improperly elevated hepcidin levels in humans and animals, making intestinal absorption of iron impossible.[24-26] Early diagnosis of iron deficiency diseases is impossible with the traditional biomarkers and is required to use the appropriate iron therapy (parenteral). Therefore, hepcidin quantification can provide a diagnostic method for IRIDA to direct genetic testing.

Hepcidin can identify iron deficiency before the development of anemia develops, generating a potential identification method in infants. Nevertheless, no trials have yet evaluated the application of hepcidin. Moreover, trials in infants revealed no correlation between prohepcidin and iron status.[27-29] Since infants cannot control intestinal absorption of iron, it is likely that it would not have any diagnostic benefit for hepcidin because hepcidin is the regulator of iron absorption.[30] Trials must explain why IRIDA does not respond to oral therapy of iron. Without inflammation, IRIDA may be suspected in patients with iron deficiency and elevated serum hepcidin. Moreover, another study demonstrated that in elderly anemic individuals with concomitant inflammation, hepcidin is not better than ferritin in the diagnosis of iron deficiency. In these patients, hepcidin has a significant positive association with ferritin and C-reactive protein.[31] Unfortunately, no trials have examined hepcidin in the diagnosis of iron deficiency.

Hepcidin in anemia of chronic diseases with or without iron deficiency anemia

Higher levels of serum hepcidin are crucial for pathogenesis of ACD. The ACD is identified by cytokines-induced macrophage iron retention, which is partly mediated by elevated serum hepcidin, triggered by interleukin-6.[26,32] ACD is associated with normochromic normocytic anemia and reduced reticulocyte numbers, accompanied by erythropoiesis inhibition.[32] It is difficult to diagnose iron deficiency in ACD patients because coexisting blood loss drug intake or inborn defect in Hb synthesis could affect them. Concerning to treatment, it is critical to differentiate between ACD with iron deficiency and ACD, where iron therapy is essential in the first case, but controversial and not currently recommended in the second.[32] Ferritin and other biochemical markers of iron are influenced by acute phase reaction. Therefore, it is difficult to distinguish between ACDs with or without iron deficiency depending on serum ferritin. In both cases, reduced iron level and low saturation of transferrin are recognized. ACD patients with IDA often have microcytes with severe anemia compared to those with ACD alone.[32] The sTfR is, newer marker, a truncated portion of the membrane receptor, which increases in deficiency of iron available for erythropoiesis. The sTfR/ferritin ratio could help differentiate ACDs with or without iron deficiency. However, this ratio is not commonly used in clinical practice because of the lack of standardization of the sTfR assays.[21] Hepcidin is controlled by inflammation and by iron in the body.[33] Hepcidin levels may be able to distinguish between ACDs with or without iron deficiency depending on the predominant regulatory mechanism. Interestingly, increased production of cytokines like interferon gamma by lymphocytes and interleukin1-β and 6 and tumor necrosis factor-alpha by macrophages reduces synthesis of endogenous erythropoietin, inhibits the erythropoiesis process, enhances serum levels of hepcidin, and, hence, activates erythrophagocytosis.[34]

Serum hepcidin levels are considerably lower in iron deficiency patients compared with healthy subjects.[17,35] Hepcidin is increases by inflammation in ACD.[36] Hepcidin levels in urine have shown to respond markedly better in acute phases after injection of lipopolysaccharide in healthy persons than serum ferritin.[19] Hepcidin also may be more likely to be more susceptible to iron imbalances than ferritin or other biomarkers. This remains completely default. Because hepcidin is involved in the acute phase reaction, the usage of hepcidin measurement is uncertain. Just few clinical trials have examined whether hepcidin levels have become a valuable biomarker for iron deficiency diagnosis in ACD patients with or without IDA. In initial trials, the predominant regulator for the hepcidin was deficient iron stores because serum hepcidin was low in IDA, irrespective of inflammation, and hence, the possibility for a hepcidin cut-off could be established to distinguish ACD with or without IDA.[26,37,38] Nevertheless, even ferritin differs considerably within the ACD subgroups with or without iron deficiency, rendering it difficult to understand a possible benefit additional to hepcidin compared to ferritin in inflammation.[26]

Till now, there have been no trials establishing a definite limit for the IDA diagnosis. A study by Lasocki et al.[37] identified an iron deficiency cut-off in patients with intensive care. Just 5 of 51 patients suffered from iron deficiency (just 3 with concurrent inflammation). Recently, studies revealed the difficulty in distinguishing between ACD with and without iron deficiency depending on the serum hepcidin. Thomas et al.[39] identified latent IDA, ID, ACD, and ACD with IDA in anemic patients, depending on ferritin index plot. ACD was not distinguished from ACD/IDA by hepcidin only. Nevertheless, Thomas et al.[39] showed that combining hepcidin and CHr instead of ferritin index plot because hepcidin could react to the hematologic state quicker than ferritin. Therefore, it is important to remember that the only rapid reaction of hepcidin seen to date is a rapid rise in the urine due to inflammation.[19] As a result, more studies must establish the variation in hepcidin among ACD, IDA and ACD with IDA. Moreover, the importance of hepcidin measurement as a diagnostic marker needs to be evaluated in patients with unclear IDA.

One proposed approach to predicting classical IRIDA is to normalize hepcidin to other iron markers such as the ratio of transferrin saturation/log hepcidin or transferrin saturation/log ferritin.[40] Another study revealed that most severe IRIDA patients are biallelic TMPRSS6 mutations and, when unrecognized, the second allele may be genetically obscure.[41] Generally, people with two allele mutations have a more severe phenotype and are less responsive to iron therapy than those with one allele mutation.[40] Interestingly, many TMPRSS6 single-nucleotide polymorphisms have been detected in blood donors to increase susceptibility to iron deficiency.[42]

Hepcidin and iron deficiency in chronic renal disorders

Erythropoietin-stimulating agents (ESA) produce a substantial rise in erythropoietic activity in chronic renal disorder, which is followed by a sharp increase in demand for bioavailable iron. Even with adequate storage of iron in the body and intake of oral iron therapy, ESA can produce a reduction in iron levels and transferrin desaturation, leading to iron deficient erythropoiesis.[21] This represents the third obstacle in the

diagnosis of iron deficiency. Diagnosis of this disease requires the appropriate dose of ESA or intravenous iron for optimal response. Iron deficiency is predicted by low ferritin, but ferritin is unpredictable because of common inflammation-induced effects.[43] The saturation of transferrin reduces with inflammation and variates with serum iron changes daily. Moreover, after several weeks after parenteral iron, it is not interpretable (100% saturation). In patients with inflammation, elevated ferritin and ~20 percent transferrin saturation, functional iron deficiency may be suspected. Although transferrin saturation and ferritin are the major parameters in the diagnosis of iron deficiency, trials to find a better index continues.[44,45] The percentage of red hypochromic cells will recognize developing IDA, but for changes in this marker, it takes long periods of iron deficient erythropoiesis. Reticulocyte number and Hb alteration can distinguish patients as "responding" or "unresponders". CHr appears to be a promising predictor of ESA dosage.[21,46] Therefore, it appears worth to investigating the additional importance of hepcidin in this situation.

Hepcidin has been recognized as a major determinant in the pathogenesis of anemia in patients with chronic kidney disease (CKD), and explains the disturbed metabolism of iron and ESA resistance.[47] Hence, hepcidin may be an effective predictor of response and guidance for ESA or parenteral iron therapy. Most patients with an ineffective ESA response have functional iron deficiency, which cannot be detected by saturation of transferrin or ferritin.[21] These patients are hypothesized to have higher levels of hepcidin, thus expected to be hyporesponsive and require higher doses of ESA. In CKD and hemodialysis, elevated hepcidin levels were identified.[17,48-50] Nevertheless, not only anemia or iron can affect hepcidin concentrations in CKD, but several other factors like hypoxia, inflammation and erythropoietin (endogenous or exogenous).[51] Furthermore, hepcidin is negatively correlated with glomerular filtration rate (GFR), contributing to elevated hepcidin levels due to a reduction in renal excretion.[49] Peters et al.[52] showed no considerable association between hepcidin-25 and eGFR. However, the same study revealed that hepcidin-25, hepcidin-20, and -22 isoforms had an inverse correlation with eGFR. In the control group, hepcidin-22 was less than the measurable value, but detectable in patients with CKD and hemodialysis. With the exception of hepcidin-25, hepcidin-20, and -22 accumulated in renal failure. However, these findings need to be verified by more trials. Another study showed that dialysis can clear hepcidin, but it increased to pre-dialysis levels before the next dialysis.[53]

Clinical trials evaluating the effect of hepcidin in differentiating responder and hypo-responder to ESA are few. One study revealed no variation in the intensities of hepcidin levels between erythropoietin responsive and hypo-responsive patients.[54] In dialysis patient, hepcidin is associated with anemia and is compatible with a possible role for elevated hepcidin levels in renal anemia.[49] However, in the same study revealed an inverse correlation between hepcidin levels and the dose of erythropoietin, which reduces the effect of hepcidin in predicting a higher need for erythropoietin. Another study revealed that unresponsive patients have reduced serum hepcidin, but these findings may be biased because unresponsive patients obtained significantly higher doses of erythropoietin than responsive patients.[55] Swinkels and Wetzels[56] recommend observing the initial hepcidin changes after a first dose of parenteral iron and/or erythropoietin because a single dose will predict patient response before starting the anemia therapy. However, further trials must elucidate the potential role of hepcidin in diagnosis.

Hepcidin and iron overload

Iron-storage disorders are the second group of disorders of iron metabolism. Nevertheless, high ferritin concentrations do not have the lack of specificity to distinguish between genetic cases with a continuous deposition of iron and moderate iron overload due to disorders that affect the liver (for example; viral hepatitis, alcoholic or non-alcoholic fatty hepatic disorder).[57,58] The pathogenic factor in iron deposition of hereditary haemochromatosis (HH) type 1 (HFE hemochromatosis), the main cause of hereditary iron overload, appears to be a reduced hepcidin production from the liver.[58] Thus, the HFE C282Y homozygous induces decreased hepcidin expression, leading to the deposition of parenchymal iron. Mutations of other genes involved in hepcidin activity, synthesis, or regulation induce less common types of HH.[59] A continues erythropoiesis decreases hepcidin in anemia associated with iron overload due to inactive erythropoiesis like thalassemia, which contributes to an overload of iron in this disorder. As a result, produced a severe reduction in hepcidin levels in types treated with a non-blood transfusion method. Whereas, hepcidin levels are higher in patients severely treated with blood transfusion than those treated with non-blood methods, because of elevated iron in the body and reduced erythropoiesis.[60]

It is unclear if a distinguishing role of hepcidin presents in cases of hyperferritinaemia. When there is a family index case, the final diagnosis of HH depends on familial screening.[58] Phlebotomy is the treatment for HH. Therapy is controlled by ferritin measurement since ferritin is correlated with iron levels in the liver and is a sensitive indicator of cirrhosis, albeit with the same non-specificity difficulty. Ferritin level <50 mg/L is characterized as a consensus therapeutic target without relevant proof of its true significance.[61]

The diagnosis is based on genotyping of HH. Hepcidin can be used as a direct measure for genetic iron overload, since hepcidin levels (or hepcidin to ferritin ratio) are reduced in HH, but elevated in ferroportin disorders.[59] Clinical characteristics like Hb (which is reduced in secondary iron overload and ferroportine disorder), family history (genetic disorder), concurrent disorder (such as, hepatitis and alcoholic) and age are used for the rational targeting of genes. To stratify genetic testing, hepcidin may then be applied.[59] Therapeutically, hepcidin has a more significant use in HFE-haemochromatosis, specifically to determine need for phlebotomy. Firstly, hepcidin appears unsuitable to this objective, since abnormal levels of hepcidin trigger the disorder and are not sensitive to stores of iron. Actually, in spite of continuous phlebotomy, a persistent decrease in hepcidin results in a persistent increase in intestinal absorption of iron. Nevertheless, low hepcidin

concentrations in serum and urine much further reduced with iron loss by flebotomy in HFE-related HH patients, and this reduction in hepcidin associated with a reduction in transferrin saturation.[62,63] These findings indicate that a phlebotomy "overshot" may have an adverse effect by further reducing hepcidin, with subsequent increase in intestinal absorption of iron. Another study proposed an upward review of the existing ferritin target (less than 50 µg/L to look for the optimum balance of reduced ferritin and a minimum reduction of hepcidin.[62] Therefore, hepcidin assessments should be determined in further clinical studies. It is not obvious if the targets of phlebotomy may be identified by hepcidin levels or by the hepcidin to ferritin ratio. There are no studies available related to treatment monitoring in another HH mutation. However, hepcidin is a possible therapeutic aim in haemochromatosis, which may considerably improve the treatment and follow-up of HH patients, rendering the possible diagnostic utility of hepcidin unclear.

Recently, the association between hepcidin and cancer-related anemia has been studied. This study showed that anemia is associated with hepcidin overexpression in patients with increased C-reactive protein, suggesting that hepcidin plays a distinct role in the development of cancer-related anemia.[64]

Hepcidin assays

Developing assays to estimate hepcidin quantity in biological fluids is challenging. It is difficult to develop antibodies for laboratory tests because hepcidin is an evolutionarily conserved small peptide, which tends to aggregate and adhere to laboratory plastics.[65] However, two major assays have been developed; mass spectrometry and classical immunoassays.[66] Although mass spectrometry-based tests are more costly, they can differentiate between hepcidin isoforms. Immunoassays often lack the specificity of hepcidin-25 and detect total levels of hepcidin. However, the importance of measuring hepcidin-25 specifically rather than total hepcidin for clinical decision-making is debatable.

Absolute hepcidin levels vary considerably (up to 10 fold) between tests in the absence of a main reference material, a reference technique, and a commutable calibrator.[67] While harmonization research is ongoing, these discrepancies now prevent the possibility of comparing the data and establishing a uniform reference range.[68] Instead, each method/lab should develop strict reference ranges for age and sex, for hepcidin to serum ferritin and hepcidin to transferrin saturation ratios, in addition to that for hepcidin. Till now, only four population studies, comprising of two in Italy (n: 1577, n: 1391),[69,70] one in the Netherlands (n: 2998),[71] and one in West Africa (n: 1316),[72] have estimated differences in serum hepcidin in the general population, clearly indicating that hepcidin levels increased considerably as the number of metabolic syndrome characteristics increased.[70] Moreover, hepcidin levels are higher in postmenopausal *versus* premenopausal women and are highly correlated with serum levels of ferritin.[69,71] Furthermore, hepcidin and hepcidin to ferritin ratio were not correlated with atherosclerosis or with cardiovascular disease.[73] Whereas findings from smaller studies revealed that the within-subject variability of hepcidin levels was relatively high. Additionally, hepcidin levels were higher in prolonged fasting,[74] and revealed both circadian rhythm and significant variation (27-50%) from day to day.[75] Values of hepcidin-25 reduce within 1-2 days with storage at room temperature but they remain stable for 1 week, 4 weeks, and 2 years at 4˚C, -20˚C, and -80˚C, respectively.[76,77]

CONCLUSION

Although its exciting findings at the beginning, the data about the diagnostic utilization of hepcidin remain limited. There have been some advances in measurement of hepcidin-25 quantitatively, but several pre-analytical issues still unanswered. Recently, trials have focused on hepcidin agonists and antagonists based on their possible therapeutic applications. Now, the question: Will hepcidin can be used in diagnosis in the future?

Ethics

Peer-review: Externally peer-reviewed.

Authorship Contributions

Concept: Z.H.F., J.A.M., Design: Z.H.F., J.A.M., Data Collection or Processing: Z.H.F., J.A.M., Z.M.Y., S.M.M., Analysis or Interpretation: Z.H.F., Literature Search: Z.H.F., J.A.M., Z.M.Y., S.M.M., Writing: Z.H.F.

Conflict of Interest: No conflict of interest was declared by the authors.

Financial Disclosure: The authors declared that this study received no financial support.

REFERENCES

1. Kali A, Charles MV, Seetharam RS. Hepcidin - a novel biomarker with changing trends. Pharmacogn Rev. 2015;9:35-40.
2. Nicolae CD, Coman OA, Ene C, Nicolae I, Fulga I. Hepcidin in neoplastic disease. J Med Life. 2013;6:355-360.
3. Reichert C, Marafon F, Levy D, Maselli L, Bagatini M, Blatt S, Bydlowski S, Celso S. In book: Current Topics in Anemia, Intechopen, Edited by Jesmine Khan. 2018.
4. Girelli D, Nemeth E, Swinkels DW. Hepcidin in the diagnosis of iron disorders. Blood. 2016;127:2809-2813.
5. Pagani A, Nai A, Silvestri L, Camaschella C. Hepcidin and anemia: a tight relationship. Front Physiol. 2019;10:1294.
6. D'Angelo G. Role of hepcidin in the pathophysiology and diagnosis of anemia. Blood Res. 2013;48:10-15.
7. Robson KJ. Hepcidin and its role in iron absorption. Gut. 2004;53:617-619.
8. Fleming RE, Sly WS. Hepcidin: a putative iron-regulatory hormone relevant to hereditary hemochromatosis and the anemia of chronic disease. Proc Natl Acad Sci U S A. 2001;98:8160-8162.
9. Ganz T, Nemeth E. Iron imports. IV. Hepcidin and regulation of body iron metabolism. Am J Physiol Gastrointest Liver Physiol. 2006;290:G199-203.
10. Ashrafian H. Hepcidin: the missing link between hemochromatosis and infections. Infect Immun. 2003;71:6693-6700.

11. Lasocki S, Longrois D, Montravers P, Beaumont C. Hepcidin and anemia of the critically ill patient: bench to bedside. Anesthesiology. 2011;114:688-694.
12. Cizmeci MN, Kara S, Kanburoglu MK, Simavli S, Duvan CI, Tatli MM. Detection of cord blood hepcidin levels as a biomarker for early-onset neonatal sepsis. Med Hypotheses. 2014;82:310-312.
13. Dudkowiak R, Neubauer K, Poniewierka E. Hepcidin and its role in inflammatory bowel disease. Adv Clin Exp Med. 2013;22:585-591.
14. Kemna EH, Tjalsma H, Willems HL, Swinkels DW. Hepcidin: from discovery to differential diagnosis. Haematologica. 2008;93:90-97.
15. Piperno A, Mariani R, Trombini P, Girelli D. Hepcidin modulation in human diseases: from research to clinic. World J Gastroenterol. 2009;15:538-551.
16. Camaschella C, Silvestri L. Molecular mechanisms regulating hepcidin revealed by hepcidin disorders. Sci World J. 2011;11:1357-1366.
17. Ganz T, Olbina G, Girelli D, Nemeth E, Westerman M. Immunoassay for human serum hepcidin. Blood. 2008;112:4292-4297.
18. Nemeth E, Valore EV, Territo M, Schiller G, Lichtenstein A, Ganz T. Hepcidin, a putative mediator of anemia of inflammation, is a type II acute-phase protein. Blood. 2003;101:2461-2463.
19. Kemna E, Pickkers P, Nemeth E, van der Hoeven H, Swinkels D. Time-course analysis of hepcidin, serum iron, and plasma cytokine levels in humans injected with LPS. Blood. 2005;106:1864-1866.
20. Brugnara C. An immunoassay for human serum hepcidin at last: Ganz klar? Blood. 2008;112:3922-3923.
21. Brugnara C. Iron deficiency and erythropoiesis: new diagnostic approaches. Clin Chem. 2003;49:1573-1578.
22. Lozoff B, Jimenez E, Wolf AW. Long-term developmental outcome of infants with iron deficiency. N Engl J Med. 1991;325:687-694.
23. Brugnara C, Zurakowski D, DiCanzio J, Boyd T, Platt O. Reticulocyte hemoglobin content to diagnose iron deficiency in children. JAMA. 1999;281:2225-2230.
24. De Falco L, Totaro F, Nai A, Pagani A, Girelli D, Silvestri L, Piscopo C, Campostrini N, Dufour C, Al Manjomi F, Minkov M, Van Vuurden DG, Feliu A, Kattamis A, Camaschella C, Iolascon A. Novel TMPRSS6 mutations associated with iron-refractory iron deficiency anemia (IRIDA). Hum Mutat. 2010;31:E1390-1405.
25. Beutler E, Van Geet C, te Loo DM, Gelbart T, Crain K, Truksa J, Lee PL. Polymorphisms and mutations of human TMPRSS6 in iron deficiency anemia. Blood Cells Mol Dis. 2010;44:16-21.
26. Theurl I, Aigner E, Theurl M, Nairz M, Seifert M, Schroll A, Sonnweber T, Eberwein L, Witcher DR, Murphy AT, Wroblewski VJ, Wurz E, Datz C, Weiss G. Regulation of iron homeostasis in anemia of chronic disease and iron deficiency anemia: diagnostic and therapeutic implications. Blood. 2009;113:5277-5286.
27. Tiker F, Celik B, Tarcan A, Kilicdag H, Ozbek N, Gurakan B. Serum pro-hepcidin levels and relationships with iron parameters in healthy preterm and term newborns. Pediatr Hematol Oncol. 2006;23:293-297.
28. Ulukol B, Orhon FS, Hanoluk A, Akar N. Serum pro-hepcidin levels and relationship with ferritin in healthy non-anaemic infants. Acta Haematol. 2007;118:70-72.
29. Orhon FS, Ulukol B, Hanoluk A, Akar N. Serum pro-hepcidin levels in infants with iron deficiency anaemia. Int J Lab Hematol. 2008;30:546-547.
30. Collard KJ. Iron homeostasis in the neonate. Pediatrics. 2009;123:1208-1216.
31. Karlsson T. Evaluation of a competitive hepcidin ELISA assay in the differential diagnosis of iron deficiency anaemia with concurrent inflammation and anaemia of inflammation in elderly patients. J Inflamm (Lond). 2017;14:21.
32. Weiss G, Goodnough LT. Anemia of chronic disease. N Engl J Med. 2005;352:1011-1023.
33. Kemna EH, Kartikasari AE, van Tits LJ, Pickkers P, Tjalsma H, Swinkels DW. Regulation of hepcidin: insights from biochemical analyses on human serum samples. Blood Cells Mol Dis. 2008;40:339-346.
34. Weiss G, Ganz T, Goodnough LT. Anemia of inflammation. Blood. 2019;133:40-50.
35. Koliaraki V, Marinou M, Vassilakopoulos TP, Vavourakis E, Tsochatzis E, Pangalis GA, Papatheodoridis G, Stamoulakatou A, Swinkels DW, Papanikolaou G, Mamalaki A. A novel immunological assay for hepcidin quantification in human serum. PLoS One. 2009;4:e4581.
36. Yacoub MF, Ferwiz HF, Said F. Effect of interleukin and hepcidin in anemia of chronic diseases. Anemia. 2020;2020:3041738.
37. Lasocki S, Baron G, Driss F, Westerman M, Puy H, Boutron I, Beaumont C, Montravers P. Diagnostic accuracy of serum hepcidin for iron deficiency in critically ill patients with anemia. Intensive Care Med. 2010;36:1044-1048.
38. Cherian S, Forbes DA, Cook AG, Sanfilippo FM, Kemna EH, Swinkels DW, Burgner DP. An insight into the relationships between hepcidin, anemia, infections and inflammatory cytokines in pediatric refugees: a cross-sectional study. PLoS One. 2008;3:e4030.
39. Thomas C, Kobold U, Balan S, Roeddiger R, Thomas L. Serum hepcidin-25 may replace the ferritin index in the Thomas plot in assessing iron status in anemic patients. Int J Lab Hematol. 2011 Apr;33(2):187-93.
40. Donker AE, Schaap CC, Novotny VM, Smeets R, Peters TM, van den Heuvel BL, Raphael MF, Rijneveld AW, Appel IM, Vlot AJ, Versluijs AB, van Gelder M, Granzen B, Janssen MC, Rennings AJ, van de Veerdonk FL, Brons PP, Bakkeren DL, Nijziel MR, Vlasveld LT, Swinkels DW. Iron refractory iron deficiency anemia: a heterogeneous disease that is not always iron refractory. Am J Hematol. 2016;91:E482-E490.
41. Heeney MM, Guo D, De Falco L, Campagna DR, Olbina G, Kao PP, Schmitz-Abe K, Rahimov F, Gutschow P, Westerman K, Ostland V, Jackson T, Klaassen RJ, Markianos K, Finberg KE, Iolascon A, Westerman M, London WB, Fleming MD. Normalizing hepcidin predicts TMPRSS6 mutation status in patients with chronic iron deficiency. Blood. 2018;132:448-452. Erratum in: Blood. 2018;132:1355.
42. Sørensen E, Rigas AS, Didriksen M, Burgdorf KS, Thørner LW, Pedersen OB, Hjalgrim H, Petersen MS, Erikstrup C, Ullum H. Genetic factors influencing hemoglobin levels in 15,567 blood donors: results from the danish blood donor study. Transfusion. 2019;59:226-231.
43. Brugnara C, Colella GM, Cremins J, Langley RC Jr, Schneider TJ, Rutherford CJ, Goldberg MA. Effects of subcutaneous recombinant human erythropoietin in normal subjects: development of decreased reticulocyte hemoglobin content and iron-deficient erythropoiesis. J Lab Clin Med. 1994;123:660-667.
44. Coyne D. Iron indices: what do they really mean? Kidney Int Suppl. 2006:S4-8.
45. Katodritou E, Zervas K, Terpos E, Brugnara C. Use of erythropoiesis stimulating agents and intravenous iron for cancer and treatment-related anaemia: the need for predictors and indicators of effectiveness has not abated. Br J Haematol. 2008;142:3-10.
46. Wish JB. Assessing iron status: beyond serum ferritin and transferrin saturation. Clin J Am Soc Nephrol. 2006;1 (Suppl 1):S4-8.

47. Nakanishi T, Kimura T, Kuragano T. The hepcidin-anemia axis: pathogenesis of anemia in chronic kidney disease. Contrib Nephrol. 2019;198:124-134.

48. Li H, Rose MJ, Tran L, Zhang J, Miranda LP, James CA, Sasu BJ. Development of a method for the sensitive and quantitative determination of hepcidin in human serum using LC-MS/MS. J Pharmacol Toxicol Methods. 2009;59:171-180.

49. Ashby DR, Gale DP, Busbridge M, Murphy KG, Duncan ND, Cairns TD, Taube DH, Bloom SR, Tam FW, Chapman RS, Maxwell PH, Choi P. Plasma hepcidin levels are elevated but responsive to erythropoietin therapy in renal disease. Kidney Int. 2009;75:976-981.

50. Zaritsky J, Young B, Wang HJ, Westerman M, Olbina G, Nemeth E, Ganz T, Rivera S, Nissenson AR, Salusky IB. Hepcidin--a potential novel biomarker for iron status in chronic kidney disease. Clin J Am Soc Nephrol. 2009;4:1051-1056.

51. Babitt JL, Lin HY. Molecular mechanisms of hepcidin regulation: implications for the anemia of CKD. Am J Kidney Dis. 2010;55:726-741.

52. Peters HP, Laarakkers CM, Swinkels DW, Wetzels JF. Serum hepcidin-25 levels in patients with chronic kidney disease are independent of glomerular filtration rate. Nephrol Dial Transplant. 2010;25:848-853.

53. Weiss G, Theurl I, Eder S, Koppelstaetter C, Kurz K, Sonnweber T, Kobold U, Mayer G. Serum hepcidin concentration in chronic haemodialysis patients: associations and effects of dialysis, iron and erythropoietin therapy. Eur J Clin Invest. 2009;39:883-890.

54. Kato A, Tsuji T, Luo J, Sakao Y, Yasuda H, Hishida A. Association of prohepcidin and hepcidin-25 with erythropoietin response and ferritin in hemodialysis patients. Am J Nephrol. 2008;28:115-121.

55. Costa E, Swinkels DW, Laarakkers CM, Rocha-Pereira P, Rocha S, Reis F, Teixeira F, Miranda V, do Sameiro Faria M, Loureiro A, Quintanilha A, Belo L, Santos-Silva A. Hepcidin serum levels and resistance to recombinant human erythropoietin therapy in haemodialysis patients. Acta Haematol. 2009;122:226-229.

56. Swinkels DW, Wetzels JF. Hepcidin: a new tool in the management of anaemia in patients with chronic kidney disease? Nephrol Dial Transplant. 2008;23:2450-2453.

57. Swinkels DW, Drenth JP. Hepcidin in the management of patients with mild non-hemochromatotic iron overload: Fact or fiction? J Hepatol. 2008;49:680-685.

58. Alexander J, Kowdley KV. HFE-associated hereditary hemochromatosis. Genet Med. 2009;11:307-313.

59. Swinkels DW, Janssen MC, Bergmans J, Marx JJ. Hereditary hemochromatosis: genetic complexity and new diagnostic approaches. Clin Chem. 2006;52:950-968.

60. Nemeth E. Hepcidin in beta-thalassemia. Ann N Y Acad Sci. 2010;1202:31-35.

61. European Association for The Study of The Liver. EASL clinical practice guidelines for HFE hemochromatosis. J Hepatol. 2010;53:3-22.

62. Piperno A, Girelli D, Nemeth E, Trombini P, Bozzini C, Poggiali E, Phung Y, Ganz T, Camaschella C. Blunted hepcidin response to oral iron challenge in HFE-related hemochromatosis. Blood. 2007;110:4096-4100.

63. Bozzini C, Campostrini N, Trombini P, Nemeth E, Castagna A, Tenuti I, Corrocher R, Camaschella C, Ganz T, Olivieri O, Piperno A, Girelli D. Measurement of urinary hepcidin levels by SELDI-TOF-MS in HFE-hemochromatosis. Blood Cells Mol Dis. 2008;40:347-352.

64. Cheng Z, Yan M, Lu Y, Pan XT. Expression of serum BMP6 and hepcidin in cancer-related anemia. Hematology. 2020;25:134-138.

65. Hunter HN, Fulton DB, Ganz T, Vogel HJ. The solution structure of human hepcidin, a peptide hormone with antimicrobial activity that is involved in iron uptake and hereditary hemochromatosis. J Biol Chem. 2002;277:37597-37603.

66. Kroot JJ, Laarakkers CM, Geurts-Moespot AJ, Grebenchtchikov N, Pickkers P, van Ede AE, Peters HP, van Dongen-Lases E, Wetzels JF, Sweep FC, Tjalsma H, Swinkels DW. Immunochemical and mass-spectrometry-based serum hepcidin assays for iron metabolism disorders. Clin Chem. 2010;56:1570-1579.

67. Kroot JJ, van Herwaarden AE, Tjalsma H, Jansen RT, Hendriks JC, Swinkels DW. Second round robin for plasma hepcidin methods: first steps toward harmonization. Am J Hematol. 2012;87:977-983.

68. van der Vorm LN, Hendriks JC, Laarakkers CM, Klaver S, Armitage AE, Bamberg A, Geurts-Moespot AJ, Girelli D, Herkert M, Itkonen O, Konrad RJ, Tomosugi N, Westerman M, Bansal SS, Campostrini N, Drakesmith H, Fillet M, Olbina G, Pasricha SR, Pitts KR, Sloan JH, Tagliaro F, Weykamp CW, Swinkels DW. Toward worldwide hepcidin assay harmonization: identification of a commutable secondary reference material. Clin Chem. 2016;62:993-1001.

69. Traglia M, Girelli D, Biino G, Campostrini N, Corbella M, Sala C, Masciullo C, Viganò F, Buetti I, Pistis G, Cocca M, Camaschella C, Toniolo D. Association of HFE and TMPRSS6 genetic variants with iron and erythrocyte parameters is only in part dependent on serum hepcidin concentrations. J Med Genet. 2011;48:629-634.

70. Martinelli N, Traglia M, Campostrini N, Biino G, Corbella M, Sala C, Busti F, Masciullo C, Manna D, Previtali S, Castagna A, Pistis G, Olivieri O, Toniolo D, Camaschella C, Girelli D. Increased serum hepcidin levels in subjects with the metabolic syndrome: a population study. PLoS One. 2012;7:e48250. Erratum in: PLoS One. 2013;8:null.

71. Galesloot TE, Vermeulen SH, Geurts-Moespot AJ, Klaver SM, Kroot JJ, van Tienoven D, Wetzels JF, Kiemeney LA, Sweep FC, den Heijer M, Swinkels DW. Serum hepcidin: reference ranges and biochemical correlates in the general population. Blood. 2011;117:e218-225.

72. Jallow MW, Campino S, Prentice AM, Cerami C. Association of common TMPRSS6 and TF gene variants with hepcidin and iron status in healthy rural Gambians. Sci Rep. 2021;11:8075.

73. Pechlaner R, Kiechl S, Mayr M, Santer P, Weger S, Haschka D, Bansal SS, Willeit J, Weiss G. Correlates of serum hepcidin levels and its association with cardiovascular disease in an elderly general population. Clin Chem Lab Med. 2016;54:151-161.

74. Troutt JS, Rudling M, Persson L, Ståhle L, Angelin B, Butterfield AM, Schade AE, Cao G, Konrad RJ. Circulating human hepcidin-25 concentrations display a diurnal rhythm, increase with prolonged fasting, and are reduced by growth hormone administration. Clin Chem. 2012;58:1225-1232.

75. Kroot JJ, Hendriks JC, Laarakkers CM, Klaver SM, Kemna EH, Tjalsma H, Swinkels DW. (Pre)analytical imprecision, between-subject variability, and daily variations in serum and urine hepcidin: implications for clinical studies. Anal Biochem. 2009;389:124-129.

76. Itkonen O, Parkkinen J, Stenman UH, Hämäläinen E. Preanalytical factors and reference intervals for serum hepcidin LC-MS/MS method. Clin Chim Acta. 2012;413:696-701.

77. Laarakkers CM, Wiegerinck ET, Klaver S, Kolodziejczyk M, Gille H, Hohlbaum AM, Tjalsma H, Swinkels DW. Improved mass spectrometry assay for plasma hepcidin: detection and characterization of a novel hepcidin isoform. PLoS One. 2013;8:e75518.

Turk J Pharm Sci 2022;19(5):610-617
DOI: 10.4274/tjps.galenos.2021.40697

REVIEW

Safety in Cosmetics and Cosmetovigilance, Current Regulations in Türkiye

İmran ALTIOKKA[1,2*], Melike ÜNER[2]

[1]University of Central Florida, Burnett School of Biomedical Science, Orlando, United States of America
[2]İstanbul University, Faculty of Pharmacy, Department of Pharmaceutical Technology, İstanbul, Türkiye

ABSTRACT

Although it is considered that cosmetics do not have side effects, studies have revealed that a significant number of consumers experience side effects. Undesirable effects arising from the use of cosmetic products have created the need for a reporting and evaluation system, which is responsible for some restrictions on the use of cosmetics ingredients and putting into cosmetic regulation effect, called cosmetovigilance. However, the new cosmetovigilance concept needs some updates to become more effective for public health. For instance, side effects related to cosmetic use have been reported more frequently recently, but this rate is still quite low. Additionally, since the current cosmetic directive does not recognize cosmeceuticals as a distinct category from cosmetics, some products named cosmetic under the laws may affect the bottom layers of dermis and cause systemic side effects. Although the manufacturers must show safety assessments to the Turkish Pharmaceutical and Medical Device Agency to get a license, after launching they do not have post-vigilance reporting to the institution, which is another problem of the system. In this review, the current cosmetovigilance system in Türkiye was discussed and some hardships encountered were criticized regarding the implementation of the system. Additionally, scientific studies are conducted on cosmetic ingredients that can have side effects and contribute to the developing cosmetovigilance concept. Because of the study, the importance of the feedback of healthcare professionals in the cosmetovigilance system, the consultancy service to be given to the consumer and patient about the contents that should be considered. Besides, there is a need for new studies to indicate the adverse reaction incidence related to cosmetics in the Turkish market. Another outcome of this review article is to understand the importance of the new regulations regarding the increase in the new active ingredients in the cosmetic market.

Key words: Adverse reactions of the skin, cosmetovigilance, side effects of cosmetics, cosmetic regulations

INTRODUCTION

The concept of cosmetovigilance was first used by Vigan, a dermatologist in 1997.[1] The meaning of cosmetovigilance is the collection, evaluation, and monitoring of spontaneous reports of undesirable effects observed with the use of cosmetic products under normal or predictable conditions. The first study on a cosmetovigilance system was conducted in France in 2002.[2] Thereafter, in line with the 76/768 EEC EU cosmetics directive, the first guideline on reporting adverse reactions was published in 2005 by COLIPA, which is called an undesirable event report (COLIPA, 2005).[3,4] In 2006, after a pilot study conducting by carried out by the Council of Europe's Committee of Experts on Cosmetic Products in 2004-2005, the EU Public Health Committee decided to establish the ResAP as a cosmetovigilance system based on case reports, which forms the basis of the current system.[5] Afterward, cosmetovigilance systems were established in Belgium, Denmark, Sweden, Italy, Germany, and Norway.

The cosmetovigilance system in our country was founded by Turkish Pharmaceutical and Medical Device Agency (TITCK) parallel to the 1223/2009 EC Regulation in 2012.[6] By force of the guide on the reporting of undesirable effects, the notification, and reporting of side effects related to cosmetics can be followed.

The necessity of a cosmetovigilance system has been proven by some pilot studies. In a pilot cosmetovigilance study conducted in the Netherlands in 2012, 1294 cases of adverse reactions related to the use of cosmetics were examined.[7] It was found that 23% of the patients were allergic to isothiazolinone, 21% to the perfume mixture, and 21% to cocamidopropyl betaine. The small number of reported cases has been thought to be because a healthcare professional was not notified, when side

*Correspondence: imranaltiokka@gmail.com, Phone: +90 212 440 00 00, ORCID-ID: orcid.org/0000-0001-7328-1964
Received: 21.07.2021, Accepted: 08.11.2021

effects occurred, the patient tried to self-medicate and ignored the side effects, and often cosmetics did not take the risk of side effects seriously enough. Simultaneously, the absence of a formal and reliable cosmetovigilance system makes it difficult to evaluate the reactions that occur as a standard.[8]

In this review, detailed information about the side effects of some cosmetic ingredients will be given, the recent regulations about the cosmetics and the current cosmetovigilance system in Türkiye will be explained.

Cosmetics and cosmeceutical concepts

Although cosmetics and cosmeceuticals represent different types of products, these two concepts are referred under "cosmetics" in the laws in Türkiye. Cosmetics are preparations that are applied externally to the skin, oral mucosa, hair, nails, sweat glands, and do not change the structure and functions of the skin. However, cosmeceuticals are products with active ingredients that reach deeper layers in the skin and display physiological effects. Therefore, the regulations related to cosmetics and cosmeceuticals should also be separately made.

Although the definition of cosmeceutical or dermocosmetic (cosmeceuticals) is unofficially included in the regulations made by the Food and Drug Administration (FDA) in the USA, the term "over-the-counter (OTC) drug" is included for products that fall between cosmetics and pharmaceuticals.[9] The FDA reports the requirements for OTC drugs in its OTC drug monographs.[10] The OTC drug monographs contain allowed ingredients and quantities, doses of active ingredients, formulations, and label rules. It decides that the cosmetic preparation should be evaluated as a cosmetic or OTC preparation with its "intended use".

With a similar approach, European countries have interpreted this class between cosmetics and pharmaceuticals differently.[11] This group, defined as "borderline products", refers to the situations, where it cannot be decided whether the product is a cosmetic or drug. The EU Commission publishes guidelines for these situations describing the cases and explaining which legislation is subject to which situation.[12] For example; although skin whitening cosmetics are included in the cosmetic class, if they are intended to treat diseases such as melasma lentigo, these products are subject to the medical product legislation.[13] Another example is that a bath foam claimed "relaxing" effect will normally be considered a cosmetic product. However, if the product is used for the treatment of cold or flu, it may be considered a medicinal product. These classifications are made by the subgroup on borderline products on the scope of application of Cosmetic Regulation EC no. 1223/2009 and then approved by the working group on the cosmetic products.

Since cosmeceuticals are not a defined group and are not subject to separate regulations from drugs and cosmetics, it is possible to say that products arising from this uncertainty confuse the cosmetovigilance system. Since the steps required for drugs to obtain a license and the procedures for cosmetics are not the same, manufacturers can market products with high active content under the name of cosmetics, as it is easier to obtain a license. However, since these intermediate products, which should be defined as cosmeceuticals, have different effects compared to cosmetics, their control and regulation should be different from cosmetics. It will be revealed in the rest of our article that the products on the market today that create a question mark in the cosmetovigilance system show much a more active cosmeceutical effectiveness than simple superficial effects.

Cosmetovigilance system in Türkiye

EC Cosmetics Regulation 1223/2009 by the European Commission under Guidelines for Reporting Serious Adverse Effects was published in 2012 and this context has been established in Türkiye by TITCK in the same year. In practice, the cosmetovigilance system is applied by healthcare professionals (pharmacists, dentists, physicians, and nurses), who observed the adverse reactions *via* their institution, manufacturer, company, or clinic with the Cosmetic Product Undesirable Effect/Serious Undesirable Effect Notification Forms.

TITCK also defines the responsibilities of cosmetic manufacturers and audits them within the cosmetovigilance system to monitor and evaluate all suspected undesirable effects of products reaching the manufacturer. The manufacturer is responsible for collecting, recording, archiving and evaluating information about the risks and reliability of the products. It ensures that up-to-date information is kept in the product information files of cosmetics, moreover, serious undesirable effect notifications are made to TITCK.[14] The notifications, pieces of information, and reports are evaluated and received by the TITCK, when necessary, opinions are taken by submitting them to the Scientific Commission. Because of the evaluations made, the changes or additions deemed to be made in the product information file or on the packaging of the product are notified to the manufacturer by TITCK. Although cosmetic product manufacturers have the responsibility to report the analysis results and regulate their contents according to legal limits when notifying cosmetic products, sometimes production conditions that do not comply with regulations may occur. In such cases, the production facility is inspected with side effect notifications related to cosmetics. The product having side effects is analyzed by TITCK and can be recalled from the market if it is not found suitable. Since feedback can prevent the occurrence of such situations, it is crucial for public health.

Difficulties encountered in the implementation of the cosmetovigilance system

Even though there is a well-established cosmetovigilance system in Türkiye, it may need some new regulations and implementations to make it more effective.

For instance, since the companies only must prove the use the safe ingredients and their use limits according to the law, the final product is usually not evaluated by the laboratories. This gap may have an adverse effect on the end cosmetic products after getting a license. According to a study conducted in Türkiye, which is the only study in this field, it has been recommended that the post-marketing vigilance systems such as using *in vitro* tests for ingredients and the end products should be done continuously and supported by the authorities.[15]

The new formation of the cosmetovigilance concept makes it difficult to follow up the side effect forms. In some studies, it has been reported that this issue is not considered sufficiently important by health professionals regarding the side effects related to cosmetics.[15,16] Unfortunately, feedback on undesirable effects related to cosmetic products is quite limited. The reason for this is that the consumer stops using the cosmetic product and treats the disorder without consulting a healthcare professional when a mild or moderate side effect is observed.[8] Since these side effects are mostly not at a worrisome level, healthcare professionals may not have time to provide feedback even if they encounter any case.

Cosmetovigilance also prevents possible risks against toxic ingredients by reporting undesirable effects caused by cosmetics. Therefore, healthcare professionals must know which ingredients may have these side effects to provide preventive health services to their patients. However, since cosmetic side effects are not generally seen as serious reactions, current cosmetovigilance training is not given to health professionals.

Another important thing to be recognized in the literature needs more study done in the Turkish cosmetic market to show the incidence of observed adverse reactions related to cosmetics in the Turkish population, identify the potential risks of end formulations, or indicate the public awareness in this matter.

Moreover, cosmetovigilance is a concept that lives and is constantly changing. Factors such as socio-economic developments, differing cosmetic trends, marketing strategies of cosmetic products increase people's cosmetic use. The increasing use of cosmetics causes people to be exposed to more chemicals. Changing cosmetic usage habits and contents creates the need to determine new regulations following the current situation.

Adverse reactions related to cosmetic ingredients

Several scientific studies have been conducted to determine the frequency of occurrence of side effects related to cosmetics. In a study, it was found that 24% of cosmetic consumers experienced any side effects.[17] Cutaneous side effects constitute 95.9% of total side effects, and 4.1% of systemic side effects. In this study, it was also reported that the most common cutaneous side effects were rash (34.8%), itching (31.5%), eczema (22.8%), and others. Systemic side effects were stated as headache (1.7%), nausea (1%), dizziness (0.6%), dyspnea (0.3%) and other conditions.

In one of the recent studies conducted in 2019, the occurrence of adverse effects in 341 subjects diagnosed with contact dermatitis induced by cosmetics was recorded using forms. The occurrence of cosmetics-related adverse events was associated with the mixing of different types of cosmetic products (31.4%), among which mixing of two different brands accounted for 65.4%.[18] Among the patients, the most common symptom recorded was contact dermatitis (n: 318), followed by rosacea and perioral dermatitis (n: 12) and acne was 3 out of 341.

A pilot study conducted in a dermatology clinic in 2019 revealed that the incidence of cutaneous adverse reactions related to cosmetics was 1.58%.[19] The most common reaction was rash and pruritus accounted for 30.9%, followed by itching 23.8%.

Twelve dermatologists from the United States examined contact dermatitis patients from 1977 to 1983 to identify the effect of cosmetic products in their dermatitis occurrence. Skincare products, hair preparations (including colors), and facial make-up was responsible for most of the reactions. One of the important findings was that half of the the patients or physicians were unaware that a cosmetic was responsible for their dermatitis.[20]

Adverse effects related to cosmetic products can be classified as contact dermatitis, acne, discoloration of the skin and its appendages, conditions caused by endocrine-disrupting components, and systemic side effects.

a. Contact dermatitis

Allergic contact dermatitis is defined as allergic or inflammatory dermatosis due to a late-type hypersensitivity reaction, which can occur with the effect of allergen substances that encounter the skin. A European standard patch test is performed to understand, which ingredients have developed allergies in patients.[21]

The European standard patch test is implemented with different types of chambers loaded with allergens at required doses. The upper back is the preferred site for patch testing and the recommended occlusion time is 2 days. Afterward, readings are performed on day 2, 3, 4 or day 7. The patch test is scored according to morphology.[22] A positive patch test reaction is

Table 1. Reading criteria of patch testing[22]

Symbol	Morphology	Assessment
-	No reaction	The negative reaction
?+	Faint erythema only	Doubtful reaction
+	Erythema, infiltration, possibly papules	Weak-positive reaction
++	Erythema, infiltration, papules, vesicles	Strong-positive reaction
+++	Erythema, infiltration, coalescing vesicles	The extreme positive reaction
IR	Various morphologies	The irritant reaction

IR: Irritant reaction

defined as a reaction that fulfills the criteria of at least one positive reaction (Table 1).

In a survey conducted in an epidemiology hospital in the Netherlands, it was reported that 70% of the side effects that patients experienced personal care product cosmetic side effects were itching, 63% dry skin, and 50% burning.[23] In a study conducted in China between 2015 and 2017, contact dermatitis was reported as the most common reaction among the side effects associated with cosmetics.[18] The applications of 151 patients who came to 3 different dermatology clinics in Sweden with the complaints of skin reaction to cosmetics were evaluated and allergic contact dermatitis was diagnosed in 28% and irritant reaction in 27%.[16] Cosmetic preparations that most commonly cause allergic contact dermatitis are hair dyes, moisturizers, deodorants, perfumes, facial cleansers, and nail polishes.

Most common cosmetic allergens, which are the causative agents of allergic contact dermatitis, can be listed as perfume ingredients, hydrogen peroxide, ammonium persulfate, butylated hydroxyanisole, butylated hydroxytoluol, Peru balm, henna, benzophenones, nickel, formaldehyde, paraben, lanolin derivatives, propylene glycol, *p*-phenylenediamine, tosylamide/formaldehyde resin, glyceryl thioglycolate, cetyl alcohol, cocoamidopropyl stearate, 2-bromo-2-nitro-propane-1,3-diol, imidazolidinyl urea, phenoxyethanol, 4-amino benzoic acid, methylisothiazolidone.[24-26] In particular, sodium lauryl sulfate that is one of the most commonly used excipients in cosmetic products, has been found to cause allergic contact dermatitis and has strong irritant properties by causing a high rate of transepidermal water loss.[27] Paraphenylenediamine used in hair dyes and benzophenone-3, which is frequently used in sunscreens, are also high-contact dermatitis allergen.[28-30] Cosmetics containing keratolytic and chemical peeling agents such as alpha and beta hydroxy acids, retinoids, trichloroacetic acid, and kojic acid may cause irritant contact dermatitis.[31]

b. Discoloration of the skin

Ochronosis, which is one of the cutaneous adverse reactions, may occur after the application of cosmetics containing hydroquinone, a skin whitening agent.[32,33] Ochronosis is a disease characterized by pigmentation in soft tissues due to lack of homogentisic acid oxidase enzyme, first described by Virchow[34] for the first time. Hydroquinone causes depigmentation as it causes necrotic destruction of melanocytes. The use of hydroquinone in cosmetics is prohibited in EU countries, as depigmentation is irreversible.[33] Another undesirable effect is related to skin bleaching cosmetics containing mercury, which is also prohibited in cosmetics at this time.[32]

c. Acne cosmetica

Kligman and Mills[35] defined the table as characterized by the acneiform eruption on the lower cheek and chin due to the use of cosmetic products in women aged 20-50 years as *Acne cosmetica*. To determine which cosmetic ingredients cause *Acne cosmetica*, many studies have performed a comedogenicity test using rabbit ear canals. The test technique consists of applying the cosmetic ingredient samples to the ears of adult female albino rabbits daily for 4 consecutive weeks according to the rabbit ear comedogenic assay. At the end of 4 weeks, each rabbit ear was biopsied and examined for evidence of comedone formation. Isopropyl myristate, isopropyl palmitate, butyl stearate, octyl palmitate, octyl stearate, petroleum jelly, lanolin, some red dyes (D&C red dyes, xanthine, and monoazoaniline), and paraffin are among the components that are considered comedogenic.[35-38]

d. Endocrine disruptor effect

An endocrine-disrupting substance is defined as an exogenous substance that causes disturbances in endocrine activity in a healthy organism or its generations.[39] Endocrine disruptors affect endocrine functions by directly or indirectly activating or inhibiting hormone receptors and hormone metabolism enzymes.[40] Endocrine-disrupting components change cellular signals by binding to hormone receptors.[41] Reproductive impairment, diabetes, obesity, and breast cancer are major health problems associated with exposure to endocrine-disrupting chemicals.

Estrogenic chemicals can stimulate or inhibit transcriptional or post-transcriptional mechanisms by binding to estrogen or androgen receptors, with their similarity to the chemical structure of estrogen.[42]

Although a direct relationship between cosmetic use and endocrine-disrupting components is not yet clear, molecules known to have endocrine-disrupting activity are also used in cosmetics by experimental studies.[43] The most common endocrine-disrupting components in cosmetics are parabens, bisphenol A and phthalates.[24,41] In addition to these, aluminum salts and triclosan are also cosmetic ingredients responsible for breast cancer by showing the estrogenic activity.[44] According to the World Health Organization (WHO), triclosan is in the endocrine disruptor class.[45]

With the detection of parabens *in vivo* and *in vitro* tests performed on breast tumor tissues, the suspicion of cosmetic preparations especially applied to the armpit has increased.[46] Methylparaben, ethylparaben, propylparaben, and *n*-butyl paraben show estrogenic activation in MCF7 breast cancer cells.[47] Also, breast cancer cells are mostly observed in the upper-outer region of the breast and one of the risk factors of this situation is the use of antiperspirants containing aluminum.[48,49]

Because of many studies, paraben derivatives are estrogen-mimetic preservatives and can cause changes in hormone levels by interacting with estrogenic receptors.[50-52] Thus, the paraben derivatives have been identified as a risk factors in the development of breast cancer.[51,52] Considering those cosmetic products containing paraben are mostly products that remain in the body without washing, it is risky to apply to most of the body for daily use. Especially during pregnancy, it is critical to make changes in cosmetic use habits, to get support from physicians and pharmacists, and to take measures to minimize the risk of exposure to endocrine-disrupting components.[43]

e. Other common systemic side effects

A cosmetic product should not permeate through the skin and enter the systemic circulation. Cosmetic products only show efficacy through the epidermis and dermis. However, changes in particle sizes and chemical properties for active ingredients to be more effective may cause them to be absorbed from the skin and participate in circulation. Here, to be able to report correctly in the cosmetovigilance system, it is necessary to measure what percentage of the applied cosmetics is in the systemic circulation or how much bioaccumulation will occur. Unfortunately, these phenomena are not easy to follow.

Percutaneous absorption of cosmetics

Systemic side effects of cosmetic substances can only occur because of percutaneous absorption. A topically applied preparation must first penetrate the lipophilic layer. However, high lipophilic content that passes the *Stratum corneum* cannot pass into the hydrophilic dermis.

Percutaneous absorption occurs in 3 stages. In the first stage, the substance adheres to the *Stratum corneum*. In the second stage, permeation occurs with the passage of the substance between the layers. In the last stage, the substance passes through the blood vessels, into the systemic circulation.[53]

Permeation from *stratum corneum* occurs *via* intracellular, intercellular, and follicular routes:

• Hydrophilic molecules undergo intracellular transmission. In the intracellular pathway, molecules do not pass through corneocytes, but through them.

• The intercellular pathway is a cross between lipids (ceramide, cholesterol, fatty acids) in the *stratum corneum*, lipophilic molecules are permeated in this way.

• The follicular pathway occurs through hair follicles or sweat glands.

Factors such as the water ratio and lipids of the *stratum corneum,* the size and diffusion coefficient of the molecule, the number of hydrogen bond donors and recipients are physicochemical factors affecting percutaneous absorption.[53] To pass the *stratum corneum*, the molecule must be of lipophilic character and of a size less than 500 Da.[54] However, lipophilic structures cannot reach the dermis even if they pass the *stratum corneum*. Therefore, lipophilic structures may cause accumulation in the *stratum corneum*.

Physical methods such as iontophoresis, phonophoresis or chemical penetration enhancers can be used to increase the permeation of molecules through the skin.

Penetration enhancers

Penetration enhancers increase penetration by changing the physicochemical structure of the *stratum corneum* and reducing its resistance to diffusion. The denaturation of proteins in the *stratum corneum* and dissolution in skin lipids is the mechanism of action of penetration enhancers. By causing conformational changes in the *stratum corneum* proteins, the penetration of polar structures increases the penetration of non-polar structures by liquefying the crystalline lipids.[55] Some penetration enhancers show these effects by two mechanisms. However, if the benefit-harm ratio of these chemicals is properly scrutinized, otherwise they may irritate [*e.g.* dimethyl sulfoxide (DMSO)]. Examples of penetration enhancers are surfactants, urea, fatty acids (oleic acid, undecanoic acid), terpenes (menthol, thymol), sugars (cyclodextrin), sulfoxides (DMSO), azone.[53,55]

Side effects related to cosmetic ingredients entering the systemic circulation

The formulation ingredients may be responsible for mutagenic, carcinogenic or genotoxic activities. The best known of these components is hexachlorophene, *p*-phenylenediamine, and zirconium complex. It has been reported that the usage of zirconium complex, which is used in antiperspirant products, in the form of aerosol causes the formation of granulomas in the lung, and the use of this substance in aerosol is prohibited.[56]

Some of the cosmetic ingredients found to be carcinogenic can be listed as *p*-phenylenediamine, aluminum, cocamide diethanolamine, butylated hydroxytoluene, coumarins, petrolatum, nickel, and mercury.[24]

In a study conducted on 169 oxidative hair dyes, 150 of them were found to be mutagenic. 2,4-diaminozole, 4-nitro-*o*-phenylenediamine, 2-nitro-*p*-phenylenediamine, 2-5-diaminoazole, 2-amino-5-nitrophenal, *o*-phenylenediamine, 2-amino-4-nitrophenol found in hair dyes and 2,5-diaminotoluene showed various levels of mutagenicity according to the Ames test. Strong mutagenic effects of *p*-phenylenediamine, 2,5-diaminotoluene, and 2,5-diaminozole were found after oxidation with hydrogen peroxide.[57]

In a study in which the absorption of oxidized amine derivative hair dyes from the skin was monitored, 3.66 mg metabolite of 2,5-diaminotoluene was found in the urine 2 days after the hair was dyed. Accordingly, it has been reported that in each hair dyeing process, approximately 4 mg content is absorbed from the scalp and many aromatic amines and diamines are absorbed from the skin.[58] Hair dyes are exposed not only through the skin but also through inhalation. For this purpose, there are various studies on the exposure of hairdressers to hair dyes.[59]

Diazolidine urea and imidazolidine urea, which are added to cosmetic preparations as preservatives, release formaldehyde. Ryu et al.[60] investigated the effects of benzalkonium chloride, diazolidine urea, and imidazolidine urea on apoptosis. Increased reactive oxygen species (ROS) production and decreased cell vital activities were observed at high concentrations of these substances in mouse cells.[60] With these results, it has been reported that benzalkonium chloride, diazolidine urea, and imidazolidine urea used as preservatives in cosmetics cause ROS induction and apoptosis. 25% of the ingredients of cosmetic products sold in the USA contain ingredients that release formaldehyde.[61]

Cadmium, chromium, and nickel are group 2 carcinogens, according to the International Agency for Research on Cancer.[62] Arsenic, cadmium, copper, nickel, manganese, lead, and cobalt are metals used in limited concentrations in lip paints.[63] However, although the formulation components have certain usage limits, cumulative effects can occur with the prolonged

use of these formulations. Unintentionally digested metals can reach vital organs through systemic circulation.[64]

Besides, it has been shown in different studies that exposure to triclosan in pregnant women can cause developmental disorders in the newborn.[65-67] Although it has been shown in studies that triclosan taken into the body with toothpaste remains within safe limits, it can have toxic effects by accumulating in adipose tissues in long-term use, and triclosan in pregnant women can pass to the placenta thanks to its pharmacokinetic properties. For this reason, healthcare professionals should recommend products that do not contain triclosan in pregnant women.

CONCLUSION

Because of all these findings, it is necessary to develop more conscious consumption habits against the unwanted side effects caused by cosmetics and cosmeceutical products, and the consultancy service to be provided by health professionals in this field become more important for public health. Therefore; it is necessary to publish guides and training to educate healthcare professionals as part of the cosmetovigilance system. Because it is known that health professionals do not pay enough attention to the side effects associated with cosmetics.[16] Side effects due to reported cosmetic products are thought to be much less than those encountered. So that, healthcare professionals need to provide feedback on the cases they encounter with the forms available on TITCK's website for the cosmetovigilance system to function properly and to prevent possible risks. For public health, these reports should be made correctly.

Factors such as socio-economic developments, differing cosmetic trends, and marketing strategies increase people's cosmetic use trends. The increasing use of cosmetics causes people to be exposed to more chemicals. As we mentioned before, some chemicals such as parabens, phatalats, and metals may enter the systemic circulation and can accumulate in the human body. Taking the increase of cosmetic consumption and the special circumstances of some patient groups (kids and cancer patients into account, these types of products' safety assessments should be different from those of other cosmetic products).

Since cosmeceuticals have different effects compared with cosmetics, their control mechanisms and regulations also should be different from cosmetics. The unnamed gap between the two groups (cosmetics and drugs) creates uncertainty in the cosmetic market, which allows manufacturers to launch their products as "cosmetics". Besides, post-vigilance reporting should be an obligation for cosmetic companies to make the control mechanism of the institution easier and more effective.

There is a need for new studies in the academic field in which new ingredients are evaluated in terms of toxicology and their penetration through the skin. Newer production technologies (nanotechnology, biotechnology) and different active ingredients are used to achieve stronger effects in cosmetics. Changing cosmetic usage habits and contents creates the need to determine new regulations following the current situation.

Overall; serious and non-serious undesirable effects can be prevented with the cosmetovigilance system. The reporting process is the key of the system, therefore as a part of the feedback system, the healthcare professionals should be trained and supported in terms of cosmetovigilance. Some updates in regulations are needed to track Turkish changing cosmetic market.

Ethics

Peer-review: Externally and internally peer-reviewed.

Authorship Contributions

Concept: İ.A., M.Ü., Design: İ.A., M.Ü., Data Collection or Processing: İ.A., M.Ü., Literature Search: İ.A., Writing: İ.A., M.Ü.

Conflict of Interest: No conflict of interest was declared by the authors.

Financial Disclosure: The authors declared that this study received no financial support.

REFERENCES

1. Vigan M. New allergens in cosmetics. Cosmetovigilance. Ann Dermatol Venereol. 1997;124:571-575.
2. Tissier MH, Lepagnol F. Cosmetovigilance: a French pharmacovigilance system for cosmetics developed by the French health products safety agency. A proposal for the future. Therapie. 2002;57:273-282.
3. 76/768 EEC Cosmetics Directive. Official Journal of the European Communities, 1976. Available from: https://www.legislation.gov.uk/eudr/1976/768/adopted
4. European Cosmetics Association, COLIPA Undesirerable Event Reports. European Comission, 2005. Available from: https://cosmeticseurope.eu
5. Council of Europe, Resolution ResAP. Committee of Ministers, 2006. Available from: https://rm.coe.int/09000016805d72f3
6. Regulation (EC) no 1223/2009 of the European Parliament and of the Council of 30 November 2009 on cosmetic products. Available from: https://health.ec.europa.eu/system/files/2016-11/cosmetic_1223_2009_regulation_en_0.pdf
7. Salverda JG, Bragt PJ, de Wit-Bos L, Rustemeyer T, Coenraads PJ, Tupker RA, Kunkeler LC, Laheij-de Boer AM, Stenveld HJ, van Ginkel CJ, Kooi MW, Bourgeois FC, van Gorcum TF, van Engelen JG, van Dijk R, de Graaf J, Donker GA, de Heer C, Bruynzeel D. Results of a cosmetovigilance survey in the Netherlands. Contact Dermatitis. 2013;68:139-148.
8. Sautebin L. Understanding the adverse effects of cosmetics: a pilot project in cosmetovigilance. Drug Saf. 2008;31:433-436.
9. FDA. Available from: https://www.fda.gov/cosmetics/cosmetics-laws-regulations/it-cosmetic-drug-or-both-or-it-soap
10. FDA. Available from: https://www.fda.gov/drugs/over-counter-otc-drug-monograph-process
11. 1223/2009 Borderline products. Available from: https://ec.europa.eu/docsroom/documents/42850
12. Available from: https://ec.europa.eu/docsroom/documents/13032/
13. European Comission, "Medical Product Legislation." Official Journal of the European Union, 2004.
14. Kozmetik ürünlerin istenmeyen etkilerinin/ciddi istenmeyen etkilerinin kuruma bildirimine ilişkin kılavuz sürüm 1.0. Türkiye İlaç ve Tıbbi Cihaz

Kurumu, 2005. Available from: https://titck.gov.tr/storage/legislation/KeaTUbu4.pdf

15. Köse Ö, Sabuncuoğlu S, Erkekoğlu P, Koçer-Gümüşel B. Cosmetovigilance: current status in Europe and Turkey, its practices and cosmetovigilance surveys. FABAD J Pharm Sci. 2018;43:79-90.
16. Berne B, Tammela M, Färm G, Inerot A, Lindberg M. Can the reporting of adverse skin reactions to cosmetics be improved? A prospective clinical study using a structured protocol. Contact Dermatitis. 2008;58:223-227.
17. Di Giovanni C, Arcoraci V, Gambardella L, Sautebin L. Cosmetovigilance survey: are cosmetics considered safe by consumers? Pharmacol Res. 2006;53:16-21.
18. Yang SL, Zheng Y, Zhang YQ, Ye CX, Yi JL, Liu YF, Lai W. Cosmetics use-related adverse events. Chin Med J (Engl). 2019;132:2135-2136.
19. Al Mulla F, Sridhar SB, Shariff A, Abu Al Hassan G. Incidence, nature and causality assessment of cutaneous adverse reactions to cosmetics: a pilot study. Int J Community Med Public Health. 2019;6:1978-1983.
20. Adams RM, Maibach HI. A five-year study of cosmetic reactions. J Am Acad Dermatol. 1985;13:1062-1069.
21. Bodamyalı P. Yüz kontakt dermatitlerinde kozmetik allerjenlerle Patch test sonuçlarının değerlendirilmesi (Thesis). Ankara: Ankara University Faculty of Medicine; 2011.
22. Johansen JD, Aalto-Korte K, Agner T, Andersen KE, Bircher A, Bruze M, Cannavó A, Giménez-Arnau A, Gonçalo M, Goossens A, John SM, Lidén C, Lindberg M, Mahler V, Matura M, Rustemeyer T, Serup J, Spiewak R, Thyssen JP, Vigan M, White IR, Wilkinson M, Uter W. European Society of Contact Dermatitis guideline for diagnostic patch testing - recommendations on best practice. Contact Dermatitis. 2015;73:195-221.
23. Groot AC, Nater JP, Lender R, Rijcken B. Adverse effects of cosmetics and toiletries: a retrospective study in the general population. Int J Cosmet Sci. 1987;9:255-259.
24. Khan AD, Alam MN. Cosmetics and their associated adverse effects: a review. J App Pharm Sci Res. 2019:1-6.
25. Orton DI, Wilkinson JD. Cosmetic allergy: incidence, diagnosis, and management. Am J Clin Dermatol. 2004;5:327-337.
26. Jansson T, Lodén M. Strategy to decrease the risk of adverse effects of fragrance ingredients in cosmetic products. Am J Contact Dermat. 2001;12:166-169.
27. Freeman S, Maibach H. Study of irritant contact dermatitis produced by repeat patch test with sodium lauryl sulfate and assessed by visual methods, transepidermal water loss, and laser Doppler velocimetry. J Am Acad Dermatol. 1988;19:496-502.
28. DeLeo VA. *p*-Phenylenediamine. Dermatitis. 2006;17:53-55.
29. Available from: https://ec.europa.eu/health/archive/ph_risk/committees/scmp/documents/out43_en.pdf
30. Warshaw EM, Wang MZ, Maibach HI, Belsito DV, Zug KA, Taylor JS, Mathias CG, Sasseville D, Zirwas MJ, Fowler JF Jr, DeKoven JG, Fransway AF, DeLeo VA, Marks JG Jr, Pratt MD, Storrs FJ. Patch test reactions associated with sunscreen products and the importance of testing to an expanded series: retrospective analysis of North American Contact Dermatitis Group data, 2001 to 2010. Dermatitis. 2013;24:176-182.
31. Pons-Guiraud A. Les allergies aux cosmétiques [Allergies to cosmetics]. Rev Prat. 2006;56:284-288.
32. Olumide YM, Akinkugbe AO, Altraide D, Mohammed T, Ahamefule N, Ayanlowo S, Onyekonwu C, Essen N. Complications of chronic use of skin lightening cosmetics. Int J Dermatol. 2008;47:344-353.
33. Desmedt B, Courselle P, De Beer JO, Rogiers V, Grosber M, Deconinck E, De Paepe K. Overview of skin whitening agents with an insight into the illegal cosmetic market in Europe. J Eur Acad Dermatol Venereol. 2016;30:943-950.
34. Virchow VR. XV. Ein fall von allgemeiner Ochronose der Knorpel und knorpelälinliclien Tlieile. De Gruyter. 1866. doi: https://doi.org/10.1515/9783112390542-015.
35. Kligman AM, Mills OH. *Acne cosmetica*. Arch Dermatol. 1972;106:843-850.
36. Fulton JE Jr, Pay SR, Fulton JE 3rd. Comedogenicity of current therapeutic products, cosmetics, and ingredients in the rabbit ear. J Am Acad Dermatol. 1984;10:96-105.
37. Singh S, Mann BK, Tiwary NK. *Acne cosmetica* revisited: a case-control study shows a dose-dependent inverse association between overall cosmetic use and post-adolescent acne. Dermatology. 2013;226:337-341.
38. Nguyen SH, Dang TP, Maibach HI. Comedogenicity in rabbit: some cosmetic ingredients/vehicles. Cutan Ocul Toxicol. 2007;26:287-292.
39. Å Bergman, Heindel JJ, Jobling S, Kidd KA, Zoeller RT. State of the Science of endocrine disrupting chemicals - 2012 an assessment of the state of the science of endocrine disruptors. Available form: https://apps.who.int/iris/bitstream/handle/10665/78102/WHO_HSE_PHE_IHE_2013.1_eng.pdf?sequence=1&isAllowed=y
40. Giulivo M, Lopez de Alda M, Capri E, Barceló D. Human exposure to endocrine disrupting compounds: their role in reproductive systems, metabolic syndrome and breast cancer. A review. Environ Res. 2016;151:251-264.
41. Natarajan R, Aljaber D, Au D, Thai C, Sanchez A, Nunez A, Resto C, Chavez T, Jankowska MM, Benmarhnia T, Yang JA, Jones V, Tomsic J, McCune JS, Sistrunk C, Doan S, Serrano M, Cardiff RD, Dietze EC, Seewaldt VL. Environmental exposures during puberty: window of breast cancer risk and epigenetic damage. Int J Environ Res Public Health. 2020;17:493.
42. Wuttke W, Jarry H, Seidlova-Wuttke D. Definition, classification and mechanism of action of endocrine disrupting chemicals. Hormones (Athens). 2010;9:9-15.
43. Marie C, Cabut S, Vendittelli F, Sauvant-Rochat MP. Changes in cosmetics use during pregnancy and risk perception by women. Int J Environ Res Public Health. 2016;13:383.
44. Darbre PD. Environmental oestrogens, cosmetics and breast cancer. Best Pract Res Clin Endocrinol Metab. 2006;20:121-143.
45. Bergman Å, Heindel JJ, Jobling S, Kidd KA, Zoeller RT. Endocrine Disrupting Chemicals 2012. WHO: UNEP, 2012.
46. Darbre PD. Underarm cosmetics and breast cancer. J Appl Toxicol. 2003;23:89-95.
47. Byford JR, Shaw LE, Drew MG, Pope GS, Sauer MJ, Darbre PD. Oestrogenic activity of parabens in MCF7 human breast cancer cells. J Steroid Biochem Mol Biol. 2002;80:49-60.
48. McGrath KG. An earlier age of breast cancer diagnosis related to more frequent use of antiperspirants/deodorants and underarm shaving. Eur J Cancer Prev. 2003;12:479-485.
49. Jennrich P, Schulte-Uebbing C, P. Does aluminium trigger breast cancer? Open Access J Sci Technol. 2016:1-6.

50. Prusakiewicz JJ, Harville HM, Zhang Y, Ackermann C, Voorman RL. Parabens inhibit human skin estrogen sulfotransferase activity: possible link to paraben estrogenic effects. Toxicology. 2007;232:248-256.

51. Darbre PD, Harvey PW. Paraben esters: review of recent studies of endocrine toxicity, absorption, esterase and human exposure, and discussion of potential human health risks. J Appl Toxicol. 2008;28:561-578.

52. Boberg J, Taxvig C, Christiansen S, Hass U. Possible endocrine disrupting effects of parabens and their metabolites. Reprod Toxicol. 2010;30:301-312.

53. Bolzinger MA, Briançon S, J. Pelletier J, Chevalier Y. Penetration of drugs through skin, a complex rate-controlling membrane. Curr Opin Colloid Interface Sci. 2012;17:156-165.

54. Massella D, Argenziano M, Ferri A, Guan J, Giraud S, Cavalli R, Barresi AA, Salaün F. Bio-functional textiles: combining pharmaceutical nanocarriers with fibrous materials for innovative dermatological therapies. Pharmaceutics. 2019;11:403.

55. Kanikkannan N, Kandimalla K, Lamba SS, Singh M. Structure-activity relationship of chemical penetration enhancers in transdermal drug delivery. Curr Med Chem. 2000;7:593-608.

56. Kaymak Y, Tırnaksız F. Side effects related to cosmetic products. Dermatose. 2007;1:39-48.

57. Ames BN, Kammen HO, Yamasaki E. Hair dyes are mutagenic: identification of a variety of mutagenic ingredients. Proc Natl Acad Sci U S A. 1975;72:2423-2427.

58. Kiese M, Rauscher E. The absorption of *p*-toluenediamine through human skin in hair dyeing. Toxicol Appl Pharmacol. 1968;13:325-331.

59. Herrinton LJ, Weiss NS, Koepsell TD, Daling JR, Taylor JW, Lyon JL, Swanson GM, Greenberg RS. Exposure to hair-coloring products and the risk of multiple myeloma. Am J Public Health. 1994;84:1142-1144.

60. Ryu O, Park BK, Bang M, Cho KS, Lee SH, Gonzales ELT, Yang SM, Kim S, Eun PH, Lee JY, Kim KB, Shin CY, Kwon KJ. Effects of several cosmetic preservatives on ROS-dependent apoptosis of rat neural progenitor cells. Biomol Ther (Seoul). 2018;26:608-615.

61. de Groot AC, Veenstra M. Formaldehyde-releasers in cosmetics in the USA and in Europe. Contact Dermatitis. 2010;62:221-224.

62. IARC Working Group on the Evaluation of Carcinogenic Risks to Humans, World Health Organization, and International Agency for Research on Cancer, eds. Some aromatic amines, organic dyes, and related exposures. Lyon: IARC Press, 2010.

63. Al-Salehl, Al-Enazi S. Trace metals in lipsticks. Toxicol Environ Chem. 2011;93:1149-1165.

64. Gao P, Lei T, Jia L, Yury B, Zhang Z, Du Y, Feng Y, Xing B. 2018;238:554-561.

65. Jackson-Browne MS, Papandonatos GD, Chen A, Calafat AM, Yolton K, Lanphear BP, Braun JM. Identifying vulnerable periods of neurotoxicity to triclosan exposure in children. Environ Health Perspect. 2018;126:057001.

66. Allmyr M, Harden F, Toms LM, Mueller JF, McLachlan MS, Adolfsson-Erici M, Sandborgh-Englund G. The influence of age and gender on triclosan concentrations in Australian human blood serum. Sci Total Environ. 2008;393:162-167.

67. Berger K, Gunier RB, Chevrier J, Calafat AM, Ye X, Eskenazi B, Harley KG. Associations of maternal exposure to triclosan, parabens, and other phenols with prenatal maternal and neonatal thyroid hormone levels. Environ Res. 2018;165:379-386.